

**DESIGN, SYNTHESIS AND BINDING
STUDIES OF NOVEL CYP26
INHIBITORS**

STEPHANE PAUTUS

A thesis submitted in accordance with the
conditions governing candidates for the degree of
PHILOSOPHIAE DOCTOR (PhD)

Welsh School of Pharmacy, School of Chemistry
Cardiff University

April, 2008

UMI Number: U584250

All rights reserved

INFORMATION TO ALL USERS

The quality of this reproduction is dependent upon the quality of the copy submitted.

In the unlikely event that the author did not send a complete manuscript and there are missing pages, these will be noted. Also, if material had to be removed, a note will indicate the deletion.



UMI U584250

Published by ProQuest LLC 2013. Copyright in the Dissertation held by the Author.
Microform Edition © ProQuest LLC.

All rights reserved. This work is protected against
unauthorized copying under Title 17, United States Code.




ProQuest LLC
789 East Eisenhower Parkway
P.O. Box 1346
Ann Arbor, MI 48106-1346



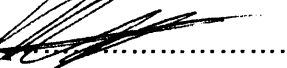
DECLARATION

This work has not previously been accepted in substance for any degree and is not concurrently submitted in candidature for any degree.

Signed  (candidate) Date 16/04/2008.....

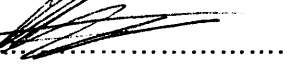
STATEMENT 1

This thesis is being submitted in partial fulfillment of the requirements for the degree of ^{PhD}..... (insert MCh, MD, MPhil, PhD etc, as appropriate)

Signed  (candidate) Date 16/04/2008.....

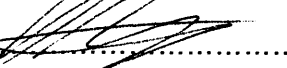
STATEMENT 2

This thesis is the result of my own independent work/investigation, except where otherwise stated. Other sources are acknowledged by explicit references.

Signed  (candidate) Date 16/04/2008.....

STATEMENT 3

I hereby give consent for my thesis, if accepted, to be available for photocopying and for inter-library loan, and for the title and summary to be made available to outside organisations.

Signed  (candidate) Date 16/04/2008.....

ACKNOWLEDGEMENT

I would like to express my gratitude to my supervisors, Dr Claire Simons and Dr Mike Coogan for their guidance, help and support throughout my PhD.

I would like to thank Cardiff University for the funding and the technical staff of both the Welsh School of Pharmacy and the School of Chemistry especially Rob Jenkins and Robin Hicks for the mass spectrometry. Thanks to the people of my groups in pharmacy: Sook-Wah, Malina, Mohammed, Pete and Ahmed and in chemistry: Richard, Vanessa, Soraya and Sarah for their guidance and advice. I would also like to thank all the people within the Welsh School of Pharmacy and the School of Chemistry for their precious help and the friendly atmosphere, especially Marco for the NMR, Andrea for the docking studies, Niek for the calculations and Damien for the CV and letters.

Special thanks to my parents, sisters, friends and Sarah for their support and encouragement.

ABSTRACT

All-*trans*-retinoic acid (ATRA) has shown spectacular success in the treatment of cancer and leukaemia, however ATRA is rapidly metabolised by the P450 enzyme CYP26. In order to enhance endogenous levels of ATRA and/or to extend the half life of externally administered ATRA, a CYP26 inhibitor is required.

Two series of CYP26 inhibitors were synthesised: a series of 4-alkyl/aryl-substituted 1-[benzofuran-2-yl-phenylmethyl]-1*H*-triazoles and a series of benzoxazol-2-yl-[phenylimidazol-1-ylmethyl]phenylamines. The triazole derivatives were prepared using methodology previously described by our group. The aminobenzoxazole derivatives were envisaged from a docking experiment using a CYP26A1 homology model (based on CYP3A4) template; docking experiments were performed with MOE. The molecular docking of the amino-benzoxazole imidazole derivatives indicated multiple hydrogen bonding in addition to coordination between the imidazole nitrogen and the P450 haem transition metal. The triazole derivatives were evaluated for CYP26A1 inhibitory activity using a MCF-7 cell-based assay. The 4-ethyl-1,2,4-triazole and the 4-phenyl-1,2,4-triazole derivatives displayed inhibitory activity (IC_{50} = 4.5 and IC_{50} = 7 μ M respectively) comparable with liarozole (IC_{50} = 7 μ M). On the other hand the aminobenzoxazole imidazole derivatives were only moderate inhibitors of the CYP26A1 enzyme in MCF-7 cells and did not achieve the promise shown in docking studies. The most potent inhibitor was the unsubstituted derivative (IC_{50} = 0.9 μ M).

Studies of the interaction of some of these inhibitors with hemin and TPP were also performed using different spectroscopic techniques (mass spectrometry, X-ray crystallography, 1 H NMR and UV/VIS spectroscopy) and the binding constant was determined from the UV/VIS data for the unsubstituted compound of the aminobenzoxazole derivative with both hemin (K_{H1} = $(1.69 \pm 0.31) \cdot 10^5$ M $^{-1}$) and TPP (K_{T2} = $(1.08 \pm 0.18) \cdot 10^7$ M $^{-2}$).

ABBREVIATIONS

Ala: alanine

Anal.: analysis

APL: acute promyelocytic leukaemia

aq: aqueous

Ar: aromatic

Arg: arginine

AROM: aromatase

Asn: Asparagine

Asp: aspartic acid

ATRA: all-*trans*-retinoic acid

BHA: butylated hydroxyanisole

bs: broad singlet

calcd: calculated

CRABP: cellular retinoic acid binding protein

Cys: cysteine

d: doublet

DCE: dichloroethane

DIEA: di-isopropyl ethylamine

DMAP: dimethyl aminopyridine

DMF: dimethyl formamide

DMSO: dimethyl sulphoxide

DoF: Degree of Freedom

DNA: Deoxyribonucleic acid

DPT: di-2-pyridyl thionocarbonate

EI: electro ionisation

ESI-MS: electro-spray ionisation- mass spectrometry

Gln: glutamine

Glu: glutamic acid

Gly: glycine

hex: hexyl
His: histidine
HL: monosubstituted haem-ligand complex
HL₂: disubstituted haem-ligand complex
HOMO: highest occupied molecular orbital
HPLC: High performance liquid chromatography
HRMS: high resolution mass spectroscopy
***i*Bu:** isobutyl
Ile: isoleucine
***i*Pr:** isopropyl
IR: infra red
KS: Kaposi's sarcoma
Leu: leucine
lit: literature
LUMO: Lowest unoccupied molecular orbital
Lys: lysine
m: multiplet
Me: methyl
Met: methionine
MMT: monomethoxytrityl
m.p.: melting point
NADP: Nicotinamide adenine dinucleotide phosphate
NMR: nuclear magnetic resonance
NOESY: Nuclear Overhauser Effect Spectroscopy
PBS: phosphate buffer solution
PE: petroleum ether
Phe: phenylalanine
ppm: part per million
Pro: proline
RAL: retinaldehyde
RAMBA: retinoic acid metabolism blocking agent
RAR: retinoic acid receptor

RAs: retinoic acids

R_f: retention factor

RPMI: Roswell Park Memorial Institute medium

rt: room temperature

RXR: retinoid X receptor

s: singlet

Ser: serine

t: triplet

TBDMS: *tert*-butyldimethylsilyl

***t*Bu: tertio-butyl**

THF: tetrahydrofuran

Thr: threonine

t.l.c.: thin layer chromatography

TPP: 5,10,15,20-tetraphenyl-21H,23H-porphine-iron(III)-chloride

Trp: tryptophane

Tyr: tyrosine

Val: valine

UV/VIS: ultra-violet/visible

TABLE OF CONTENTS

CHAPTER1: Introduction	PAGE
1) GENERAL INTRODUCTION	1
<u>1.1) The cytochrome P450 enzyme system</u>	1
<u>1.2) Reactions catalysed by cytochrome P450 and catalytic cycle</u>	7
<u>1.3) Specific target: the CYP26 enzymes</u>	11
<i><u>1.3.1) Retinoid family</u></i>	11
<i><u>1.3.2) General mode of action of retinoic acid</u></i>	13
<i><u>1.3.3) Retinoids and cancer</u></i>	16
<i><u>1.3.4) Role of CYP26</u></i>	18
<i><u>1.3.5) Known CYP26 inhibitors or retinoic acid metabolism blocking agents (RAMBAs)</u></i>	20
<i><u>(a) Liarozole (LiazalTM) and ketoconazole</u></i>	20
<i><u>(b) R115866 and R116010</u></i>	22
<i><u>(c) RAMBAs recently developed</u></i>	24
<i><u>(d) RAMBAs previously developed in our laboratory</u></i>	26
2) AIMS AND OBJECTIVES	28
CHAPTER2: FIRST SERIES: 1-[benzofuran-2-yl-(4-alkyl-phenyl)-methyl]triazole and 1-[benzofuran-2-yl-(4-alkyl-phenyl)methyl]tetrazole	30
1) SYNTHESIS AND DISCUSSION	30
<u>1.1) General chemistry</u>	30

<u>1.2) Preparation of the 4'-alkylacetophenone bromide</u>	31
<u>1.3) Preparation of the benzofurans</u>	33
<u>1.4) Reduction of the α-ketones</u>	35
<u>1.5) Addition of the aza-ring (triazole or tetrazole)</u>	36
2) BIOLOGICAL ASSAY	39
<u>2.1) Materials and equipment</u>	39
<u>2.2) Cell-lines used</u>	40
<u>2.3) General method for the MCF-7 wild type ATRA assay</u>	41
<u>2.4) Experimental results</u>	42
<u>2.5) Molecular modeling</u>	44
3) EXPERIMENTAL	47
<u>3.1) General material and method</u>	47
<u>3.2) Experimental results</u>	48
<u>3.2.1) General procedure for the preparation of the 4'-alkylacetophenone bromide 1-6</u>	48
<u>3.2.2) General procedure for the preparation of the Benzofuran-2-yl-(4-alkyl-phenyl)-methanone 7-12</u>	50
<u>3.2.3) General procedure for the preparation of the Benzofuran-2-yl-(4-alkyl-phenyl)-methanol 13-18</u>	53
<u>3.2.4) Preparation of the 1-{Benzo[b]furan-2-yl}[4-fluorophenyl]methyl}-1H-tetrazole 19</u>	56

<u>3.2.5) General procedure for the preparation of the 1-(Benzo[b]furan-2-yl)4-alkyl-(phenyl)methyl)-1H-[1,2,4] triazole 20-24 and 1-(benzo[b]furan-2-yl)4-alkyl-(phenyl)methyl)-1H-[1,3,4] triazole 20' and 21'</u>	57
CHAPTER 3:SECOND SERIES: Benzooxazol-2-yl-[phenyl-imidazol-1-yl-methyl)phenyl]-amine	62
1) MOLECULAR DOCKING	62
<u>1.1) Introduction</u>	62
<u>1.2) Docking studies</u>	64
<u>1.2.1) Docking of ATRA</u>	64
<u>1.2.2) Docking of R115866</u>	65
<u>1.2.3) Docking of benzooxazol-2-yl-[phenyl-[1,2,4]imidazol-1-yl-methyl)-phenyl]-amine derivatives</u>	67
<u>1.2.4) Investigation of other substitutions</u>	72
<u>1.2.5) Substitution on the benzooxazole ring and change in the aza-ring</u>	78
2) SYNTHESIS AND DISCUSSION	81
<u>2.1) Retrosynthesis</u>	81
<u>2.2) Synthesis of the 4-substituted aminobenzophenone</u>	82
<u>A</u>	
<u>2.2.1) Formation of A by a Friedel-Crafts acylation</u>	82
<u>2.2.2) Formation of A by a Negishi coupling</u>	85
<u>2.2.3) Formation of A by Samietz method</u>	87
<u>2.2.4) Reduction of the nitro-group</u>	89
<u>2.3) Formation of the benzooxazole ring C</u>	90
<u>2.4) Addition of the aza-ring</u>	94

<u>2.5) Synthesis of the other substituents</u>	95
<u>2.6) Synthesis of the unsubstituted, methyl, methoxy and hydroxy substituted phenyl derivatives</u>	97
<i><u>2.6.1) Synthesis of the benzooxazol-2-yl-[4-substituted-1-yl-phenyl-methyl]-phenyl-amine (52), (53), (53'), (54).</u></i>	97
<i><u>2.6.2) Synthesis of the methyl derivative (59)</u></i>	99
<i><u>2.6.3) Synthesis of the methoxy (67) and the hydroxy (68) derivatives</u></i>	100
<u>2.7) Substitution on the other positions of the phenyl ring</u>	102
<i><u>2.7.1) Synthesis of a di-meta derivative</u></i>	102
<i><u>2.7.2) Synthesis of the dimethyl derivatives 84, 85 and 86</u></i>	103
<u>2.8) Biological evaluation</u>	105
3) EXPERIMENTAL	108
<u>3.1) Experimental results for the preparation of the methyl ester derivatives 45 and 46 and the carboxylic acid derivatives 47 and 48</u>	108
<u>3.2) Experimental results for the preparation of the unsubstituted derivatives 52, 53, 53' and 54</u>	123
<u>3.3) Experimental results for the preparation of the methyl derivative 59</u>	129
<u>3.4) Experimental results for the preparation of the methoxy derivative 67 and the hydroxy derivative 68</u>	133
<u>3.5) Experimental results for the preparation of the dimethyl derivatives 84, 85 and 86</u>	140

CHAPTER 4: Haem and haem model binding studies	152
1) INTRODUCTION	152
2) MASS SPECTROMETRY STUDIES	156
<u>2.1) Material and method</u>	156
<u>2.2) Experimental results and discussion</u>	157
3) FORMATION OF COMPLEXES AND X-RAY CRYSTALLOGRAPHY STUDIES	167
4) ¹H NMR STUDIES	170
<u>4.1) Materials and method</u>	171
<u>4.2) Experimental results and discussion</u>	171
5) UV/VIS ANALYSIS AND DETERMINATION OF THE BINDING CONSTANT	175
<u>5.1) UV/VIS analysis</u>	175
<u>5.2) Binding constant determination</u>	179
<u>5.2.1) Stoichiometry of the reaction</u>	180
<u>5.2.2) Equations used</u>	181
<u>5.2.3) Fit of the data and binding constant determination</u>	183
6) CONCLUSION	193
CHAPTER 5: Conclusion and future investigations	195

1) GENERAL INTRODUCTION

1.1) The cytochrome P450 Enzyme

The P450 enzymes consist of a large family of single polypeptide chains in the order of 45000 to 55000 Da. All these proteins contain a single iron protoporphyrin IX prosthetic group coordinated to the four pyrrole nitrogen atoms as a haem¹. The fifth coordination site has the thiolate anion from a cysteine residue and the sixth is probably coordinated to the imidazole group from a histidine residue² (Figure 1.1).

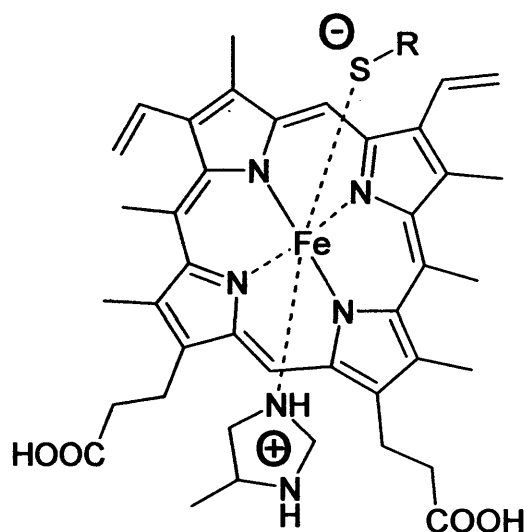


Figure 1.1: Structure of protoporphyrin IX³

The name cytochrome P450 comes from pigment at 450 nm as their UV/VIS spectrum displays a strong absorbance near 450 nm when the haem iron is reduced

¹ De Matteis F.; In *Iron in biochemistry and medicine*, 2nd Ed. Academic Press, London, New York, 1980, 5293-324.

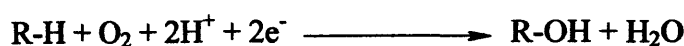
² Poulos T.L.; Cytochrome P450: Molecular architecture, mechanism and prospects for rational inhibitor design. *Pharm. Res.*, 1988, 5, 67-75.

³ McMurry T.J. and Groves J.T.; Metalloporphyrin models for cytochrome P450. In: Ortiz de Montellano, P.R., Ed. *Cytochrome P450: Structure and biochemistry*, New York: Plenum Press, 1986, 1-28.

with sodium dithionate and complexed to carbon monoxide⁴. This is called a reduced CO difference spectrum⁵.

In mammals, the P450 enzymes can be found in most tissues, except the muscles, neurones and red blood cells⁶. These enzymes are located in the endoplasmic reticulum and are highly concentrated in the liver and small intestine⁷.

These enzymes are monooxygenases, able to insert one oxygen atom of the oxygen molecule (O₂) into a large number of substrates, while reducing the other oxygen atom by two electrons to form water⁸.



Where R-H is a hydrophobic substrate

They are involved in the synthesis or the degradation of a large number of endogenous compounds such as steroids and fatty acids, and can also transform new synthesised compounds such as drugs⁹.

The P450 enzymes are often designated by the abbreviation CYP followed by a number indicating their gene family, a capital letter indicating the subfamily and another number for the individual gene. Members of the same family should share at least 40 % of the amino acids in their protein sequence while members of the same subfamily should share at least 55 % of their amino acids in their protein sequence.

In humans, 57 genes and more than 59 pseudogenes divided among 18 families of cytochrome P450 genes and 43 subfamilies have been identified¹⁰. The 18

⁴ Meunier B., De Visser S.P. and Shaik S.; Mechanism of oxidation reactions catalysed by cytochrome P450 enzymes. *Chem. Rev.*, 2004, 104, 3947-3980.

⁵ Omura T. and Sato R.; The carbon monoxide-binding pigment of liver microsomes. *J. Biol. Chem.*, 1964, 239, 2370-2378.

⁶ Waterman M.R., John M.E. and Simpson E.R.; Regulation of synthesis and activity of cytochrome P-450 enzymes in physiological pathways; In: Ortiz de Montellano, P.R., Ed. *Cytochrome P450: Structure and biochemistry*; New York: Plenum Press, 1986, 345-386.

⁷ Nerbert D.W. and Gonzalez F.J.; P450 genes: structure, evolution and regulation. *Ann. Rev. Biochem.*, 1987, 56, 945-993.

⁸ Dawson J.H.; Probing structure-function relations in heme-containing oxygenases and peroxidases. *Science*, 1988, 240, 433-439.

⁹ Simmons D.L., Lalley P.A. and Kapser C.B.; Chromosomal assignments of genes coding for components of the mixed-function oxidase system in mice: Genetic localisation of the cytochrome P450 PB gene families and the NADPH-cytochrome P450 oxidoreductase and epoxide hydratase genes. *J. Biol. Chem.*, 1985, 260, 515-521.

families found in human are CYP1, CYP2, CYP3, CYP4, CYP5, CYP7, CYP8, CYP11, CYP17, CYP19, CYP20, CYP21, CYP24, CYP26, CYP27, CYP39, CYP46, CYP51¹⁰.

Their functions and substrates are variable (Table 1.1). The majority of them (CYP1, CYP2, CYP3, CYP7, CYP11, CYP17, CYP21, CYP39, CYP46, CYP51) are involved in the metabolism of drugs and steroids such as the sex hormone (oestrogen, testosterone) and cholesterol which is involved in cardiovascular disease^{11,12}. Some others such as CYP4 and CYP5 are involved in the metabolism of fatty acids (especially arachidonic acid)¹³. Some of them also have a very specific function and substrate such as CYP24 responsible for the degradation of calcitriol¹⁴ and the CYP26 responsible of the metabolism of retinoic acid¹⁵. They can also display different functions depending on their subfamily such as the CYP8 and the CYP27 families. CYP8A1 is involved in the degradation of prostacyclin, which is a metabolite of the arachidonic acid acting as an effective vasodilator¹⁶, while CYP8B1 is involved in the biosynthesis of bile acid¹⁷. Concerning the CYP27 family, CYP27A1 is involved in bile acid biosynthesis¹⁸ while CYP27B1 is connected with the degradation of vitamin D¹⁹ and the function of the third member

¹⁰ Nelson D.R., Zeldin D.C., Hoffman S.M.G., Maltais L.J., Wain H.M. and Nebert N.W.; Comparison of cytochrome P450 (CYP) genes from the mouse and human genomes, including nomenclatures recommendations for genes, pseudogenes and alternative-splice variant. *Pharmacogenetics*, 2004, 14, 1-18.

¹¹ Nagata K. and Yamazoe Y.; Genetic polymorphism of human cytochrome P450 involved in drug metabolism. *Drug Metabol. Pharmacokin.*, 2002, 17, 167-189.

¹² Honkakoski P. and Negishi M.; Regulation of cytochrome P450 (CYP) genes by nuclear receptor. *Biochem. J.*, 2000, 347, 321-337.

¹³ Baer B.R. and Rettie A.E.; CYP4B1: an enigmatic P450 at the interface between xenobiotic and endobiotic metabolism. *Drug Met. Rev.*, 2006, 38, 451-476.

¹⁴ Schuster I., Egger H., Astecker N., Herzig G., Schussler M. and Vorisek G.; Selective inhibitors of CYP24: mechanistic tools to explore vitamin D metabolism in human keratinocytes. *Steroids*, 2001, 66, 451-462.

¹⁵ Abu-Abed S.S., Beckett B.R., Chiba H., Chitalen V.J., Jones G., Metzger D., Chambon P. and Petkovic M.; Mouse *P450RAI* (CYP26) expression and retinoic acid-inducible retinoic acid metabolism in F9 cells are regulated by retinoic acid receptor γ and retinoid X receptor α . *J. Biol. Chem.*, 1998, 273, 2409-2415.

¹⁶ Chiang C.W., Yeh H.C., Wang L.H. and Chan N.L.; Crystal structure of the human prostacyclin synthase. *J. Mol. Biol.*, 2006, 364, 266-274.

¹⁷ Zhang M. and Chiang J.Y.L.; Transcriptional regulation of the human sterol 12 α -hydroxylase gene (CYP8B1). *J. Biol. Chem.*, 2001, 276, 41690-41699.

¹⁸ Bjorkhem I., Araya Z., Rudling M., Angelin B., Einarsson C. and Wikvall K.; Differences in the regulation of the classical and the alternative pathway for bile acid synthesis in human liver. *J. Biol. Chem.*, 2002, 277, 26804-26807.

¹⁹ Farhan H., Wahala K. and Cross H.S.; Genistein inhibits vitamin D hydroxylases CYP24 and CYP27B1 expression in prostate cells. *J. Steroid Biochem. Mol. Biol.*, 2003, 84, 423-429.

of the family CYP27C1 is still unknown. The function of the CYP20 family is still to be discovered.

Table 1.1: Families and function of the different cytochrome P450 in human²⁰.

Family	Function	Members	Names
CYP1	Drug and steroid (especially oestrogen) metabolism	3 subfamilies, 3 genes, 1 pseudogenes	CYP1A1, CYP1A2, CYP1B1
CYP2	Drug and steroid metabolism	13 subfamilies, 16 genes, 16 pseudogenes	CYP2A6, CYP2A7, CYP2A13, CYP2B6, CYP2C8, CYP2C9, CYP2C18, CYP2C19, CYP2D6, CYP2E1, CYP2F1, CYP2J2, CYP2R1, CYP2S1, CYP2U1, CYP2W1
CYP3	drug and steroid (including testosterone) metabolism	1 subfamily, 4 genes, 2 pseudogenes	CYP3A4, CYP3A5, CYP3A7, CYP3A43
CYP4	arachidonic acid or fatty acid metabolism	6 subfamilies, 11 genes, 10 pseudogenes	CYP4A11, CYP4A22, CYP4B1, CYP4F2, CYP4F3, CYP4F8, CYP4F11, CYP4F12, CYP4F22, CYP4V2, CYP4X1, CYP4Z1
CYP5	thromboxane synthase A ₂	1 subfamily, 1 gene	CYP5A1
CYP7	bile acid biosynthesis 7-alpha hydroxylase	2 subfamilies, 2 genes	CYP7A1, CYP7B1

²⁰ Nebert D.W. and Russell D.W.; Clinical importance of the cytochromes P450. *The Lancet*, 2002, 360, 1155-1162.

	of steroid nucleus		
CYP8	<i>varied</i>	2 subfamilies, 2 genes	CYP8A1 (prostacyclin synthase), CYP8B1 (bile acid biosynthesis)
CYP11	steroid biosynthesis	2 subfamilies, 3 genes	CYP11A1, CYP11B1, CYP11B2
CYP17	steroid biosynthesis, 17-alpha hydroxylase	1 subfamily, 1 gene	CYP17A1
CYP19	steroid biosynthesis: aromatase synthesizes oestrogen	1 subfamily, 1 gene	CYP19A1
CYP20	unknown function	1 subfamily, 1 gene	CYP20A1
CYP21	steroid biosynthesis	2 subfamilies, 2 genes, 1 pseudogene	CYP21A2
CYP24	vitamin D degradation	1 subfamily, 1 gene	CYP24A1
CYP26	retinoic acid hydroxylase	3 subfamilies, 3 genes	CYP26A1, CYP26B1, CYP26C1
CYP27	<i>varied</i>	3 subfamilies, 3 genes	CYP27A1 (bile acid biosynthesis), CYP27B1 (vitamin D3 1-alpha hydroxylase, activates vitamin D3), CYP27C1 (unknown function)
CYP39	7-alpha hydroxylation of 24-hydroxycholesterol	1 subfamily, 1 gene	CYP39A1

CYP46	cholesterol hydroxylase	24-	1 subfamily, 1 gene	CYP46A1
CYP51	cholesterol biosynthesis		1 subfamily, 1 gene, 3 pseudogenes	CYP51A1 (lanosterol 14-alpha demethylase)

The subfamilies CYP1A, CYP2C and CYP3A are the most predominant P450 enzymes in humans, representing 65 % of all cytochrome P450 enzymes in the liver. The CYP2A (8 %) subfamily as well as the CYP2D6 (4 %) and CYP2E1 (6 %) are also highly expressed in the human liver. All the other families are present in low concentration and together represent only 17 % of all P450 enzymes (Figure 1.2).

CYP3A4, which is involved in drug metabolism, is the most abundant of all the CYPs in the human liver²¹, and is known to metabolise more than 120 different drugs such as codeine, diazepam, erythromycin and taxol and is responsible for many drug interactions in humans²².

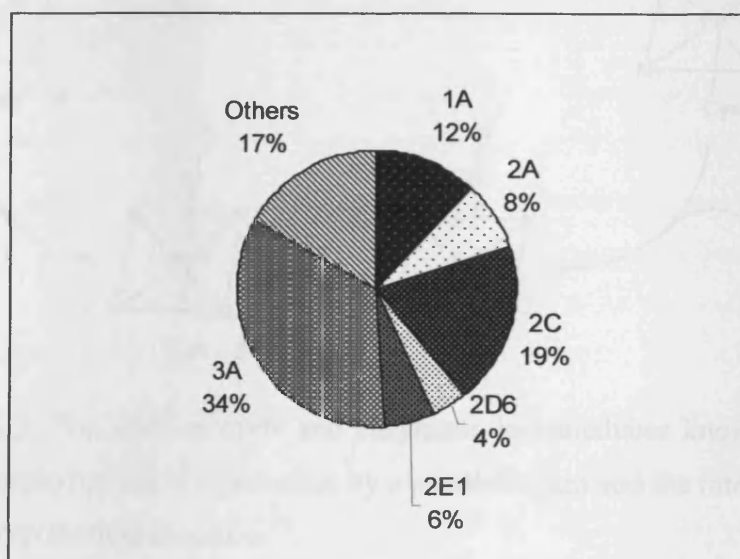


Figure 1.2: Distribution of P450 enzymes in human liver²³

²¹ Waxman D.J.; P450 gene induction by structurally diverse xenochemicals: central role of nuclear receptors CAR, PXR and PPAR. *Archiv. Biochem. Biophys.*, **1999**, 369, 11-23.

²² Kenworthy K.E., Bloomer J.C., Clarke S.E. and Houston J.B.; CYP3A4 drug interactions: correlation of 10 *in vitro* probe substrate. *Br. J. Clin. Pharmacol.*, **1999**, 48, 716-727.

²³ Guengerich F.P.; Human cytochrome P-450 enzymes; In: Ortiz de Montellano, P.R., Ed. *Cytochrome P450*; New York: Plenum Press, **1995**, 473-535.

1.2) Reactions catalysed by cytochrome P450 and catalytic cycle

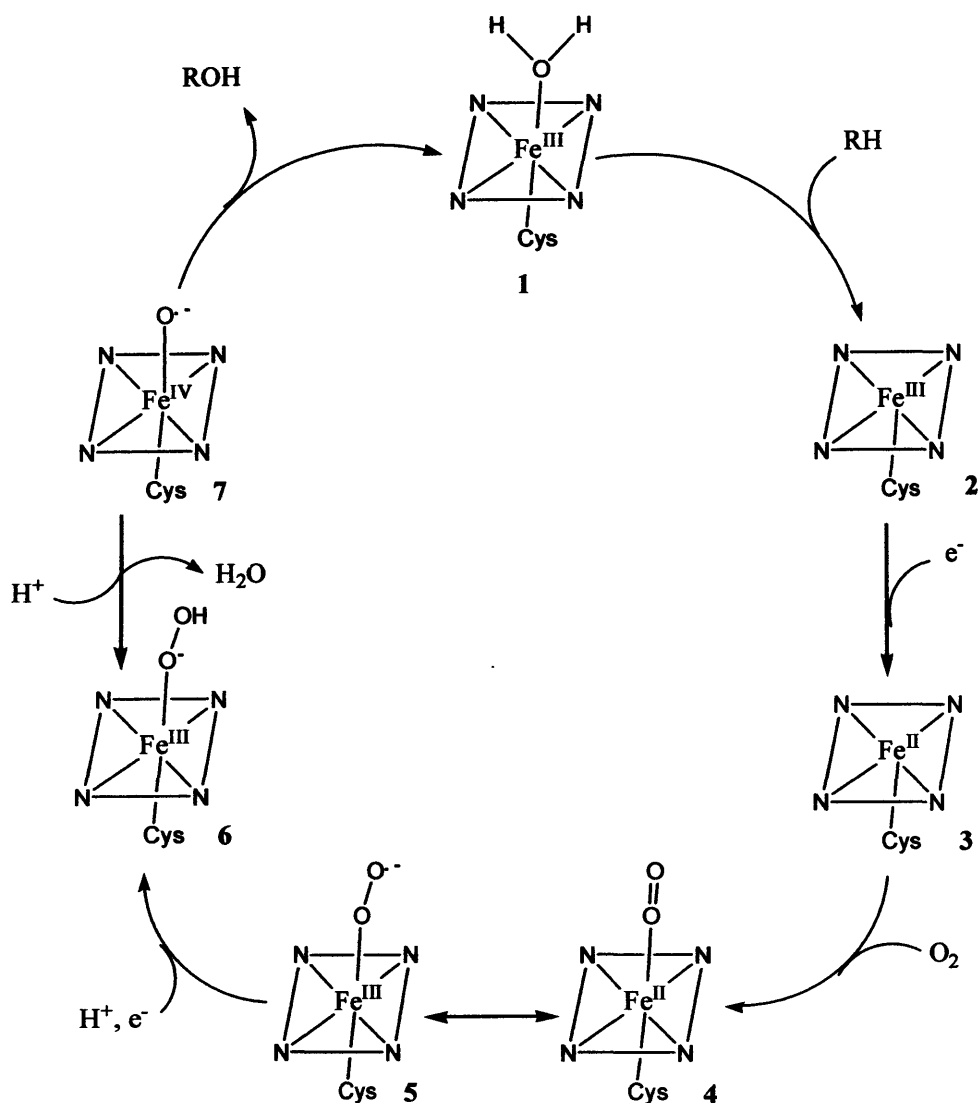
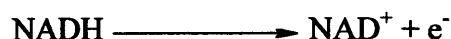


Figure 1.3: The reaction cycle and enzymatic intermediates known in P450 reactions; the porphyrin ring is represented by a parallelogram and the intermediate 6 and 7 are only hypothetical structures²⁴.

The catalytic cycle of cytochrome P450 is shown in Figure 1.3. In its resting state, the P450 enzyme generally exists as a hexacoordinate low-spin Fe^{III} species containing a water molecule *trans* to its cysteine ligand (1). Binding of a RH

²⁴ Van Vauwe J.P. and Janssen P.A.J.; Is there a case for P450 inhibitors in cancer treatment? *J. Med. Chem.*, 1989, 32, 2231-2239.

substrate in the protein site changes the haem system into a pentacoordinate Fe^{III} complex (2). Then, there is a reduction by an electron to give the pentacoordinated Fe^{II} high spin complex (3). This electron comes from the cofactor of the enzyme, which can be NADH or NADPH depending on the type of P450 system.



Then in the third step, the ferrous form of the enzyme combines with a molecule of oxygen to form a ferric-oxy intermediate (4), which can also be in its Fe^{III} mesomeric form 5. This is followed by a second reduction step that leads to a short-lived activated oxygen species. Protonation of the distal oxygen of 5 produces a hydroperoxo-iron complex (6), which can then be transformed after losing a water molecule into an activated iron-oxo complex (7). Finally the oxygen atom transfers from the iron-oxo complex to the substrate yielding the oxidised ROH product and the iron complex returns to its resting state.

Although mono-oxygenation of substrate is the main function of P450 enzymes, some other unusual catalytic functions such as oxidations involving C-C or C=N bond cleavage, dehydration, dehydrogenation or isomerisation have also been reported (Figures 1.4 and 1.6).²⁵ In some P450s, an oxidase type activity with the formation of O₂⁻, H₂O₂ and H₂O from reduction of O₂ could be observed²⁶. This is due to a partial decoupling between the electron transfer from NADPH to O₂ and the transfer of an oxygen atom to the substrate. Some P450s also have been found to be able to act as a peroxidase and catalyse the oxidative coupling of phenol²⁷. This involves the oxidation of the phenol function into its phenoxy radical, followed by coupling of two of these radicals. Dehydrogenation of alkane CH-CH bonds and

²⁵ Mansuy D.; The great diversity of reactions catalysed by cytochromes P450. *Comp. Biochem. Biophys. C*, 1998, 121, 5-14.

²⁶ Bast A., Brenninkmeijer J.W., Savenije-Chapel E.M. and Noordhoek J.; Cytochrome P450 oxidase activity and its role in NADPH dependent lipid peroxidation. *FEBS Lett.*, 1983, 151, 185-188.

²⁷ Stadler R. and Zenk M.H.; The purification and characterization of a unique cytochrome P450 enzyme from *Berberis stolonifera* plant cell cultures. *J. Biol. Chem.*, 1993, 268, 823-831.

formation of the corresponding double bond have also been observed with some substrates such as testosterone, valproic acid and lovastatin²⁸.

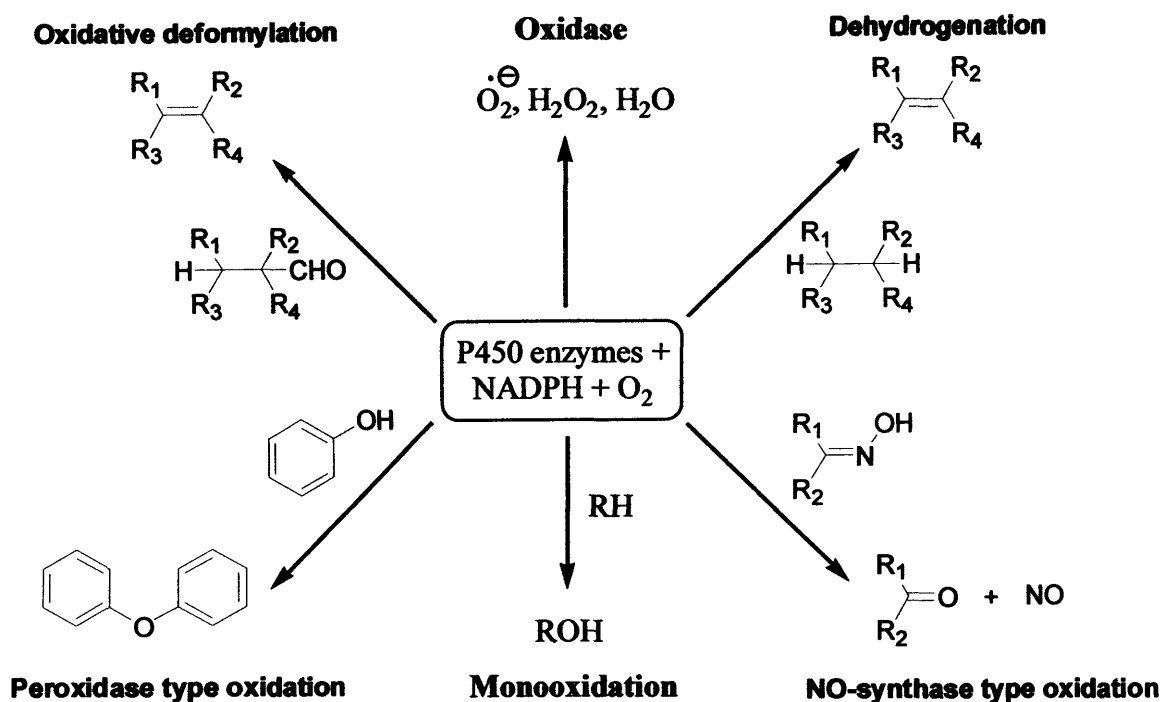


Figure 1.4: Atypical oxidation reactions catalysed by cytochrome P450²⁵

The cleavage of a C-C bond *via* oxidative deformylation has also been proven. A good example is the oxidative demethylation observed with P450 aromatase which is responsible for the last step of the biosynthesis of oestrone (Figure 1.5). The oxidative cleavage of C=N-OH bond can also be achieved using P450 enzymes. This non-classical monooxygenation has been found to be catalysed by liver microsomal P450s²⁹.

P450 enzymes are also able to catalyse non-oxidative reactions (Figure 1.6). Two particular P450s, prostacyclin synthase (CYP8A1) and thromboxane synthase (CYP5A1) are able to act as an isomerase catalysing the formation of prostacyclin

²⁸ Mansuy D. and Renaud J.P.; Heme-thiolate proteins different from cytochrome P450 catalysing monooxygenations; In: Ortiz de Montellano, P.R., Ed. *Cytochrome P450: structure, mechanism and biochemistry*; New York: Plenum Press, 1995, 537-574.

²⁹ Andronik-Lion V., Boucher J.L., Delaforge M., Henry Y. and Mansuy D.; Formation of nitric oxide by cytochrome P450-catalysed oxidation of aromatic amidoximes. *Biochem. Biophys. Res. Commun.*, 1992, 185, 452-458.

and thromboxane through isomerisation of prostaglandin H₂^{30, 31}. Several P450s are also able to catalyse the reduction of azo-compounds, nitroaromatics, polyhalogenated compounds, tertiary amine, *N*-oxides and arene oxide³². This is due to the ability of the Fe(II) intermediate in the catalytic cycle to transfer an electron to substrates other than O₂ containing electron-accepting properties²⁵. Dehydration of substrate is also a possible function of P450 enzymes, and can occur on two forms: the conversion of hydroperoxides into allenes oxide³³ and the transformation of aldoximes into nitriles³⁴. In both cases, the reaction is catalysed by the reduced Fe(II) species and does not require any reducing agent.

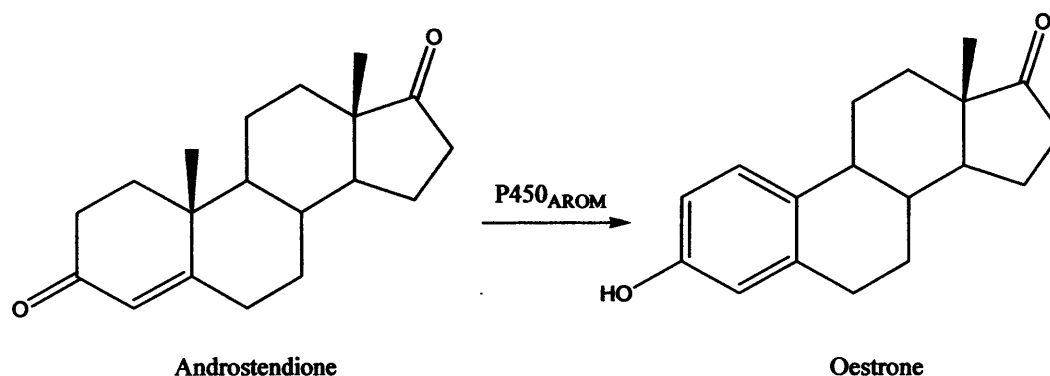


Figure 1.5: Transformation of androgens to oestrogens catalysed by the P450 aromatase enzyme, CYP19 (P450_{AROM}).

The ability of the cytochrome P450 haem iron to exist under different oxidation states with different reactivity is one of the main causes of the great diversity of reactions catalysed by P450 enzymes³⁵.

³⁰ Wang L.H., Tsai A.L. and Hsu P.Y.; Substrate binding is the rate limiting step in thromboxane synthase catalysis. *J. Biol. Chem.*, **2001**, *276*, 14737-14743.

³¹ Chiang C.W., Yeh H.C., Wang L.H. and Chan N.L.; Crystal structure of the human prostacyclin synthase. *J. Mol. Biol.*, **2006**, *364*, 266-274.

³² Mansuy D., Battioni P. and Battioni J.P.; Chemical model systems for drug -metabolizing cytochrome P450-dependant monooxygenase. *Eur. J. Biochem.*, **1989**, *184*, 267-285.

³³ Song W.C. and Brach A.R.; Purification of an allene oxide synthase and identification of the enzyme as a cytochrome P450. *Science*, **1991**, *253*, 781-784.

³⁴ De Master E.G., Shirota F.N. and Nagasawa H.T.; A Beckmann-type dehydration of *n*-butyraldoxime catalysed by cytochrome P450. *J. Org. Chem.*, **1992**, *57*, 5074-5075.

³⁵ Pylypenko O. and Schlichting I.; Structural aspects of ligand binding to and electron transfer in bacterial and fungal P450s. *Ann. Rev. Biochem.*, **2004**, *73*, 991-1018.

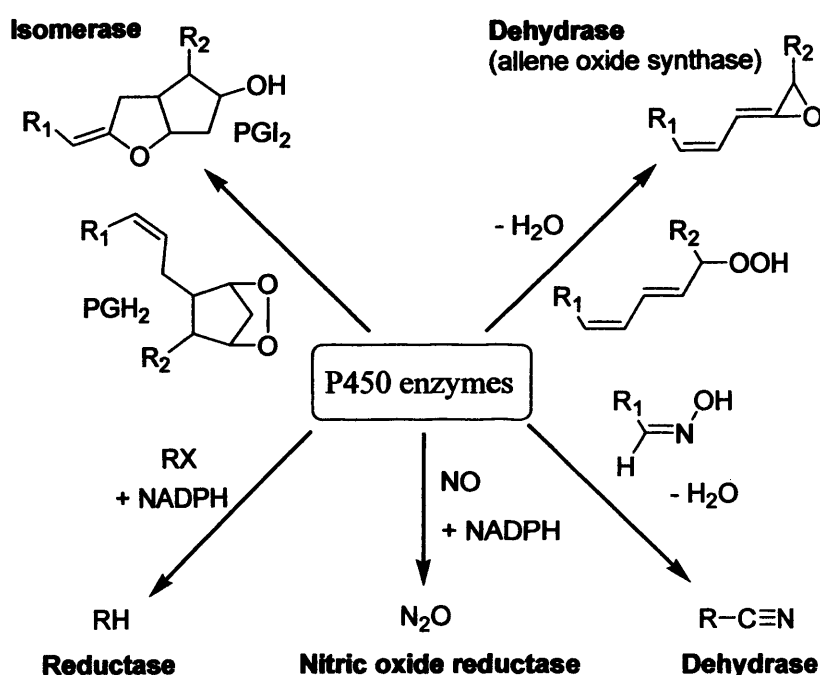


Figure 1.6: Non oxidative reactions catalysed by cytochrome P450²⁵.

1.3) Specific target: the CYP26 enzymes

1.3.1) Retinoid family

Retinoids are chemically derived from vitamin A, including natural metabolites and synthetic analogues. Provitamin A (carotenoids) from vegetables (carrots, spinach and broccoli) and retinyl esters from animal origin are the main sources of vitamin A³⁶. Carotenoids are converted into retinol after a central oxidative cleavage in the intestine and then a reduction to retinol. Conversely, lipases or esterases from the intestine hydrolyse the retinyl esters into retinol³⁷. Then, in the body retinol is converted into retinaldehyde (RAL) and retinoic acids (RAs). Cytochrome P450 enzymes (CYPs 1A1, 1A2 and 3A4 particularly) are responsible

³⁶ Underwood B.A. and Arthur P.; The contribution of vitamin A to public health. *FASEB*, 1996, 10, 1040-1048.

³⁷ Curley R.W. and Robarge M.J.; Retinoid structure, chemistry and biologically active derivatives. In G.V. S. (Ed). *Retinoids: their physiological function and therapeutic potential*, 1997, JAI Press Inc, London, 1-34.

for the metabolism of retinaldehyde to ATRA in human³⁸. Then, retinoic acids are hydroxylated to 4-hydroxy all-*trans* retinoic acid and more polar metabolites (Figure 1.7).

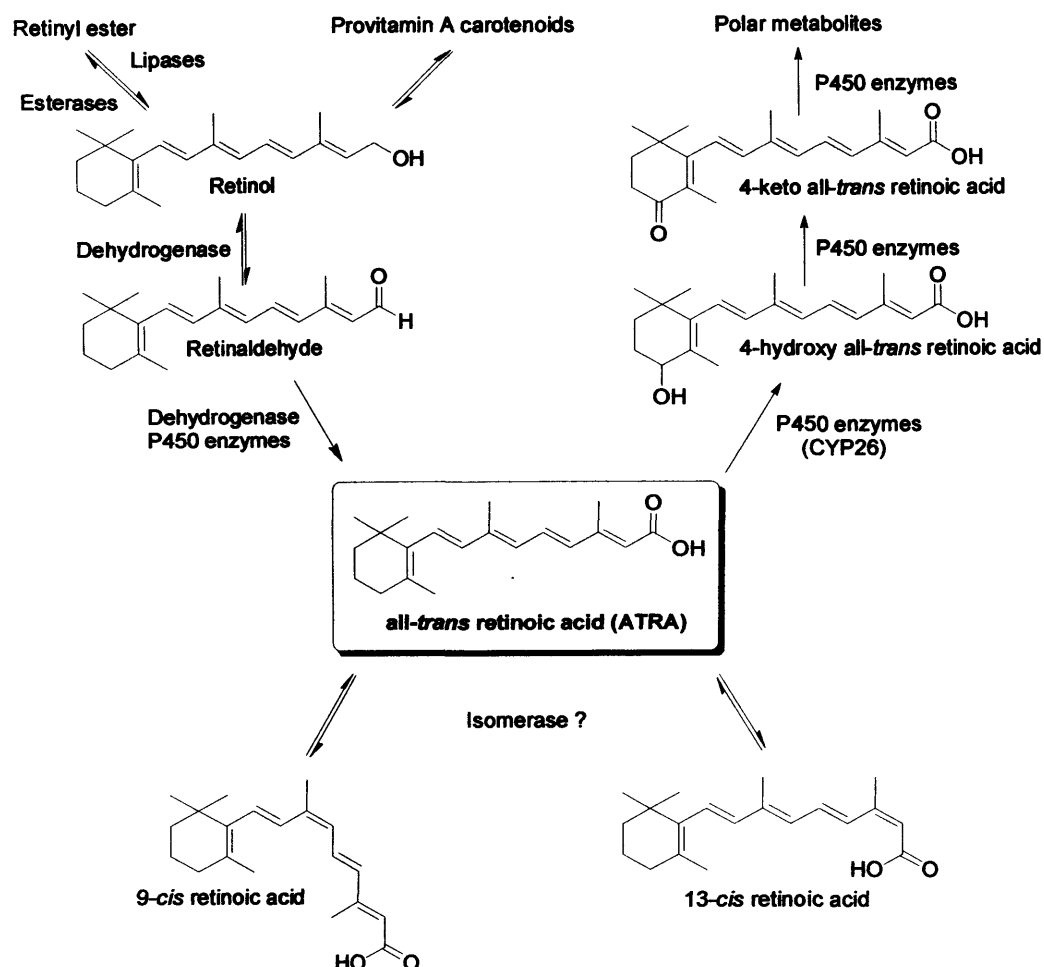


Figure 1.7: Biosynthesis and metabolism of all-*trans* retinoic acid.

RAs are the most interesting compounds; they play an important role in development, differentiation and homeostasis in our body³⁹. There are three major forms: all-*trans*-retinoic acid (ATRA) and its two isomeric forms 9-*cis*-retinoic acid (9-*cis*-RA) and 13-*cis*-retinoic acid (13-*cis*-RA) (Figure 1.8). The temperature-dependent interconversion of these transformations suggests that they may be

³⁸ Zhang Q.Y., Dunbar D. and Kaminsky L.; Human cytochrome P450 metabolism of retinals to retinoic acids. *Drug Met. Dispo.*, 2000, 28, 292-297.

³⁹ Chambon P.; A decade of molecular biology of retinoic acid receptors. *FASEB*, 1996, 10, 940-954.

catalysed by an isomerase^{40,41}, but no specific retinoid isomerase has been identified yet (Figure 1.7).

1.3.2) General mode of action of retinoic acid

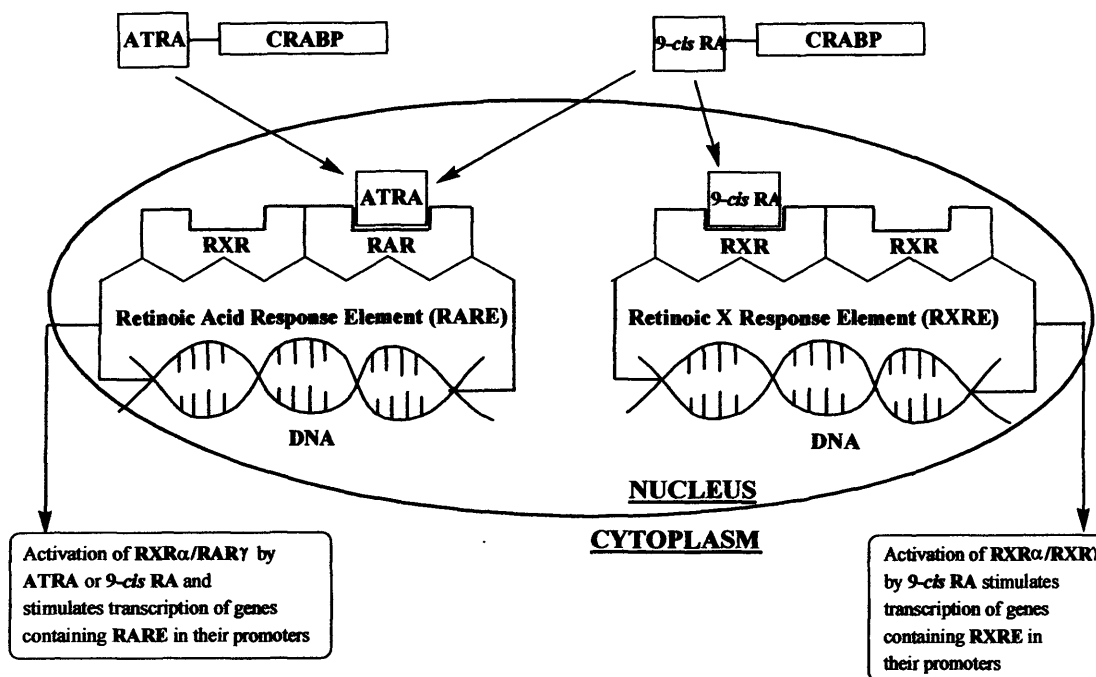


Figure 1.8: The bonding of ATRA and 9-cis RA to the RAR and RXR nuclear receptor respectively in the nucleus.

Retinoids are small hydrophobic molecules and are able to cross biological membranes and enter cells where they can bind to specific receptors³⁷. These receptors are divided into two sub-families: the retinoic acid receptors (RARs) and the retinoid X receptors (RXRs). Each receptor is composed of three subtypes (α , β , γ). The RAR family is activated by both ATRA and 9-cis RA⁴² whereas the RXR

⁴⁰ Chen H. and Juchau M.R.; Biotransformation of 13-cis- and 9-cis-retinoic acid to all-trans-retinoic acid in rat conceptual homogenates. *Drug Met. Dispo.*, 1998, 26, 222-228.

⁴¹ Giguere V.; Retinoic acid receptors and cellular retinoid binding proteins: complex interplay in retinoid signaling. *Endocrin. Rev.*, 1994, 15, 61-79.

⁴² Mangelsdorf D.J., Thummel C., Beato M., Herrlich P., Schutz G., Umenoso K., Blumberg B., Kastner P., Mark M., Chambon P. and Evans R.M.; The nuclear receptor superfamily – the 2nd decade. *Cell*, 1995, 83, 835-839.

family is activated only by 9-*cis* RA⁴³ (Figure 1.8). The binding of other ATRA stereoisomers e.g. 13-*cis* RA is still unclear; however the reported antitumour efficacy of 13-*cis* RA⁴⁴, suggest that 13-*cis*-RA is isomerised intracellularly to ATRA or 9-*cis*-RA or acts without obvious interaction with the known retinoid receptors^{45, 46}.

Most of the action of retinoids is due to their binding to the RAR site of the RAR/RXR heterodimer, RXR being the silent partner, as it is not able to activate the RAR/RXR heterodimer on its own. However it has been shown that binding of a ligand to the RXR allosterically improves the potencies of the RAR ligands⁴⁷. These receptors (heterodimer RAR/RXR or homodimer RXR/RXR) bind to DNA as RA-inducible transcriptional regulatory proteins in the RAREs (retinoic acid response elements) or RXREs (retinoid X response elements) regions^{39, 48}.

In the absence of ligand, the RAR/RXR heterodimer binds to the RARE and complex with a corepressor protein such as nuclear receptor corepressor (NCoR) and/or silencing mediator for retinoid and thyroid receptors (SMRT)⁴⁷. These corepressors by recruiting histone deacetylases which catalyse the removal of acyl group from lysine residues cause DNA to be inaccessible to the transcriptional machinery⁴⁹. On the other hand, binding of ATRA or an agonist to the RAR result in a conformational change which lead to dissociation of the corepressor and recruitment of a coactivator protein⁵⁰ which in turn promotes transcriptional activation by interacting directly with the basal transcriptional activation or by

⁴³ Heyman R.A., Mangelsdorf D.J., Dyck J.A., Stein R.B., Eichele G., Evans R.M. and Thaller C.; 9-*cis* retinoic acid is a high affinity ligand for the retinoid X receptor. *Cell*, 1992, 68, 397-406.

⁴⁴ Stearns M.E., Wang M. and Fudge K.; Liarozole and 13-*cis*-retinoic acid anti-prostatic tumor activity. *Cancer Res.*, 1993, 53, 3073-3077.

⁴⁵ Njar V.C.O., Gediya L., Purushottamachar P., Chopra P., Vasaitis T.S., Khandelwal A., Mehta J., Huynh C., Belosay A. and Patel J.; Retinoic acid metabolism blocking agent (RAMBAs) for treatment of cancer and dermatological diseases. *Bioorg. Med. Chem.*, 2006, 14, 4323-4340.

⁴⁶ Armstrong J.L., Redfern C.P.F. and Veal G.J.; 13-*cis* retinoic acid and isomerisation in paediatric oncology-is changing shape the key to success? *Biochem. Pharm.*, 2005, 69, 1299-1306.

⁴⁷ Kurokawa R., Soderstrom M., Horlein A., Halachmi S., Brown M., Rosenfeld M.G. and Glass C.K.; Polarity-specific activities of retinoic acid receptors determined by a co-repressor. *Nature*, 1995, 377, 451-454.

⁴⁸ Altuchi L. and Gronemeyer H.; The promise of retinoids to fight cancer. *Nat. Rev. Cancer*, 2001, 1, 181-193.

⁴⁹ Loinder K. and Soderstrom M.; The nuclear corepressor (NCoR) modulates basal and activated transcription of genes controlled by retinoic acid. *J. Steroid. Biochem. Mol. Biol.*, 2003, 84, 15-21.

⁵⁰ Pogenberg V., Guichou J.F., Vivat-Hannah V., Kammerer S., Perez E., Germain P., De Lera A.R., Gronemeyer H., Royer C.A. and Bourguet W.; Characterization of the interaction between retinoic acid receptor/retinoid X receptor (RAR/RXR) heterodimers and transcriptional coactivators through structural and fluorescence anisotropy studies. *J. Biol. Chem.*, 2005, 280, 1625-1633.

encoding histone acetyl transferase activity (HAT) which causes chromatin to relax and increases the access to DNA⁵¹.

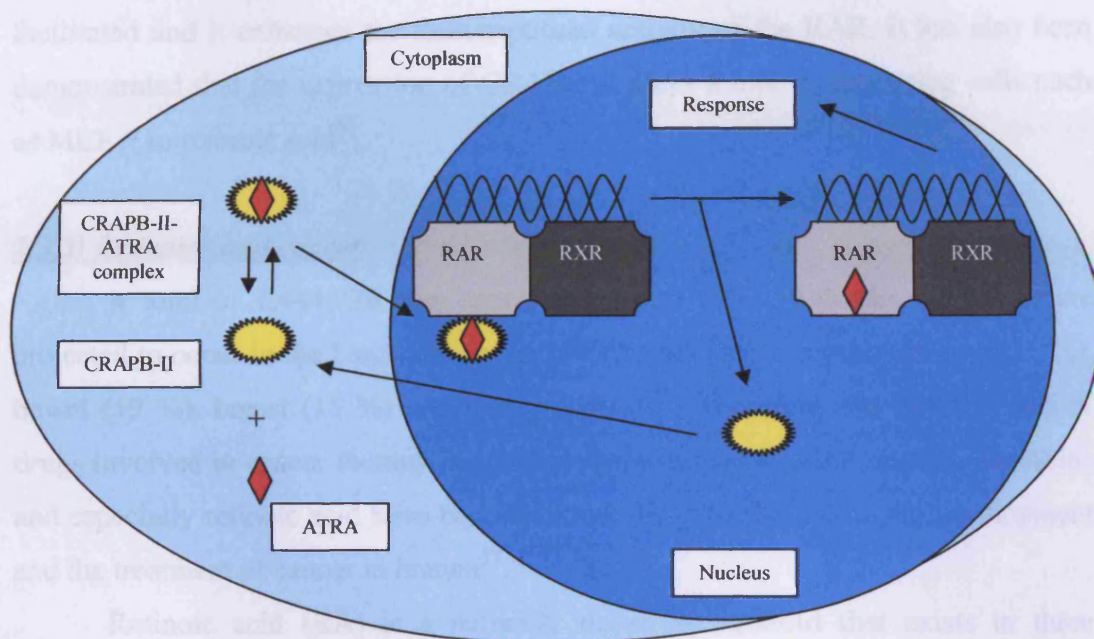


Figure 1.9: Mechanism of action of the cellular retinoic acid binding protein II (CRABP II)³³.

Two binding proteins, CRABP I and CRABP II (cellular retinoic acid-binding proteins I and II) are also involved in the mechanism of actions of ATRA. Their role is to solubilise and stabilise retinoic acid in aqueous milieu and then to transport it in different compartments of the cell⁵². Although they are very similar, the two isoforms of CRABP serve different functions in the cell. This might be due to their different binding affinity with retinoic acid⁵³. CRABP I has been shown to moderate the cellular response to ATRA by facilitating its catabolism. The retinoic acid bound

⁵¹ Dilworth F.J., Fromental-Ramain C., Remboutsika E., Benecke A. and Chambon P.; Ligand-dependant activation of transcription *in vitro* by retinoic acid receptor α /retinoid X receptor α heterodimers that mimics transactivation by retinoids *in vitro*. *Proc. Natl. Acad. Sci. USA*, **1999**, *96*, 1995-2000.

⁵² Noy N.; Retinoid-binding protein: mediators of retinoid action. *Biochem. J.*, **2000**, *348*, 481-495.

⁵³ Norris A.W., cheng L., Giguere V., Rosenberger M. and Li E.; Measurement of subnanomolar retinoic acid binding affinities for cellular retinoic acid binding proteins by fluorometric titration. *Biochim. Biophys. Acta*, **1994**, *1209*, 10-18.

to CRABP I is metabolised by CYP26 enzymes resulting in the formation of more polar metabolites⁵⁴. While CRABP I acts as a passive vehicle which binds and release its ligand, CRABP II delivers retinoic acid to the RAR in a direct collisional process³⁹ (Figure 1.9). As a result, the ligation of the RAR by retinoic acid is facilitated and it enhances the transcriptional activity of the RAR. It has also been demonstrated that the expression of CRABP II plays a role in sensitising cells such as MCF-7 to retinoic acid⁵⁵.

1.3.3) Retinoids and cancer

A total of 1,444,920 new cancer cases and 589,650 deaths for cancer are projected to occur in the United States in 2007⁵⁶. The most common are lung (31 %), bowel (19 %), breast (15 %) and prostate (9 %)⁵⁶. Therefore, the development of drugs involved in cancer therapy and chemoprevention is of main interest. Retinoids and especially retinoic acid have been known to be associated with the development and the treatment of cancer in human⁵⁷.

Retinoic acid (RA) is a naturally occurring retinoid that exists in three isomeric forms: *all-trans*-RA (ATRA), *9-cis*-RA (9cRA) and *13-cis*-RA (13cRA) (Table 1.2). Retinoic acid is an essential regulator of embryogenesis, high concentrations of retinoic acid has shown to be teratogenic (capable of causing malformation in the embryo), while insufficient vitamin A concentration can also cause severe malformation⁴⁸.

RA is commonly used as a therapeutic treatment for dermatological disease such as acne, psoriasis and ichthyosis^{58, 59} (Table 1.2). However side effects such as skin irritation constitute a limit to their prolonged use⁶⁰.

⁵⁴ Fujii H., Sato T., Kaneko S., Gotoh O., Fujii-Kuriyama Y., Osawa K., Kato S. and Hamada H.; Metabolic inactivation of retinoic acid by a novel P450 differentially expressed in developing mouse embryos. *EMBO J.*, 1997, 16, 4163-4173.

⁵⁵ Manor D., Schmidt E.N., Budhu A., Flesken-Nikitin A., Zgola M., Page R., Nikitin Y.A. and Noy N.; Mammary carcinoma suppression by cellular retinoic acid binding protein II. *Cancer Res.*, 2003, 63, 4426-4433.

⁵⁶ Jemal A., Siegel R., Ward E., Murray T., Xu J. and Thun M.J.; Cancer statistics, 2007. *CA Cancer J. Clin.*, 2007, 57, 43-66.

⁵⁷ Zanardi S., Serrano D., Argusti A., Barile M., Puntoni M. and Decensi A.; Clinical trials with retinoids for breast cancer prevention. *Endocrin. Rel. Cancer*, 2006, 13, 51-68.

⁵⁸ Kuijpers A.L., Van Pelt P.T., Bergers M., Boegeheim P.J., Den Bakker J.E., Siegenthaler G., Van der Kerkhof P.C. and Achalkwijk J.; The effects of oral liarozole on epidermal proliferation and differentiation in severe plaque psoriasis are comparable with those of acitretin. *Br. J. Dermatol.*, 1998, 139, 380-389.

ATRA has been proven to be an effective treatment in cancer chemoprevention and in differentiation therapy of cancer. Clinical studies have shown the efficacy of RA in reversing human premalignant lesions and in the prevention of primary tumour of head and neck, liver, skin and breast cancer^{61, 62}. Retinoids have also been known to have anti-proliferative effects on the growth of various tumour cells *in vitro*, including prostate cancer (LNCap)⁶³, breast carcinoma (MCF-7, ZR-75.1)⁶⁴ and human leukaemia cells (HL60)⁶⁵. The most impressive effect of ATRA therapy has been observed in the treatment of acute promyelocytic leukaemia (APL) for which a complete remission was observed with high dose of ATRA^{66, 67} (Table 1.2).

The two others stereoisomers 13-*cis*-RA (Isotretinoin) and 9-*cis*-RA (Alitretinoin) are also used clinically for the treatment of dermatologic diseases such as acne⁵⁸, psoriasis⁵⁹ and also in the treatment of APL⁶⁶ and Kaposi's sarcoma (KS)⁶⁸ (Table 1.2).

⁵⁹ Thacher S.M., Vasudenvan J., Tsang K.Y., Nagpal S. and Chandraratna R.A.S.; New dermatological agents for the treatment of psoriasis. *J. Med. Chem.*, 2001, 44, 281-297.

⁶⁰ Esgleyes-Ribot T., Chandraratna R.A.S., Lew-Kaya D.A., Sefton J. and Duvic M.; Response of psoriasis to a new topical retinoid, AGN 190168. *J. Am. Acad. Dermatol.*, 1994, 30, 581-590.

⁶¹ Sun S.Y. and Lotan R.; Retinoids and their receptors in cancer development and chemoprevention. *Crit. Rev. Oncol. Hematol.*, 2002, 41, 41-55.

⁶² Miller W.H.; The emerging role of retinoids and retinoic acid metabolism blocking agents in the treatment of cancer. *Cancer*, 1998, 83, 1471-1482.

⁶³ Shen J.C., Wang T.T., Chang S. and Hursting S.D.; Mechanistic studies of the effects of the retinoid *N*-(4-hydroxyphenyl)retinamide on prostate cancer cell growth and apoptosis. *Mol. Carcinogen.*, 1999, 281, 1598-1604.

⁶⁴ Van Heusden J., Wouters W., Ramakaers F.C.S., Krekels M.D.W.G., Dillen L., Borgers M. and Smets G.; The anti-proliferative activity of ATRA catabolites and isomers is differentially modulated by liarazole-fumarate in MCF-7 human breast cancer cells. *Br. J. Cancer*, 1998, 77, 1229-1235.

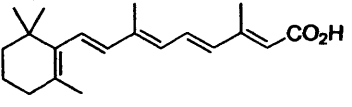
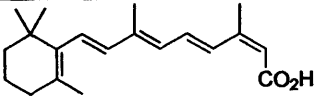
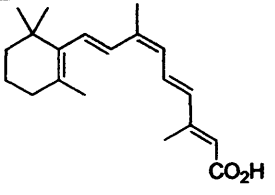
⁶⁵ Fontana J.A., Dawson M.I., Leid M., Rishi A.K., Zhang Y., Hsu C.A., Lu J.S., Peterson V.J., Jong L., Hobbs P., Chao W.R., Shroot B. and Reichert U.; Identification of a unique binding protein specific for a novel retinoid inducing cellular apoptosis. *Int. J. Cancer*, 2000, 86, 474-479.

⁶⁶ Huang M., Ye Y., Chen S., Chai J., Lu J., Zhou L., Gu L. and Wang Z.; Use of all-*trans*-retinoic acid in the treatment of acute promyelocytic leukaemia. *Blood*, 1988, 72, 567-572.

⁶⁷ Witcher M. and Miller W.H. Jr; Cytokine and retinoic acid therapy for APL: new tricks from an old combination. *Leukemia Res.*, 2004, 28, 447-448.

⁶⁸ Guo W.X., Gill P.S. and Antakly T.; Inhibition of AIDS-Kaposi's sarcoma cell proliferation following retinoic acid receptor activation. *Cancer Res.*, 1995, 55, 823-829.

Table 1.2: Structure and therapeutic application of retinoic acid isomers used clinically

Retinoid	Structure	Target	Application
Tretinoin (ATRA)		RAR agonist	APL, Acne
Isotretinoin (13- <i>cis</i> -RA)		RAR agonist	Acne
Alitretinoin (9- <i>cis</i> -RA)		RAR and RXR agonist	Psoriasis, APL, KS

Despite the anti-cancer properties of RA, its use in the therapy of human cancer in the clinic has been quite disappointing⁶⁹. The metabolism and catabolism of RA by P450 enzymes seem to be the cause of its reduced therapeutic effects⁷⁰. Although few P450 enzymes are known to be involved in retinoid metabolism⁷¹ (CYP2C8, CYP3A4, CYP2C9 and CYP26), the CYP26 is the only of these enzymes to have a high specificity for RA⁷².

1.3.4) Role of CYP26

CYP26 is membrane bound and is located in the endoplasmic reticulum, it is found in highest levels in adult liver, heart, pituitary gland, adrenal gland, testis, duodenum, colon, placenta and regions of the brain^{73, 74}. Studies by Taimi *et al.*⁷⁵

⁶⁹ Trump D.L., Smith D.C., Stiff D., Adedoyin A., Day R., Banhson R.R., Hofacker J. and Branch R.A.; A phase II trial of all-*trans*-retinoic acid in hormone-refractory prostate cancer: a clinical trial with detailed pharmacokinetic analysis. *Cancer Chem. Pharm.*, 1997, 39, 349-356.

⁷⁰ Huynh C.K., Brodie A.M.H. and Njar V.C.O.; Inhibitory effects of retinoic acid metabolism blocking agents (RAMBAs) on the growth of human prostate cancer cells and LNCaP prostate tumour xenografts in SCID mice. *Br. J. Cancer*, 2006, 94, 513-523.

⁷¹ Marill J., Cresteil T., Lanotte M. and Chabot G.G.; Identification of human cytochrome P450s involved in the formation of all-*trans*-retinoic acid principal metabolites. *Mol. Pharmacol.*, 2000, 58, 1341-1348.

⁷² Njar V.C.O.; Cytochrome P450 retinoic acid 4-hydroxylase inhibitors: potential agents for cancer therapy. *Min. Rev. Med. Chem.*, 2002, 2, 261-269.

⁷³ Ray W.J., Bain G., Yao M. and Gottlieb D.I.; CYP26 a novel mammalian cytochrome P450, is induced by retinoic acid and defines a new family. *J. Biol. Chem.*, 1997, 272, 18702-18708.

⁷⁴ Lampen A., Meyer S. and Nau H.; Effects of receptor-selective retinoids on CYP26 gene expression and metabolism of all-*trans*-retinoic acid in intestinal cells. *Drug Met. Dispo.*, 2001, 29, 742-747.

showed the existence of three different types of CYP26: CYP26A1, CYP26B1 and CYP26C1. More recently, a fourth CYP26 enzyme CYP26D1 has also been identified in zebrafish⁷⁶.

CYP26 plays a key role in retinoic acid metabolism. It acts on retinoids, including all-*trans*-retinoic acid (ATRA) and its stereoisomer 9-*cis*-retinoic acid (9-*cis*-RA) and 13-*cis*-retinoic acid (13-*cis*-RA) (Figure 1.7), capable of both 4-hydroxylation and 18-hydroxylation responsible for the generation of several hydroxylated forms of retinoic acid, including 4-hydroxy-retinoic acid, 4-oxo-retinoic acid and 18-hydroxy-retinoic acid (Figure 1.7). These enzymes exhibit a high degree of specificity for ATRA (ATRA>>>9-*cis*-RA>13-*cis*-RA>retinaldehyde>retinol)⁷⁷. However CYP26C1, which shares many similarities with the other member of its family CYP26A1 and CYP26B1, is also able to metabolise the ATRA stereoisomer 9-*cis*-RA⁷⁵. The role of the CYP26 enzymes is to regulate the level of intracellular ATRA in the body and to protect tissues from inappropriate level of ATRA⁷⁸.

Induction of CYP26 enzyme by ATRA has been observed in a large number of normal and cancer cells such as MCF-7, T47D, NB4, HepG2, HPK1A and LNCaP⁴⁵. An inappropriate metabolism of ATRA by CYP26 is also related to some dermatological diseases such as acne, psoriasis and ichthyosis⁷⁹.

CYP26 enzymes are involved in the regulation of both normal and therapeutic level of ATRA. They may also be involved in the limited effect of retinoic acid treatment observed in the clinic. Inhibition of these enzymes would consequently lead to an increase in the level of endogenous and co-administered ATRA. The development of retinoic acid metabolism blocking agents (RAMBAs) or

⁷⁵ Taimi M., Helvig C., Wisniewski J., Ramshaw H., White J., Amad M., Korczak B. and Petkovich M.; A novel human cytochrome P450 CYP26C1, involved in metabolism of 9-*cis* and all-*trans* isomers of retinoic acid. *J. Biol. Chem.*, 2004, 279, 77-85.

⁷⁶ Gu X., Xu F., Song W., Wang X., Hu P., Yang Y., Gao X. and Zao Q.; A novel cytochrome P450, zebrafish Cyp26D1, is involved in the metabolism of all-*trans*-retinoic acid. *Mol. Endo.*, 2006, 20, 1661-1672.

⁷⁷ Sonneveld E., Van den Brink C.E., Van der Leede B.J.M., Schulkes R.K.A.M., Petkovic M., Van der Burgh B. and Van der Saag P.T.; Human retinoic acid (RA) 4-hydroxylase (CYP26) is highly specific for all-*trans*-RA and can be induced through RA receptors in human breast and colon carcinoma cells. *Cell Growth Differ.*, 1998, 9, 629-637.

⁷⁸ Perlmann T.; Retinoids metabolism: a balancing act. *Nature Gen.*, 2002, 31, 7-8.

⁷⁹ Orfanos C.E., Zouboulis C.C., Almond-Roestler B. and Geilen C.C.; Current use and future potential role of retinoids in dermatology. *Drugs*, 1997, 53, 358-388.

CYP26 inhibitors thus emerged as a good therapy for cancer chemoprevention or treatment and dermatological disease.

1.3.5) Known CYP26 inhibitors or retinoic acid metabolism blocking agents (RAMBAs)

The development of retinoic acid metabolism blocking agents (RAMBAs) has been a major subject of research in the past 20 years resulting in an important number of drugs.

(a) Liarozole (LiazalTM) and ketoconazole

Well established inhibitors are the two imidazole compounds: ketoconazole⁸⁰ and liarozole⁸¹ (Figure 1.10).

Ketoconazole was one of the first oral treatments for fungal infections and is still sold as an anti-dandruff shampoo branded Nizoral® by Janssen Pharmaceutica⁸². It is also well-known to be an efficient inhibitor of some P450 enzymes including CYP26⁸³. However it has a poor activity with an IC₅₀ of 18 µM and a very poor selectivity for CYP26⁸⁴.

Liarozole displayed an IC₅₀ of 6 µM for CYP26 inhibition⁸¹ and has also been proven to be a potent inhibitor of CYP17 (IC₅₀= 260 nM) and CYP19^{85, 86}. Liarozole remains the only RAMBA so far to have been evaluated clinically for cancer and dermatological diseases.

⁸⁰ Heeres J., Backx L.J., Mostmans J.H. and Van Cutsem J.; Antimycotic imidazoles. Part 4. Synthesis and antifungal activity of ketoconazole, a new potent orally active broad-spectrum antifungal agent. *J. Med. Chem.*, 1979, 22, 1003-1005.

⁸¹ Freyne E., Raemackers A., Venet M., Sanz G., Wouters W., De Coster R. and Van Wauwe J.; Synthesis of LIAZALTM, a retinoic acid metabolism blocking agent (RAMBA) with potential clinical applications in oncology and dermatology. *Bioorg. Med. Chem. Lett.*, 1998, 8, 267-272.

⁸² Bulmer A.C. and Bulmer G.S.; The antifungal action of dandruff shampoo. *Mycopathologia*, 1999, 147, 63-65.

⁸³ Van Wauwe J.P., Coene M.C., Goosens J., Van Nigen G., Cools W. and Lauwers W.; Ketoconazole inhibits the in vitro and in vivo metabolism of all-trans-retinoic acid. *J. Pharm. Exp. Ther.*, 1988, 245, 718-722.

⁸⁴ Yee S.W. and Simons C.; Synthesis and CYP24 inhibitory activity of 2-substituted-3,4-dihydro-2H-naphthalen-1-one (tetralones) derivatives. *Bioorg. Med. Chem. Lett.*, 2004, 14, 5651-5654.

⁸⁵ Leze M.P., Le Borgne M., Marchand P., Loquet D., Kogler M., Le Baut G., Paluszczak A. and Hartmann R.W.; 2- and 3-[(aryl)(azolyl)methyl]indoles as potential non-steroidal aromatase inhibitor. *J. Enz. Inhib. Med. Chem.*, 2004, 19, 549-557.

⁸⁶ Van Ginckel R., De Coster R., Wouters W., Vanherck W., Van der Veer R., Goeminne N., Jagers E., Van Canteren H., Wouters L., Distelmans W. and Janssen P.; Antitumoral effects of R75251 on the growth of transplantable R3327 prostatic adenocarcinoma in rats. *Prostate*, 1990, 16, 313-323.

Anti-tumour activity has been observed in the treatment of prostate cancer in immunodepressed mice⁸⁷ and in rat prostate carcinoma⁴⁴. It has also shown *in vivo* anti-tumour activity for breast cancer therapy⁸⁸. These studies also revealed that the anti-tumour properties of liarozole were correlated to its inhibition of ATRA metabolism. Studies have shown that treatment with liarozole will increase the level of endogenous ATRA⁸⁹ and also increase the half-life of exogenous administered ATRA⁹⁰.

As a result, liarozole progressed to a phase III clinical trial for prostate cancer⁹¹. The study showed that liarozole was efficient in improving life expectancy, pain reduction and maintaining the quality of life of patients and was therefore a good treatment for prostate cancer.

However, despite these very encouraging results in preclinical and clinical studies, side effects due its lack of CYP specificity and moderate potency in CYP26 inhibition appeared to be a strong limitation for its use in cancer therapy. Consequently, the clinical development of liarozole has been stopped⁹².

⁸⁷ Smets G., Van Ginckel R., Daneels G., Moeremans M., Van Wauwe J., Coene M.C., Romarehers F.C., Schalken J.A., Borgers M. and De Coster R.; Liarozole, an antitumor drug, modulates cytokeratin expression in the dunning AT-6sq prostatic carcinoma through in situ accumulation of all-trans retinoic acid. *Prostate*, 1995, 27, 129-140.

⁸⁸ Goss P.E., Strasser K., Marques R., Clemons M., Oza A., Goel R., Blackstein M., Kaizer L., Sterns E.E., Nabholz J.M., De Coster R., Crump M., Abdolell M. and Qi S.; Liarozole fumarate (R85246): in the treatment of ER negative tamoxifen refractory or chemotherapy resistant postmenopausal metastatic breast cancer. *Breast Cancer Res. Treat.*, 2000, 64, 177-188.

⁸⁹ Van Wauwe J.P., Coene M.C., Goosens J., cools W. and Monbaliu J.; Effects of cytochrome P450 inhibitors on the in vivo metabolism of all-trans retinoic acid in rats. *J. Pharmacol. Exp. Ther.*, 1990, 252, 365-369.

⁹⁰ Achkar C.C., Bentel J.M., Boylan J.F., Scher H.I., Gudas L.J. and Miller W.H. Jr; Differences in the pharmacokinetic properties of orally administrated all-trans retinoic acid and 9-cis-retinoic acid in the plasma of nude mice. *Biochem. Pharmacol.*, 1994, 47, 737-741.

⁹¹ Debruyne F.J.M., Murray R., Fradet Y., Johansson J.E., Tyrrel C., Boccardo F., Denis L., Marberger J., Brune D., Rasswiler J., Vangeneugden T., Bruynseels J., Janssens M. and De Porre P.; Liarozole-a novel treatment approach for advance prostate cancer: results of a large randomized trial versus cyproteron acetate. *Urology*, 1998, 52, 72-81.

⁹² Goss P.E., Strasser K., Marques R., Clemons M., Oza A., Goel R., Blackstein M., Kaizer L., Sterns E.E., Nabholz J.M., Coster R.D., Crump M., Abdolell M. and Qi S.; Liarozole fumarate (R85246): in the treatment of ER negative, tamoxifen refractory or chemotherapy resistant postmenopausal metastatic breast cancer. *Breast Cancer Res. Treat.*, 2000, 64, 177-188.

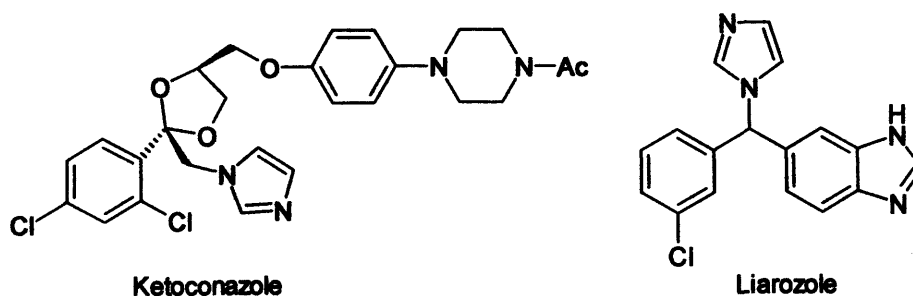


Figure 1.10: Chemical structure of ketoconazole⁸⁰ and liarozole⁸¹.

Because of the contribution of ATRA in some skin disorders, liarozole has also been studied for dermatological diseases. Clinical studies showed that liarozole was in fact an effective therapy for psoriasis^{93,94} and ichthyosis⁹⁵. As a result liarozole has been recently approved (2004) in Europe and in the USA as an orphan drug for the treatment of congenital ichthyosis⁹⁶.

(b) R115866 and R116010

Two benzothiazolamines compounds with high potency and selectivity for CYP26 inhibition have been developed: R115866⁹⁷ (IC_{50} = 4 nM) and R116010⁹⁸ (IC_{50} = 8.7 nM), (Figure 1.11). They displayed about 1000 fold more potency than liarozole (IC_{50} = 6 μ M)⁸¹.

R115866 has been shown to be very specific for CYP26 inhibition with moderate inhibitory activity versus CYP19 (IC_{50} = 2.6 μ M), CYP17 (IC_{50} = 1.2 μ M),

⁹³ Dockx P., Decree J. and Degree H.; Inhibition of the metabolism of endogenous retinoic acid as treatment for severe psoriasis: an open study with oral liarozole. *Br. J. Dermatol.*, 1995, 133, 426-432.

⁹⁴ Berth-Jones J., Todd G., Hutchinson P.E., Thestrup-Petersen K. and Vanhoutte F.P.; Treatment of psoriasis with oral liarozole: a dose-ranging study. *Br. J. Dermatol.*, 2000, 143, 1170-1176.

⁹⁵ Lucker G.P.H., Heremans A.M.C., Boegheim P.J., Van der Kerkhof P.C.M. and Steijlen P.P.M.; Oral treatment of ichthyosis by the cytochrome p450 inhibitor liarozole. *Br. J. Dermatol.*, 1997, 136, 71-75.

⁹⁶ Lucker G.P.H., Verfaillie C.J., Heremans A.M.C., Vanhoutte F.P., Boegheim P.J. and Steijlens P.P.M.; Topical liarozole in ichthyosis: a double-blind, left-right comparative study followed by a long term open maintenance study. *Br. J. Dermatol.*, 2005, 152, 566-568.

⁹⁷ Stoppie P., Borgers M., Borghraef P., Dillen L., Goossens J., Sanz G., Szel H., Van Hove C., Van Nyen G., Nobels G., Van den Bossche H., Venet M., Willemsens G. and Van Wauwe J.; R115866 inhibits all-*trans*-retinoic acid metabolism and exerts retinoid effects in rodents. *J. Pharmacol. Exp. Ther.*, 2000, 293, 304-312.

⁹⁸ Van Heusden J., Van Ginckel R., Bruwiere H., Moelans P., Janssen B., Floren W., Van des Leede B.J., Van Dun J., Sanz G., Venet M., Dillen L., Van Hove C., Willemsens G., Janicot M. and Wouters W.; Inhibition of all-*trans*-retinoic acid metabolism by R116010 induces antitumour activity. *Brit. J. Cancer*, 2002, 86, 605-611.

CYP2C11 ($IC_{50}= 7.2 \mu\text{M}$), CYP2A1 ($IC_{50}= 9.1 \mu\text{M}$) and CYP3A4 (20 % inhibition at $10 \mu\text{M}$)⁹⁷ and should thus be less likely to show any unwanted side effects. *In vivo* studies have also proved that R115866 is able to enhance endogenous retinoic acid levels and also to mimic the effects of retinoic acid⁸³. As a result, R115866 was found to exert retinoidal activities and displayed some potential in dermatological therapy: in the treatment of severe facial acne vulgaris and plaque-type psoriasis R115866 exhibited a modulating effect on epithelial growth and differentiation in various animal models of keratinisation^{99,100,101}.

R116010 also displayed specificity for CYP26 inhibition. R116010 inhibition activity versus other CYPs is quite low. It is superior at $10 \mu\text{M}$ for CYP2A1, CYP2B1, CYP2B2, CYP2C11, CYP3A and CYP19 and moderate for CYP17 ($IC_{50}= 0.25 \mu\text{M}$)⁹⁸. R116010 has shown anti-tumour activity as a single agent and enhanced the anti-proliferative property of retinoic acid both *in vitro* and *in vivo*⁹⁸. R116010 has also shown potency in the treatment of neuroblastoma while co-administrated with 13-*cis*-RA¹⁰².

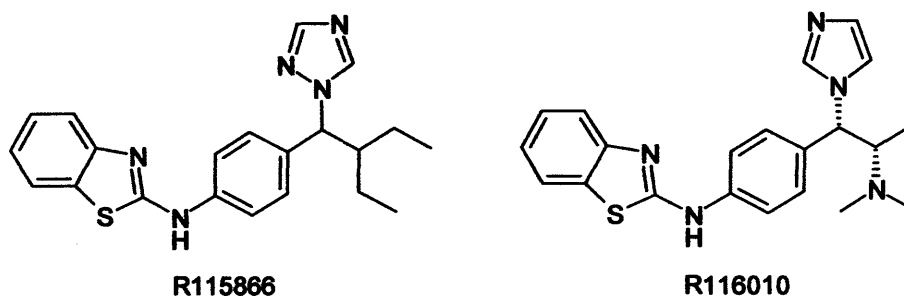


Figure 1.11: Chemical structure of R115866⁹⁷ and R116010⁹⁸.

⁹⁹ Verfaillie C.J., Coel M., Boersma I.H., Mertens J., Borgers M. and Roseeuw D.; Oral R115866 in the treatment of moderate to severe facial acne vulgaris: an exploratory study. *Br. J. Dermatol.*, 2007, 157, 122-126.

¹⁰⁰ Verfaillie C.J., Thissen C.A.C.B., Bovenshen H.J., Mertens J., Steijlen P.M. and Van der Kerkhof P.C.M.; Oral R115866 in the treatment of moderate to severe plaque-type psoriasis. *J. Eur. Acad. Dermatol. Venereol.*, 2007, 21, 1038-1046.

¹⁰¹ Bovenschen H.J., Otero M.E., Langewouters A.M.G., Van Vlijmen-Willems I.M.J.J., Van Rens D.W.A., Seyger M.M.B. and Van der Kerkhof P.C.M.; Oral retinoic acid metabolism blocking agent Rambazole™ for plaque psoriasis: an immunohistochemical study. *Br. J. Dermatol.*, 2007, 156, 263-270.

¹⁰² Armstrong J.L., Taylor G.A., Thomas H.D., Boddy A.V., Redfern C.P.F. and Veal G.J.; Molecular targeting of retinoic acid metabolism in neuroblastoma: the role of CYP26 inhibitor R116010 *in vitro* and *in vivo*. *Br. J. Cancer*, 2007, 96, 1675-1683.

R115866 and R116010 are thus two very interesting RAMBAs showing both high potency and high specificity for CYP26 inhibition. They also displayed promising results in cancer and dermatological therapy.

(c) RAMBAs recently developed

Few very potent RAMBAs displaying activities in the nanomolar range have been developed in the last few years. Three series of compounds hold our attention: a series of benzeneacetic acid^{103, 104}, a series of 2,6-disubstituted naphthalene^{105, 106} and a series of azolyl retinoids¹⁰⁷ (Figure 1.12).

A series of benzeneacetic acid derivatives have recently been developed^{103, 104}. The most potent inhibitor of the series containing an acetylene linker between an aromatic moiety and a substituted chromain as well as two cyclopropyl rings (Figure 1.12) displayed a CYP26 inhibitory activity of 14 nM in HeLa cells.

Mulvihill *et al.*^{105, 106} proposed a series of 2,6-disubstituted naphthalenes which mimic the haem-binding imidazolyl-propylamino moiety of R116010 with a naphthalene core substituted at the 6-position by an ether group. The most potent inhibitor of the series displayed a very potent activity (IC_{50} = 1.3 nM in T47D cells) as well as a high specificity over CYP3A4 enzyme (IC_{50} = 3300 nM)¹⁰⁵ (Figure 1.12). The potent activity of these 2,6-disubstituted naphthalenes as well as their selectivity

¹⁰³ Vasudevan J., Johnson A.T., Huang D. and Chandraratna R.A.; Preparation of compounds having activity as inhibitors of cytochrome P450RAI. *U.S. Patent*, 2001, 68 pp.

¹⁰⁴ Vasudevan J., Johnson A.T., Huang D., Wang L. and Chandraratna R.A.; Preparation of tetrahydronaphthalenes, tetrahydroisoquinolines, chromans, spirobenzopyrancyclopropanes and related compounds as cytochrome P450RAI inhibitors. *U.S. Patent*, 2002, 269 pp.

¹⁰⁵ Mulvihill M.J., Kan J.L.C., Cooke A., Bhagwat S., Beck P., Bittner M., Cesario C., Keane D., Lazarescu V., Nigro A., Nillson C., Panicker B., Smith V., Srebernak M., Sun F.L., O'Connor M., Russo S., Fischetti G., Vrkljan M., Winski S., Castelhana A.L., Emerson D. and Gibson N.W.; 3-[6-(2-Dimethylamino-1-imidazol-1-yl-butyl)-naphthalen-2-yloxy]-2,2-dimethyl-propionic acid as a highly potent and selective retinoic acid metabolism blocking agent. *Bioorg. Med. Chem. Lett.*, 2006, 16, 2729-2733.

¹⁰⁶ Mulvihill M.J., Kan J.L.C., Beck P., Bittner M., Cesario C., Cooke A., Keane D.M., Nigro A.I., Nillson C., Smith V., Srebernak M., Sun F.L., Vrkljan M., Winski S.L., Castelhana A.L., Emerson D. and Gibson N.; Potent and selective [2-imidazol-1-yl-2-(6-alkoxy-naphthalen-2-yl)-1-methyl-ethyl]-dimethyl-amines as retinoic acid metabolism blocking agents. *Bioorg. Med. Chem. Lett.*, 2005, 15, 1669-1673.

¹⁰⁷ Patel J.B., Huynh C.K., Handratta V.D., Gediya L., Brodie A.M.H., Goloubeva O.G., Clement O.O., Nnane I.P., Soprano D.R. and Njar V.C.O.; Novel retinoic acid metabolism blocking agents endowed with multiple biological activities are efficient growth inhibitors of human breast and prostate cancer cells in vitro and a human breast tumor xenograft in nude mice. *J. Med. Chem.*, 2004, 47, 6716-6729.

for CYP26 over CYP3A4 make them good candidates for further development as therapeutic agents in dermatology and oncology.

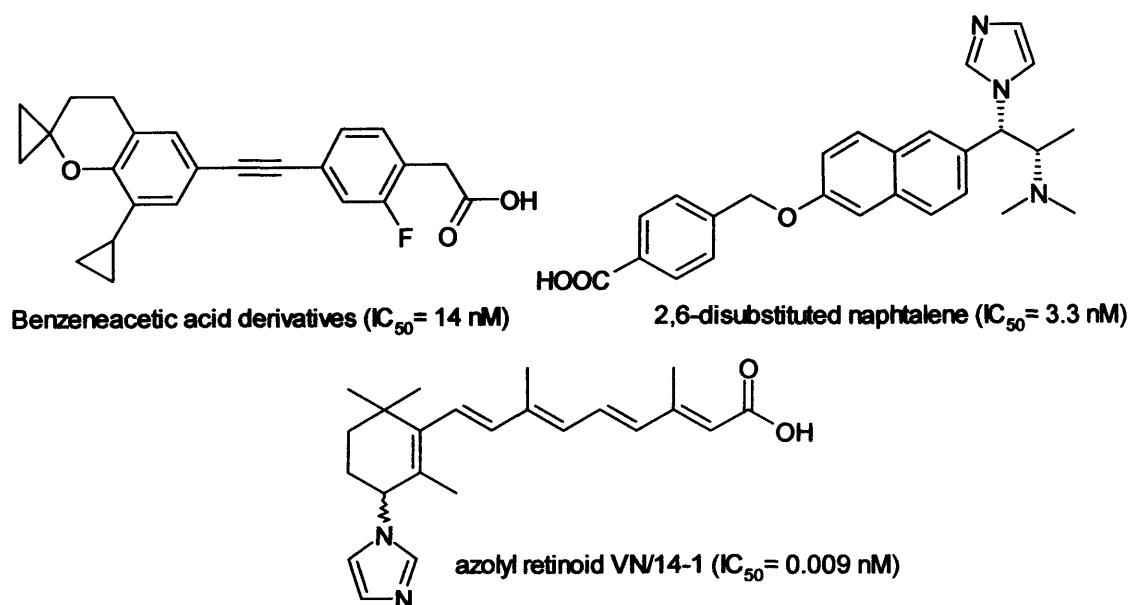


Figure 1.12: Chemical structure of the most potent compound of the benzeneacetic derivatives^{103, 104}, the 2,6-disubstituted naphthalene derivative^{105, 106} and the azolyl derivative¹⁰⁷.

The most potent CYP26 inhibitor to date has been described by the Njar group¹⁰⁷. As the presence of an azole ring seems to be essential in the design of RAMBAs, their compounds have been designed by introducing an azole ring at the C-4 position of ATRA, which is the position of the initial enzymatic hydroxylation (Figure 1.12). Compound VN/14-1 with an imidazole ring as a substituent appeared to be the most potent inhibitor of CYP26 with an inhibitory activity of 0.009 nM so almost 100000 fold the activity of liarozole (IC_{50} = 6000 nM)⁸¹. These compounds as well as being potent inhibitors of ATRA metabolism exhibited multiple biological activities such as induction of apoptosis and differentiation and antiproliferative activity on a number of human cancer cells^{108, 70}.

¹⁰⁸ Belosay A., Brodie A.M.H. and Njar V.C.O.; Effects of novel retinoic acid metabolism blocking agent (VN/14-1) on letrozole-insensitive breast cancer cells. *Cancer Res*, 2006, 66, 11485-11493.

(d) RAMBAs previously developed in our laboratory

Our group has been interested in inhibition of CYPs including CYP19¹⁰⁹, CYP24⁸⁴ and CYP26 for a number of years. However the emerging role of RAMBAs as potential anti-cancer agents focussed our interest in the development of CYP26 inhibitors. Two main type of structures were investigated: a series of pyrrolidin-2,5-diones derivatives¹¹⁰ and a series of tetralone derivatives¹¹¹ (Figure 1.13).

A series of pyrrolidin-2,5-dione derivatives substituted by a long alkyl chain or an aryl group at the 1-, 3- or 1,3-position was first investigated. They appeared to be weak inhibitors of ATRA metabolism against rat liver microsomes (68-80 % inhibition at 100 μ M) compared to ketoconazole (85 % inhibition at 100 μ M)¹¹⁰. The most potent compound **I1** of the series contained a long alkyl chain (C₆H₁₃) in position -1 and no substitution in position -3.

The tetralone derivatives displayed more promising results. The tetralone **I2** (IC₅₀= 12.75 μ M) was 2 fold more potent than ketoconazole (IC₅₀= 22.15 μ M) against rat liver microsomal RA-metabolising enzymes¹¹¹. Also no difference in the activity was observed between the two isomer (+) and (-). A later study by Angotti *et al.*¹¹² also showed that tetralone **I2** was able to enhance the endogenous plasma concentration of retinoic acid and that the tetralone inhibitory activity was comparable to ketoconazole. Transformation of the tetralone derivatives into a benzylidene tetralone **I3** or a benzyltetralone derivatives **I4** increased the activity to a level comparable with liarozole with measured IC₅₀ of 5 to 9 μ M in MCF-7 cells (liarozole IC₅₀= 7 μ M)¹¹³.

¹⁰⁹ Saberi M.R., Vinh T.K., Yee S.W., Griffiths B.J.N., Evans P.J. and Simons C.; Potent CYP19 (aromatase) 1[(benzofuran-2-yl)(phenylmethyl)pyridine, -imidazole, and -triazole inhibitors: synthesis and biological evaluation. *J. Med. Chem.*, **2006**, *49*, 1016-1022.

¹¹⁰ Kirby A.J., Le Lain R., Mason P., Maharlouie F., Nicholls P.J., Smith H.J. and Simons C.; Some 3-(4-aminophenyl)pyrrolidine-2,5-dinones as all-*trans*-retinoic acid metabolizing enzyme inhibitors (RAMBAs). *J. Enz. Inhib. Med. Chem.*, **2002**, *17*, 321-327.

¹¹¹ Kirby A.J., Le Lain R., Maharlouie F., Mason P., Nicholls P.J., Smith H.J. and Simons C.; Inhibition of retinoic acid metabolizing enzymes by 2-(4-aminophenylmethyl)-6-hydroxy-3,4-dihydronaphtalen-1(2H)-one and related compounds. *J. Enz. Inhib. Med. Chem.*, **2003**, *18*, 27-33.

¹¹² Angotti M., Hartmann R.W., Kirby A.J., Simons C., Nicholls P.J., Sewell R.D.E. and Smith H.J.; Effect of 2-(4-aminophenylmethyl)-6-hydroxy-3,4-dihydronaphtalen-1(2H)-one on all-*trans* and 13-*cis* retinoic acid levels in plasma quantified by high performance liquid chromatography coupled to tandem mass spectrometry. *J. Enz. Inhib. Med. Chem.*, **2005**, *20*, 219-226.

¹¹³ Yee S.W., Jarno L., Gomaa M.S., Elford C., Ooi L.L., Coogan M.P., McClelland R., Nicholson R.I., Evans B.A.J., Brancale A. and Simons C.; Novel tetralone-derived retinoic acid metabolism blocking agents: synthesis and in vitro evaluation with liver microsomal and MCF-7 CYP26A1 cell assays. *J. Med. Chem.*, **2005**, *48*, 7123-7131.

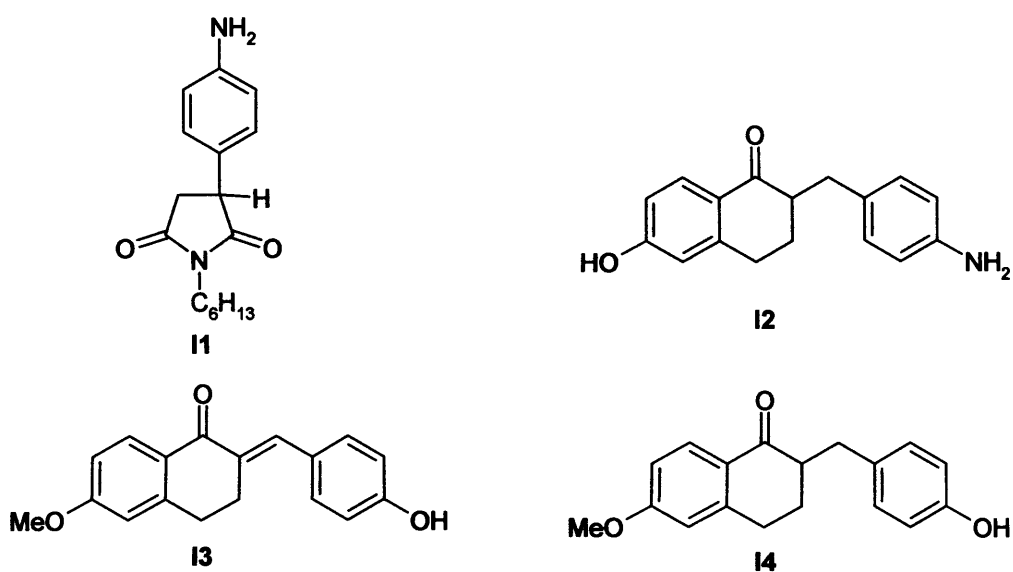


Figure 1.13: Chemical structure of the most potent compounds previously developed in our laboratory.

In conclusion, the pyrrolidin-2,5-dione derivatives and the tetralone derivatives displayed a weak to moderate activity towards CYP26 inhibition. The tetralone derivatives were the most interesting compounds (IC_{50} = 5-9 μ M) displaying results comparable with liarozole (IC_{50} = 7 μ M). These structures were consequently not investigated further as they seem unlikely to lead to potent inhibitors.

2) AIMS AND OBJECTIVES

The inhibition of CYP26 enzyme responsible for the metabolism of ATRA is an important target for the treatment of several cancers, leukaemia and some dermatological diseases and the use of RAMBAs has been proven to be effective in inhibiting the CYP26 enzyme and thus increasing the endogenous levels of ATRA.

Our research focussed on the design, synthesis and biological evaluation of new inhibitors for the CYP26 enzyme as well as a study of their binding interactions with a mimic of the active site of the enzyme using different spectroscopic techniques.

Some compounds have been previously synthesised in our group at the Welsh School of Pharmacy which affect activity of cytochrome P450 enzymes involved in retinoic acid catabolism^{110, 111}. However, they displayed a low activity compared to the best known inhibitors and the design of a new series of inhibitor is clearly needed.

Two new series of compounds were thus developed: a series of benzofuran derivatives and a series of benzoxazole derivatives. The first series of compounds is based on the 1-[benzofuran-2-yl-(4-alkylphenyl)methyl]triazole derivatives described by Vinh *et al.*^{114, 115}. A lipophilic alkyl chain attached to the 4-position of the phenyl ring of the benzofuran derivatives may mimic the lipophilic chain structure of ATRA (Figure 1.13).

The second series, the benzoxazol-2-yl-[phenylimidazol-1-ylmethyl]phenylamine (Figure 1.13), is based on docking studies performed with R115866⁹⁷ using a model of the CYP26A1 enzyme. As they display multiple hydrophobic interactions and hydrogen bonding with the active site, the benzoxazole

¹¹⁴ Vinh T.K., Ahmadi M., Delgado P.O., Perez S.F., Walters H.M., Smith H.J., Nicholls P.J. and Simons C.; 1-[(Benzofuran-2-yl)phenylmethyl]-triazoles and tetrazoles – potent inhibitors of aromatase. *Bioorg. Med. Chem. Lett.*, 1999, 9, 2105-2108.

¹¹⁵ Vinh T.K., Yee S.W., Kirby A.J., Nicholls P.J. and Simons C.; 1-[(Benzofuran-2-yl)-methylphenyl] triazoles as steroidogenic inhibitors: synthesis and *in vitro* inhibition of human placental CYP19 aromatase. *Anti-cancer Drug Des.*, 2001, 16, 217-225.

derivatives were scheduled for synthesis with various substituents on the 4-position of the phenyl ring including CO₂Me, COOH, CONH₂, OMe, OH, CH₃, F and H.

These two new series of compounds were then to be evaluated for CYP26 inhibition against MCF-7 cells using a method previously developed in our laboratory.

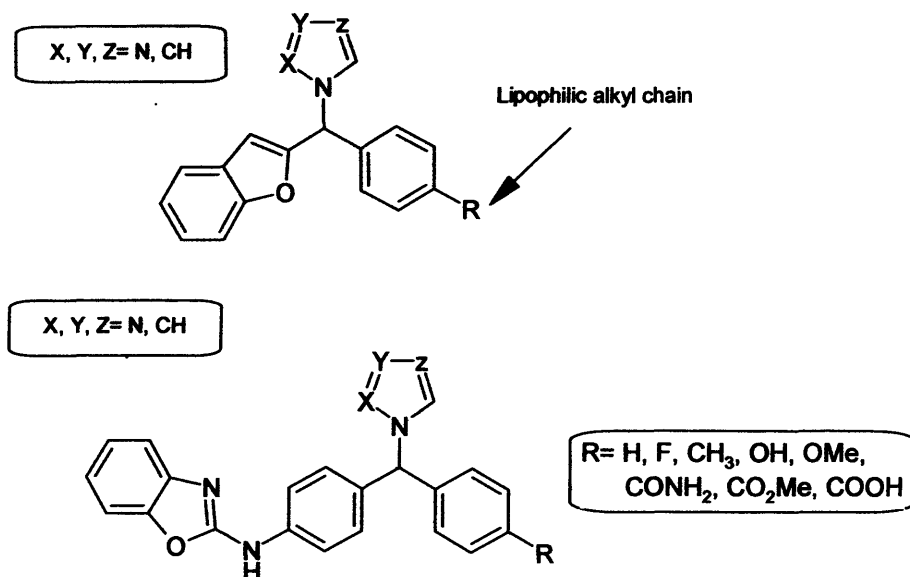


Figure 1.13: 1-[Benzofuran-2-yl-(4-alkylphenyl)methyl]triazole and benzoxazol-2-yl-[phenylimidazol-1-ylmethyl]phenyl]amine derivatives

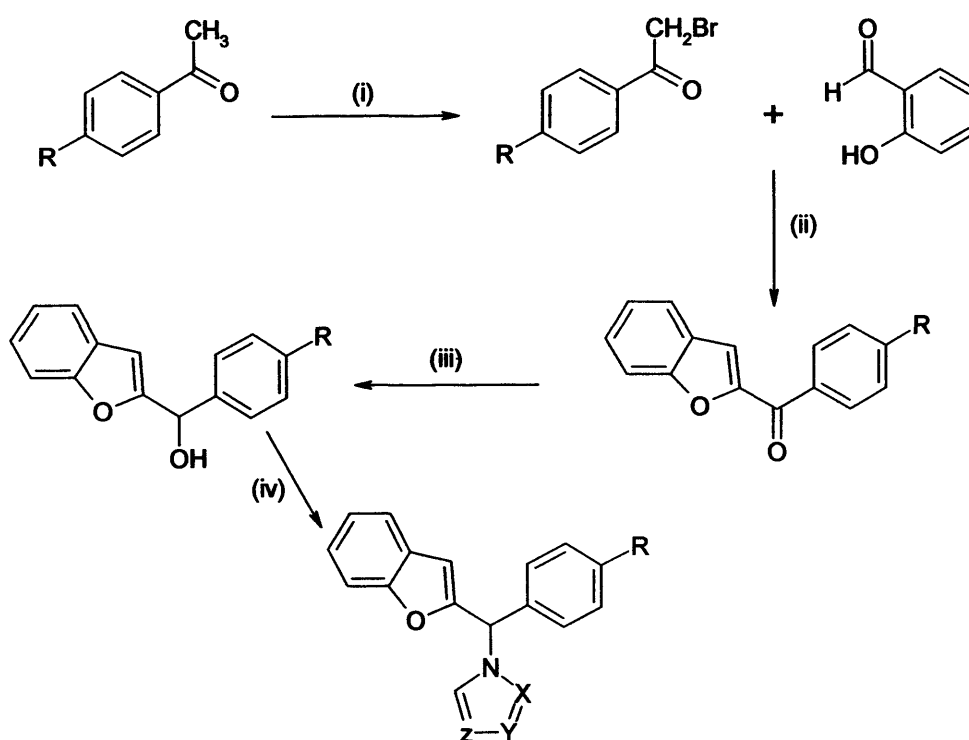
The second part of our work was to study the interaction of some of our drugs with a model of the haem enzyme active site. Different techniques such as X-ray crystallography, mass spectrometry, ¹H NMR spectroscopy and UV/VIS spectroscopy will be investigated in order to determine the binding constant of our inhibitors. A crystal structure of the haem-drug complex could also allow us to study the length and the angle of the Fe-N bond. The aim of this study was to correlate the binding properties of the drugs in the active site with their activity and therefore determine which type of azole ring or substituent is the more appropriate to enhance the activity.

CHAPTER 2

**FIRST SERIES: 1-[benzofuran-2-yl-
(4-alkylphenyl)methyl]triazole and
1-[benzofuran-2-yl-(4-
alkylphenyl)methyl]tetrazole**

1) SYNTHESIS AND DISCUSSION

1.1) General chemistry



R= F, *i*-Pr, *t*-Bu, cyclohexyl, *i*-Bu, *n*-Pr
X, Y, Z= N, CH

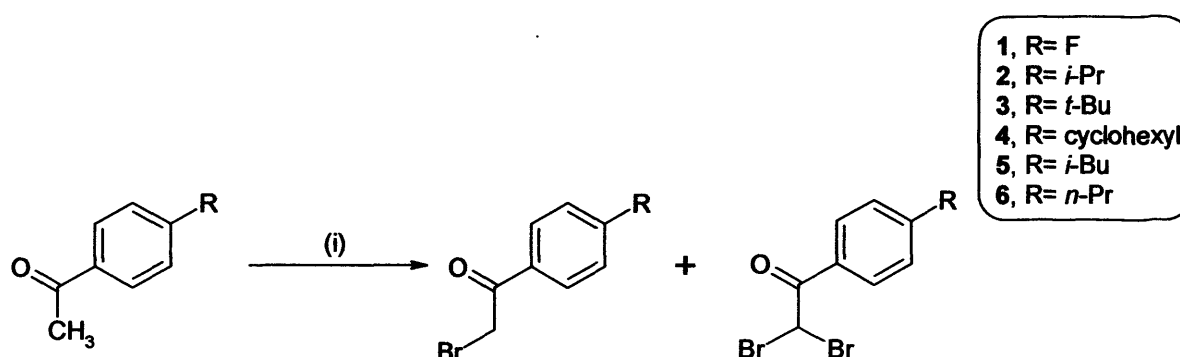
Scheme 2.1: General reaction scheme for the synthesis of 1-[benzofuran-2-yl-(4-alkylphenyl)methyl]triazole and 1-[benzofuran-2-yl-(4-alkylphenyl)methyl]tetrazole. *Reagents and conditions:* (i) Br₂, AlCl₃, Et₂O, 0 °C, 1 h; (ii) NaH, DMF, 80 °C, 1.5 h, then NaOCH₃, 80 °C, 1 h; (iii) NaBH₄, dioxan, rt, 3-6 h; (iv) SOCl₂, triazole or tetrazole, CH₃CN, 10 °C, 1 h, then K₂CO₃, 3-7 days.

The synthesis of 1-[benzofuran-2-yl-(4-alkylphenyl)methyl]triazole and 1-[benzofuran-2-yl-(4-alkylphenyl)methyl]tetrazole involved a sequence of four steps (Scheme 2.1):

- The generation of 4'-alkylacetophenone bromide by reaction of the appropriate acetophenone with bromine and aluminium trichloride.
- The preparation of the ketones by the Rap-Störmer reaction involving reaction of salicylaldehyde with the corresponding 4'-alkylacetophenone bromide.
- The reduction of the ketones to alcohols in quantitative yield using sodium borohydride.
- The addition of the aza-ring (triazole or tetrazole) using *N-N'*-thionyl-di-triazole or -tetrazole.

The reactions shown in Scheme 2.1 involve a procedure described previously in the laboratory by Vinh *et al.*^{114, 115}.

1.2) Preparation of the 4'-alkylacetophenone bromide



Scheme 2.2: Reagents and conditions (i) Br₂, AlCl₃, Et₂O, 1-2 h, rt, 58-100 %.

In this reaction, bromine was added dropwise over 20 min to the mixture composed of 4-substituted acetophenone and aluminium chloride as catalyst in anhydrous ether (Scheme 2.2)¹¹⁶. The reaction time was shorter than 2 h to prevent the formation of any side products and particularly the di-brominated products, but this time was enough to complete the reaction. The mechanism of the reaction reviewed by Fieser¹¹⁷ is described in Figure 2.1.

¹¹⁶ Cowper R.M. and Davidson L.H.; Phenacyl bromide (Acetophenone, α -bromo-). *Org. Synth., Coll. Vol II*, 1943, 480-481.

¹¹⁷ Fieser L.F. and Fieser M.; Reagents for organic synthesis. USA: John Wiley and Sons, Inc. 1967.

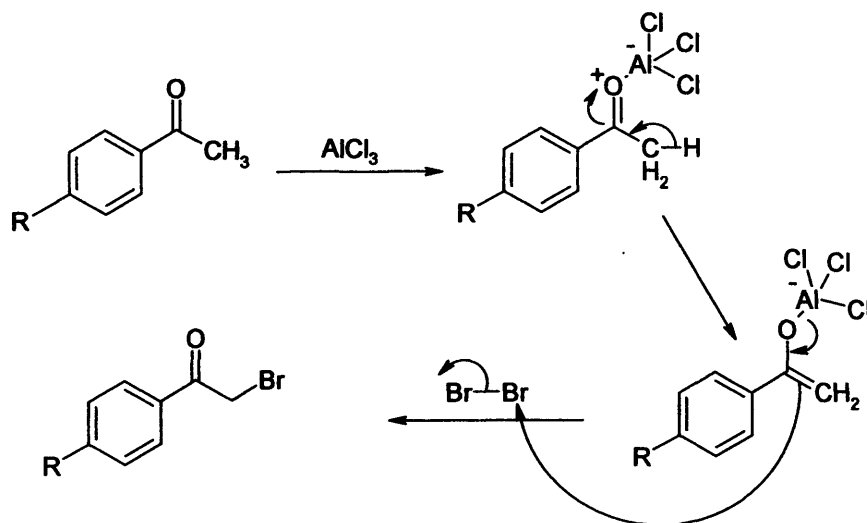


Figure 2.1: Proposed mechanism of the bromination of acetophenone by AlCl_3 catalyst.

In the first step, aluminium chloride, acting as a Lewis acid, forms a complex with the oxygen to give the enolate. Then, this enolate attacks bromine yielding the 2-bromoacetophenone and liberating the catalyst AlCl_3 and hydrogen bromide. The di-brominated product can also be formed during this reaction. The ratio of mono-brominated/di-brominated was calculated by proton NMR. The mono-brominated products were confirmed by the presence of a CH_2 singlet at approximately δ 4.5 ppm and the di-brominated products by a CH singlet about δ 6.7 ppm. The crude product was used for the next reaction.

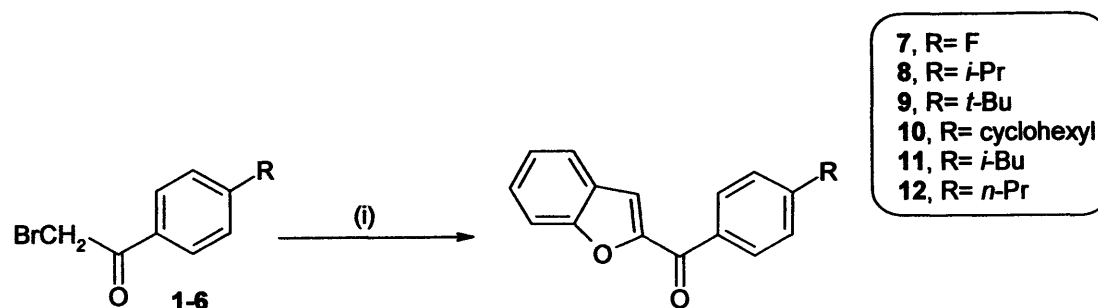
Table 2.1: Yield of the bromination in mono-brominated product:

R	YIELD ^(a)	COMPOUND NUMBER
F	65 %	1
Isopropyl	100 %	2
<i>Tert</i> -butyl	100 %	3
Cyclohexyl	58 %	4
Isobutyl	75 %	5
<i>n</i> -propyl	95 %	6

(a) Yield of the crude mono-brominated product only.

The proportion of di-brominated product was very variable (Table 2.1). None was detected in 2, 3 and 6 while the ratio was about 1:2 (di:mono) in 1 and 5 and about 1:1 in 4.

1.3) Preparation of the benzofurans



Scheme 2.3: Reagents and conditions (i) (a) NaH, salicylaldehyde, DMF, 2-3 h, 80 °C (b) NaOCH₃, 3-5 h, 80 °C, 29-50 %.

The formation of these α -ketones was achieved by a Rap-Stöermer reaction (Scheme 2.3), which involved two steps¹¹⁸, the mechanism of which is shown in Figure 2.2.

In the first step, salicylaldehyde is mixed with sodium hydride and DMF as solvent. Sodium hydride, which is a strong base, deprotonates the alcohol to form the sodium salt (a) and hydrogen gas. Nucleophilic substitution between the sodium salt and the 2-bromoacetophenone results in the non-cyclic compound (b).

In the second step, NaOCH₃ deprotonates the acidic α -proton of the ketone (b), with the resulting carbanion (c) attacking the aldehyde carbonyl to close the benzofuran ring (d). Then the molecule loses water to form the more stable conjugated product (f).

In conclusion, the synthesis of these α -ketones showed usually a moderate yield (29-50 %, Table 2.2). This may be due to the difficulty in purification of the product. In some case, the starting material was not pure (1, 4 and 5) and the two steps of the reactions were generally not complete. As a result the product was

¹¹⁸ Buu-Hoi N.P., Bisagni E., Royer R., Routier C.; Oxygen related compounds. *J. Chem. Soc.*, 1957, 625-628.

obtained with purification by recrystallisation from methanol (7, 8, 9, 11 and 12) or ethyl acetate (10).

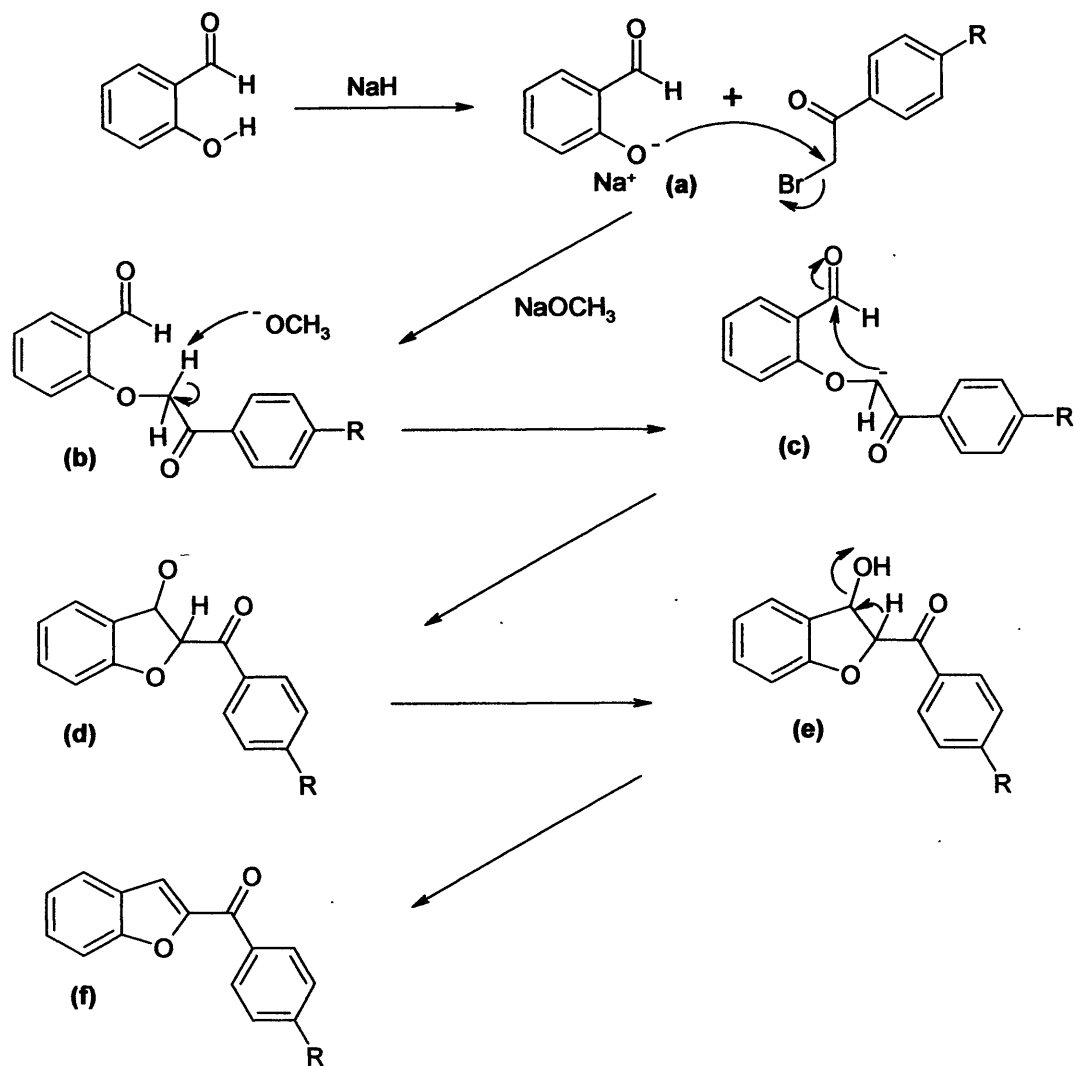


Figure 2.2: Mechanism of α -ketone formation by a Rap-Stoermer reaction

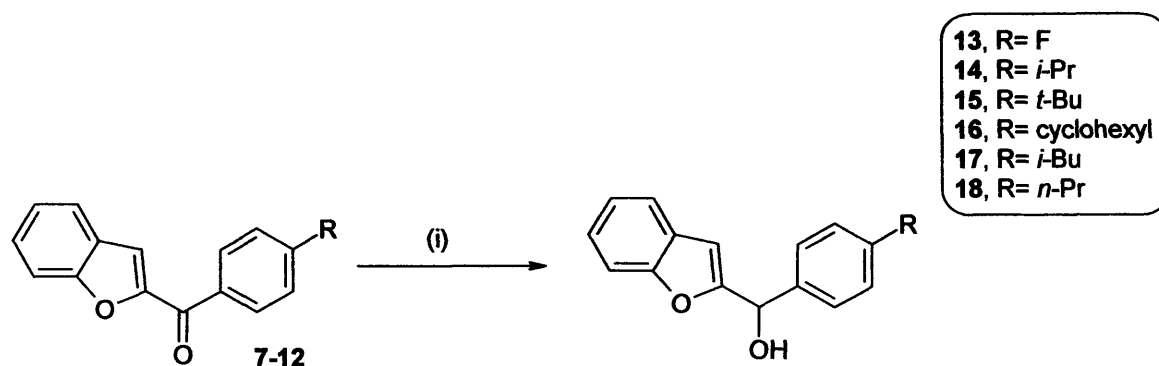
Table 2.2: Results of the preparation of benzofurans:

R	MELTING POINT	YIELD ^(a)	COMPOUND NUMBER
F	132-134 °C	42 %	7
Isopropyl	93-95 °C	44 %	8
<i>tert</i> -Butyl	103-105 °C	32 %	9
Cyclohexyl	92-94 °C	29 %	10

Isobutyl	62-63 °C	50 %	11
<i>n</i> -Propyl	64-66 °C	42 %	12

(a) Yield calculated after recrystallisation from methanol or ethyl acetate.

1.4) Reduction of the α -ketones



Scheme 2.4: Reagents and conditions (i) NaBH₄, dioxan, 2-3 h, rt, 90-99 %.

The reduction was achieved in mild conditions and very high yields (Table 2.3) using the reducing agent NaBH₄ and anhydrous dioxane as solvent (Scheme 2.4)¹¹⁹. The reactions were complete after 2 to 4 h. The reduction involved the transfer of one hydride ion H⁻ from NaBH₄ to the carbonyl carbon. Then, the excess NaBH₄ was quenched with 1 M HCl and the product obtained after extraction was pure enough for the next step.

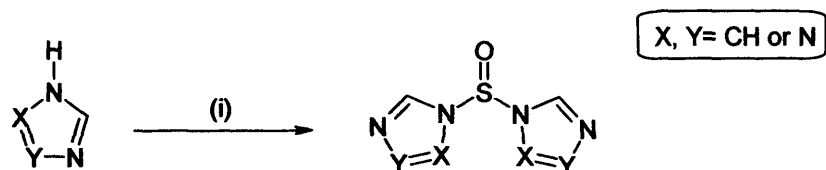
Table 2.3: Results of the reduction:

R	MELTING POINT	YIELD	COMPOUND NUMBER
F	-	99 %	13
Isopropyl	69-70 °C	96 %	14
<i>tert</i> -Butyl	87-88 °C	99 %	15
Cyclohexyl	67-68 °C	98 %	16

¹¹⁹ Ghelardoni M., Russo F. and Pestellini V.; Derivati del benzofurano ad attivita' coronarodilatatrice. *Boll. Chim. Farm.*, 1970, 109, 45-58.

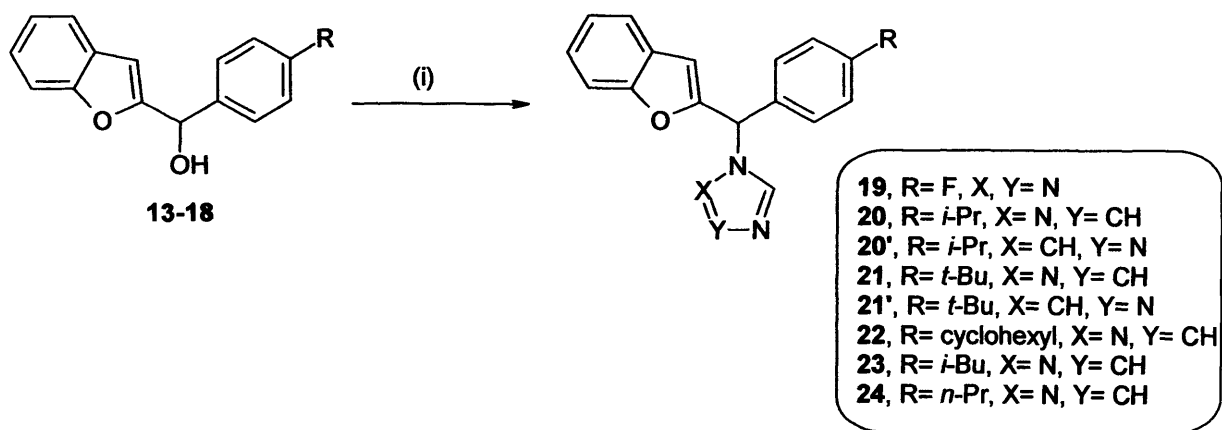
Isobutyl	-	98 %	17
<i>n</i> -Propyl	-	90 %	18

1.5) Addition of the aza-ring (triazole or tetrazole)



Scheme 2.5: Reagents and conditions (i) SOCl₂, CH₃CN, 1 h, 10 °C.

The required triazole and tetrazole compounds were prepared by using the Staab method¹²⁰. In this reaction, it is necessary to form *in situ* the reactive species *N-N'*-thionyl diaza-ring by coupling the aza-ring (triazole or tetrazole, 4 equivalents) and thionyl chloride (2 equivalents) during 1 h at 10 °C with anhydrous acetonitrile as solvent¹²¹ (Scheme 2.5).



Scheme 2.6: Reagents and conditions (i) *N-N'*-thionyl ditriazole or *N-N'*-thionyl ditetrazole, K₂CO₃, CH₃CN, 3-5 days, rt, 4-78 %.

¹²⁰ Staab A.H.; New methods of preparative organic chemistry IV. Syntheses using heterocyclic amides (azolides). *Angew. Chem. Int. Ed.*, **1962**, *1*, 351-367.

¹²¹ Humburg G., Mildenerger H. and Hoechst A.G.; 1,5-Disubstituted 1,2,4-triazole compounds. *Liebigs Ann. Chem.*, **1982**, *7*, 1387-1393.

Then, a solution of the carbinol (13-18) in dry CH_3CN was added to the mixture, followed by activated potassium carbonate. Next, the suspension was stirred under nitrogen at room temperature for 3 to 5 days (Scheme 2.6). The mechanism of the reaction is described in Figure 2.3.

The carbinol is first attacked by the base (K_2CO_3) to form the potassium salt of the carbinol. Then, this salt attacks the thionyl group of the *N-N'*-thionyl diazaring previously formed *in situ*, producing the carbinol with a very good leaving group in place of the hydroxyl. Then the aza-ring in the reaction can substitute the leaving group to form the final product and liberate SO_2 and triazole or tetrazole.

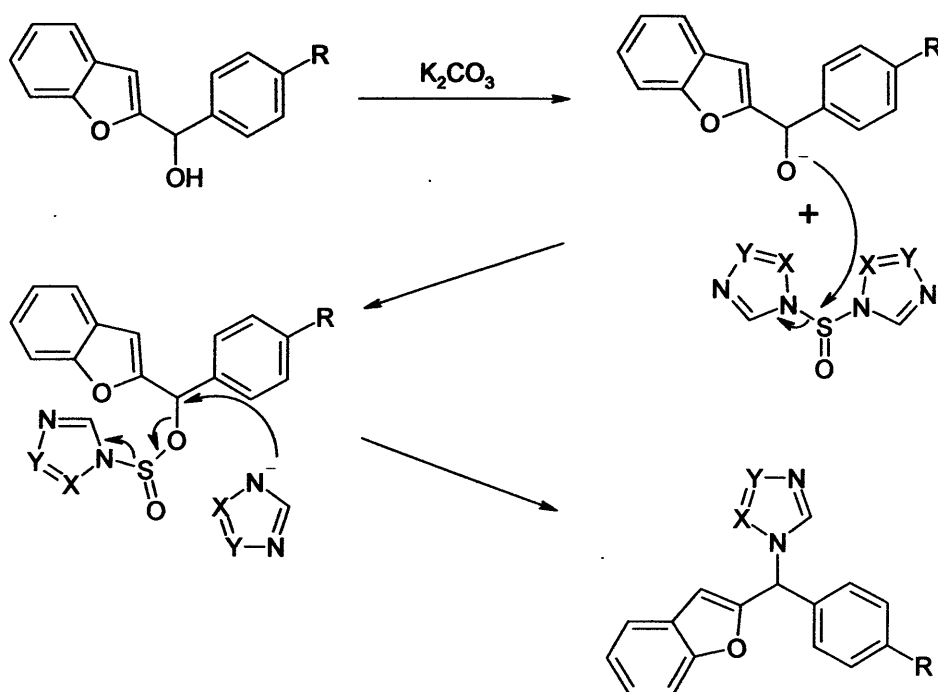


Figure 2.3: General mechanism of the formation of 1-[benzofuran-2-yl-(4-alkylphenyl)methyl]triazole and 1-[benzofuran-2-yl-(4-alkylphenyl)methyl]tetrazole.

Table 2.4: Results of the addition of the aza-ring

R	X	Y	YIELD^(a)	COMPOUND NUMBER
F	N	N	41 %	19
<i>i</i> -Pr	N	CH	78 %	20
<i>i</i> -Pr	CH	N	7 %	20'
<i>t</i> -Bu	N	CH	62 %	21
<i>t</i> -Bu	CH	N	4 %	21'
Cyclohexyl	N	CH	14 %	22
Cyclohexyl	CH	N	0 %	22'
<i>i</i> -Bu	N	CH	56 %	23
<i>i</i> -Bu	CH	N	0 %	23'
<i>n</i> -Pr	N	CH	59 %	24
<i>n</i> -Pr	CH	N	0 %	24'

(a) Yield calculated after purification by flash column chromatography

The final compounds with 1,2,4-triazole (**20**, **21**) and 1,3,4-triazole (**20'**, **21'**) are formed together in the same reaction with *i*-Pr and *t*-Bu as substituents. The 1,3,4-triazole compounds were not formed with the cyclohexyl, the isobutyl and the *n*-propyl derivatives (Table 2.4). Flash column chromatography was used to separate the regioisomer mixture, a 9:1 v/v petroleum ether/ethyl acetate mixture was used for the 1,2,4-triazole products while a 95:5 v/v dichloromethane/methanol mixture was used to obtain the 1,3,4-triazole products. The ratio of 1,3,4-triazole compounds was generally very low (4 to 7 %) however this was adequate for biological evaluation. The 1,2,4-triazole compounds were obtained generally with a good yield (Table 2.4), except for **22** (14 %).

After purification the products were confirmed by proton NMR. One proton at about δ 8.8 ppm was observed for the tetrazole compound **19** and two protons about δ 8.2 and δ 8.1 ppm respectively were observed for the 1,2,4-triazole compounds **20**, **21**, **22**, **23** and **24** instead of one two protons singlet at about δ 8.3 ppm for the 1,3,4-triazole compounds **20'** and **21'**.

2) BIOLOGICAL ASSAY

These assays were performed using *all-trans* retinoic acid as substrate and used methods previously developed by our group^{122,123}

2.1) Materials and equipment

Material/Chemical/Equipment	Source
<i>All-trans</i> retinoic acid	Sigma Chemicals (Dorset, UK)
[³ H-11,12]-ATRA (9.25 MBq, 250 µCi)	Perkin Elmer Life Science Ltd. (Massachussets, USA)
HPLC grade solvent (acetonitrile, methanol)	Fisher Scientific (Leicestershire, UK)
Ethyl acetate, ethanol, ammonium acetate	Sigma Chemicals, UK
Optiflow Safe 1 liquid scintillation cocktail	Fisons Chemical, UK
Ketoconazole	Sigma Chemicals (Dorset, UK)
Borosilicate tubes (12 × 75 mm and 13 × 100 mm)	Corning (New York, USA)
Centrifuge	MSE Harrier 18/80, Santo, Japan
Pump	Milton-Roy
Water bath with shaker	Grant, UK
Rotating evaporator	Christ Alpha RVC (Germany)
10 µm C ₁₈ µBondapak [®] 309 × 300 mm column	Waters, UK

¹²² Yee S.W.; PhD thesis: Synthesis and evaluation of inhibitors against vitamin D₃ and *all-trans* retinoic acid metabolising enzymes as potential therapy for androgen-independent prostate cancer. In *Welsh School of Pharmacy, Cardiff University, Cardiff, 2005*.

¹²³ Jarno L.; PhD thesis: Studies on the action and metabolism of retinoic acid in MCF-7 human breast cancer cells. In *Welsh School of Pharmacy, Cardiff University, Cardiff, 2003*.

Beta-Ram online scintillation detector	LKB Wallace 1217 Rackbeta
Computer	Compaq™
Laura data acquisition and analysis software	Lablogic Ltd

[³H-11,12]-ATRA stock solution was prepared using the following method: 100 µL of 1.2 nM ATRA in EtOH was diluted with 900 µL of iPrOH:EtOH 1:1 v/v. To this was added 10 µL of [³H-11,12] ATRA (9.25 MBq, 250 µCi).

The HPLC system was equipped with a high pressure pump (Milton-Roy pump), injector with a 50 µL loop connected to a β-RAM radioactivity detector, connected to a Compaq™ computer running Laura® data acquisition and analysis software. This enabled on-line detection and quantification of radioactive peaks. The HPLC column (10 µM C₁₈ µBondapak™ 3.9 × 300 mm HPLC column from Waters, UK) operating at ambient temperature was used to separate the metabolites which were eluted with acetonitrile/1 % ammonium acetate in water/acetic acid (75:25:0.1 v/v/v) at a flow rate of 1.9 mL/min. Ecoscint™ was used as the flow scintillation fluid.

2.2) Cell-lines used

Retinoids have been known to have anti-proliferative effects on the growth of breast carcinoma cells (MCF-7, ZR-75.1)⁶¹. The wild type MCF-7 cell lines were chosen because of their availability at the Welsh school of Pharmacy from the Tenovus group.

The MCF-7 wild type cell line is also known as the MCF-7 human mammary-carcinoma cell line and is oestrogen receptor-positive. These cells were grown in RPMI medium with 5 % (v/v) foetal calf serum (FCS), antibiotics (streptomycin and penicillin) and fungizone at a concentration of 10 iU/mL.

The MCF-7 cells are cultured in 75 cm² sterile flasks and are passaged every 7 days. To work on the retinoic acid metabolism, the cells are seeded at 1 × 10⁶ cells per well plate (12 wells).

2.3) General method for the MCF-7 wild type ATRA assay

- On the day of the assay:

1. Place PBS (phosphate buffer solution) in a water bath at 37 °C.
2. Prepare the experimental media solution as follow in the laminar flow.
3. Add 20 µL of EtOH or MeCN as control or inhibitor to labelled glass tubes.
4. Add the media (white RPMI + 5 % stripped-charcoal foetal calf serum + antibiotics). Need 1 mL of this media per well.
5. Cover each tube before removing it from the laminar flow to keep the experimental media as sterile as possible.
6. Add the [³H] ATRA to the tubes (20 µL per tube) in a dark room.
7. Place the tubes in the water bath and shake gently for about 10-15 min.
8. Take the MCF-7 cells from the incubator.
9. Remove the media from each well and then add 1 mL PBS.
10. Remove the PBS from the wells and add the corresponding experimental media to the corresponding well.
11. Incubate the plate in the incubator for 24 hours.

- After 24 h incubation time:

1. Remove the cells from the incubator.
2. Add 100 µL of 1 % acetic acid to each well. Shake it gently.
3. Add 2 mL of ethyl acetate/0.05 % butylated hydroxyanisole (BHA) into each labelled glass tube.
4. Remove the media from each well.
5. Add 200 µL of distilled water into each well.
6. Scrap the cells using the rubber end of the 1 mL syringe.
7. After scrapping the cells from each well, wash the rubber end with 200 µL of distilled water. Remove this 400 µL of distilled water with cells into the corresponding glass tube.
8. Vortex each tube for 15 s.
9. Remove 1 mL from each glass tube into the corresponding glass tube.

10. Add 1 mL ethyl acetate/ 0.05 % BHA and 100 μ L of MeOH into each tube.
Vortex it for 10 s.
11. Place the glass tube in the centrifuge for 15-18 min, the cells/serum in the media will settle in between the organic and water layer.
12. Remove the organic layer and place it in corresponding tubes.
13. Centrifuge the tube with the pump switched on for about 60 min.
14. Add 60 μ L of MeOH to each tube and vortex.
15. Inject to the HPLC, run it for 20 min, flow rate 1.9 mL/min. Psi is usually around 115-117.

2.4) Experimental results

The IC₅₀ of our final compounds can be measured using HPLC and Laura data acquisition software. Two major peaks can be observed on the HPLC. The first peak (retention time about 2 min) corresponds to the metabolites of ATRA (4-oxo-ATRA, 4-hydroxy-ATRA and other polar metabolites) which are metabolised by the action of CYP26 on ATRA and the second peak (retention time about 5.5 min) corresponds to the ATRA itself.

Consequently, a disappearance of the first peak would be observed if an inhibitor is added to the media. The separated metabolites were quantitatively calculated from the area under the curves and the percentage inhibition was calculated from: $100[\text{metabolites (control)} - \text{metabolites (inhibitors)} / \text{metabolites (control)}]$.

The tested compounds were the 1-[benzofuran-2-yl-(4-alkylphenyl)methyl]triazole and 1-[benzofuran-2-yl-(4-alkylphenyl)methyl]tetrazole:

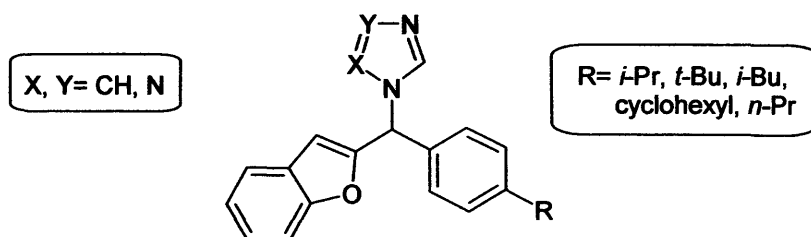


Table 2.5: IC_{50} of the 1-[benzofuran-2-yl-(4-alkylphenyl)methyl]triazole and 1-[benzofuran-2-yl-(4-alkylphenyl)methyl]tetrazole:

R	X	Y	IC_{50}	COMPOUND NUMBER
<i>i</i> -Pr	N	CH	20-40 μ M	20
<i>i</i> -Pr	CH	N	50-100 μ M	20'
<i>t</i> -Bu	N	CH	10-25 μ M	21
<i>t</i> -Bu	CH	N	-	21'
Cyclohexyl	N	CH	5-15 μ M	22
<i>i</i> -Bu	N	CH	30-40 μ M	23
<i>n</i> -Pr	N	CH	50-100 μ M	24
Me	N	CH	> 40 μ M ¹²⁴	25
Me	CH	N	> 40 μ M ¹²⁴	25'
Et	N	CH	4.5 μ M ¹²⁴	26
Et	CH	N	5 μ M ¹²⁴	26'
Ph	N	CH	7 μ M ¹²⁴	27
Ph	CH	N	9 μ M ¹²⁴	27'
<i>p</i> -Cl-C ₆ H ₅	N	CH	20-40 μ M	28
<i>p</i> -Cl-C ₆ H ₅	CH	N	20-40 μ M	28'

Compounds **25**, **25'**, **26**, **26'**, **27**, **27'**, **28** and **28'** were synthesised previously in the laboratory by Sook-Wah Yee¹²⁴.

The 4-ethyl (**26**, IC_{50} = 4.5 μ M and **26'**, IC_{50} = 5 μ M) and the 4-phenyl (**27**, IC_{50} = 7 μ M and **27'**, IC_{50} = 9 μ M) derivatives displayed inhibitory activity of CYP26 comparable with that of liarozole (IC_{50} = 7 μ M), and the cyclohexyl (**22**, IC_{50} = 5-15 μ M) and the *t*-Bu (**21**, IC_{50} = 10-25 μ M) derivatives displayed moderate activity, the remaining alkyl/aryl derivatives were all poor CYP26 inhibitors of retinoic acid metabolism (IC_{50} > 20 μ M) (Table 2.5). All the 1-[benzofuran-2-yl-(4-

¹²⁴ Pautus S., Yee S.W., Jayne M., Coogan M.P. and Simons C.; Synthesis and CYP26A1 inhibitory activity of 1-[benzofuran-2-yl-(4-alkyl/aryl-phenyl)-methyl]-1*H*-triazoles. *Bioorg. Med. Chem.*, 2006, 14, 3643-3653.

alkyl/arylphenyl)methyl]-1*H*-triazoles were considerably less active than R115866⁹⁴ (IC₅₀= 5 nM).

The 4-methyl derivative **25** has previously been evaluated as an aromatase (CYP19) inhibitor (IC₅₀ = 0.59 μM)¹⁰⁶. The 4-ethyl **26** and the 4-phenyl **27** derivatives were also screened against CYP19 to determine selectivity, both having an inhibitory IC₅₀ > 100 μM. The negligible CYP19 inhibitory activity of **26** and **27** was expected from SAR studies¹⁰³ which had shown that only small substituents, for example, F, Cl, CH₃ and CN were tolerated at the 4-position of the phenyl ring for CYP19 inhibitors.

2.5) Molecular modeling

In order to rationalise the results obtained, MOE (Molecular Operating Environment)¹²⁵ docking studies of the inhibitors were performed using a human CYP26A1 model¹²⁶, built using the recently crystallised human CYP3A4¹²⁷ as a template. Docking interactions at the enzyme active site were shown to be comparable with those of the CYP26 inhibitor liarozole with the benzofurans positioned above the haem with multiple hydrophobic interactions. The inhibitor compounds are all racemic therefore both enantiomers of all the compounds were docked to determine any preference for (*R*)- or (*S*)-configuration; no preference was observed with both enantiomers exhibiting a similar 'fit' in the active site with the nitrogen of the heterocyclic ring coordinating with the Fe³⁺ of the haem.

Docking of the 4-alkyl derivatives with a chain length of >2 indicated that steric hindrance was encountered preventing close (2.5-3.5 Å) interaction with the haem. The phenyl derivatives (**27** and **27'**, IC₅₀= 7-9 μM) have a greater inhibitory activity despite its size owing to favourable conformation and enhanced hydrophobic

¹²⁵ Molecular Operating Environment (MOE). Chemical Computing Group, Inc. Montreal, Quebec, Canada. <http://www.chemcomp.com>. Code 'scoring svl' obtained from SVL Exchange website <http://svl.chemcomp.com>, Chemical computing Group, Inc. Montreal, Canada.

¹²⁶ Gomaa M.S., Yee S.W., Milbourne C.E., Barbera M., Simons C. and Brancale A.; Homology model of human retinoic acid metabolising enzyme cytochrome P450 26A1 (CYP26A1): active site architecture and ligand binding. *J. Enz. Inhib. Med. Chem.* **2006**, *21*, 361-369.

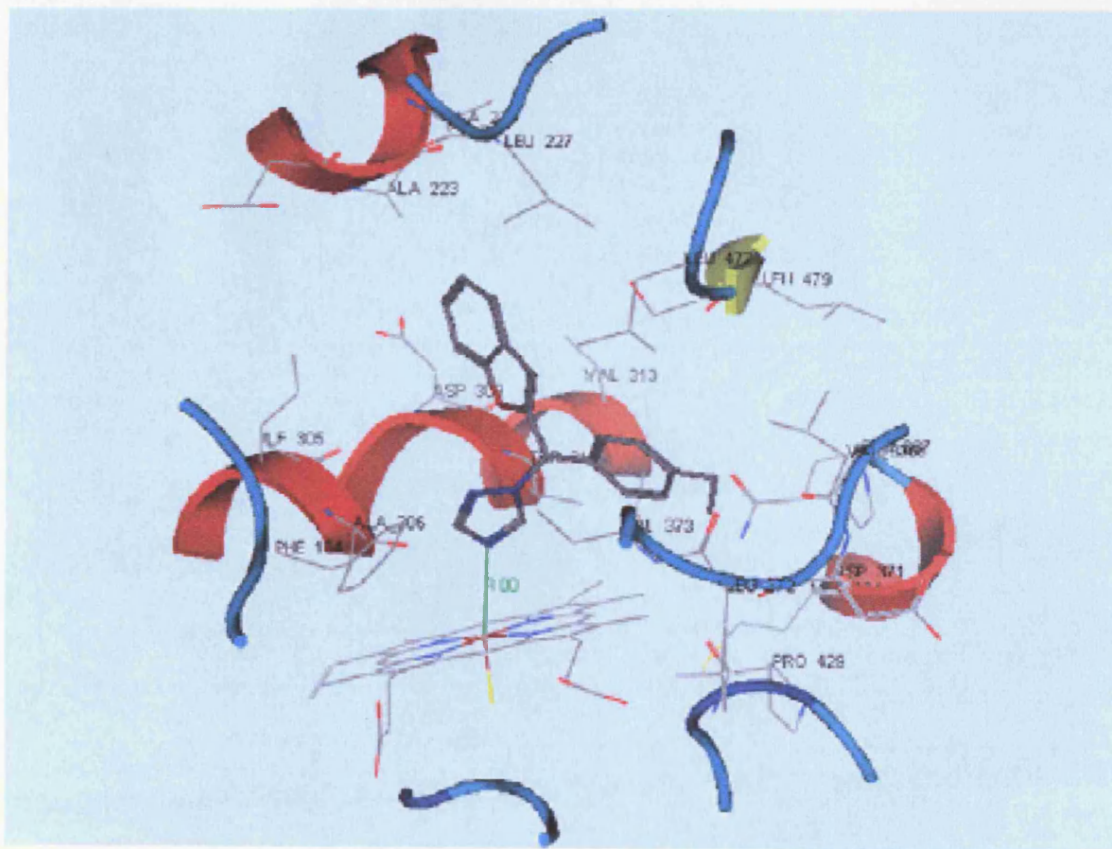
¹²⁷ Yano J.K., Wester M.R., Schoch G.A., Griffin K.J., Stout C.D. and Johnson E.F.; The structure of human microsomal cytochrome P450 3A4 determined by X-ray crystallography to 2.05- Å resolution. *J. Biol. Chem.*, **2004**, *279*, 38091-38094.

bonding (Figure 2.4). This may strengthen the interaction of the phenyl derivative increasing its potency as an inhibitor of the enzyme; however, the unsubstituted phenyl was the limit with the introduction of the chloro substituent (**28**, $IC_{50} = 20\text{-}40\ \mu\text{M}$) resulting in a reduction of inhibitory activity owing to steric/electronic factors.

The docking studies however failed to shed any light on the poor results obtained for the methyl compound (**25**, $IC_{50} > 40\ \mu\text{M}$), which was expected to possess potency similar to that of the ethyl derivative.

A series of 4-alkyl/aryl benzofuran phenyl triazole derivative has been successfully prepared with the ethyl and phenyl derivatives shown to possess comparable inhibitory activity with that of the known CYP26 inhibitor liarozole.

a



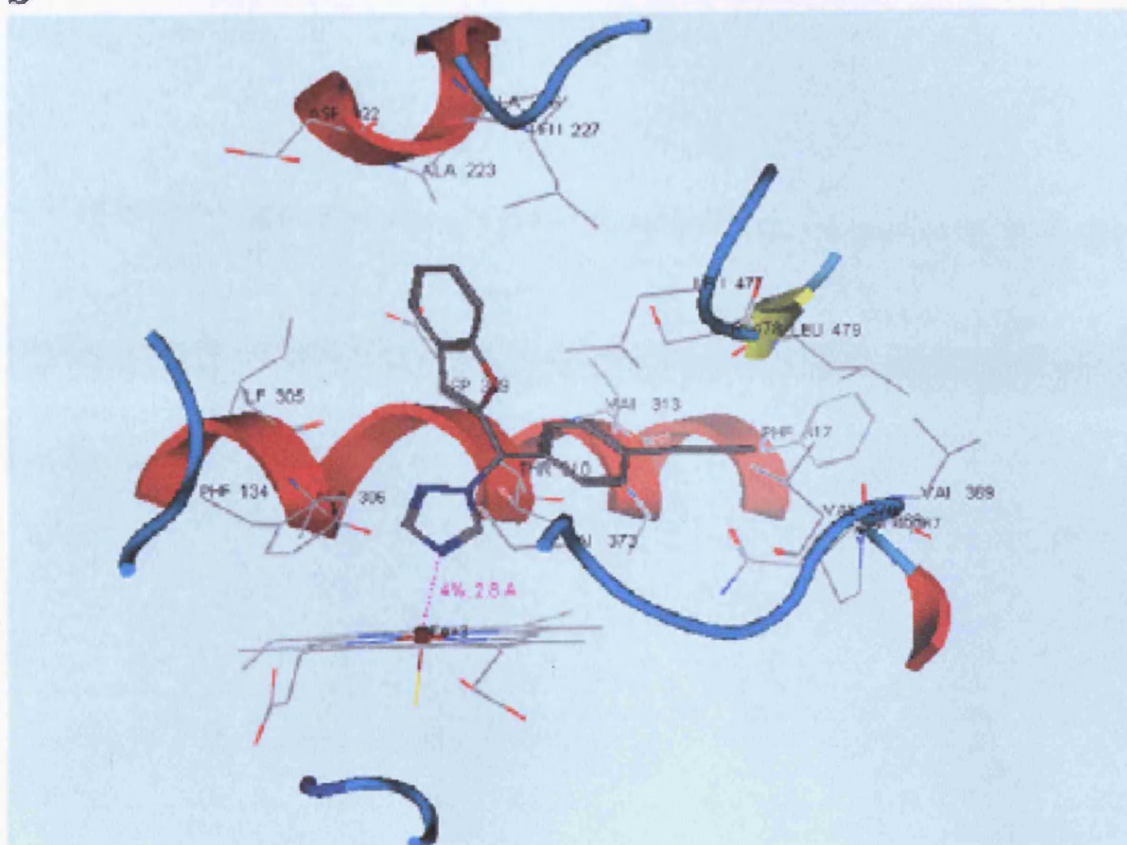
b

Figure 2.4: Active site region of CYP26A1 model showing (a) *S-26* and (b) *S-27* in ball and stick form. The distance from the haem is indicated with a green line, transition metal interaction with a purple line. Amino-acid residues identified are involved in hydrophobic interactions¹²⁴.

3) EXPERIMENTAL

3.1) General materials and methods

All reactions were carried out under an atmosphere of nitrogen when necessary. All reagents and solvents employed were of general purpose or analytical grade and purchase from Fluka, Agros chemicals and Sigma-Aldrich Chemical Company. Then solvents were appropriately dried over molecular sieves (3 Å) or when necessary by distillation.

N.M.R. spectra were recorded on a Bruker Advance 500 MHz. The chemical shifts are given in parts per million (ppm) relative to the internal standard tetramethyl silane (TMS), the coupling constants (J) are in Hertz and the multiplicity is denoted as s (singlet), d (doublet), t (triplet) and m (multiplet).

Silica gel Fluka Kieselgel 60 was used for column chromatography in a glass column. Flash column chromatography was performed with the aid of a pump.

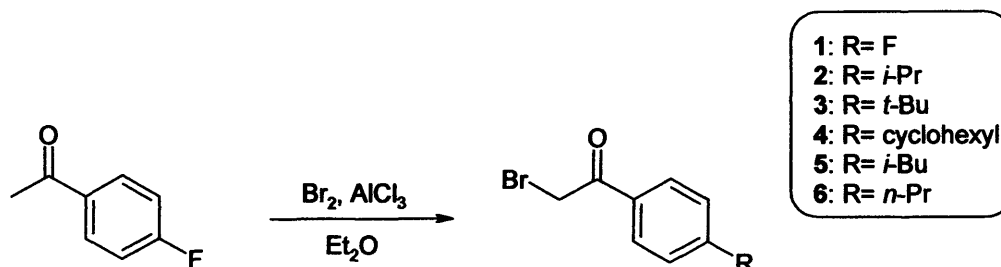
Thin layer chromatography was achieved on pre-coated silica plates (Merck Kieselgel 60 F₂₅₄) and visualised with UV light (254 nm) and/or vanillin stain.

Melting points were determinate using a Gallenkamp melting point apparatus and are uncorrected. Mass spectroscopy was performed at the EPSRC National Mass Spectrometry Service Centre Swansea and microanalyses were obtained from Medac Ltd., Brunel Science Centre Surrey.

3.2) Experimental results

3.2.1) General procedure for the preparation of the 4'-alkylacetophenone bromide 1-

6



To a cooled solution (0 °C) of 4'-alkylacetophenone (30.82 mmol) in anhydrous Et₂O (50 mL) was added a catalytic amount of aluminium chloride (3.08 mmol). Bromine (30.82 mmol) was added dropwise to the solution (to give an orange solution) over a period of 20 min and the reaction was stirred for further 1 h until the orange solution faded to a yellow coloration. The reaction mixture was then quenched with H₂O (100 mL) and stirred for 10 min. H₂O was separated from the ether and the organic layer was dried with MgSO₄, filtered and reduced *in vacuo*.

3.2.1.1) 4'-Fluoroacetophenone bromide (1, R= F)¹²⁸

Green syrup (65 % mono-brominated product), ratio monobrominated product-dibrominated product 3:1. t.l.c system petroleum ether-ethyl acetate 4:1, R_f= 0.89.

¹H NMR: δ (CDCl₃): 7.89 (d, 2H, J= 8.4 Hz, Ar), 7.09 (d, 2H, J= 8.3 Hz, Ar), 6.76 (s, 2H, CH₂Br).

3.2.1.2) 4'-Isopropylacetophenone bromide (2, R= *i*-Pr)¹²⁹

Brown syrup (100 %). t.l.c system: petroleum ether-ethyl acetate 4:1, R_f= 0.74.

¹²⁸ Bahner C.T., Easley W.K., Walden B.G., Lyons H.D. and Biggerstaff G.E.; p-Fluorophenacyl bromide salts. *J. Am. Chem. Soc.*, **1952**, *74*, 3960.

¹²⁹ Rebstock M.C. and Stratton C.D.; Some compound related to chloromycetin. *J. Am. Chem. Soc.*, **1955**, *77*, 4054-8.

$^1\text{H NMR}$: δ (CDCl_3): 7.96 (d, 2H, J = 8.2 Hz, Ar), 7.37 (d, 2H, J = 8.1 Hz, Ar), 4.48 (s, 2H, CH_2Br), 3.01 (m, 1H, i -Pr), 1.29 (d, 6H, J = 6.9 Hz, i -Pr).

3.2.1.3) 4'-*Tert*-butylacetophenone bromide (3, R= *t*-Bu)¹³⁰

Yellow syrup (100 %). t.l.c system: petroleum ether-ethyl acetate 4:1, R_f = 0.63.

$^1\text{H NMR}$: δ (CDCl_3): 7.92 (d, 2H, J = 8.4 Hz, Ar), 7.56 (d, 2H, J = 8.4 Hz, Ar), 4.48 (s, 2H, CH_2Br), 1.38 (s, 9H, *t*-Bu).

3.2.1.4) 4'-Cyclohexylacetophenone bromide (4, R= Cyclohexyl)¹²⁸

Yellow syrup (58 % in mono-brominated product), ratio monobrominated product-dibrominated product 1:1. t.l.c system: petroleum ether-ethyl acetate 4:1, R_f = 0.66.

$^1\text{H NMR}$: δ (CDCl_3): 8.01 (d, 2H, J = 8.3 Hz, Ar), 7.33 (m, 2H, J = 8.4 Hz, Ar), 4.46 (s, 2H, CH_2Br), 2.18 (m, 1H, cyclohexyl), 1.58 (m, 10H, cyclohexyl).

3.2.1.5) 4'-Isobutylacetophenone bromide (5, R= *i*-Bu)¹³¹

Yellow solid (75 % in mono-brominated product), ratio mono-brominated product-di-brominated product 3:1. t.l.c system: petroleum ether-ethyl acetate 4:1, R_f = 0.69.

$^1\text{H NMR}$: δ (CDCl_3): 7.83 (d, 2H, J = 8.3 Hz, Ar), 7.19 (m, 2H, J = 8.3 Hz, Ar), 4.36 (s, 2H, CH_2Br), 2.49 (d, J = 8.04 Hz, 2H, *i*-Bu), 1.72 (m, 1H, *i*-Bu), 0.83 (d, 6H, J = 6.8 Hz, *i*-Bu).

3.2.1.6) 4'-*n*-Propylacetophenone bromide (6, R= *n*-Pr)¹³²

Yellow solid (95 %). t.l.c system: petroleum ether-ethyl acetate 4:1, R_f = 0.66.

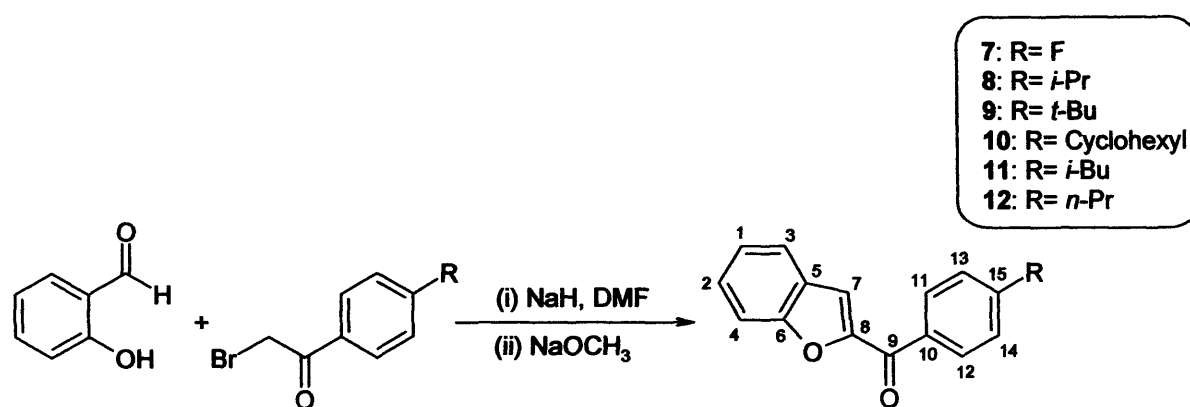
¹³⁰ Pesson M., Antoine M., Girard P., Benichon J.L., Chabassier S., De Lajudie P., Patte S., Roquet F. and Montay G.; Synthetic antibacterial agents. Pipemidic acid derivatives. *Eur. J. Med. Chem.*, 1980, 15, 263-8.

¹³¹ Pal M., Batcher V.R., Khanna S. and Yeleswaparau K.R.; Regioselective aluminium chloride induced heteroacylation of pyrrolo[1,2-*b*]pyridazines: its scope and application. *Tetrahedron*, 2002, 58, 9933-9940.

¹³² Zaszke H., Nitsche K., Schubert H.; Liquid-crystalline 3,6-diphenyl-1,2,4-triazines. *J. Prakt. Chem.*, 1977, 319, 475-484.

$^1\text{H NMR}$: δ (CDCl_3): 7.90 (d, 2H, $J= 8.3$ Hz, Ar), 7.29 (d, 2H, $J= 8.3$ Hz, Ar), 4.44 (s, 2H, CH_2Br), 2.65 (m, 2H, $n\text{-Pr}$), 1.67 (m, 2H, $n\text{-Pr}$), 0.94 (m, 3H, $n\text{-Pr}$).

3.2.2) General procedure for the preparation of the Benzofuran-2-yl-(4-alkylphenyl)methanone 7-12



To a solution of sodium hydride (60 % in mineral oil, 11 mmol) in dry DMF (10 mL) was added a solution of salicylaldehyde (10 mmol) in dry DMF (6 mL) dropwise. Hydrogen gas was liberated to give a yellow solution of the sodium salt. A solution of the 4'-alkylacetophenone bromide 1-6 (10 mmol) in dry DMF (10 mL) was then added dropwise and the reaction mixture was heated under nitrogen at 80 °C for 1.5-3 h. Sodium methoxide (2.5 mmol) was added to the mixture and heating was continued for 2-4 h. After cooling, the reaction mixture was evaporated to about a third its volume, diluted with CH_2Cl_2 (100 mL), washed with H_2O (100 mL), dried (MgSO_4) and concentrated under reduced pressure.

3.2.2.1) Benzofuran-2-yl-(4-fluoro-phenyl)-methanone (7, R= F)¹³³

Light yellow crystalline solid (55 %) after recrystallisation from MeOH, mp: 132-134 °C (lit mp 133-135 °C)¹³³. t.l.c system: petroleum ether-ethyl acetate 4:1, $R_f= 0.62$.

$^1\text{H NMR}$: δ (CDCl_3): 7.90 (m, 2H, Ar), 7.52 (m, 2H, Ar), 7.34 (m, 4H, Ar), 7.33 (s, 1H, H-7).

¹³³ Clementi S., Linda P. and Marino G.; Electrophilic substitutions in five membered heteroaromatic systems. Part XII. A quantitative study on the reactivities of the α - and β - positions of benzofuran and benzothiophen in electrophilic substitutions. *J. Chem. Soc.*, 1971, (B), 79-82.

3.2.2.2) Benzofuran-2-yl-(4-isopropylphenyl)methanone (8, R= *i*-Pr)

Pale orange solid (44 %) after recrystallisation from MeOH, mp: 93-95 °C.

t.l.c system: petroleum ether-ethyl acetate 4:1, $R_f = 0.64$.

$^1\text{H NMR}$: δ (CDCl_3): 7.85 (m, 2H, Ar), 7.53 (m, 2H, Ar), 7.35 (m, 2H, Ar), 7.34 (s, 1H, H-7), 7.32 (m, 2H, Ar) 3.05 (m, 1H, *i*-Pr), 1.32 (d, 6H, $J = 6.9$ Hz, *i*-Pr).

$^{13}\text{C NMR}$: δ (CDCl_3): 186.36 (C, C-9), 155.81 (C, C-15), 154.60 (C, C-6), 154.39 (C, C-10), 152.39 (C, C-8), 134.89 (C, C-5), 131.15 (CH, C-11, C-12), 129.74 (CH, C-13, C-14), 126.62 (CH, C-1), 124.22 (CH, C-2), 123.27 (CH, C-3), 115.76 (CH, C-4), 111.20 (CH, C-7), 34.24 (CH, *i*-Pr), 23.82 ($\text{CH}_3 \times 2$, *i*-Pr).

Microanalysis: Calculated for $\text{C}_{18}\text{H}_{16}\text{O}_2$. theoretical: %C 81.79, %H 6.10, found %C 81.58, %H 6.07.

3.2.2.3) Benzofuran-2-yl-(4-*tert*-butylphenyl)methanone (9, R= *t*-Bu)

Yellow solid (32 %) after recrystallisation from MeOH, mp: 103-105 °C. t.l.c system: petroleum ether-ethyl acetate 4:1, $R_f = 0.58$.

$^1\text{H NMR}$: δ (CDCl_3): 7.87 (m, 2H, Ar), 7.67 (m, 2H, Ar), 7.53 (m, 2H, Ar), 7.34 (s, 1H, H-7), 7.32 (m, 2H, Ar), 1.35 (s, 9H, H-17, H-18, *t*-Bu).

$^{13}\text{C NMR}$: δ (CDCl_3): 184.08 (C, C-9), 167.76 (C, C-15), 156.77 (C, C-6), 155.95 (C, C-10), 155.95 (C, C-8), 134.54 (C, C-5), 130.89 (CH, C-11, C-12), 129.51 (CH, C-13, C-14), 127.09 (CH, C-1), 125.55 (CH, C-2), 123.92 (CH, C-3), 116.14 (CH, C-4), 112.57 (CH, C-7), 68.17 (C, *t*-Bu), 31.15 ($\text{CH}_3 \times 3$, *t*-Bu).

Microanalysis: Calculated for $\text{C}_{19}\text{H}_{18}\text{O}_2 \cdot 0.5 \text{H}_2\text{O}$; theoretical: %C 78.92, %H 6.69, found: %C 79.17, %H 7.06.

3.2.2.4) Benzofuran-2-yl-(4-cyclohexylphenyl)methanone (10, R= cyclohexyl)¹³⁴

Light yellow crystalline solid (29 %) after recrystallisation from EtOAc, mp: 92-94 °C. t.l.c system: petroleum ether-ethyl acetate 4:1, $R_f = 0.71$.

$^1\text{H NMR}$: δ (CDCl_3): 7.93 (m, 2H, Ar), 7.24 (m, 2H, Ar), 7.19 (m, 4H, Ar), 6.62 (s, 1H, H-7), 2.51 (m, 1H, cyclohexyl), 1.56 (m, 10H, cyclohexyl).

$^{13}\text{C NMR}$: δ (CDCl_3): 184.08 (C, C-9), 155.94 (C, C-6), 153.70 (C, C-15), 152.52 (C, C-8), 134.94 (C, C-10), 129.76 (CH, C-13, C-14), 128.17 (CH, C-11, C-

¹³⁴ Richter P.H., Elsner H. and Vogt B.; Preparation of benzo[b]furan-derived ketone amidinohydrazome classIII antiarrhythmic agents. *Eur. Pat. Appl.*, 1997, 32 pp.

12), 127.07 (CH, C-2), 123.91 (CH, C-1), 123.23 (CH, C-3), 116.06 (CH, C-4), 112.56 (CH, C-7), 44.78 (CH, C-16), 34.17 (CH₂, C-17, C-18), 26.76 (CH₂, C-19, C-20), 26.07 (CH₂, C-21).

HRMS (EI): Found: 305.1537(M)⁺, Calculated: 305.1536.

3.2.2.5) Benzofuran-2-yl-(4-isobutylphenyl)methanone (11, R= *i*-Bu)

White solid (50 %) after recrystallisation from MeOH, mp: 62-63 °C. t.l.c system: petroleum ether-ethyl acetate 4:1, R_f= 0.63.

¹H NMR: δ (CDCl₃): 7.90 (m, 2H, Ar), 7.59 (m, 2H, Ar), 7.52 (m, 2H, Ar), 7.34 (m, 2H, Ar), 7.32 (s, 1H, H-7), 2.56 (d, J= 8.06 Hz, 2H, *i*-Bu), 1.96 (m, 1H, *i*-Bu), 1.01 (d, 6H, J= 6.8 Hz, *i*-Bu).

¹³C NMR: δ (CDCl₃): 184.08 (C, C-9), 155.95 (C, C-6), 152.50 (C, C-8), 147.55 (C, C-10), 134.86 (C, C-15), 129.63 (CH, C-11, C-12), 129.30 (CH, C-13, C-14), 128.19 (CH, C-1), 127.08 (CH, C-5), 123.92 (CH, C-2), 123.25 (CH, C-3), 116.09 (CH, C-4), 112.55 (CH, C-7), 45.48 (CH₂, *i*-Bu), 30.16 (CH, *i*-Bu), 22.39 (CH₃ × 2, *i*-Bu).

Microanalysis: Calculated for C₁₉H₁₈O₂; theoretical: %C 81.99, %H 6.52, found %C 81.55, %H 6.45.

3.2.2.6) Benzofuran-2-yl-(4-propylphenyl)methanone (12, R= *n*-Pr)

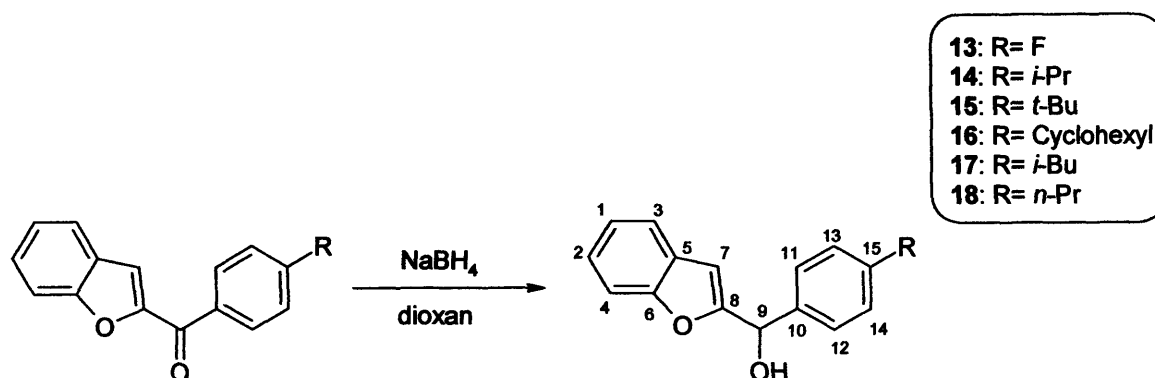
Cream crystalline solid (42 %) after recrystallisation from MeOH, mp: 64-66 °C. t.l.c system: petroleum ether-ethyl acetate 4:1, R_f= 0.52.

¹H NMR: δ (CDCl₃): 7.92 (d, 2H, J= 8.2 Hz, Ar), 7.65 (d, 2H, J= 7.9 Hz, Ar), 7.57 (m, 1H, Ar), 7.46 (m, 1H, Ar), 7.42 (m, 1H, Ar), 7.26 (m, 3H, Ar), 2.62 (m, 2H, H-16), 1.64 (m, 2H, H-17), 0.91 (t, 3H, J= 7.3 Hz, H-18).

¹³C NMR: δ (CDCl₃): 184.09 (C, C-9), 155.95 (C, C-6), 152.51 (C, C-8), 148.50 (C, C-10), 134.84 (C, C-15), 129.67 (CH, C-11, C-12), 128.68 (CH, C-13, C-14), 128.19 (CH, C-1), 127.08 (CH, C-5), 123.92 (CH, C-2), 121.71 (CH, C-3), 116.07 (CH, C-4), 112.56 (CH, C-7), 38.12 (CH₂, C-16), 24.25 (CH₂, C-17), 13.75 (CH₃, C-18).

HRMS (EI): Found: 265.1224 (M)⁺, Calculated: 265.1223.

3.2.3) General procedure for the preparation of the Benzofuran-2-yl-(4-alkylphenyl)methanol 13-18



To a cooled (0 °C) solution of benzofuran-2-yl-(4-alkyl-phenyl)-methanone (5 mmol) in anhydrous dioxane (15 mL) was added sodium borohydride (5 mmol) and then the mixture was allowed to stir at room temperature under nitrogen for 2-4 h. The solvent was concentrated under reduced pressure and aqueous HCl (1 M, 10 mL) was added to the residue. The oil formed was extracted with Et₂O or EtOAc (2 × 50 mL), the organic layers were combined and dried (MgSO₄) and the solvent concentrated under reduced pressure.

3.2.3.1) Benzofuran-2-yl-(4-fluorophenyl)methanol (13, R= F)¹³⁵

Yellow-brown oil (99 %). t.l.c system: petroleum ether-ethyl acetate 4:1 v/v, R_f = 0.67.

¹H N.M.R.: δ (CDCl₃): 7.54 (m, 4H, Ar), 7.30 (m, 2H, Ar), 7.13 (m, 2H, Ar), 6.57 (s, 1H, H-7), 5.98 (s, 1H, H-9), 3.74 (bs, 1H, OH).

3.2.3.2) Benzofuran-2-yl-(4-isopropylphenyl)methanol (14, R= *i*-Pr)

White solid (96 %), mp: 69-70 °C. t.l.c system: petroleum ether-ethyl acetate 4:1, R_f = 0.74.

¹H NMR: δ (CDCl₃): 7.42 (m, 2H, Ar), 7.34 (m, 2H, Ar), 7.16 (m, 2H, Ar), 7.11 (m, 2H, Ar), 6.45 (s, 1H, H-7), 5.81 (s, 1H, H-9), 2.82 (m, 1H, *i*-Pr), 2.59 (bs, 1H, OH), 1.18 (d, 6H, J= 6.9 Hz, *i*-Pr).

¹³⁵ Vinh K.T.; Design and synthesis of inhibitors of steroidogenesis. *PhD Thesis*, Cardiff University, 2001

¹³C NMR: δ (CDCl₃): 157.64 (C, C-8), 154.03 (C, C-15), 148.10 (C, C-10), 136.71 (CH, C-11, C-12), 127.03 (CH, C-13, C-14), 125.81 (CH, C-2), 125.65 (CH, C-1), 123.16 (CH, C-3), 110.28 (CH, C-4), 102.82 (CH, C-7), 69.54 (CH, C-9), 32.84 (CH, *i*-Pr), 22.93 (CH₃ \times 2, *i*-Pr).

Microanalysis: Calculated for C₁₈H₁₉O₂ \cdot 0.5 H₂O; theoretical: %C 78.23, %H 7.29, found %C 78.14, %H 7.05.

3.2.3.3) Benzofuran-2-yl-(4-*tert*-butylphenyl)methanol (15, R= *t*-Bu)

White solid (99 %), mp: 87-88 °C. t.l.c system: petroleum ether-ethyl acetate 4:1, R_f= 0.72.

¹H NMR: δ (CDCl₃): 7.39 (m, 2H, Ar), 7.34 (m, 2H, Ar), 7.30 (m, 2H, Ar), 7.12 (m, 2H, Ar), 6.41 (s, 1H, H-7), 5.78 (s, 1H, H-9), 2.58 (bs, 1H, OH), 1.21 (s, *t*-Bu).

¹³C NMR: δ (CDCl₃): 158.74 (C, C-8), 155.14 (C, C-15), 151.24 (C, C-10), 130.72 (CH, C-11, C-12), 129.36 (CH, C-13, C-14), 128.15 (CH, C-2), 126.64 (CH, C-1), 125.93 (CH, C-3), 111.39 (CH, C-4), 103.92 (CH, C-7), 70.57 (CH, C-9), 34.66 (C, *t*-Bu), 31.39 (CH₃ \times 3, *t*-Bu).

Microanalysis: Calculated for C₁₉H₂₀O₂; theoretical: %C 81.40, %H 7.19, found %C 81.22, %H 7.01.

3.2.3.4) Benzofuran-2-yl-(4-cyclohexylphenyl)methanol (16, R= cyclohexyl)

White solid (98 %), mp: 67-68 °C. t.l.c system: petroleum ether-ethyl acetate 4:1, R_f= 0.63.

¹H NMR: δ (CDCl₃): 7.59 (m, 1H, Ar), 7.48 (m, 3H, Ar), 7.25 (m, 4H, Ar), 6.58 (s, 1H, H-7), 5.89 (s, 1H, H-9), 3.72 (bs, 1H, OH), 2.61 (m, 1H, cyclohexyl), 1.58 (m, cyclohexyl).

¹³C NMR: δ (CDCl₃): 159.28 (C, C-4), 155.46 (C, C-8), 144.09 (C, C-15), 134.90 (C, C-10), 128.72 (CH, C-11, C-12), 128.59 (CH, C-13, C-14), 124.00 (CH, C-1), 122.77 (CH, C-2), 120.91 (CH, C-3), 111.25 (CH, C-4), 103.24 (CH, C-7), 67.63 (CH, C-9), 45.00 (CH, cyclohexyl), 35.40 (CH₂, cyclohexyl), 27.65 (CH₂, cyclohexyl), 26.95 (CH₂, cyclohexyl).

HRMS (ED): Found: 306.1612(M)⁺, Calculated: 306.1614.

3.2.3.5 Benzofuran-2-yl-(4-isobutylphenyl)methanol (17, R= *i*-Bu)

Yellow syrup (99 %). t.l.c system: petroleum ether-ethyl acetate 4:1, R_f = 0.73.

$^1\text{H NMR}$: δ (CDCl_3): 7.53 (m, 1H, Ar), 7.48 (m, 1H, Ar), 7.41 (m, 2H, Ar), 7.20 (m, 4H, Ar), 6.57 (s, 1H, H-7), 5.95 (s, 1H, H-9), 3.72 (bs, 1H, OH), 2.52 (d, J = 8.06 Hz, 2H, *i*-Bu), 1.91 (m, 1H, *i*-Bu), 0.96 (d, 6H, J = 6.8 Hz, *i*-Bu).

$^{13}\text{C NMR}$: δ (CDCl_3): 158.74 (C, C-8), 155.12 (C, C-6), 142.05 (C, C-10), 137.66 (C, C-15), 129.38 (CH, C-11, C-12), 128.10 (CH, C-5), 126.63 (CH, C-13, C-14), 124.23 (CH, C-2), 122.81 (CH, C-1), 121.12 (CH, C-3), 111.34 (CH, C-4), 103.89 (CH, C-7), 70.66 (CH, C-9), 45.16 (CH_2 , C-16), 30.21 (CH, C-17), 22.38 (CH_3 , C-18, C-19).

Microanalysis: Calculated for $\text{C}_{19}\text{H}_{20}\text{O}_2 \cdot 0.5 \text{H}_2\text{O}$; theoretical: %C 81.40, %H 7.19, found %C 81.07, %H 7.43.

3.2.3.6 Benzofuran-2-yl-(4-propylphenyl)methanol (18, R= *n*-Pr)

Yellow syrup (90 %). t.l.c system: petroleum ether-ethyl acetate 4:1, R_f = 0.64.

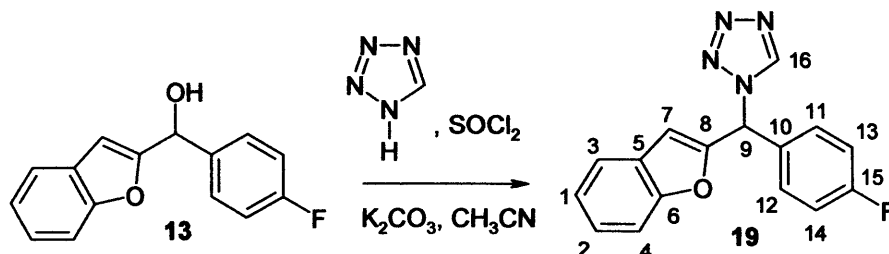
$^1\text{H NMR}$: δ (CDCl_3): 7.50 (m, 4H, Ar), 7.26 (m, 4H, Ar), 5.70 (s, 1H, H-9), 2.64 (m, 2H, *n*-Pr), 2.50 (bs, 1H, OH), 1.69 (m, 2H, *n*-Pr), 0.10 (m, 3H, *n*-Pr).

$^{13}\text{C NMR}$: δ (CDCl_3): 157.20 (C, C-8), 155.25 (C, C-6), 142.95 (C, C-15), 135.72 (C, C-10), 128.76 (CH, C-13, C-14), 128.15 (CH, C-11, C-12), 127.57 (CH, C-5), 126.78 (CH, C-2), 124.25 (CH, C-1), 122.82 (CH, C-3), 111.48 (CH, C-4), 105.09 (CH, C-7), 75.22 (CH, C-9), 37.85 (CH_2 , *n*-Pr), 24.51 (CH_2 , *n*-Pr), 13.93 (CH_3 , *n*-Pr).

Microanalysis: Calculated for $\text{C}_{19}\text{H}_{20}\text{O}_2$; theoretical: %C 81.17, %H 6.81, found %C 80.87, %H 6.92.

3.2.4) Preparation of the 1-{Benzofuran-2-yl}[4-fluorophenyl]methyl}-1H-tetrazole 19

135

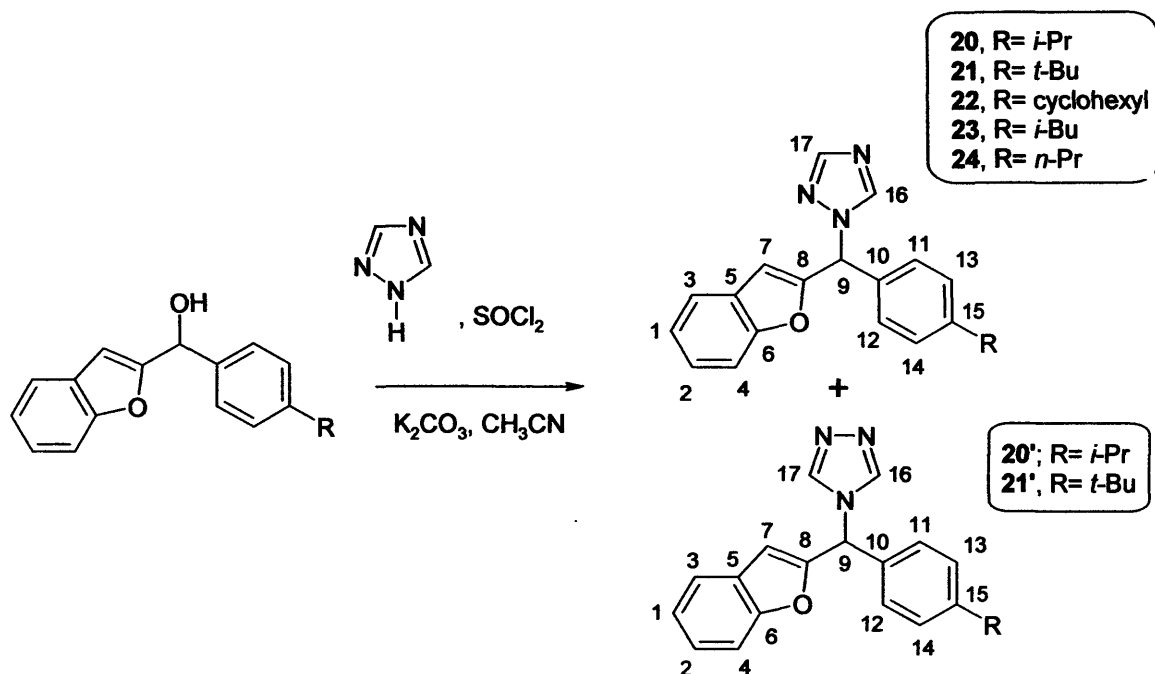


Thionyl chloride (0.17 g, 1.43 mmol) in anhydrous CH₃CN (2 mL) was added dropwise to a stirred solution of 1H-tetrazole (0.40 g, 5.71 mmol) in anhydrous CH₃CN (5 mL) at a temperature of 10 °C. The white suspension formed was allowed to stand for 1 h at 10 °C. A solution of 3 (0.34 g, 1.43 mmol) in anhydrous CH₃CN (5 mL) was added to the mixture followed by activated potassium carbonate (0.40 g, 2.86 mmol). The suspension was stirred under nitrogen at room temperature for 3 to 5 days. The resulting suspension was filtered and the filtrate was evaporated *in vacuo* to yield a brownish oil. The oil was extracted with CH₂Cl₂ (50 mL) and washed with H₂O (3 × 50 mL). The organic layer was dried (MgSO₄), filtered and reduced *in vacuo* to give an orange oil. The crude product was purified by flash column chromatography (CHCl₃-MeOH 99:1 v/v increasing to 97:3 v/v) to give the crude product as a yellow syrup. Preparative TLC was performed on glass plates (CHCl₃-MeOH 95:5 v/v). The product was collected and washed with CH₂Cl₂ (2 × 20 mL), CHCl₃ (3 × 20 mL) and then with MeOH (3 × 20 mL), filtered and reduced *in vacuo* to give a yellow syrup. Yield: 0.18 g (41 %). t.l.c system: petroleum ether-ethyl acetate 1:1, R_f = 0.63.

¹H N.M.R.: δ (CDCl₃): 8.16 (s, 1H, H-16), 7.47 (m, 2H, Ar), 7.35 (m, 4H, Ar), 7.30 (m, 2H, Ar), 6.31 (s, 1H, H-7), 5.48 (s, 1H, H-9).

¹³C NMR: δ (CDCl₃): 167.04 (C, C-15), 157.42 (C, C-6), 143.85 (CH, C-16), 139.77 (C, C-8), 134.90 (CH, C-11, C-12), 130.38 (C, C-5), 123.37 (CH, C-2), 122.14 (CH, C-1), 119.91 (CH, C-3), 119.09 (CH, C-13, C-14), 110.25 (CH, C-4), 98.76 (CH, C-9).

3.2.5) General procedure for the preparation of the 1- (Benzofuran-2-yl)4-alkyl(phenyl)methyl)-1H-[1,2,4] triazole 20-24 and 1- (benzofuran-2-yl)4-alkyl(phenyl)methyl)-1H-[1,3,4] triazole 20' and 21'



Thionyl chloride (4 mmol) in anhydrous CH₃CN (10 mL) was added dropwise to a stirred solution of 1,2,4-triazole (16 mmol) in anhydrous CH₃CN (10 mL) at a temperature of 10 °C. The white suspension formed was stirred for 1 h at 10 °C. A solution of benzofuran-2-yl-(4-alkyl-phenyl)-methanol (**13-18**) (4 mmol) in anhydrous CH₃CN (10 mL) was added to the mixture followed by activated potassium carbonate (8 mmol). The suspension was stirred under nitrogen at room temperature for 4 days. The resulting suspension was filtered and the filtrate was evaporated *in vacuo* to yield a light brown oil. The oil was extracted with CH₂Cl₂ (150 mL) and washed with H₂O (3 × 100 mL). The organic layer was dried (MgSO₄), filtered and reduced *in vacuo*.

3.2.5.1) 1- (Benzofuran-2-yl)4-isopropyl(phenyl)methyl)-1*H*-[1,2,4] triazole (20, R= *i*-Pr) and 1- (benzofuran-2-yl)4-isopropyl(phenyl)methyl)-1*H*-[1,3,4] triazole (20', R= *i*-Pr).

Purified by column chromatography (hexane/EtOAc, 9:1 v/v) to give the [1,2,4]triazole **20**, further elution (CH₂Cl₂/MeOH, 9:1 v/v) gave the [1,3,4]triazole **20'**.

Data for 20: Yellow syrup (78 %). t.l.c system: petroleum ether-ethyl acetate 1:1, R_f = 0.72.

¹H NMR: δ (CDCl₃): 8.42 (s, 1H, H-17), 8.33 (s, 1H, H-16), 7.31 (m, 1H, Ar), 7.24 (m, 2H, Ar), 7.06 (m, 5H, Ar), 6.62 (s, 1H, H-7), 6.37 (s, 1H, H-9), 2.73 (m, 1H, *i*-Pr), 1.05 (d, 6H, J = 6.9 Hz, *i*-Pr).

¹³C NMR: δ (CDCl₃): 155.25 (C, C-6), 153.15 (CH, C-16), 152.11 (CH, C-17), 149.79 (C, C-15), 143.35 (C, C-8), 133.09 (C, C-10), 127.76 (CH, C-11, C-12), 126.84 (CH, C-13, C-14), 125.04 (CH, C-2), 123.22 (CH, C-1), 112.44 (CH, C-3), 111.42 (CH, C-4), 107.07 (CH, C-7), 62.03 (CH, C-9), 34.47 (CH, *i*-Pr), 24.16 (CH₃ × 2, *i*-Pr).

HRMS (EI): Found: 318.1601(M)⁺, Calculated: 318.1601.

Data for 20': Yellow syrup (7 %). t.l.c system: petroleum ether-ethyl acetate 1:1, R_f = 0.11.

¹H NMR: δ (CDCl₃): 8.12 (s, 2H, H-16, H-17), 7.47 (m, 1H, Ar), 7.39 (m, 1H, Ar), 7.27 (m, 1H, Ar), 7.20 (m, 3H, Ar), 7.13 (m, 2H, Ar), 6.56 (s, 1H, H-7), 6.49 (s, 1H, H-9), 2.75 (m, 1H, *i*-Pr), 1.18 (d, 6H, J = 6.9 Hz, *i*-Pr).

¹³C NMR: δ (CDCl₃): 155.39 (C, C-6), 152.30 (C, C-15), 150.63 (CH, C-8), 142.47 (CH, C-16, C-17), 132.46 (C, C-6), 127.72 (C, C-5), 127.52 (CH, C-13, C-14), 127.21 (CH, C-11, C-12), 125.58 (CH, C-2), 123.58 (CH, C-1), 121.59 (CH, C-3), 111.64 (CH, C-4), 107.67 (CH, C-7), 58.08 (CH, C-9), 33.89 (C, *i*-Pr), 23.85 (CH₃ × 2, *i*-Pr).

HRMS (EI): Found: 318.1601(M)⁺, Calculated: 318.1603.

3.2.5.2) 1- (Benzofuran-2-yl)4-*tert*-butyl(phenyl)methyl)-1*H*-[1,2,4] triazole (21, R= *t*-Bu) and 1- (benzofuran-2-yl)4-*tert*-butyl(phenyl)methyl)-1*H*-[1,3,4] triazole (21', R= *t*-Bu).

Purified by column chromatography (hexane/EtOAc, 9:1 v/v) to give the [1,2,4]triazole **21**, further elution (CH₂Cl₂/MeOH, 9:1 v/v) gave the [1,3,4]triazole **21'**.

Data for 21: Yellow syrup (62 %). t.l.c system: petroleum ether-ethyl acetate 1:1, R_f= 0.61.

¹H NMR: δ (CDCl₃): 8.15 (s, 1H, H-17), 8.01 (s, 1H, H-16), 7.49 (m, 1H, Ar), 7.40 (m, 3H, Ar), 7.25 (m, 3H, Ar), 7.19 (m, 3H, Ar), 6.76 (s, 1H, H-7), 6.57 (s, 1H, H-9), 1.32 (s, 9H, *t*-Bu).

¹³C NMR: δ (CDCl₃): 156.98 (C, C-6), 154.16 (CH, C-17), 150.30 (C, C-15), 148.52 (CH, C-16), 136.47 (C, C-8), 132.56 (CH, C-11, C-12), 129.94 (C, C-5), 129.08 (C, C-10), 127.92 (CH, C-13, C-14), 123.37 (CH, C-2), 122.14 (CH, C-1), 120.55 (CH, C-3), 110.82 (CH, C-4), 101.37 (CH, C-7), 61.90 (CH, C-9), 34.80 (C, *t*-Bu), 31.41 (CH₃ × 3, *t*-Bu).

HRMS (EI): Found: 332.1761 (M)⁺, Calculated: 332.1757.

Data for 21': Yellow syrup (4 %). t.l.c system: petroleum ether-ethyl acetate 1:1, R_f= 0.08.

¹H NMR: δ (CDCl₃): 8.12 (s, 2H, H-16, H-17), 7.47 (m, 1H, Ar), 7.39 (m, 3H, Ar), 7.25 (m, 1H, Ar), 7.18 (m, 2H, Ar), 7.10 (m, 1H, Ar), 6.56 (s, 1H, H-7), 6.51 (s, 1H, H-9), 1.24 (s, 9H, *t*-Bu).

¹³C NMR: δ (CDCl₃): 158.26 (C, C-6), 150.02 (C, C-15), 158.22 (CH, C-16, C-17), 140.15 (CH, C-8), 131.84 (CH, C-11, C-12), 131.22 (C, C-5), 129.20 (CH, C-13, C-14), 127.93 (C, C-10), 123.49 (CH, C-2), 122.25 (CH, C-1), 120.28 (CH, C-3), 111.63 (CH, C-4), 107.64 (CH, C-7), 62.05 (CH, C-9), 34.71 (C, *t*-Bu), 31.23 (CH₃ × 3, *t*-Bu).

HRMS (EI): Found: 332.1762 (M)⁺, Calculated: 332.1757.

3.2.5.3) 1- (Benzofuran-2-yl)4-cyclohexyl(phenyl)methyl-1H-[1,2,4] triazole (22, R= cyclohexyl).

Purified by column chromatography (hexane/EtOAc, 9:1 v/v) to give the [1,2,4]triazole **22** as a yellow syrup (14 %). t.l.c system: petroleum ether-ethyl acetate 1:1, $R_f = 0.70$.

$^1\text{H NMR}$: δ (CDCl_3): 8.12 (s, 1H, H-17), 7.99 (s, 1H, H-16), 7.50 (m, 2H, Ar), 7.41 (m, 2H, Ar), 7.26 (m, 2H, Ar), 7.20 (m, 2H, Ar), 6.71 (s, 1H, H-7), 6.55 (s, 1H, H-9), 2.50 (m, 1H, cyclohexyl), 1.54 (m, 10H, cyclohexyl).

$^{13}\text{C NMR}$: δ (CDCl_3): 156.98 (C, C-6), 154.16 (CH, C-17), 148.52 (CH, C-16), 143.74 (C, C-15), 136.47 (C, C-8), 131.56 (CH, C-11, C-12), 129.81 (CH, C-13, C-14), 128.64 (C, C-10), 123.37 (CH, C-1), 122.14 (CH, C-2), 120.55 (CH, C-3), 110.89 (CH, C-4), 101.37 (CH, C-7), 56.50 (CH, C-9), 45.00 (CH_2 , cyclohexyl), 35.40 ($\text{CH}_2 \times 2$, cyclohexyl), 27.65 ($\text{CH}_2 \times 2$, cyclohexyl), 26.95 (CH_2 , cyclohexyl).

HRMS (EI): Found: 358.1910 (M^+), Calculated: 358.1914.

3.2.5.4) 1- (Benzofuran-2-yl)4-isobutyl(phenyl)methyl-1H-[1,2,4] triazole (23, R= *i*-Bu).

Purified by column chromatography (hexane/EtOAc, 9:1 v/v) to give the [1,2,4]triazole **23** as a yellow syrup (56 %). t.l.c system: petroleum ether-ethyl acetate 1:1, $R_f = 0.63$.

$^1\text{H NMR}$: δ (CDCl_3): 8.28 (s, 1H, H-17), 8.22 (s, 1H, H-16), 7.60 (m, 2H, Ar), 7.40 (m, 2H, Ar), 7.31 (m, 2H, Ar), 7.23 (m, 2H, Ar), 6.82 (s, 1H, H-7), 6.54 (s, 1H, H-9), 2.54 (d, $J = 8.06$ Hz, 2H, *i*-Bu), 1.95 (m, 1H, *i*-Bu), 1.02 (d, 6H, $J = 6.9$ Hz, *i*-Bu).

$^{13}\text{C NMR}$: δ (CDCl_3): 155.27 (C, C-6), 153.21 (CH, C-17), 152.11 (CH, C-16), 136.47 (C, C-8), 132.51 (CH, C-11, C-12), 131.47 (CH, C-13, C-14), 131.36 (C, C-15), 129.94 (C, C-5), 128.88 (C, C-10), 123.37 (CH, C-2), 122.14 (CH, C-1), 120.55 (CH, C-3), 110.89 (CH, C-4), 101.37 (CH, C-7), 56.50 (CH, C-9), 45.54 (CH_2 , *i*-Bu), 27.57 (CH, *i*-Bu), 22.23 ($\text{CH}_3 \times 2$, *i*-Bu).

Microanalysis: Calculated for $\text{C}_{21}\text{H}_{21}\text{N}_3\text{O} \cdot 0.3 \text{H}_2\text{O}$; theoretical: %C 74.89, %H 6.46, %N 12.48, found %C 74.87, %H 6.45, %N 12.15.

3.2.5.5) 1- (Benzofuran-2-yl)4-propyl(phenyl)methyl)-1*H*-[1,2,4] triazole (24, R= *n*-Pr).

Purified by column chromatography (hexane/EtOAc, 9:1 v/v) to give the [1,2,4]triazole **24** as a yellow syrup (59 %). t.l.c system: petroleum ether-ethyl acetate 4:1, $R_f = 0.25$.

^1H NMR: δ (CDCl_3): 8.03 (s, 1H, H-17), 7.94 (s, 1H, H-16), 7.46 (d, 1H, $J = 7.7$ Hz, Ar), 7.38 (d, 1H, $J = 8.3$ Hz, Ar), 7.23 (m, 1H, Ar), 7.16 (m, 5H, Ar), 6.74 (s, 1H, H-7), 6.49 (s, 1H, H-9), 2.53 (t, 2H, $J = 7.6$ Hz, *n*-Pr), 1.57 (m, 2H, *n*-Pr), 0.87 (t, 3H, $J = 7.3$ Hz, *n*-Pr).

^{13}C NMR: δ (CDCl_3): 154.32 (C, C-8), 151.92 (C, C-6), 151.17 (CH, C-17), 148.22 (CH, C-16), 142.96 (C, C-5), 131.77 (C, C-10), 128.17 (CH, C-11, C-12), 126.61 (CH, C-13, C-14), 126.53 (C, C-15), 124.13 (CH, C-2), 122.27 (CH, C-1), 120.46 (CH, C-3), 110.52 (CH, C-4), 106.55 (CH, C-7), 61.11 (CH, C-9), 36.68 (CH_2 , *n*-Pr), 23.34 (CH_2 , *n*-Pr), 12.79 (CH_3 , *n*-Pr).

HRMS (EI): Found: 318.1601 (M)⁺, Calculated: 318.1601.

CHAPTER 3

SECOND SERIES: Benzoxazol-2-yl-
[phenylimidazol-1-
ylmethyl)phenyl]amine

1) MOLECULAR DOCKING

1.1) Introduction

The active site of the P450 enzyme is composed of a single iron protoporphyrin IX prosthetic group coordinated to the four pyrrole nitrogen atoms as a haem¹ as shown previously in Figure 1.1.

Our group recently constructed a three-dimensional model of CYP26A1 based on the three known crystal structures of membrane bound human cytochrome P450: P450 2C9¹³⁶, P450 2C8¹³⁷ and P450 3A4¹²⁷. Molecular Operating Environment (MOE)¹²⁵ and FLEXX (TRIPOS Inc.)¹³⁸ software were used to build the three models based on the templates, P450 2C8 (PDB code: 1PQ2), P450 2C9 (1R90), P450 3A4 (ITQN). After performing docking with known CYP26 inhibitors such as liarozole and R115866, the model based on the P450 3A4 template was chosen. Further active site optimisation generated a final CYP26A1 model.

The CYP26A1 active site in human contains 497 amino-acids in its chain; the full sequence is given in Figure 3.1. The protein residues within a 7 Å radius of the haem were selected (Figure 3.2). All the other residues in the active site were too far to interact with a ligand. These residues formed a large hydrophobic pocket above the haem molecule which will be able to accommodate the substrate.

¹³⁶ Williams P.A., Cosme J., Ward A., Angrove H.C., Vinkovic D.M. and Johti H.; Crystal structure of human cytochrome P450 2C9 with bound warfarin. *Nature*, **2003**, *424*, 464-468.

¹³⁷ Schoch G.A., Yano J.K., Wester M.R., Griffin K.J., Stout C.D. and Johnson E.F.; Structure of human microsomal cytochrome P450 2C8. *J. Biol. Chem.*, **2004**, *279*, 9497-9503.

¹³⁸ Tripos SYBYL 7.0; Tripos Inc., 1699 South Hanley Rd, St. Louis, Missouri 63144, USA.
<http://www.tripos.com>.

	1	2	3	4	5	6	7	8	9	10	11	12	13	14	15	
1	Met	Gly	Leu	Pro	Ala	Leu	Leu	Ala	Ser	Ala	Leu	Cys	Thr	Phe	Val	15
16	Leu	Pro	Leu	Leu	Leu	Phe	Leu	Ala	Ala	Ile	Lys	Leu	Trp	Asp	Leu	30
31	Tyr	Cys	Val	Ser	Gly	Arg	Asp	Arg	Ser	Cys	Ala	Leu	Pro	Leu	Pro	45
46	Pro	Gly	Thr	Met	Gly	Phe	Pro	Phe	Phe	Gly	Glu	Thr	Leu	Gln	Met	60
61	Val	Leu	Gln	Arg	Arg	Lys	Phe	Leu	Gln	Met	Lys	Arg	Arg	Lys	Tyr	75
76	Gly	Phe	Ile	Tyr	Lys	Thr	His	Leu	Phe	Gly	Arg	Pro	Thr	Val	Arg	90
91	Val	Met	Gly	Ala	Asp	Asn	Val	Arg	Arg	Ile	Leu	Leu	Gly	Asp	Asp	105
106	Arg	Leu	Val	Ser	Val	His	Trp	Pro	Ala	Ser	Val	Arg	Thr	Ile	Leu	120
121	Gly	Ser	Gly	Cys	Leu	Ser	Asn	Leu	His	Asp	Ser	Ser	His	Lys	Gln	135
136	Arg	Lys	Lys	Val	Ile	Met	Arg	Ala	Phe	Ser	Arg	Glu	Ala	Leu	Glu	150
151	Cys	Tyr	Val	Pro	Val	Ile	Thr	Glu	Glu	Val	Gly	Ser	Ser	Leu	Glu	165
166	Gln	Trp	Leu	Ser	Cys	Gly	Glu	Arg	Gly	Leu	Leu	Val	Tyr	Pro	Glu	180
181	Val	Lys	Arg	Leu	Met	Phe	Arg	Ile	Ala	Met	Arg	Ile	Leu	Leu	Gly	195
196	Cys	Glu	Pro	Gln	Leu	Ala	Gly	Asp	Gly	Asp	Ser	Glu	Gln	Gln	Leu	210
211	Val	Glu	Ala	Phe	Glu	Glu	Met	Thr	Arg	Asn	Leu	Phe	Ser	Leu	Pro	225
226	Ile	Asp	Val	Pro	Phe	Ser	Gly	Leu	Tyr	Arg	Gly	Met	Lys	Ala	Arg	240
241	Asn	Leu	Ile	His	Ala	Arg	Ile	Glu	Gln	Asn	Ile	Arg	Ala	Lys	Ile	255
256	Cys	Gly	Leu	Arg	Ala	Ser	Glu	Ala	Gly	Gln	Gly	Cys	Lys	Asp	Ala	270
271	Leu	Gln	Leu	Leu	Ile	Glu	His	Ser	Trp	Glu	Arg	Gly	Glu	Arg	Leu	285
286	Asp	Met	Gln	Ala	Leu	Lys	Gln	Ser	Ser	Thr	Glu	Leu	Leu	Phe	Gly	300
301	Gly	His	Glu	Thr	Thr	Ala	Ser	Ala	Ala	Thr	Ser	Leu	Ile	Thr	Tyr	315
316	Leu	Gly	Leu	Tyr	Pro	His	Val	Leu	Gln	Lys	Val	Arg	Glu	Glu	Leu	330
331	Lys	Ser	Lys	Gly	Leu	Leu	Cys	Lys	Ser	Asn	Gln	Asp	Asn	Lys	Leu	345
346	Asp	Met	Glu	Ile	Leu	Glu	Gln	Leu	Lys	Tyr	Ile	Gly	Cys	Val	Ile	360
361	Lys	Glu	Thr	Leu	Arg	Leu	Asn	Pro	Pro	Val	Pro	Gly	Gly	Phe	Arg	375
376	Val	Ala	Leu	Lys	Thr	Phe	Glu	Leu	Asn	Gly	Tyr	Gln	Ile	Pro	Lys	390
391	Gly	Trp	Asn	Val	Ile	Tyr	Ser	Ile	Cys	Asp	Thr	His	Asp	Val	Ala	405
406	Glu	Ile	Phe	Thr	Asn	Lys	Glu	Glu	Phe	Asn	Pro	Asp	Arg	Phe	Met	420
421	Leu	Pro	His	Pro	Glu	Asp	Ala	Ser	Arg	Phe	Ser	Phe	Ile	Pro	Phe	435
436	Gly	Gly	Gly	Leu	Arg	Ser	Cys	Val	Gly	Lys	Glu	Phe	Ala	Lys	Ile	450
451	Leu	Leu	Lys	Ile	Phe	Thr	Val	Glu	Leu	Ala	Arg	His	Cys	Asp	Trp	465
466	Gln	Leu	Leu	Asn	Gly	Pro	Pro	Thr	Met	Lys	Thr	Ser	Pro	Thr	Val	480
481	Tyr	Pro	Val	Asp	Asn	Leu	Pro	Ala	Arg	Phe	Thr	His	Phe	His	Gly	495
496	Glu	Ile														

Figure 3.1: Sequence of the 497 amino acid of the CYP26A1 enzyme in human¹³⁹.

In order to find new potent CYP26 inhibitors, ligand docking was performed on this CYP26A1 model using the MOE software. These ligands should fit in the active site (have no steric clashes), have optimal binding with the protein residues by forming hydrogen and hydrophobic bonds and coordinate with the iron atom from the haem at a distance of 3 Å or less.

¹³⁹<http://www.expasy.org/uniprot/O43174>

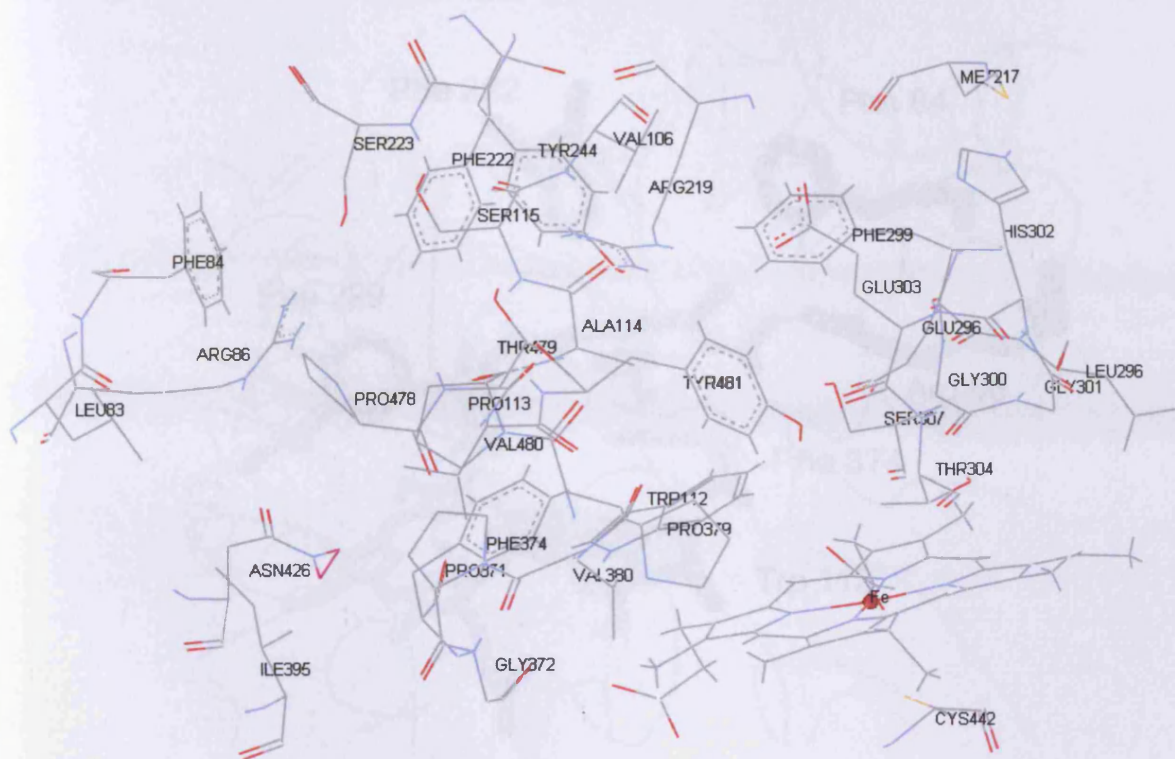


Figure 3.2: 3D Structure of the CYP26A1 model based on P450 3A4 template with residues within 7 Å radius of the haem molecule. These residues may form the main skeleton of the active site. Colour coding of the atoms: grey= carbon, red= oxygen, blue= nitrogen and brown= iron¹²⁶.

1.2) Docking studies

1.2.1) Docking of ATRA

ATRA is the natural substrate of the CYP26A1 enzyme. The result of the docking study is shown on Figure 3.3. The C-4 atom is positioned perpendicular at a distance of 5.3 Å from the haem iron. This distance would accommodate a molecule of water which will then be responsible for the 4-hydroxylation of the substrate. ATRA also interacts with the protein residues by forming multiple hydrophobic interactions as well as a hydrogen bond between its carboxylic acid group and ARG_86 which will hold the molecule in the active site¹²⁶.

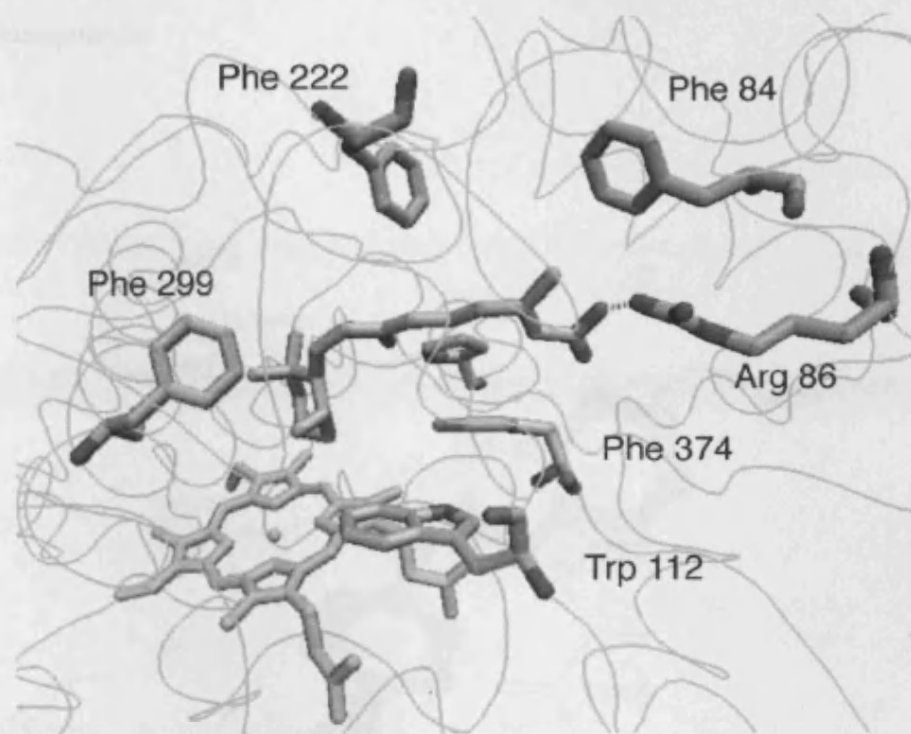


Figure 3.3: ATRA docked in the CYP26A1 active site, hydrogen bond between ATRA and ARG_86 is represented by a dashed line¹²⁶.

1.2.2) Docking of R115866

The triazole compound R115866 synthesised by Stoppie *et al.*⁹⁷ is one of the most potent CYP26 inhibitors ($IC_{50} = 4$ nM). Therefore the interaction of this drug with our active site model was evaluated.

As observed with other triazole and imidazole derivative inhibitors, the nitrogen atom of the aza-ring of both R115866 enantiomers is coordinated to the iron atom of the haem with a distance of 2.13 Å (*S*-) and 2.38 Å (*R*-). Multiple hydrophobic interactions with the side chains residues were observed (TRP_112, ALA_114, SER_115, MET_217, ARG_219, PHE_222, TYR_234, GLU_296, LEU_297, PHE_299, GLU_303, THR_304, PRO_369, VAL_370, PRO_371, PHE_374, THR_479) as well as a very interesting hydrogen bonding interaction between the secondary nitrogen of the *S*-enantiomer and the peptide carbonyl group

of ALA_114 (Figure 3.4). This hydrogen bond could contribute to the potent activity of these compounds.

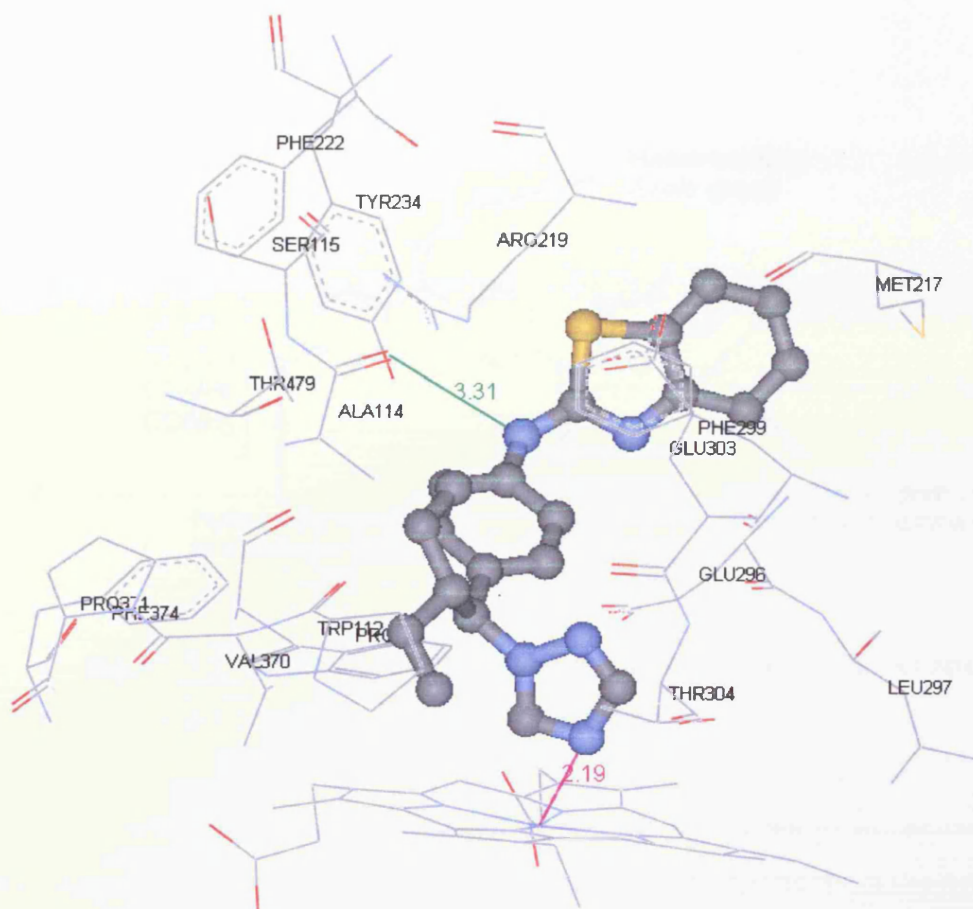


Figure 3.4: Active site region of CYP26A1 model after dynamics showing the *S*-enantiomer of the inhibitor ligand R115866 as a ball and stick form. Hydrogen bonding interactions are shown as green lines and distance from the haem is indicated with a purple line. Colour coding of the atoms: grey= carbon, red= oxygen, blue= nitrogen, brown= iron and yellow= sulphur. Amino-acid residues identified are involved in hydrophobic interactions.

As a consequence a new series of compounds which interact closely with the haem (less than 3 Å) and keep the hydrogen bonding of R115866 with ALA_114 was envisaged.

1.2.3) Docking of benzoxazol-2-yl-[phenylimidazol-1-ylmethyl]phenyl]amine derivatives

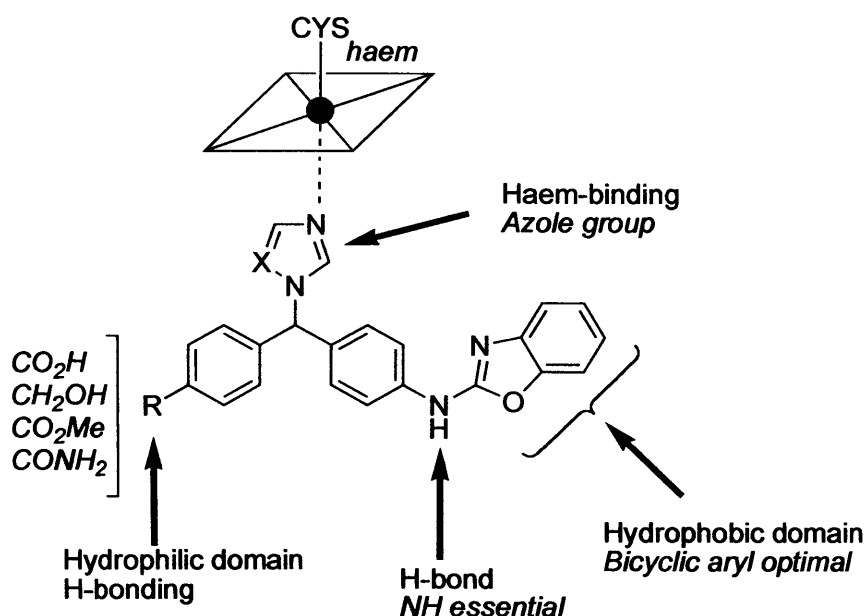


Figure 3.5: Structure and key binding interactions of the benzoxazol-2-yl-[phenylimidazol-1-ylmethyl]phenyl]amine derivatives

A new molecule with hydrogen bonds on both sides of the active site was investigated. These two hydrogen bonds could hold the molecule in the hydrophobic tunnel of the active site and thus increase the activity. After further investigations, the replacement of the alkyl chain of R115866 by a substituted phenyl ring showed interesting results with OH, OMe, OAc, CN, CH₂OH, COOH, COOMe and CONH₂ as substituents (Figure 3.5).

In some cases, the hydrogen bond, observed in R115866 docking, between the benzoxazole nitrogen and ALA_114 was kept (**B** and **K'**) or replaced by another hydrogen bond with the next peptide SER_115 (**B'**, **H**, **H'** and **J**).

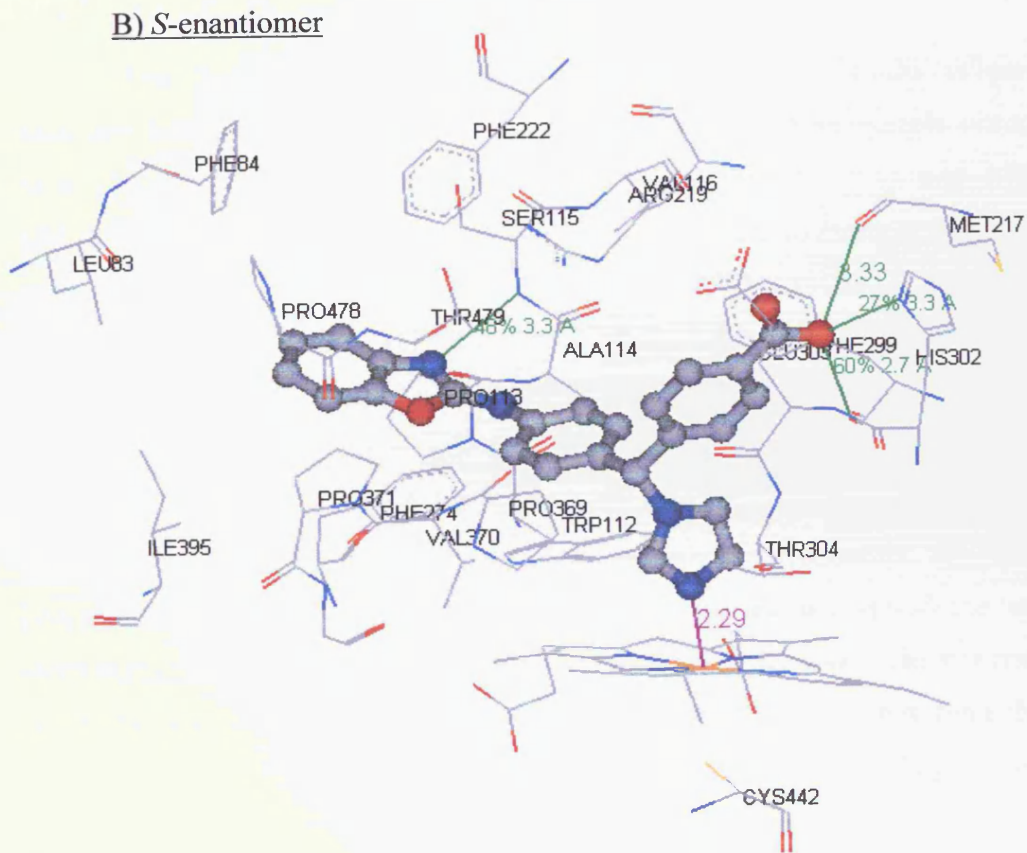
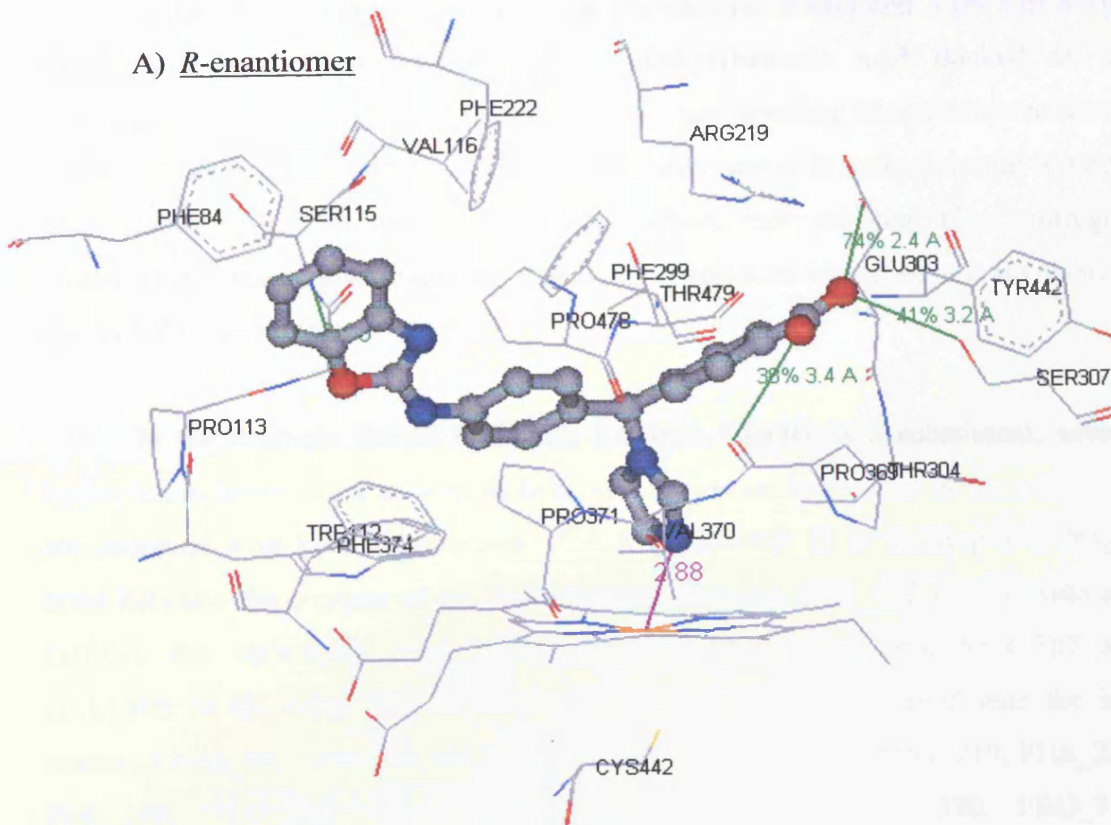


Figure 3.6: Diagram showing both enantiomers *R* (**H**) and *S* (**H'**) of 4-{[4-(benzoxazol-2-ylamino)phenyl]imidazol-1-ylmethyl}benzoic acid docked at the active site region of the CYP26A1 model. Hydrogen bonding interactions are shown as green lines and co-ordination with the transition metal is indicated with a purple line. Colour coding of the atoms: grey= carbon, red= oxygen, blue= nitrogen, brown= iron and yellow= sulphur. Amino-acid residues identified are involved in hydrophobic interactions.

In the example shown in Figure 3.6 with COOH as a substituent, several hydrophobic interactions as well as hydrogen bonds on both sides of the active site are observed with both enantiomers. The *R*-enantiomer **H** is forming a hydrogen bond between the oxygen of the benzoxazole ring and SER_115 on one side and between the carboxylic acid group and THR_479, PRO_369, SER_307 and GLU_303 on the other side. Hydrophobic interactions are observed with the side chains of PHE_84, TRP_112, PRO_113, SER_115, VAL_116, ARG_219, PHE_222, PHE_299, GLU_303, THR_304, SER_307, PRO_369, VAL_370, PRO_371, PHE_374, TYR_442, PRO_478 and THR_479.

The *S*-enantiomer **H'** displayed also interesting results (Figure 3.5), hydrogen bonds were observed on one side between the benzoxazole nitrogen and SER_115 and on the other side between the carboxylic acid and MET_217, HIS_302, PHE_299. A large number of hydrophobic interactions are also observed with the residues LEU_83, PHE_84, TRP_112, PRO_113, ALA_114, SER_115, VAL_116, MET_217, ARG_219, PHE_222, PHE_274, PHE_299, HIS_302, GLU_303, THR_304, PRO_369, VAL_3770, PRO_371, ILE_395, PRO_478 and THR_479. Both enantiomers are also interacting closely with the haem with a distance of respectively 2.88 Å for **H** and 2.29 Å for **H'**.

The docking of the other para-substituted compounds displayed also interesting results (Table 3.1). They all showed a good interaction with the haem iron atom between 1.85 Å and 3.40 Å, except the methoxy derivative (**E**, **E'**) and the *R*-enantiomer of the methyl derivative (**C**) that fit in the active site but don't show any interaction with the haem (Table 3.1). They also display a large number of

hydrophobic interactions and most of them form hydrogen bonds with the protein residues.

Although they show good interaction with the haem, the small substituents (H, F, Me, OH, OMe and CN) seem to be too far from the edge of the active site to form any hydrogen bond with the protein residues. The only one observed is with the hydroxy group of compound **D'** and HIS_271. The presence of larger substituents seems to be required.

In fact, the use of larger substituents (CO₂Me, COOH, CH₂OH, CONH₂, OAc), as expected, allowed the formation of hydrogen bonds with different protein residues (SER_307, ARG_219, THR_479, PRO_369, SER_307, GLU_303, MET_217, HIS_302, PHE_299) depending on the orientation of the molecule and the enantiomer. However only compounds **H**, **H'**, **J** and **K'** are able to hold the molecule on both sides of the active site.

Table 3.1: Interactions observed between the different inhibitors and the active site:

R	Enantiomer	Distance from haem (Å)	Hydrogen bonding	Name
H	<i>R</i>	2.57	-	A
H	<i>S</i>	2.77	-	A'
F	<i>R</i>	2.12	ALA_114	B
F	<i>S</i>	3.16	SER_115	B'
Me	<i>R</i>	-	-	C
Me	<i>S</i>	2.11	-	C'
OH	<i>R</i>	2.78	-	D
OH	<i>S</i>	2.73	HIS_271	D'
OMe	<i>R</i>	-	-	E
OMe	<i>S</i>	-	-	E'
CN	<i>R</i>	2.98	-	F
CN	<i>S</i>	2.26	-	F'
CO ₂ Me	<i>R</i>	3.12	SER_307	G
CO ₂ Me	<i>S</i>	1.85	ARG_219	G'

COOH	<i>R</i>	2.88	SER_115, THR_479, PRO_369, SER_307, GLU_303	H
COOH	<i>S</i>	2.29	MET_217, HIS_302, PHE_299, SER_115,	H'
CH ₂ OH	<i>R</i>	3.28	PRO_369	I
CH ₂ OH	<i>S</i>	3.28	ARG_219, GLU_303	I'
CONH ₂	<i>R</i>	2.84	SER_115, ARG_219	J
CONH ₂	<i>S</i>	2.31	-	J'
OAc	<i>R</i>	2.94	HIS_302	K
OAc	<i>S</i>	3.40	ALA_114, ARG_219	K'

These substituents are also convenient because it is possible to synthesise a large variety of compounds from the same skeleton by simple reactions such as oxidation, reduction, esterification and amidation (Figure 3.7).

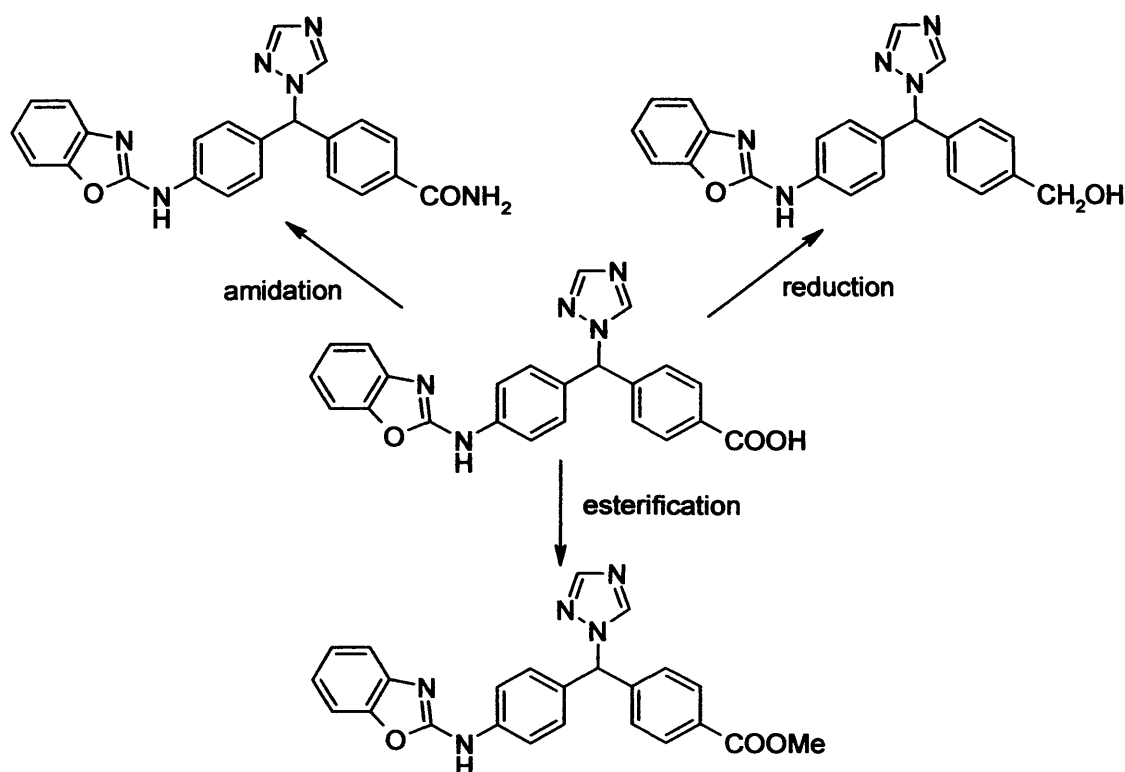


Figure 3.7: Possible transformation of the substituents by simple reactions.

1.2.4) Investigation of other substitutions

After the interesting results observed for the benzoxazol-2-yl-[phenylimidazol-1-ylmethyl]phenyl]amine derivatives with a para substituent, ortho and meta substitution as well as a di-substitution on the phenyl ring were also investigated. As examples, three substituents of different size and properties were employed: CH₂OH, OH and Me. Results are reported in Table 3.2.

Table 3.2: Interactions observed on the other positions:

R	Position	Enantiomer	Distance from haem (Å)	Hydrogen bonds	Name
Me	Ortho	R	2.85	-	L
Me	Ortho	S	1.49	-	L'
OH	Ortho	R	2.87	GLU_303	M
OH	Ortho	S	1.82	GLU_296	M'

CH ₂ OH	Ortho	<i>R</i>	1.82	-	N
CH ₂ OH	Ortho	<i>S</i>	2.02	-	N'
Me	Meta	<i>R</i>	2.25	GLU_296	O
Me	Meta	<i>S</i>	1.73	-	O'
OH	Meta	<i>R</i>	1.57	PHE_299	P
OH	Meta	<i>S</i>	2.17	-	P'
CH ₂ OH	Meta	<i>R</i>	-	-	Q
CH ₂ OH	Meta	<i>S</i>	1.86	-	Q'
Me	2, 3	<i>R</i>	2.98	-	R
Me	2, 3	<i>S</i>	2.10	-	R'
OH	2, 3	<i>R</i>	1.91	PHE_299	S
OH	2, 3	<i>S</i>	1.35	GLY_372	S'
CH ₂ OH	2, 3	<i>R</i>	-	-	T
CH ₂ OH	2, 3	<i>S</i>	1.82	-	T'
Me	2, 4	<i>R</i>	-	-	U
Me	2, 4	<i>S</i>	1.63	GLU_296	U'
OH	2, 4	<i>R</i>	1.66	-	V
OH	2, 4	<i>S</i>	1.96	-	V'
CH ₂ OH	2, 4	<i>R</i>	-	-	W
CH ₂ OH	2, 4	<i>S</i>	-	-	W'
Me	2, 5	<i>R</i>	2.74	-	X
Me	2, 5	<i>S</i>	3.75	-	X'
OH	2, 5	<i>R</i>	1.54	-	Y
OH	2, 5	<i>S</i>	2.63	-	Y'
CH ₂ OH	2, 5	<i>R</i>	1.33	GLU_296	Z
CH ₂ OH	2, 5	<i>S</i>	2.64	PHE_299 GLU_303	Z'
Me	2, 6	<i>R</i>	2.14	-	AA
Me	2, 6	<i>S</i>	3.49	-	AA'
OH	2, 6	<i>R</i>	1.80	-	AB

OH	2, 6	<i>S</i>	1.80	-	AB'
CH ₂ OH	2, 6	<i>R</i>	1.36	GLY_300 PHE_299	AC
CH ₂ OH	2, 6	<i>S</i>	2.08	-	AC'
Me	3, 4	<i>R</i>	-	-	AD
Me	3, 4	<i>S</i>	-	-	AD'
OH	3, 4	<i>R</i>	1.35	GLU_303	AE
OH	3, 4	<i>S</i>	1.60	PRO_338	AE'
CH ₂ OH	3, 4	<i>R</i>	3.31	-	AF
CH ₂ OH	3, 4	<i>S</i>	4.02	-	AF'
Me	3, 5	<i>R</i>	2.03	-	AG
Me	3, 5	<i>S</i>	2.36	-	AG'
OH	3, 5	<i>R</i>	1.99	GLU_296	AH
OH	3, 5	<i>S</i>	1.88	-	AH'
CH ₂ OH	3, 5	<i>R</i>	1.98	PRO_369 PHE_299 GLU_303	AI
CH ₂ OH	3, 5	<i>S</i>	2.02	PRO_369	AI'

In the ortho position (compounds **L**, **L'**, **M**, **M'**, **N**, **N'**), the 6 compounds showed a good coordination with the haem (1.49 Å to 2.87 Å). However, only the compounds with the hydroxy substituent are able to form some hydrogen bonds, between the benzoxazole nitrogen and GLU_296 for the *S*-enantiomer and between the OH substituent and GLU_303 for the *R*-enantiomer.

Concerning the meta derivative (**O**, **O'**, **P**, **P'**, **Q**, **Q'**), The *R*-enantiomer of both small substituent CH₃ and OH (**O** and **P**) gave the best results. They are respectively 2.25 Å and 1.57 Å from the haem and formed hydrogen bonds with GLU_296 (secondary amine of **O**) and PHE_299 (OH substituent of **P**). The 4 others compounds interact also well with the haem, except **Q'** but do not form any hydrogen bonds with the protein residues. In conclusion, the size of the substituent may be an issue in this position especially with the *R*-enantiomer.

Then compounds with a di-substitution were investigated using the same three substituents. The 2,3-substitution (compounds **R**, **R'**, **S**, **S'**, **T**, **T'**) gave similar results than the single ortho and meta substitution, the compounds of most interest were the OH-derivatives **S** and **S'** which are respectively 1.91 Å and 1.35 Å from the haem and form hydrogen bond with their OH substituent and PHE_299 for **S** and GLY_372 for **S'**. Compounds **R**, **R'** and **T'** are also quite close to the haem, respectively 2.98 Å, 1.91 Å and 1.82 Å although they do not form hydrogen bonds with the protein residues. As for the meta substitution, the *R*-enantiomer of the CH₂OH compound fitted in the active site but did not interact with the haem. It confirms that a large substituent in the meta position may not be tolerated.

The ortho-para (2,4) substituted compounds (**U**, **U'**, **V**, **V'**, **W**, **W'**) did not fit as well in the active site. Although **U**, **W** and **W'** fit in the active site, they do not form any interaction with the haem. Large substituents do not seem to be tolerated in these positions. The OH derivatives **V** and **V'** and the *S*-enantiomer of the methyl derivative **U'** are interacting strongly with the haem with transition metal coordination at 1.66 Å, 1.96 Å and 1.63 Å respectively. However, the methyl compound **U'** is the only one forming a hydrogen bond on GLU_296 using its secondary amine.

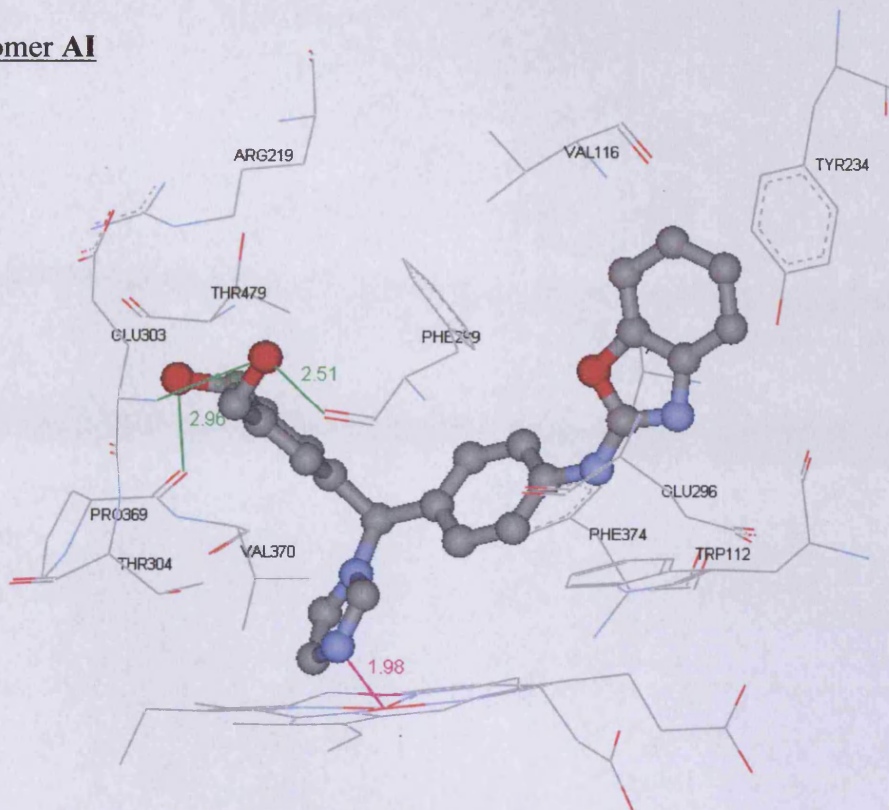
The 2,5-substituted compounds (**X**, **X'**, **Y**, **Y'**, **Z**, **Z'**) interacted with the haem iron between 1.33 Å and 3.75 Å. Compounds with a methyl or a hydroxy substitution (**X**, **X'**, **Y**, **Y'**) did not form any hydrogen bonds with the protein residues. The presence of a larger group seems to be required. Compounds **Z** and **Z'** with CH₂OH as a substituent had transition metal coordination with the haem and formed hydrogen bonding: the *S*-enantiomer with GLU_296 using its secondary amine and the *R*-enantiomer with PHE_299 and GLU_303 using one of its OH substituents.

Compounds with a di-ortho (2,6) substitution (**AA**, **AA'**, **AB**, **AB'**, **AC**, **AC'**) also allow the three different substituents. They displayed very similar results to the 2,5-derivatives, interacting well with the haem (between 3.49 Å and 1.36 Å) but only the introduction of a CH₂OH substituent allowed formation of hydrogen bonding. The CH₂OH substituent of the *R*-enantiomer **AC** interacts with GLY_300 and PHE_299.

In the 3,4 position, the presence of an electron donating substituent seems to be essential. Both enantiomers of the methyl substituted compounds (**AD**, **AD'**) are not able to interact with the haem. The presence of the CH₂OH substituent as well gave disappointing results. Although they fit in the active site, both enantiomers are quite far to the haem (3.31 Å for the *R*-enantiomer **AF** and 4.02 Å for the *S*-enantiomer **AF'**) and no hydrogen bonds were observed. On the other hand, the OH substituted compounds **AE** and **AE'** displayed interesting results. They are both very close to the haem, respectively 1.35 Å and 1.60 Å and form hydrogen bonds with some protein residues with their OH groups (GLU_303 for **AE** and PRO_369 for **AE'**).

The di-meta derivatives (**AG**, **AG'**, **AH**, **AH'**, **AI**, **AI'**) are the most promising compounds. They are all at a short distance from the haem (between 2.36 Å and 1.88 Å). The presence of a large electron donating substituent (CH₂OH) also seems to improve their correlation in the active site by forming some hydrogen bonds with the protein residues. The *R*-enantiomer **AI** formed hydrogen bonds with each of its CH₂OH group and the amino-acid PRO_369, PHE_299 and GLU_303, these two hydrogen bonds are able to hold the molecule on two different sides of the hydrophobic pocket. The *S*-enantiomer **AI'** interacts with only one of its CH₂OH substituents and PRO_369 (Figure 3.8). The OH derivative **AH** was also able to form hydrogen bond with the protein residue GLU_296. However di-meta compounds **AI** (TRP_112, ALA_114, VAL_116, ARG_219, TYR_234, GLU_296, PHE_299, GLU_303, THR_304, PRO_369, VAL_370, PHE_374 and THR_479) and **AI'** (TRP_112, ALA_114, VAL_116, ARG_219, PHE_222, TYR_234, GLU_296, PHE_299, GLU_303, THR_304, PRO_369, VAL_370, PRO_371, PHE_374, THR_479) do not display as many hydrophobic interactions with the protein residues as the para-substituted compounds **H** and **H'**.

R-enantiomer AI



S-enantiomer AI'

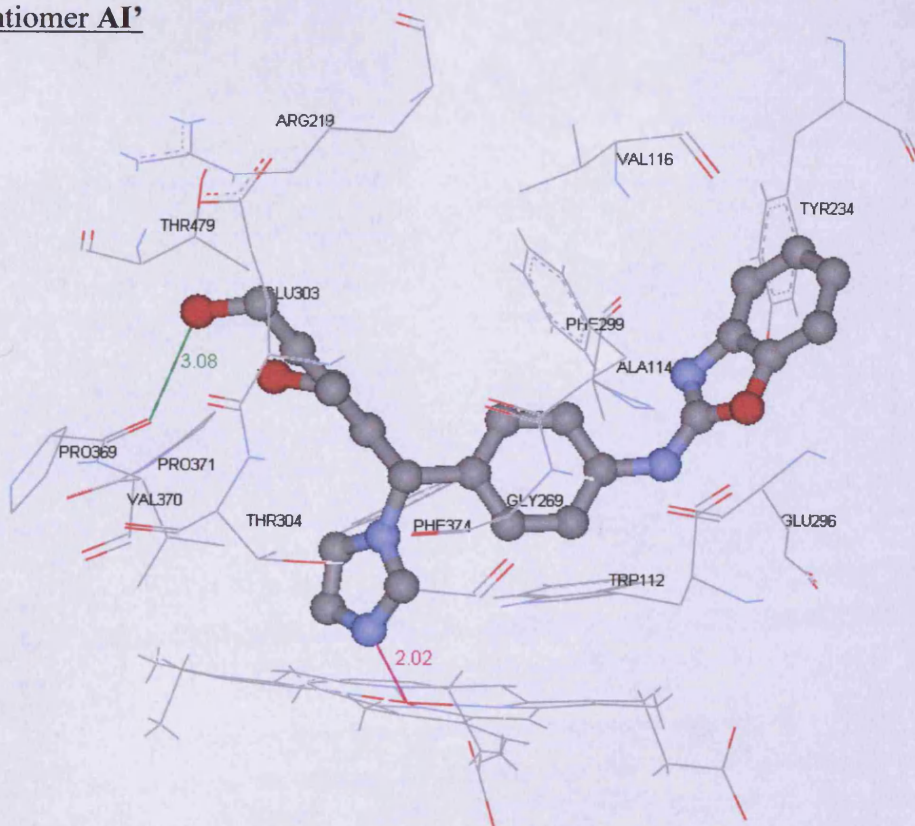
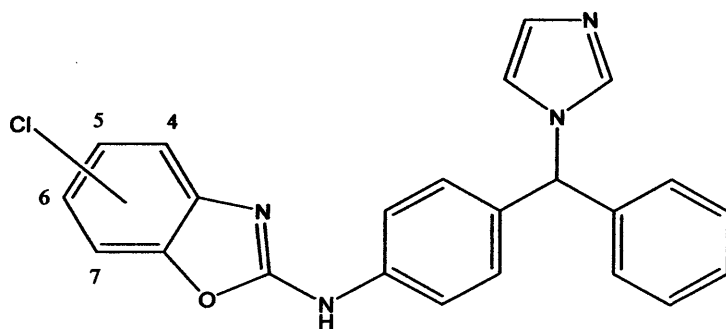


Figure 3.8: Diagram showing both enantiomers *R*-(AI) and *S*-(AI') of (3-{[4-(benzoxazol-2-ylamino)phenyl]imidazol-1-ylmethyl}-5-hydroxymethylphenyl)methanol docked at the active site region of the CYP26A1 model. Hydrogen bonding interactions are shown as green lines and co-ordination with the transition metal is indicated with a purple line. Colour coding of the atoms: grey= carbon, red= oxygen, blue= nitrogen, brown= iron and yellow= sulphur. Amino-acid residues identified are involved in hydrophobic interactions.

Although most of these compounds displayed interesting results and especially a very close interaction with the haem iron, none was able to keep the hydrogen bond observed in R115866 with SER_115 and thus to hold the molecule on both sides of the active site. They also appear to be very challenging to synthesise, our effort will thus focus on the synthesis of para-derivatives.

1.2.5) Substitution on the benzoxazole ring and change in the aza-ring

After looking at different substituents on the phenyl ring of the molecule, other changes such as a halogen substitution of the benzoxazole ring and a change of the imidazole ring into a triazole or tetrazole ring were investigated. The results are reported in Tables 3.3 and 3.4.



In the case of the halogen substitution on the benzoxazole ring, the chlorine atom was used as an example (Table 3.3). This substitution seemed to be tolerated; all compounds except the 4-substituted AM' fitted nicely in the active site. Though none were able to form any hydrogen bonds with the protein residues, they appear to be closer to the haem than the unsubstituted compounds A and A' which displayed a distance of respectively 2.57 Å and 2.77 Å. Consequently, a chlorine substitution on

position 4, 5 and 6 of the benzoxazole ring (compounds AJ, AJ', AK, AK', AL, AL') could improve the activity.

Table 3.3: Effects of a chlorine substitution on the benzoxazole ring:

Position	Enantiomer	Distance from haem (Å)	Hydrogen bonds	Name
4	<i>R</i>	1.97	-	AJ
4	<i>S</i>	1.92	-	AJ'
5	<i>R</i>	2.20	-	AK
5	<i>S</i>	1.62	-	AK'
6	<i>R</i>	1.92	-	AL
6	<i>S</i>	2.00	-	AL'
7	<i>R</i>	1.99	-	AM
7	<i>S</i>	-	-	AM'

The replacement of the imidazole ring by a 1,2,4-triazole, a 1,3,4-triazole and a tetrazole ring also seems to decrease the distance between the aza-ring nitrogen and the haem (Table 3.4). All compounds are very close to the haem iron (between 2.47 Å and 1.26 Å), even if, as the imidazole compounds, they are not able to form any hydrogen bonds with the amino-acid residues.

However because of its enhanced binding properties with the haem¹¹⁴, the imidazole ring should display a lower IC₅₀ than the other azoles, especially the 1,3,4-triazole and the tetrazole ring.

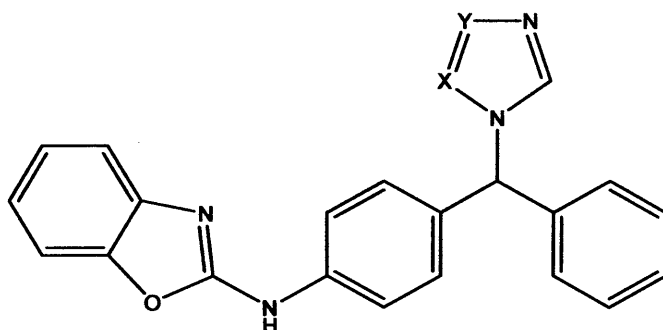


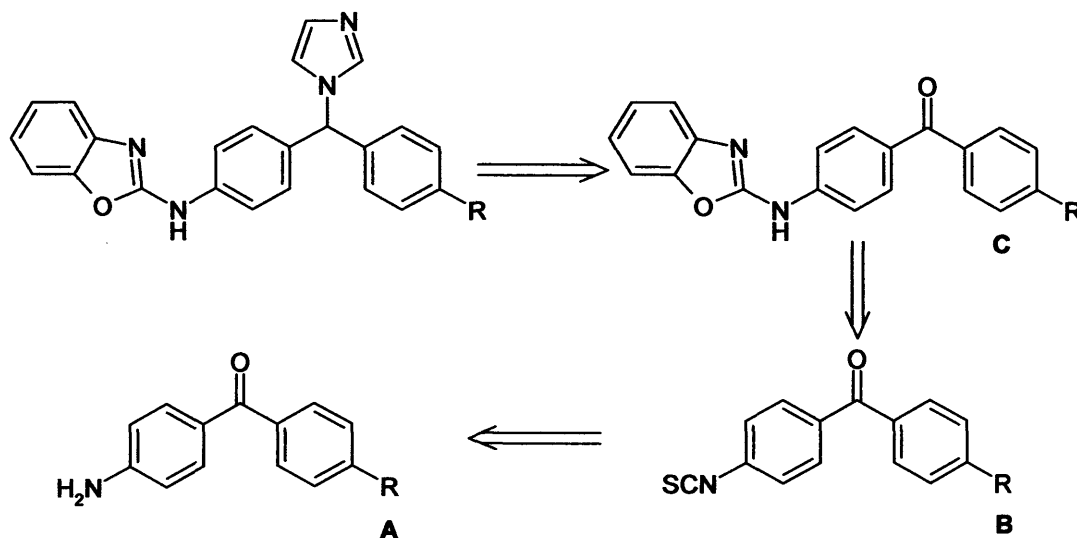
Table 3.4: Effects of a change in the aza-ring:

X	Y	Enantiomer	Distance from haem (Å)	Hydrogen bonds	Name
CH	CH	<i>R</i>	2.57	-	A
CH	CH	<i>S</i>	2.77	-	A'
N	CH	<i>R</i>	1.91	-	AN
N	CH	<i>S</i>	2.47	-	AN'
CH	N	<i>R</i>	1.56	-	AO
CH	N	<i>S</i>	1.26	-	AO'
N	N	<i>R</i>	1.56	-	AP
N	N	<i>S</i>	1.39	-	AP'

This new series of benzoxazole derivatives showed very promising results on docking studies with our CYP26A1 active site model. They displayed close interaction with the haem iron as well as multiple hydrophobic interactions and hydrogen bonds with the protein residues. A method for their synthesis was thus investigated, starting with the para-substituted compounds.

2) SYNTHESIS AND DISCUSSION

2.1) Retrosynthesis



Scheme 3.1: Disconnective strategy toward substituted *N*-phenylbenzo[*d*]oxazolamines

The benzoxazol-2-yl-[phenylimidazol-1-ylmethyl]phenylamine could be envisaged from the corresponding benzophenone C. This benzophenone could be transformed, as in the first series, by a reduction of the ketone followed by the addition of the triazole ring using the Staab method¹²⁰ (Scheme 3.1).

The benzoxazole ring of C could be obtained by the reaction of the isothiocyanate B and 2-hydroxyaniline with nickel peroxide as a catalyst¹⁴⁰.

Then, the isothiocyanate B could be prepared by the action of di-2-pyridyl thionocarbonate (DPT)¹⁴¹ or thiophosgene¹⁴² on the aminobenzophenone A.

¹⁴⁰ Ogura H., Mineo S. and Nakagawa K.; Studies on heterocyclic compounds. Synthesis of 2-substituted aminobenzoxazoles with nickel peroxide. *Chem. Pharm. Bull.*, **1981**, *29*, 1518-1524.

¹⁴¹ Kim S. and Yi K.Y.; Di-2-pyridyl thionocarbonate. A new reagent for the preparation of isothiocyanates and carbodiimides. *Tetrahedron Lett.*, **1985**, *26*, 1661-1664.

¹⁴² Bertha F., Hornyak G., Lempert K.Z.K. and Toht E.P.G.; Benzoxadiazocines, benzothiadiazocines and benzotriazocines-III: The synthesis of 2-(subst.)amino- and 2-(2-subst.hydrazino)-6-(alkylsulfonyl and arylsulfonyl)-5,6-dihydro-4H-3,1,6-benzothiadiazocines. *Tetrahedron*, **1983**, *39*, 1203.

2.2) Synthesis of the 4-substituted aminobenzophenone A

Three methods were envisaged to synthesise these aminobenzophenones: a Friedel-Crafts acylation, a Negishi coupling and a method developed by Samietz in 1895¹⁴³.

2.2.1) Formation of A by a Friedel-Crafts acylation

The Friedel-Crafts acylation is the most important method for the preparation of aryl ketones. This electrophilic aromatic substitution allows the synthesis of monoacylated products from the reaction between arenes and acyl chlorides.



The mechanism of this reaction involves the formation of the acyl cation by the action of the Lewis acid (generally aluminum chloride) on the acyl chloride. This acyl cation is then attacked by an ion pair of the aryl ring to form the aryl ketone (Figure 3.9).

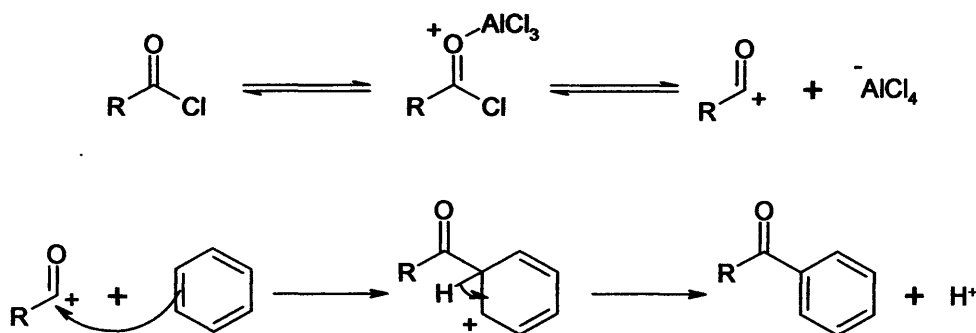


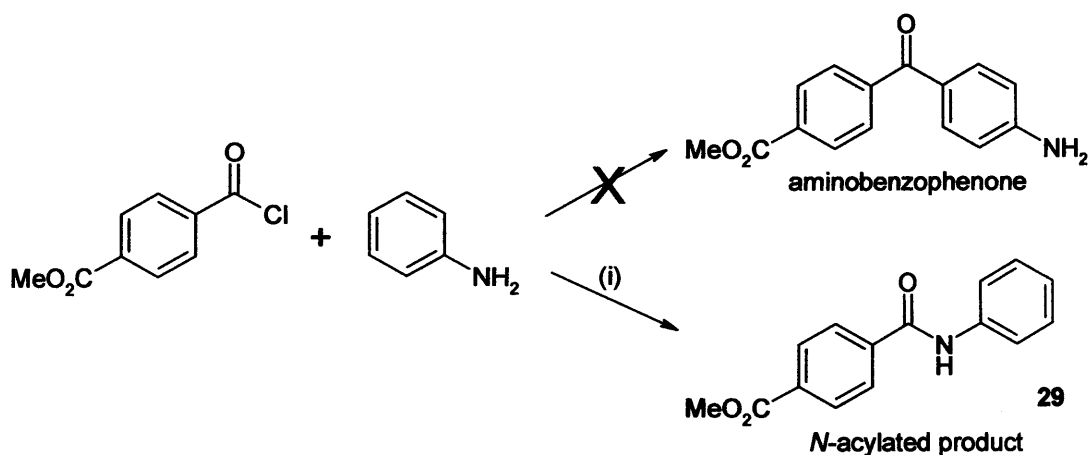
Figure 3.9: Mechanism of the Friedel-Crafts acylation¹⁴⁴

The Friedel-Crafts acylation was applied to the synthesis of the aminobenzophenone A.

¹⁴³ Samietz E.; *p*-Nitrophenyl-tolylketon. *Ann. Chem.*, 1895, 321-332.

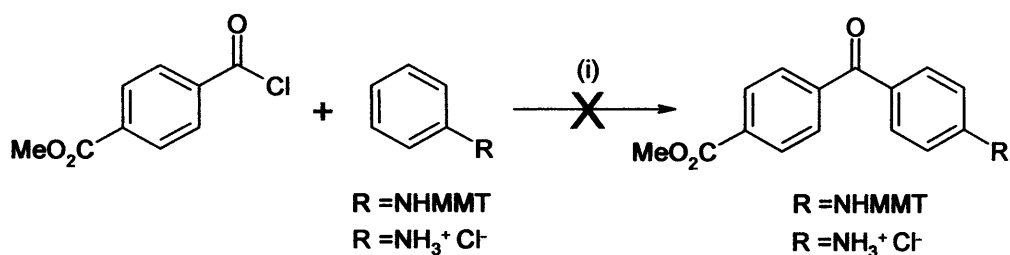
¹⁴⁴ Smith M.B. and March J.; *March's advanced organic chemistry: reactions, mechanisms and structure* 5th edition. *John Wiley and Sons, Inc.* 2001, 712-715.

The first attempt was the reaction between methyl-4-chlorocarbonylbenzoate and aniline with an excess of AlCl_3 (3 equivalents) and CH_2Cl_2 as solvent. This reaction did not form the aminobenzophenone but resulted in the *N*-acylated product **29** with a low 20 % yield (Scheme 3.2).



Scheme 3.2: Reagents and Conditions (i) AlCl_3 , CH_2Cl_2 , o/n, rt, 20 %.

The problem of the *N*-acylation could be solved by protecting the amino group of the aniline. The protecting group should be stable to the conditions of the Friedel-Crafts acylation (Lewis acid) and subsequently cleaved easily without loss of the ester. The MMT (monomethoxytrityl) group was suitable for these conditions.



Scheme 3.3: Reagents and Conditions (i) AlCl_3 , CH_2Cl_2 , o/n, rt.

The MMT protected aniline was prepared by reaction of aniline with 4-monomethoxytrityl chloride in anhydrous pyridine and Et_3N overnight¹⁴⁵. The reaction did not go to completion resulting in a 34 % yield (Scheme 3.3). The poor yield could be explained by steric limitations.

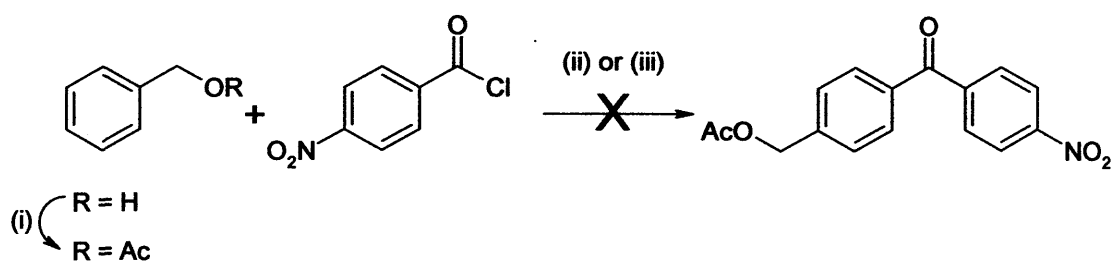
¹⁴⁵ Will D.W., Breipohl G., Langner D., Knolle J. and Uhlmann E.; Two recent examples of the use of MMT as an amino protecting group. *Tetrahedron*, 1995, 51, 12069-12082.

Then, the Friedel-Crafts acylation was attempted again using the protected aniline; however no reaction was observed (Scheme 3.3).

The size of the protecting group could be a problem to achieve the acylation. So, a reaction with a smaller group was envisaged: the aniline hydrochloride. The chloride salt should be a good enough protection for this type of reaction. Unfortunately no reaction was observed with this amine salt (Scheme 3.3). The reason could be the problem of solubility of the aniline hydrochloride in dichloromethane.

A new method with different starting material (protected benzyl alcohol and 4-nitrobenzoyl chloride) was then investigated¹⁴⁶.

The acetyl protecting group was chosen for the benzyl alcohol as it is stable to the Friedel-Crafts conditions and to the hydrogenation envisaged at the next step to reduce the nitro group to an amino group.



Scheme 3.4: Reagents and Conditions (i) Ac_2O , pyridine, DMAP, o/n, rt, 98 %; (ii) AlCl_3 , CH_2Cl_2 , o/n, rt then reflux, 2h; (iii) AlCl_3 , CS_2 , o/n, rt.

Acetic anhydride was added to a solution of benzyl alcohol and DMAP in dry pyridine and the mixture was stirred at room temperature overnight (Scheme 3.4). The reaction went to completion with a 98 % yield, and the product could be used in the next step without any chromatographic purification¹⁴⁷.

Then for the Friedel-Crafts acylation, an excess of benzylacetate and aluminum chloride (two equivalents) were added to a solution of 4-nitrobenzoyl

¹⁴⁶ Carrol R.D., Miller M.W., Mylari B.L., Chappel L.R., Howes H.L., Lynch M.J., Lynch J.E., Gupta S.K., Rash J.J. and Koch R.C.; Anticoccidial derivatives of 6-azauracil. 5. Potentiation by benzophenone side chains. *J. Med. Chem.*, **1983**, *26*, 96-100.

¹⁴⁷ Weber H. and Khorana H.G.; CIV. Total synthesis of the structural gene for an alanine transfer ribonucleic acid from yeast. Chemical synthesis of an iscosadesoxyribonucleotide corresponding to the nucleotide sequence 21 to 40. *J. Mol. Biol.*, **1972**, *72*, 219-249.

chloride and dichloromethane as solvent. The reaction was stirred at room temperature overnight and refluxed for two hours, but again no reaction was observed. Employing carbon disulphide instead of dichloromethane as solvent¹⁴⁸ was also unsuccessful (Scheme 3.4).

No efficient methods to synthesise the aminobenzophenone **A** by a Friedel-Crafts acylation could be found, so a new method using a Negishi coupling was investigated.

2.2.2) Formation of **A** by a Negishi coupling

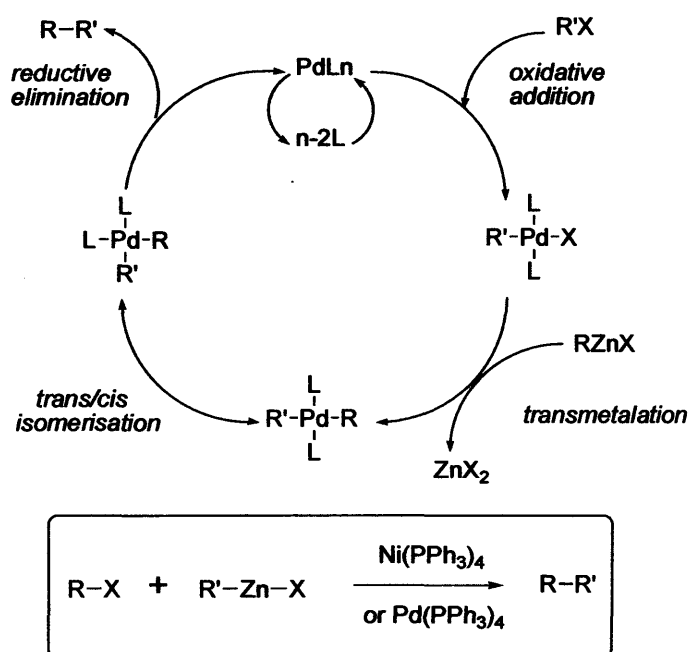


Figure 3.10: Mechanism of the Negishi coupling

¹⁴⁸ De Souza A.O., Hemerly F.P., Busallo A.C., Melo P.S., Machado G.M.C., Miranda C.C., Santa-Rita R.M., Haun M., Leon L.L., Sato D.N., De Castro S.L. and Duran N.; 3-[4'-bromo-(1,1'-biphenyl)-4-yl]-*N,N*-dimethyl-3-(2-thienyl)-2-propen-1-amine: synthesis, cytotoxicity, and leishmanicidal, trypanocidal and antimycobacterial activities. *J. Antimicrob. Chemother.*, 2002, 50, 629-637.

The Negishi Coupling, published in 1977, was the first reaction that allowed the preparation of unsymmetrical biaryls in good yields. It is a Pd- or Ni-catalysed cross-coupling reaction forming a carbon-carbon bond¹⁴⁹.

The mechanism of this reaction involves four steps (Figure 3.10):

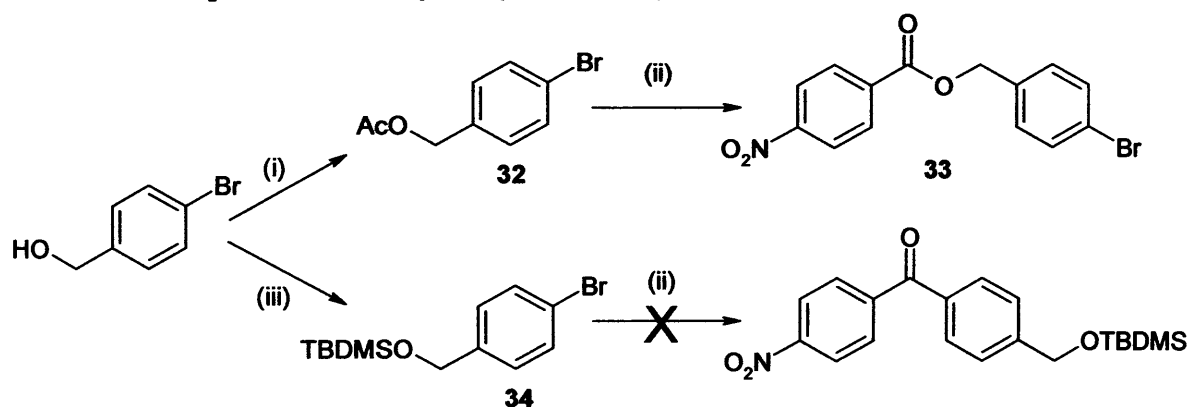
- The oxidative addition: The alkyl halide R'X coordinates to the metal which loses two of its ligands.

- The transmetalation: The alkyl of the zinc metal is exchanged with the halide of the palladium to form the four coordinated palladium with two ligands and the two alkyl groups R and R'.

- The *trans/cis* isomerisation: The two alkyl groups are transformed from the *trans* to the *cis* conformation.

- The reductive elimination: The palladium is reduced to its second oxidative state by losing the two alkyl groups which form the expected product RR'.

The Negishi coupling was attempted to synthesise the aminobenzophenone A. A protection of the alcohol function was needed to avoid the possible esterification, again the acetyl protecting group was chosen. The acetylation was performed using acetic anhydride with DMAP and pyridine¹⁴⁷ and the product 32 was obtained pure with 99 % yield (Scheme 3.5).



Scheme 3.5: Reagents and Conditions (i) Ac₂O, pyridine, DMAP, o/n, rt, 99 %; (ii) (a) nBuLi, THF, -78 °C, (b) ZnCl₂, -78 °C to rt, (c) Pd(PPh₃)₄, 4-nitrobenzoyl chloride, o/n, rt, 85 %; (iii) TBDMSCl, imidazole, DMF, 4 h, rt, 95 %.

¹⁴⁹ Huo S.; Highly efficient, general procedure for the preparation of alkylzinc reagents from unactivated alkyl bromides and chlorides. *Org. Lett.*, 2003, 5, 423-425.

The Negishi coupling was performed in three steps¹⁵⁰. In the first step, *n*-butyllithium was added dropwise to a solution of 4-bromobenzylacetate in tetrahydrofuran at -78 °C. Then a THF solution of zinc chloride was added to the mix and the reaction allowed warming to room temperature. Finally, the reaction was cooled to 0 °C and a catalytic amount of tetrakis(triphenylphosphine)palladium(0) was added followed by the addition of 4-nitrobenzoyl chloride (Scheme 3.5). The reaction mixture was stirred overnight. Unfortunately, the acetyl group was not stable under these conditions and as a result the ester **33** was formed with 85 % yield.

A new protecting group was consequently envisaged. A silyl group such as TBDMS (*tert*-butyldimethylsilyl) was considered as quite stable to a variety of organic reactions and particularly to basic conditions. It is also quite easy to introduce and can be removed under mild conditions¹⁵¹.

The TBDMS protection was performed using *tert*-butyldimethylsilyl chloride in dry DMF and imidazole as a catalyst¹⁵² (Scheme 3.5). The mixture was allowed to stir at room temperature during four hours. This reaction resulted in 95 % yield of pure product **34** after the extraction, no further purification was required.

Then the Negishi coupling was applied to this protected 4-bromobenzyl alcohol **34** following the same method previously described (Scheme 3.5). The TBDMS protection was stable to the reaction conditions, however no reaction was observed.

The Negishi cross-coupling reaction was thus not suitable for the formation of the required benzophenone **A**; therefore the method developed by Samietz in 1895 was attempted.

2.2.3) Formation of **A** by Samietz method¹⁴³

This method allowed the synthesis of **A** in three steps: (1) a Friedel-Crafts acylation between toluene and nitrobenzoyl chloride in order to form 4-Methyl-

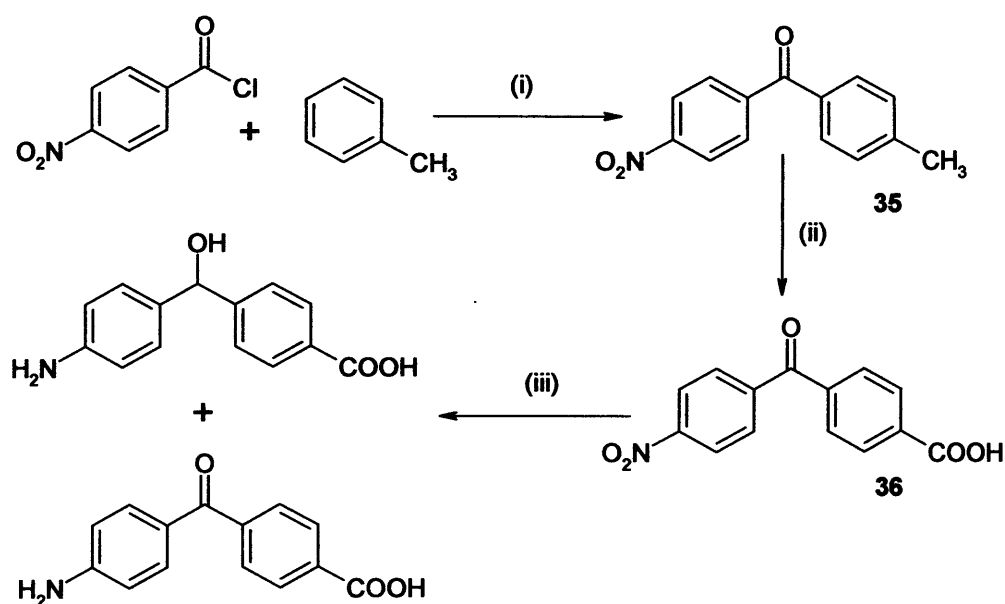
¹⁵⁰ Ottosen E.R., Sørensen M.D., Björkling F., Skak-Nielsen T., Fjording M.S., Aaes H. and Binderup L.; Synthesis and structure-activity relationship of aminobenzophenones. A novel class of p38 MAP kinase inhibitors with high antiinflammatory activity. *J. Med. Chem.*, **2003**, *46*, 5651-5662.

¹⁵¹ Greene T.W. and Wuts P.G.M.; Protective groups in organic synthesis. *John Wiley and Sons, Inc.*, **1991**, 77-79.

¹⁵² Ogilvie K.K., Schifman A.L. and Penney C.L.; The synthesis of oligoribonucleotides III. The use of silyl protecting groups in nucleoside and nucleotides chemistry VIII. *Can. J. Chem.*, **1979**, *57*, 2230-2238.

4'-nitrobenzophenone, (2) a Jones oxidation to the carboxylic acid, and (3) a selective reduction of the nitro group (Scheme 3.6).

For the Friedel-Crafts acylation, an excess of aluminium chloride was added to a mixture of *p*-nitrobenzoyl chloride dissolved in toluene. After one hour stirring, water was added to the mix to precipitate the catalyst. After extraction the product was recrystallised from a mixture of chloroform and hexane to give the product as a single isomer with 92 % yield. The mechanism of this reaction is similar to the one shown in Figure 3.9.

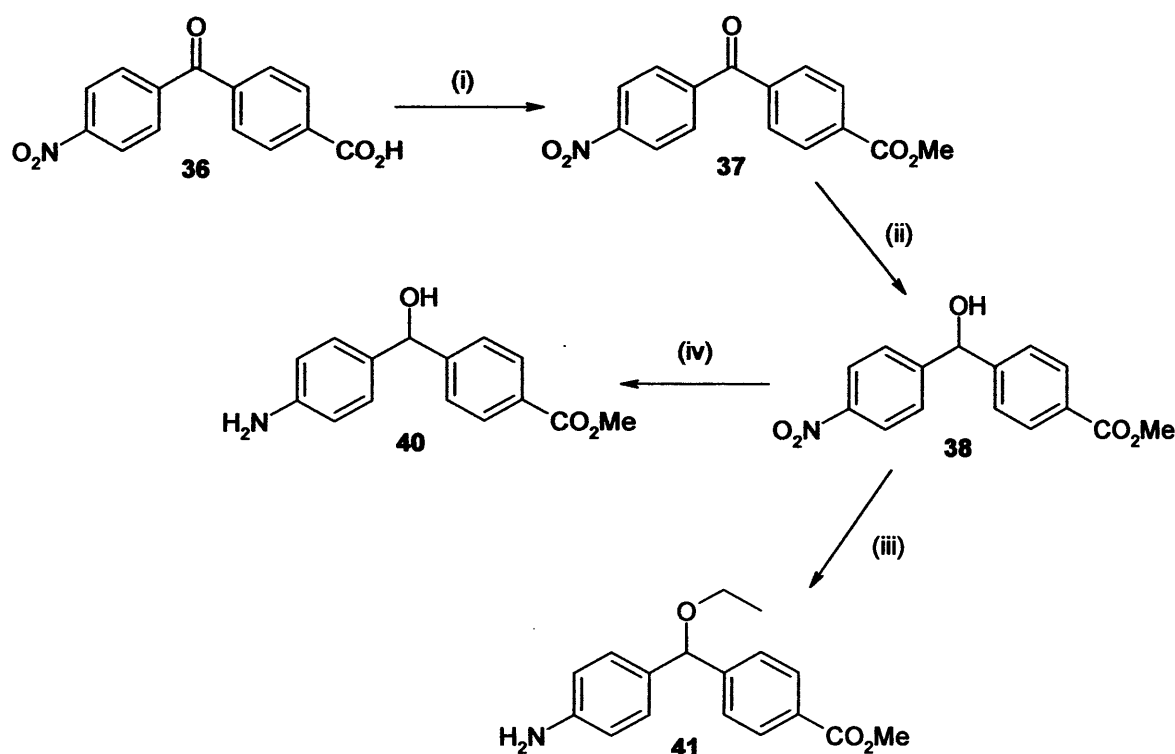


Scheme 3.6: Reagents and Conditions (i) AlCl₃, toluene, 2 h, rt, 92 %; (ii) CrO₃, AcOH, H₂O, 1 h, reflux, 93 %; (iii) SnCl₂, EtOH, rt, 95 %.

The second step involved the oxidation of the methyl group into a carboxylic acid, using a mixture of chromium oxide with acetic acid and sulphuric acid known as Jones reagent. The mixture was stirred under reflux for 1 h. After cooling, cold water was added into the flask and the solid that precipitated was collected and washed with cold water until perfectly white to give the expected carboxylic acid 36 with 93 % yield. This result was confirmed by proton NMR by the disappearance of the methyl peak at δ 2.49 ppm and the presence of a broad singlet at δ 13.35 ppm, which corresponds to the acid proton.

Selective reduction of the nitro group into an amino group using tin chloride as a catalyst was unsuccessful. After 30 min stirring at 70 °C, it afforded a mixture of three different compounds, the starting material, the expected compound and the “amino-alcohol” product (Scheme 3.6). Owing to the limited solubility of the mixture, further purification was not attempted.

2.2.4) Reduction of the nitro-group



Scheme 3.7: Reagents and Conditions (i) H₂SO₄, MeOH, 30 min, reflux, 89 %; (ii) NaBH₄, dioxane, 5 h, rt, 99 %; (iii) SnCl₂, EtOH, rt, 76 %; (iv) Pd/C, H₂ (1 atm), EtOH, 30 min, rt, 80 %.

Before investigating other routes, the carboxylic acid was transformed to a methyl ester 37, using standard methodology, to improve solubility (Scheme 3.7). Attempts to selectively reduce the nitro group of the ester derivative using SnCl₂, H₂/Pd on C, nickel-catalysed formic acid reductions were all unsuccessful. According to the literature, this latter method should be selective for the reduction of

nitro compounds over carbonyl substituents¹⁵³. However in all cases complex mixtures and over reduction were observed. After the lack of success of selective reduction of the nitro group the selective reduction of the carbonyl group was performed in very high yield using NaBH₄ and dioxane as solvent (38). The reaction was complete after 5 h stirring at room temperature and the result confirmed by proton NMR by the CH singlet peak at δ 5.88 ppm and the disappearance of the carbonyl peak in the carbon NMR.

Reduction of the nitro group using catalytic tin chloride resulted in a surprising *O*-alkylation by the solvent ethanol (41). However Pd/C hydrogenation using a hydrogen balloon at atmospheric pressure instead of the hydrogenator at 20-30 psi resulted in a complete and selective reduction of the nitro group (40) after 30 min stirring at room temperature (Scheme 3.7). If the reaction was left for longer removal of the hydroxy group was observed. The same type of result was obtained with an acetyl protection of the alcohol; the acetyl protection was cleaved under these conditions.

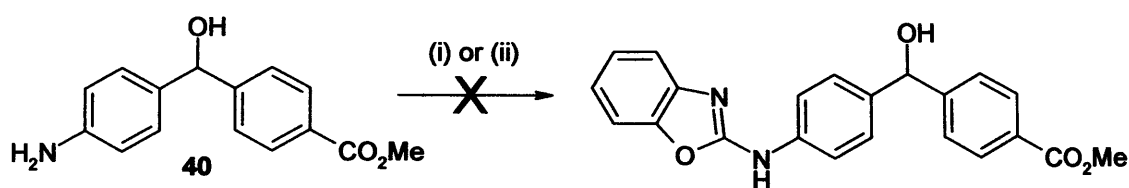
2.3) Formation of the benzoxazole ring C

The benzoxazole ring could be attached by a simple nucleophilic substitution between 2-chlorobenzoxazole and the amine (40). Two different methods have been found to execute this reaction (1) using 2 equivalents of diisopropylethylamine as a base and dichloromethane as a solvent¹⁵⁴, and (2) using 2 equivalents of Et₃N as a base and dioxane as a solvent (Scheme 3.8)¹⁵⁵. Both reactions have been shown to work with a primary amine as the nucleophilic species, but unfortunately in this case no reaction was observed presumably owing to the reduced nucleophilicity of the aromatic amine.

¹⁵³ Gowda D.C., Gowda A.S.P., Baba A.R. and Gowda S.; Nickel-catalysed formic acid reductions. A selective method for the reduction of nitro compounds. *Synth. Com.*, 2000, 30, 2889-2895.

¹⁵⁴ Lazer E.S., Miao C.K., Wang H.C., Sorcek R., Spero D.M., Gilman A., Pal K., Behuke M., Graham A.G., Watraus J.M., Homan C.A., Nagel J., Shah A., Guindon Y., Farina P.R. and Adams J.; Benzoxazolamines and benzothiazolamines: potent, enantioselective inhibitors of leukotriene biosynthesis with a novel mechanism of action. *J. Med. Chem.*, 1994, 37, 913-923.

¹⁵⁵ Haviv F., Ratajczyk J.D., De Net R.W., Kerdesky F.A., Walters R.L., Schmidt S.P., Holms J.H., Young P.R. and Carter G.W.; 3-[1-(2-Benzoxazolyl)hydrazine]propanenitrile derivatives: Inhibitors of immune complex induced inflammation. *J. Med. Chem.*, 1988, 31, 1719-1728.



Scheme 3.8: *Reagents and Conditions* (i) 2-chlorobenzoxazole, DIEA, CH_2Cl_2 , o/n, rt; (ii) 2-chlorobenzoxazole, Et_3N , dioxane, o/n, rt.

However, studies by Ogura *et al*¹⁴⁰ have shown that the benzoxazole ring could also be formed by attaching 2-aminophenol to an isothiocyanate. This leads to a thiourea derivative that can then be cyclised using nickel peroxide as a catalyst.

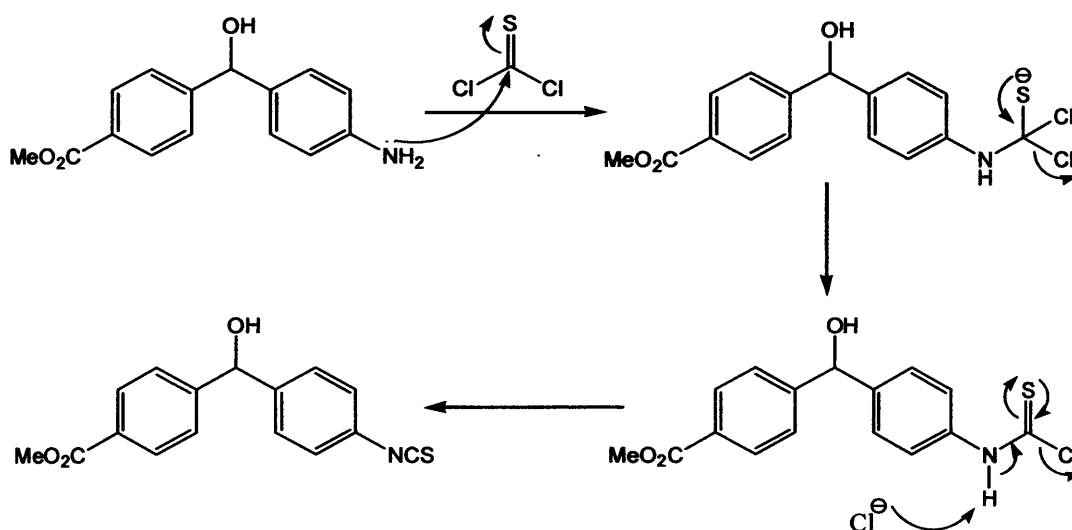
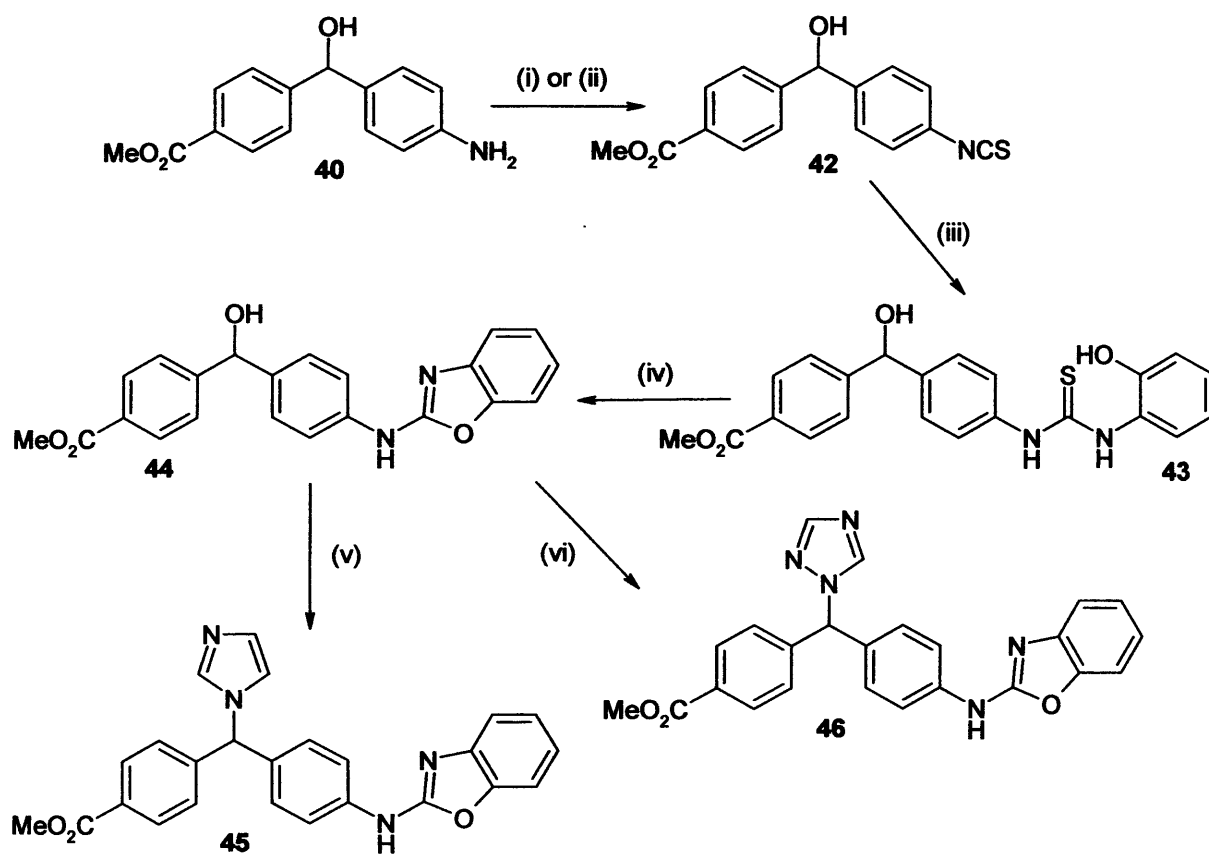


Figure 3.11: Mechanism of the formation of the isothiocyanate using thiophosgene as a reagent

The isothiocyanate (42) could be formed by two different methods: one employing expensive di-pyridyl-thiocarbonate (DPT)¹⁴⁰ and the other involving thiophosgene¹⁴¹ (Scheme 3.9). The DPT reaction was performed by adding DPT to the amine (40) in dichloromethane, the mixture was left overnight at room temperature, washed with water and then purified by column chromatography to give the product 42 in 78 % yield. The thiophosgene reaction was performed by adding thiophosgene to a mixture of amine (40), dichloromethane, ice and water, the

reaction was stirred overnight at 0 °C then the thiophosgene residue and the hydrochloric acid formed during the reaction were removed by washing the organic layer thoroughly with water and sodium bicarbonate. The product 42 was obtained in 89 % yield and could be used in the next step without further purification.

The mechanism of the thiophosgene reaction (Figure 3.11) involves the attack of the nitrogen lone pair on the thiophosgene thiocarbonyl group. The chloride released during this process is then acting like a base and catch the hydrogen on the nitrogen atoms. The electrons are then coming between the nitrogen and the carbon to form the isothiocyanate and the last chloride is released. The mechanism of the DPT reaction is similar.



Scheme 3.9: Reagents and Conditions (i) DPT, CH₂Cl₂, 12 h, rt, 78 %; (ii) CS₂, CH₂Cl₂, H₂O, 12 h, rt, 89 %; (iii) 2-aminophenol, EtOH, 12 h, rt, then (iv) NiPO, CH₃CN, 24 h, rt, 61 %; (v) 1,1'-carbonyldiimidazole, imidazole, CH₃CN, 12 h, rt, 89 %; (vi) 1H-1,2,4-triazole, SOCl₂, K₂CO₃, CH₃CN, 72 h, rt, 43 %.

The isothiocyanate (42) derivative was then reacted with 2-aminophenol at room temperature overnight. On a small scale (100 mg), the thiourea product (43) could be isolated after purification by column chromatography with 76 % yield. On a large scale (9 g), a mixture of the thiourea derivative (43) and the cyclised benzoxazole (44) was observed; this mixture was difficult to separate by column chromatography and was used as a mixture for the cyclisation. After the nickel peroxide cyclisation¹⁴⁰, the product (44) was formed with an overall 61 % yield (Scheme 3.9).

The difference between the thiourea and the benzoxazole could be seen by NMR; the thiourea gave 2 broad NH protons at δ_{H} 8.09 ppm and 7.79 ppm instead of only one for the benzoxazole at δ_{H} 7.92 ppm. In the ¹³C NMR, the thiourea C=S signal of 43 was observed at δ_{C} 178.96 ppm while the quaternary carbon of 44, which links the benzoxazole ring to the rest of the molecule was observed at δ_{C} 158.13 ppm.



Figure 3.12: Redox reaction between the peroxide and the nickel¹⁵⁶

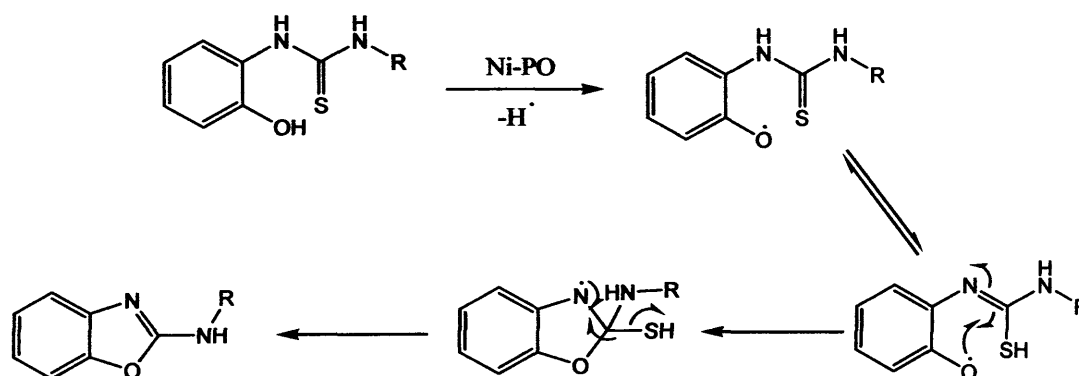


Figure 3.13: Proposed mechanism for the radical cyclisation of the benzoxazole by Ni-PO.

The mechanism of the reaction involved radical species. The reaction starts by a redox reaction involving a one-electron transfer generating the hydroxy radical

¹⁵⁶ Sykes P.; A guidebook to mechanism in organic chemistry 6 ed. Longman Singapore publishers Pte Ltd. 1986, p 306.

OH[•] (Figure 3.12). This radical will be able to react with the molecule to form a phenoxy radical which will then attack the thiourea function to close the ring. Then the ring is stabilised by aromatisation and the thiyl radical SH[•] is released (Figure 3.13).

2.4) Addition of the aza-ring

The imidazole compound (45) was prepared in 89% yield by direct reaction of the carbinol (44) with 1,1'-carbonyldiimidazole in the presence of excess imidazole as previously reported¹⁵⁷ (Scheme 3.8). The addition of the triazole ring employed the Staab method¹²⁰, i.e. reaction of the carbinol (44) with *in situ* prepared *N,N'*-di(1*H*-1,2,4-triazol-1-yl)sulphoxide. After purification by column chromatography the triazole benzoxazole (46) was obtained in 43% yield (Scheme 3.9). The 1,2,4-triazole isomer was confirmed by ¹H NMR with the presence of the two singlet protons of the triazole at approximately δ 7.97 and 8.02, no 1,3,4-triazole isomer was formed during the reaction.

The mechanism of the imidazole reaction is described in Figure 3.14. This mechanism is similar to the triazole reaction mechanism previously described. In this case the reagent 1,1' carbonyl diimidazole is commercially available and does not need to be prepared *in situ*.

The carbinol (44) is first attacked by the imidazole to form the anion species. Then, the negatively charged oxygen attacks the carbonyl of the 1-1' carbonyl diimidazole yielding the product with a very good leaving group instead of the hydroxyl and releasing 1 mole of imidazole anion. Finally the leaving group is substituted by the imidazole anion to form the product and liberate carbon dioxide and another mole of imidazole.

¹⁵⁷ Aelterman W., Lang Y., Willemsens B., Vervest I., Leurs S. and De Knaep F.; Conversion of the laboratory synthetic route of the *N*-aryl-2-benzothiazolamine R116010 to a manufacturing method. *Org. Proc. Res. Dev.* 2001, 5, 467-471.

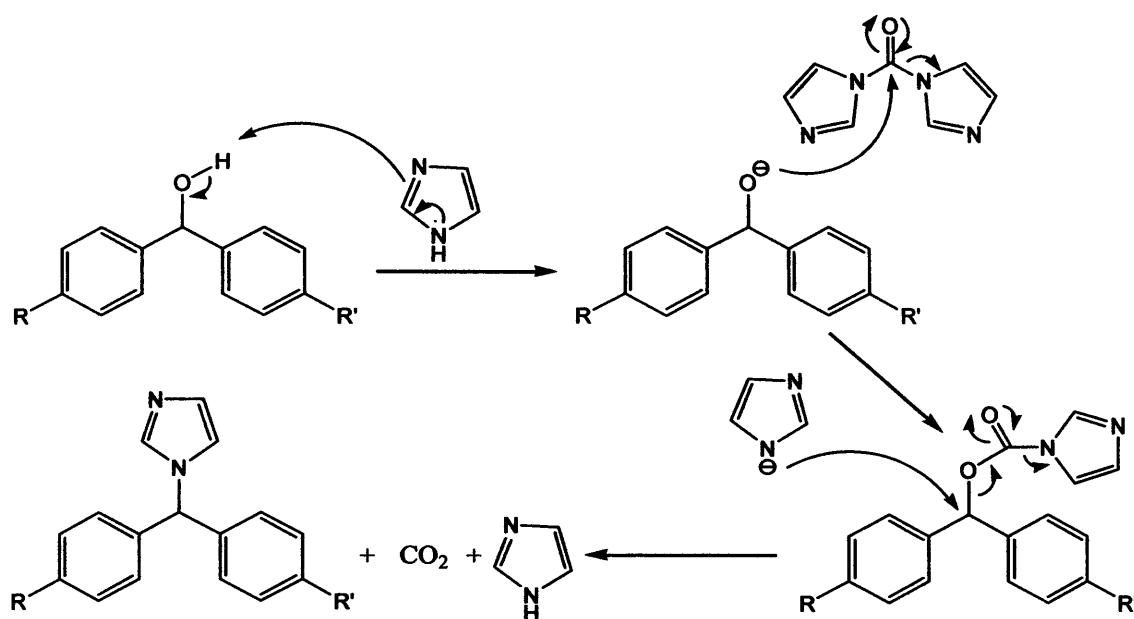


Figure 3.14: Mechanism of the addition of the imidazole ring

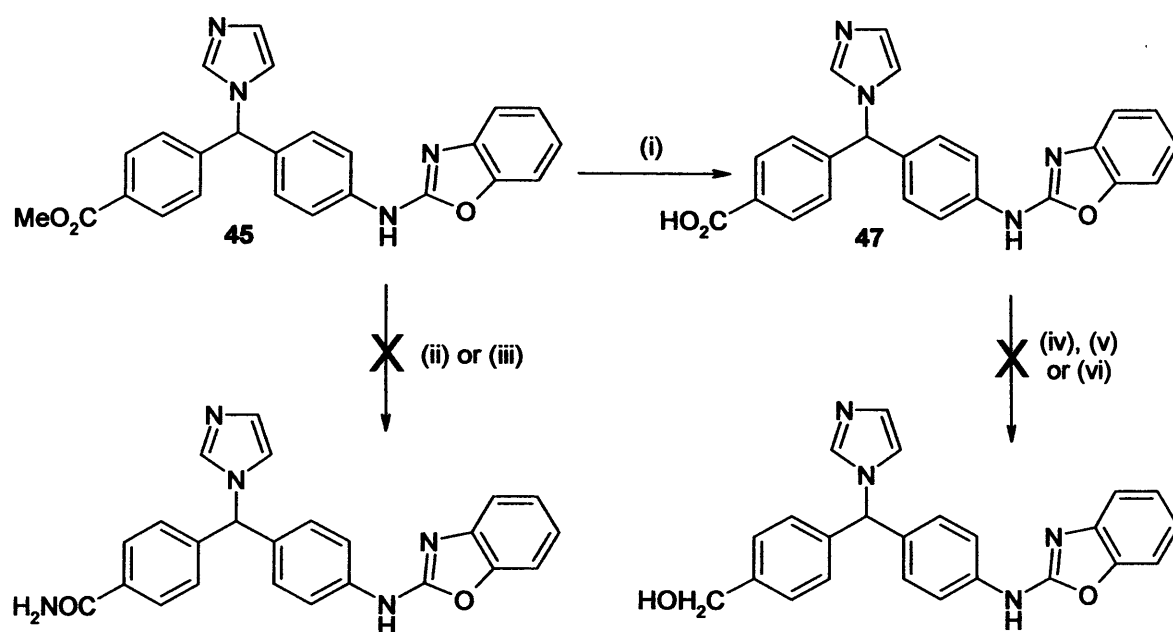
2.5) Synthesis of the other substituents

The previous docking experiments have shown interesting results for three other substituents other than the ester: the carboxylic acid COOH, the alcohol CH₂OH and the amide CONH₂.

The saponification of the ester **45** to the carboxylic acid **47** was achieved using a solution of 2 M aqueous NaOH and methanol as solvent in a 1:2 ratio. This allowed the compound to be synthesised after 30 min reflux with 62 % yield (Scheme 3.10).

Then the reduction of both the ester **45** and the carboxylic acid **47** into the alcohol was investigated. Several methods have been found to perform this reaction (Scheme 3.10).





Scheme 3.10: Reagents and Conditions (i) 2 M aq. NaOH, MeOH, 30 min, reflux, 62 %; (ii) 28 % NH₄OH aq., o/n, rt; (iii) NH₃/MeOH, o/n, rt; (iv) LiAlH₄, THF, 4 h, 0 °C; (v) NaBH₄, ethane dithiol, THF, 4 h, reflux; (vi) NaBH₄, BF₃/Et₂O, THF, 5 h, rt.

The conventional method using the reductive agent LiAlH₄ in THF¹⁵⁸ was attempted but no reaction was observed. In the other methods, sodium borohydride was used as the reducing agent. Sodium borohydride cannot reduce carboxylate ester and carboxylic acid on its own, however some studies have shown that its reducing power can be increased. It has been shown that the addition of ethanedithiol to sodium borohydride leads to a sulfurated sodium borohydride species with a stronger reducing power^{159, 160}. The mixture NaBH₄/BF₃·Et₂O in THF has also been

¹⁵⁸ Hartmann R.W., Paluszczak A., Lacan F., Ricci G. and Ruzziconi R.; CYP 17 and CYP 19 inhibitors. Evaluation of fluorine effects on the inhibiting activity of regioselectively fluorinated 1-(naphthalen-2-ylmethyl)imidazoles. *J. Enz. Inh. Med. Chem.*, 2004, 19, 145-155.

¹⁵⁹ Guida W.C., Entreken E.E. and Guida A.R.; Reduction of esters and other carboxylates by sodium borohydride/ethanedithiol: Improved procedures and an investigation into the nature of the reducing species. *J. Org. Chem.*, 1984, 49, 3024-3026.

¹⁶⁰ Maki Y. and Kikuchi K.; Thiol-activated sodium borohydride reduction of carboxylate ester. *Tetrahedron Lett.*, 1975, 38, 3295-3296.

shown to reduce carboxylic acids and esters^{161, 162}. The treatment of sodium borohydride with boron trifluoride etherate produces borane which is a good reducing agent. Unfortunately both of these methods were ineffective in that case and no reaction was observed (Scheme 3.10).

The transformation of either **45** or **47** into the amide derivative was also attempted (1) using a 28 % ammonium hydroxide aqueous solution¹⁶³ and (2) using a saturated methanolic ammonia solution. Unfortunately no reaction was observed in both cases (Scheme 3.10).

2.6) Synthesis of the unsubstituted, methyl, methoxy and hydroxy substituted phenyl derivatives

2.6.1) Synthesis of the benzoxazol-2-yl-[4-substituted-1-ylphenylmethyl]phenylamine (52), (53), (53'), (54).

The unsubstituted derivative was prepared using the same strategy as seen before for the methyl ester derivative. However as the 4-aminobenzophenone is commercially available the synthesis was much easier with only 4 steps instead of 8 (Scheme 3.11).

4-aminobenzophenone was first transformed into the corresponding isothiocyanate **49** with 99 % yield using thiophosgene. Then the benzoxazole ring was added. As seen previously 2-aminophenol reacted on **49** to form the thiourea. For the cyclisation step, the expensive nickel peroxide reaction (Scheme 3.9) has been changed by a cheap mercury (II) oxide reaction in ethanol catalysed by a small amount of sulphur powder¹⁶⁴. This allowed the formation of **50** with an overall yield of 54 %. The reduction of the ketone **50** to the alcohol **51** was performed using

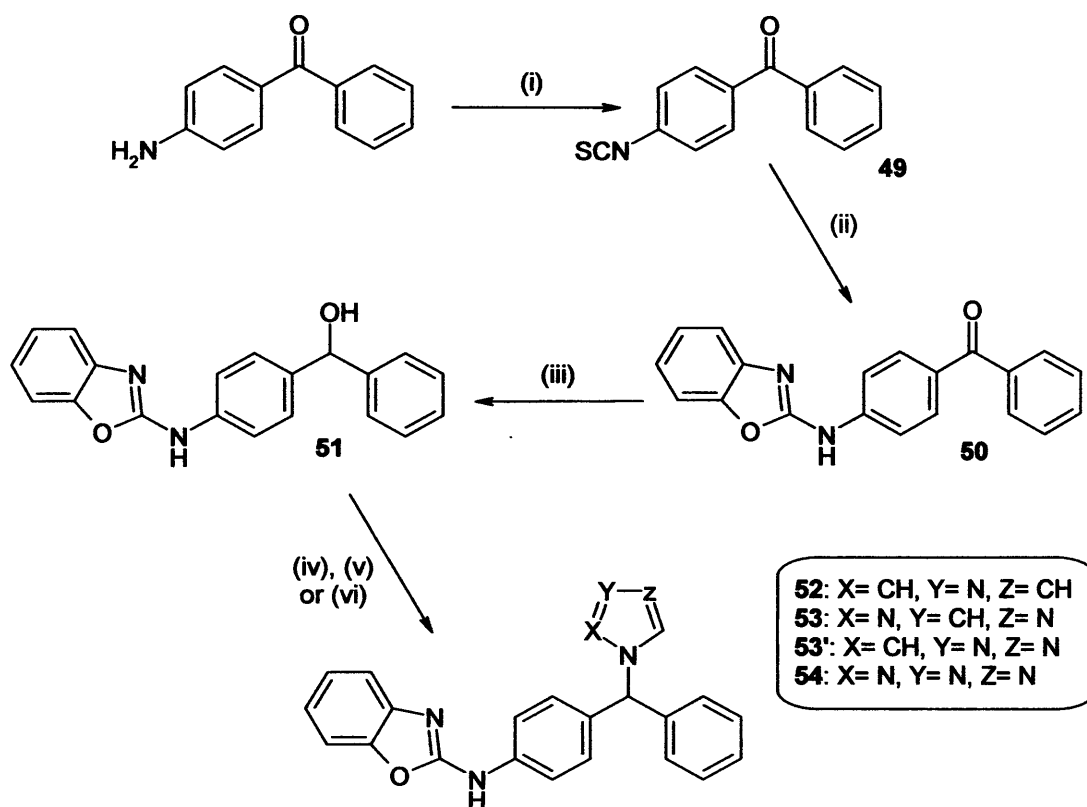
¹⁶¹ Cho S., Park Y., Kim J., Falck J.R. and Yoon Y.; Facile reduction of carboxylic acids, esters, acid chloride, amides and nitriles to alcohols or amines using NaBH₄/BF₃·Et₂O. *Bull. Korean Chem. Soc.*, **2004**, *25*, 407-409.

¹⁶² Brown H.C. and Subba Rao B.C.; Hydroboration. III. The reduction of organic compounds by diborane, an acid-type reducing agent. *J. Am. Chem. Soc.*, **1960**, *82*, 681-686.

¹⁶³ Pan Y., Holmes C.P. and Tumelty D.; Novel α,α -Difluorohomophthalimides via Copper-Catalyzed Tandem Cross-Coupling-Cyclization of 2-Halobenzamides with α,α -Difluoro Reformatskii Reagent. *J. Org. Chem.*, **2005**, *70*, 4897-4900.

¹⁶⁴ Janssens F., Torremans J., Janssen M., Stokbroekx R.A., Luyckx M. and Janssen P.A.J.; New antihistaminic N-heterocyclic 4-piperidinamines. Synthesis and antihistaminic activity of N-(4-piperidinyl)-1H-benzimidazol-2-amines. *J. Med. Chem.*, **1985**, *28*, 1925-1933.

NaBH₄ in dioxane. Because of the poor solubility of **50** in dioxane, the reaction had to be left overnight to give **51** in 86 % yield. The imidazole (**52**), 1,2,4 triazole (**53**), 1,3,4 triazole (**53'**) and tetrazole (**54**) ring were then added to the carbinol **50** using methods previously described (Scheme 3.9 and Figure 3.14) with variable yield (12 to 74 %) depending on the azole ring (Table 3.5).



Scheme 3.11: Reagents and Conditions (i) CSCl₂, CH₂Cl₂, H₂O, 12 h, rt, 99 %; (ii) (1) 2-aminophenol, EtOH, 12 h, rt (2) HgO, S, EtOH, 4 h, reflux, 54 %; (iii) NaBH₄, dioxane, o/n, 86 %; (iv) 1,1'-carbonyldiimidazole, imidazole, CH₃CN, 12 h, rt, 74 %; (v) 1H-1,2,4-triazole, SOCl₂, K₂CO₃, CH₃CN, 72 h, rt, **53**: 35 %, **53'**: 12 %; (vi) 1H-tetrazole, SOCl₂, K₂CO₃, CH₃CN, 72 h, rt, **54**: 32 %.

Table 3.5: Results of the addition of the aza-ring

X	Y	Z	YIELD^(a)	COMPOUND NUMBER
CH	N	CH	74 %	52
N	CH	N	35 %	53
CH	N	N	12 %	53'
N	N	N	32 %	54

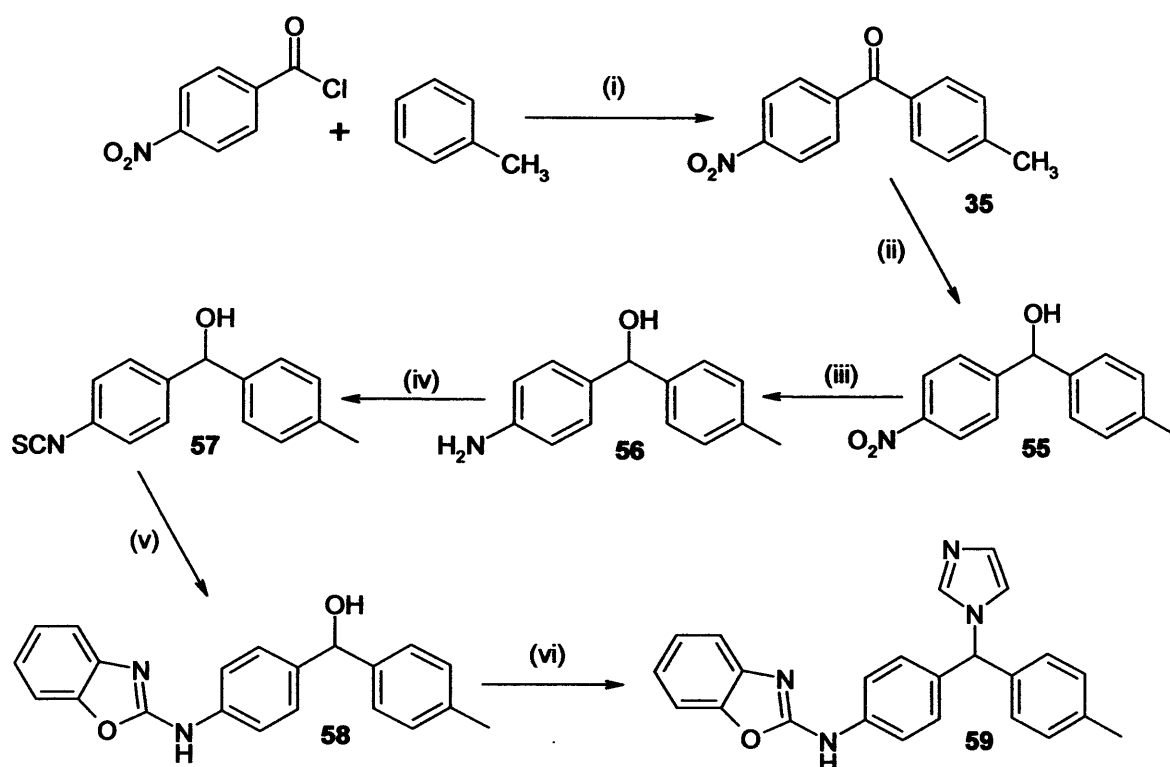
^(a) Yield calculated after purification by flash column chromatography

2.6.2) Synthesis of the methyl derivative (59)

The synthesis of the methyl derivatives could be achieved in 6 steps (Scheme 3.12). This method followed the procedure used for the synthesis of the methyl ester derivative. **35** formed by a Friedel-Crafts acylation between 4-nitro-benzoyl chloride and toluene was reduced to the corresponding alcohol **55** using NaBH₄ in methanol. Then the nitro group was reduced to an amino group using a hydrogen atmosphere (P= 1 atm). This reduction was performed on a large scale (6 g), and after 1.5 h stirring at room temperature the reaction was still not complete however reduction of the alcohol was occurring leading to a mixture of three different compounds. The expected product could be isolated by column chromatography in only 48 % yield.

The benzoxazole ring was attached using the mechanism described in Scheme 3.10 for **50**. The formation of the isothiocyanate **57** was completed using thiophosgene with 88 % yield. Then 2-aminophenol was added and after an overnight stirring at room temperature, mercury oxide and sulphur were added to the mixture and left under reflux for 2 h to form **58** with 35 % yield (Scheme 3.12).

The imidazole was finally attached to **58** using the conventional method with 1,1'-carbonyldiimidazole and imidazole to give, after overnight stirring at room temperature, **59** with 66 % yield.



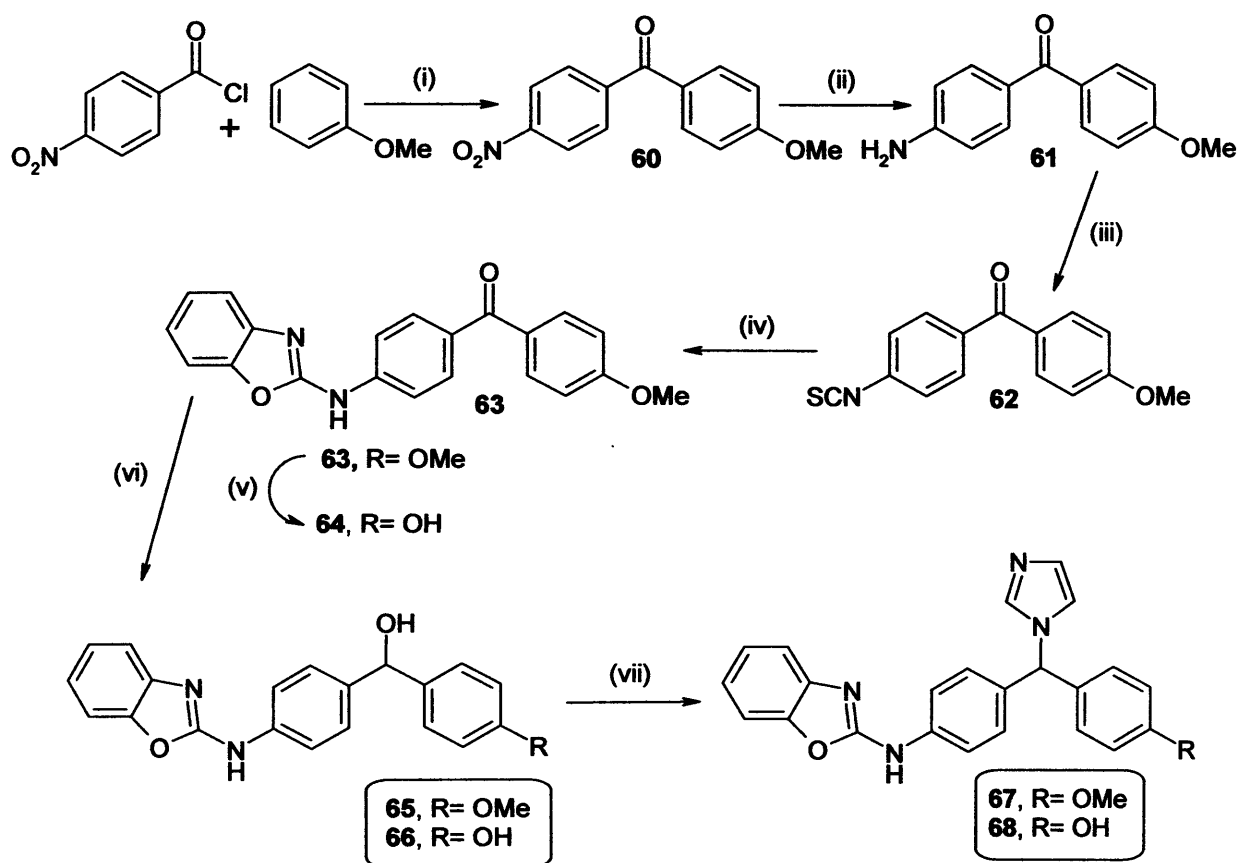
Scheme 3.12: Reagents and Conditions (i) AlCl_3 , toluene, 2 h, rt, 92 %; (ii) NaBH_4 , MeOH, 1 h, rt, 86 %; (iii) Pd/C, H_2 balloon, EtOH, 1.5 h, rt, 48 %; (iv) CSCl_2 , CH_2Cl_2 , H_2O , 12 h, rt, 88 %; (v) (1) 2-aminophenol, EtOH, 12 h, rt (2) HgO , S, EtOH, 4 h, reflux, 35 %; (vi) 1,1'-carbonyldiimidazole, imidazole, CH_3CN , 12 h, rt, 66 %.

2.6.3) Synthesis of the methoxy (67) and the hydroxy (68) derivatives

The synthesis of the methoxy derivative was performed in 6 steps following the method for the synthesis of the unsubstituted compound 52; the reduction of the ketone took place after the formation of the benzoxazole ring (Scheme 3.13). The benzophenone 60 was formed by a Friedel-Crafts acylation between *p*-nitrobenzoyl chloride and anisole. In contrast with the methyl derivative, the nitro group of 60 was first reduced to the amine. Only 10 min under a hydrogen atmosphere (1 atm) and Pd/C catalyst afforded the corresponding amine 61 with 95 % yield.

After transformation into the isothiocyanate 62 using thiophosgene with 97 % yield, the benzoxazole ring was attached using the same method seen previously. 62

was stirred overnight with 2-aminophenol in toluene instead of ethanol because of its poor solubility and then sulphur and HgO were added to the mixture which was refluxed for 1.5 h to give **63** with 46 % yield. The carbinol **65** was then formed by a reduction of the ketone using NaBH₄ in methanol with 91 % yield.



Scheme 3.13: Reagents and Conditions (i) AlCl₃, anisole, CH₂Cl₂, 12 h, rt, 69 %; (ii) Pd/C, H₂ balloon, EtOH, 10 min, rt, 95 %; (iii) CSeCl₂, CH₂Cl₂, H₂O, 12 h, rt, 97 %; (iv) (1) 2-aminophenol, EtOH, 12 h, rt (2) HgO, S, toluene, 4 h, reflux, 46 %; (v) HBr, AcOH, 6 h, reflux then 12 h, rt, 77 %; (vi) NaBH₄, MeOH, 1 h, rt, **65**: 91 %, **66**: 44 %; (vii) 1,1'-carbonyldiimidazole, imidazole, CH₃CN, 12 h, rt, **67**: 38 %, **68**: 74 %.

The imidazole was finally attached to **65** using the conventional method with 1,1'-carbonyldiimidazole and imidazole to give, after overnight reflux, **67** with only

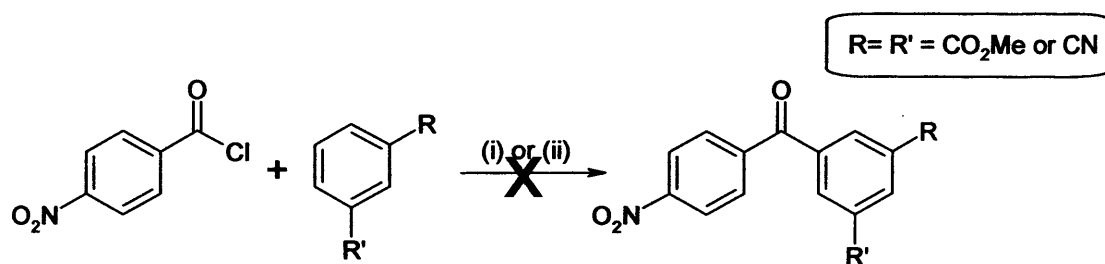
38 % yield. The poor yield of this reaction could be explained by the fact that the reaction did not go to completion because of the poor solubility of **65** in CH₃CN.

The hydroxy derivative **68** was formed in 3 steps after deprotection of the methoxy function of **63** (Scheme 3.13). A first attempt using a 1 M solution of BBr₃ in CH₂Cl₂ was found unsuccessful¹⁶⁵. Then, another method involving a 48 % solution of HBr in acetic acid gave the hydroxy product **64** in 77 % yield after 6 h reflux followed by overnight stirring¹⁶⁶. This product was then reduced to the alcohol **66** using NaBH₄ in methanol. In that case the reaction did not go to completion and afforded the product after purification by column chromatography with a moderate 44 % yield. The imidazole ring was then attached using the usual method to form **68** with 74 % yield.

2.7) Substitution on the other positions of the phenyl ring

Docking studies in the previous chapter showed that substitution on the ortho and the meta positions of the phenyl ring could be of interest. Better results were also observed in the case of a di-substitution; however the synthesis of these compounds appeared to be very challenging.

2.7.1) Synthesis of a di-meta derivative



Scheme 3.14: Reagents and Conditions (i) AlCl₃, CH₂Cl₂, rt; (ii) AlCl₃, DCE, reflux.

¹⁶⁵ Grieco P.A., Nishizawa M., Oguri T., Burke S.D. and Marinovic N.; Sesquiterpene lactones: total synthesis of vernolepin and vernomenin. *J. Am. Chem. Soc.*, 1977, 99, 5773-5780.

¹⁶⁶ Plattner J.J., Martin Y.C., Smital J.R., Lee C.M., Fung A.K.L., Horram B.W., Orowley S.R., Pernet A.G., Bunnell P.R. and Kim K.H.; [(Aminomethyl)aryloxy]acetic acid esters. A new class of high-ceiling diuretics. 3. Variation in the bridge between the aromatic rings to complete mapping of the receptor. *J. Med. Chem.*, 1985, 28, 79-93.

Synthesis of a di-meta derivative by a Friedel-Crafts acylation requires having 2 withdrawing groups on the 2 meta positions.

Friedel-Crafts acylation were attempted with 4-nitrobenzoyl chloride and both dimethyl isophthalate and 1,3-dicyanobenzene with CH_2Cl_2 as a solvent at room temperature and with dichloroethane as a solvent at reflux (Scheme 3.14). Unfortunately no reaction was observed.

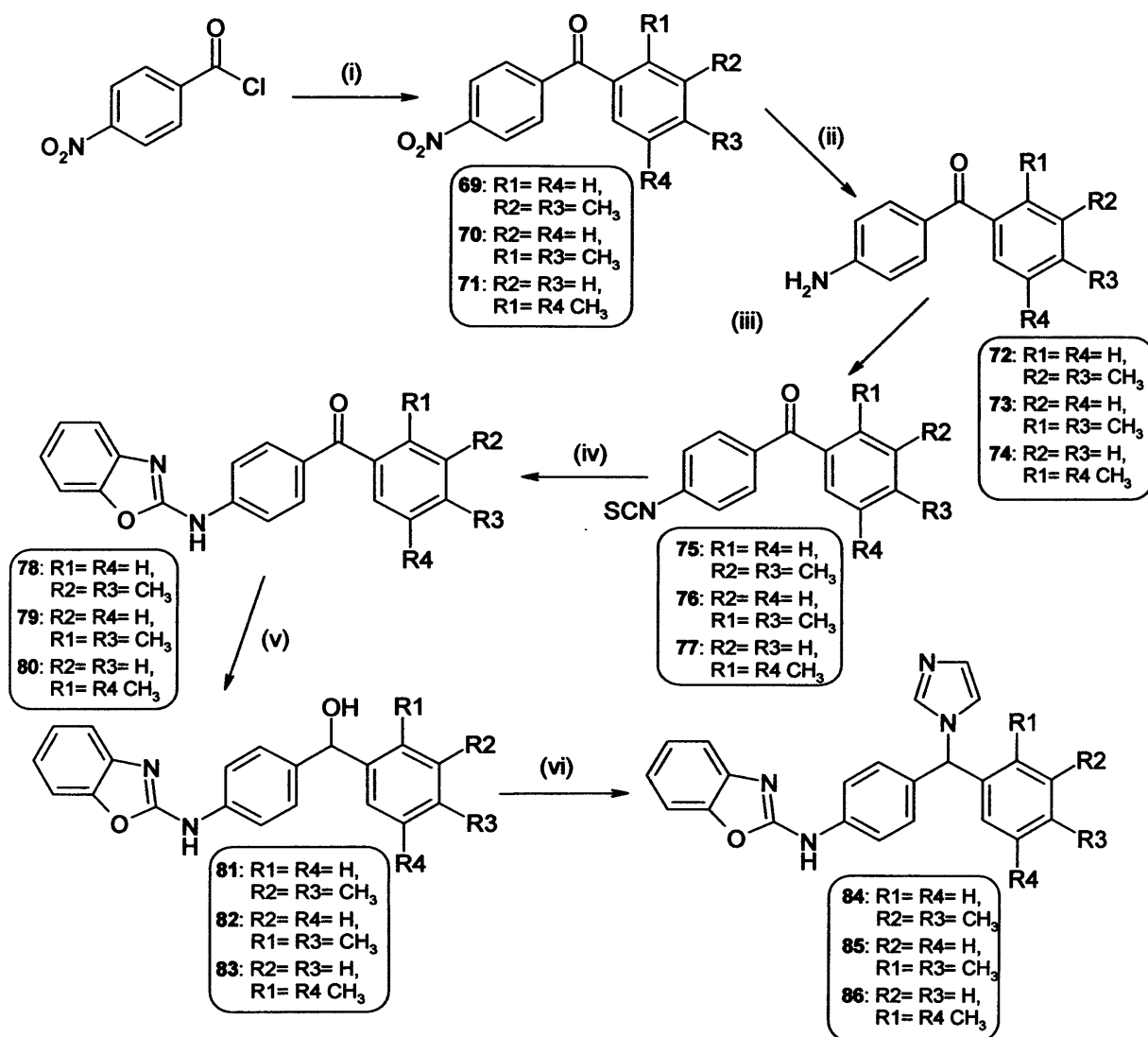
2.7.2) Synthesis of the dimethyl derivatives 84, 85 and 86

A simple method to obtain some di-substituted compounds was to perform a Friedel-Crafts acylation between 4-nitrobenzoyl chloride and ortho, meta and para-xylene. This led to the formation of three dimethyl derivatives, the 3,4-dimethyl **84**, the 2,4-dimethyl **85** and the 2,5-dimethyl **86**. Their synthesis is described in Scheme 3.15.

The Friedel-Crafts acylation was performed at room temperature for 3-4 h and gave the products **69**, **70** and **71** respectively with 41 %, 85 % and 90 % yield. These products were obtained pure as a single isomer after extraction except **69** which required purification by column chromatography (PE/EtOAc 80:20 v/v). Formation of **69** and **70** was confirmed by proton NMR with the presence of respectively an aromatic singlet at 7.46 ppm and two aromatic doublets at 7.34 ppm and 7.10 ppm integrating for one proton for **69** and an aromatic singlet at 6.86 ppm and 2 aromatic doublets at 7.04 and 6.86 integrating for one proton for **70**. Because of the symmetry of the para-xylene compound **71** was the only possible product of the reaction.

The rest of the synthesis involved the usual method for this type of compound (Scheme 3.15) with first a reduction of the nitro-group which led to the amino-benzophenone **72** (94 %), **73** (96 %) and **74** (94 %) followed by a transformation of the amino group into an isothiocyanate (compound **76** was pure enough after extraction and obtained with 96 % yield while compounds **75** and **77** required purification by column chromatography (petroleum ether/ethyl acetate 80:20 v/v) and were respectively obtained with 75 % and 61 % yield). Then the benzoxazole ring was added in high yield to give compounds **78** (87 %), **79** (66 %) and **80** (64 %), the

ketone was reduced (compounds **81**, **82** and **83**) and finally the imidazole ring attached to give the three dimethyl derivatives **84**, **85** and **86**.



Scheme 3.15: Reagents and Conditions (i) AlCl₃, o,m or p-xylene, CH₂Cl₂, 3-4 h, rt, **69**: 41 %, **70**: 85 %, **71**: 90 %; (ii) Pd/C, H₂ balloon, EtOH, 20-25 min, rt, **72**: 94 %, **73**: 96 %, **74**: 94 %; (iii) CSCl₂, CH₂Cl₂, H₂O, 12 h, rt, **75**: 75 %, **76**: 96 %, **77**: 61 %; (iv) (1) 2-aminophenol, EtOH, 12 h, rt (2) HgO, S, EtOH, 4-6 h, reflux, **78**: 87 %, **79**: 66 %, **80**: 64 %; (v) NaBH₄, MeOH, 3-4 h, rt, **81**: 73 %, **82**: 97 %, **83**: 99 %; (vi) 1,1'-carbonyldiimidazole, imidazole, CH₃CN, 12 h, rt, **84**: 78 %, **85**: 84 %, **86**: 72 %.

2.8) Biological evaluation

The biological activity of the benzoxazole derivatives was measured following the same procedure as previously described with the MCF-7 cell line and [³H-11,12]-all-*trans* retinoic acid. The results are reported in Table 3.6.

Compounds **45**, **46**, **47** and **48** which showed very interesting results in the docking studies were unfortunately not as active as expected ($IC_{50} > 20 \mu M$), and were 2 to 3 times less active than the most potent 1-[(benzofuran-2-yl)phenylmethyl]triazole series previously described ($IC_{50} = 5 \mu M$) and liarozole ($IC_{50} = 6 \mu M$)⁸¹. On the other hand **52** which is the same compound with no substituent showed a good activity ($0.9 \mu M$) as well as the methyl derivative (**59**, $IC_{50} = 8 \mu M$) and the hydroxy derivative (**68**, $IC_{50} = 12 \mu M$). Also the presence of a methoxy (**67**) or a dimethyl substitution (**84**, **85** and **86**) gave disappointing results. The accurate IC_{50} of compounds **53'**, **54**, **65**, **84**, **85** and **86** were not calculated as they appeared to be weak inhibitors of CYP26 and showed less than 50 % inhibition at a $20 \mu M$ concentration. Their percentage inhibition at $20 \mu M$ is showed in Table 3.7.

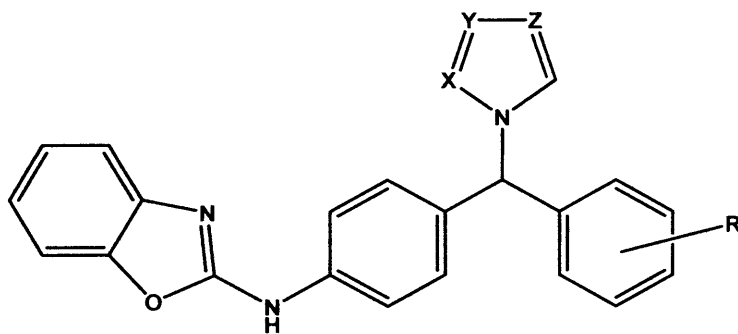


Table 3.6: IC_{50} of the benzoxazole derivatives

R	X	Y	Z	IC_{50} (μM)	COMPOUND NUMBER
4-CO ₂ Me	CH	N	CH	20	45
4-CO ₂ Me	N	CH	N	50	46
4-COOH	CH	N	CH	50	47

4-COOH	N	CH	N	50	48
H	CH	N	CH	0.9	52
H	N	CH	N	18	53
H	CH	N	N	>20	53'
H	N	N	N	>20	54
4-CH ₃	CH	N	CH	8	59
4-OMe	CH	N	CH	>20	67
4-OH	CH	N	CH	12	68
3,4-CH ₃	CH	N	CH	>20	84
2,4-CH ₃	CH	N	CH	>20	85
2,5-CH ₃	CH	N	CH	>20	86

A large drop in the activity can also be observed when the imidazole ring (**52**, IC₅₀ = 0.9 μM) is replaced by a triazole ring (**53**, IC₅₀ = 18 μM for the 1,2,4 triazole and > 20 μM for the 1,3,4 triazole **53'**) or a tetrazole ring (**54**, IC₅₀ > 20 μM).

Table 3.7: % inhibition at 20 μM

COMPOUND NUMBER	% INHIBITION AT 20 μM
53'	19.12 %
54	39.32 %
67	40.5 %
84	34.62 %
85	31.82 %
86	36.15 %

Consequently, comparison between the activity of the unsubstituted compound (**52**, IC₅₀ = 0.9 μM) and the different substituted ones (**45**, IC₅₀ = 20 μM; **47**, IC₅₀ = 50 μM; **59**, IC₅₀ = 8 μM; **67**, IC₅₀ > 20 μM; **68**, IC₅₀ = 12 μM) showed that no substitution on the phenyl ring seem to be tolerated at the para-position. The moderate activity observed for the small substituent CH₃ (**59**, IC₅₀ = 8 μM) and OH (IC₅₀ = 12 μM) suggests that this is due to steric limitations with the active site. The

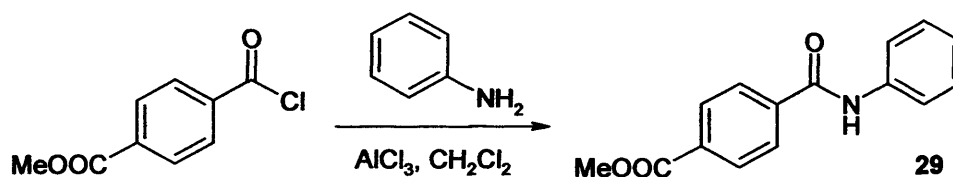
poor activity of the three dimethyl compounds **84**, **85** and **86** ($IC_{50} > 20 \mu M$) also showed that substitution on the other position of the phenyl ring did not need to be investigated further. The imidazole ring also appears to be the best choice in theazole ring as the unsubstituted compounds appeared to be much more potent with an imidazole ring than a triazole or a tetrazole.

As a result, the presence of a substituted phenyl ring displayed disappointing results. The difference observed in the docking studies and the activity also showed the limitations of our CYP26A1 model. The model should consequently be improved and the replacement of the phenyl ring by a more flexible alkyl chain should now be considered in the design of new potential CYP26 inhibitors.

3) EXPERIMENTAL

3.1) Experimental results for the preparation of the methyl ester derivatives 45 and 46 and the carboxylic acid derivatives 47 and 48

3.1.1) Terephthalanilic acid (29)¹⁶⁷

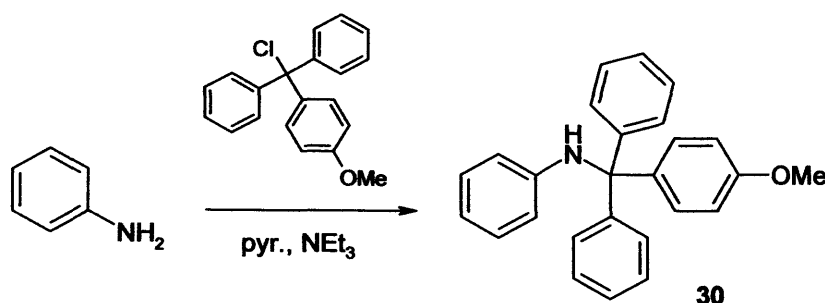


To a suspension of aniline (38 mg, 0.41 mmol) in CH₂Cl₂ (10 mL), was added aluminum chloride (0.16 g, 1.23 mmol) at 0 °C. The reaction mixture was stirred for 30 min, during which time the reaction temperature was allowed to rise to room temperature. Methyl-4-chlorocarbonylbenzoate (0.10 g, 0.45 mmol) was added over a period of 1 h maintaining the temperature below 30 °C. The reaction mixture was stirred overnight at room temperature and then 2 N aqueous HCl (2 mL) was slowly added. The solvent was removed and water was added. The resulting precipitate was filtered, washed with H₂O (3 × 20 mL) and dried to give the *N*-acylated product as a yellow syrup. Yield: 21 mg (20 %). t.l.c system: petroleum ether-ethyl acetate 1:1, R_f= 0.83.

¹H NMR: δ (DMSO-*d*₆): 8.09 (m, 2H, Ar), 7.84 (m, 2H, Ar), 7.61 (m, 2H, Ar), 7.31 (m, 2H, Ar), 7.13 (m, 1H, Ar), 3.88 (s, 3H, CH₃).

¹⁶⁷ Schoenberg A. and Heck R.F.; Palladium-catalyzed amidation of aryl, heterocyclic, and vinylic halides. *J. Org. Chem.*, 1974, 39, 3327-3331.

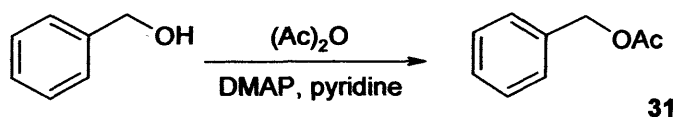
3.1.2) [(4-Methoxyphenyl)diphenylmethyl]phenylamine (30)¹⁶⁸



Aniline (1.33 g, 14.25 mmol) was dissolved in anhydrous pyridine (27 mL) and triethylamine (0.6 mL). To this solution was added a solution of 4-monomethoxytrityl chloride (4 g, 12.95 mmol) in anhydrous pyridine (15 mL) in 3 aliquats at 45 min intervals. The reaction was stirred at room temperature for 3 h then quenched by the addition of MeOH (3 mL). The solution was evaporated to give a yellow syrup and coevaporated 3 times with toluene to remove traces of pyridine. The residue was dissolved in EtOAc (30 mL) and washed with saturated aqueous KCl solution (2 × 25 mL). The organic phase was dried (MgSO₄), filtered and evaporated *in vacuo*. The residue was purified by column chromatography (hexane: EtOAc: diethylamide 49.5: 49.5: 1) to give the product as a yellow syrup. Yield: 1.59 g (34 %). t.l.c system: dichloromethane, R_f = 0.89.

¹H NMR: δ (CDCl₃): 7.56 (m, 3H, Ar), 7.43 (m, 2H, Ar), 7.39 (m, 5H, Ar), 7.35 (m, 2H, Ar), 7.09 (m, 2H, Ar), 6.98 (m, 2H, Ar), 6.72 (m, 1H, Ar), 6.54 (m, 2H, Ar), 5.28 (bs, 1H, NH), 3.87 (s, 3H, CH₃).

3.1.3) Benzyl acetate (31)¹⁶⁹



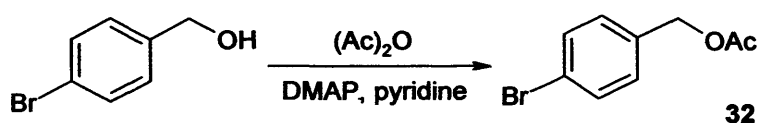
¹⁶⁸ Moises Comle L., Demirtas I. and Maskill H.; Substituent effects upon rates deamination and base strengths of substituted *N*-tritylamines. *J. Chem. Soc., Perkin Transactions 2*, 2001, 9, 1748-1752.

¹⁶⁹ Bryant D.R., McKeon J.E. and Ream B.C.; Palladium-catalyzed synthesis of benzyl esters from methyl benzenes. *J. Org. Chem.*, 1968, 33, 4123-4127.

To a solution of benzyl alcohol (15 g, 0.14 mol) and DMAP (1.86 g, 15.26 mmol) in dry pyridine (150 mL) was added acetic anhydride (42.48 g, 0.42 mol) and the reaction was stirred under nitrogen at room temperature overnight. EtOH (60 mL) was added to quench the reaction, and the solvent concentrated under reduced pressure. The residue was then diluted with CH₂Cl₂ (100 mL) and washed with saturated aqueous NaHCO₃ (2 × 100 mL) and 10 % aqueous NaCl (2 × 100 mL) solution. The organic layer was dried with MgSO₄ to give a yellow syrup. Yield: 20.40 g (98 %). t.l.c system: petroleum ether-ethyl acetate 4:1, R_f= 0.51.

¹H NMR: δ (CDCl₃): 7.39 (m, 5H, Ar), 5.13 (s, 2H, CH₂), 2.11 (s, 3H, CH₃).

3.1.4) 4-Bromobenzyl acetate (32)¹⁷⁰

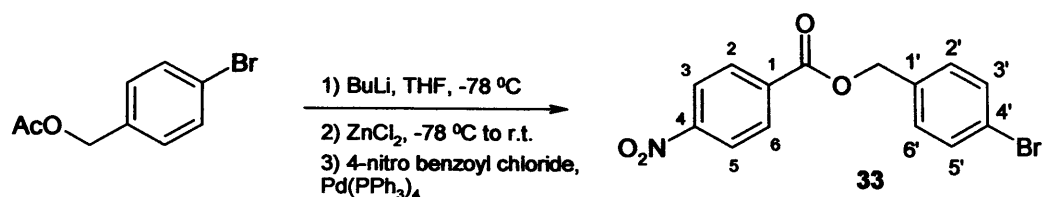


To a solution of 4-bromobenzyl alcohol (6 g, 32.07 mmol) and DMAP (0.43 g, 3.53 mmol) in dry pyridine (50 mL) was added acetic anhydride (6.55 g, 64.14 mmol) and the reaction was stirred under nitrogen at room temperature overnight. EtOH (30 mL) was added to quench the reaction, which was then diluted with CH₂Cl₂ (60 mL). The solution was washed with saturated aqueous NaHCO₃ (2 × 50 mL) and 10 % NaCl solution (2 × 50 mL). The organic layer was dried with MgSO₄ to give a yellow syrup. Yield: 7.30 g (99 %). t.l.c system: petroleum ether-ethyl acetate 3:1, R_f= 0.59.

¹H NMR: δ (CDCl₃): 7.47 (d, J= 8.1 Hz, 2H, Ar), 7.22 (d, J= 8.1 Hz, 2H, Ar), 5.05 (s, 2H, CH₂), 2.10 (s, 3H, CH₃).

¹⁷⁰ Gilman H. and Helstrom D.S.; Organolithium compounds with hydroxyl, nitrilo and sulfonamido groups. *J. Am. Chem. Soc.*, **1948**, *70*, 4177-4179.

3.1.5) 4-Bromobenzyl 4-nitrobenzoate (33)¹⁷¹



n-Butyllithium (5.86 mL, 8.73 mmol) was added dropwise (10 min) to a solution of 4-bromobenzyl acetate (2 g, 8.73 mmol) in THF (20 mL) at -78 °C, and the resulting mixture was stirred for 30 min. A THF solution of dry ZnCl₂ (1.0 M, 12 mL) was added with a syringe and the reaction mixture was allowed to warm to room temperature. After 2 h the reaction mixture was cooled to 0 °C, and tetrakis(triphenylphosphine)palladium(0) (0.49 g, 0.43 mmol) was added followed by the addition of 4-nitrobenzoyl chloride (1.78 g, 9.6 mmol) in THF (5 mL). The stirring mixture was allowed to warm to room temperature overnight. The reaction was concentrated under reduced pressure. The residue was partitioned between EtOAc (50 mL) and 1 N HCl (100 mL) and the aqueous phase was extracted with EtOAc (50 mL). The combined organic extracts were washed with brine (3 × 50 mL), dried over MgSO₄ and concentrated *in vacuo*. The residue obtained was washed with MeOH to give a white solid. Yield: 2.56 g (85 %). t.l.c analysis was impossible owing to limited solubility.

¹H NMR: δ (DMSO-*d*₆): 8.41 (d, J= 7.8 Hz, 2H, Ar), 8.29 (d, J= 7.8 Hz, 2H, Ar), 7.67 (d, J= 8.1 Hz, 2H, Ar), 7.54 (d, J= 8.1 Hz, 2H, Ar), 5.42 (s, 2H, H-8).

¹³C NMR: δ (DMSO-*d*₆): 164.07 (C, C=O), 150.33 (C, C-4), 135.06 (C, C-1'), 135.84 (C, C-1), 131.48 (CH, C-2, C-6), 130.74 (CH, C-3', C-5'), 130.35 (CH, C-2', C-6'), 123.91 (CH, C-3, C-5), 121.52 (C, C-4'), 66.25 (CH₂).

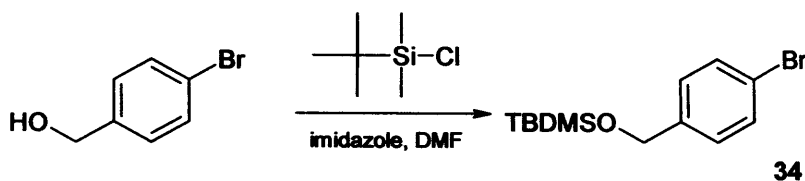
IR (NaCl)/ cm⁻¹ 1714 (C=O); 1524.7 (NO₂); 1348.8 (NO₂).

Melting point: 106-108 °C.

Microanalysis: Calculated for C₁₄H₁₀BrNO₄; theoretical: %C 50.03, %H 3.00, %N 4.17, found %C 49.80, %H 3.14, %N 3.95.

¹⁷¹ Bowie J.H. and Nussey B.; Electron-impact studies. LXXXIV. Substituent effects in the negative ion mass spectra of aryl esters. *Org. Mass Spec.*, 1974, 9, 310-320.

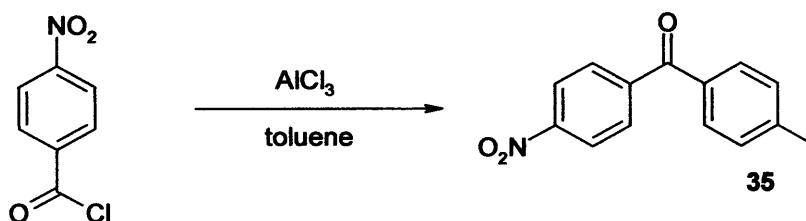
3.1.6) (4-Bromophenoxy)-tert-butyl-dimethyl-silane (34)¹⁷²



TBDMSCl (1.01 g, 6.68 mmol) in dry DMF (5 mL) was added to a dry DMF (25 mL) solution of 4-bromo-benzylalcohol (1 g, 5.35 mmol) and imidazole (0.91 g, 13.36 mg). The mixture was stirred at room temperature for 4 h and then quenched with MeOH (10 mL). The solvent are removed under reduced pressure and the residue diluted with EtOH (30 mL). The mixture was washed with H₂O (3 × 20 mL) and the recombined organic layers were dried (MgSO₄), filtered and concentrated *in vacuo* to give a pure yellow syrup. Yield: 1.54 g (95 %). t.l.c system: petroleum ether-ethyl acetate 2:1, R_f= 0.75.

¹H NMR: δ (DMSO-*d*₆): 6.61 (d, J= 8.1 Hz, 2H, Ar), 6.48 (d, J= 8.1 Hz, 2H, Ar), 3.82 (s, 2H, CH₂), 2.10 (s, 3H, Me), 2.05 (s, 3H, Me), 0.14 (s, 9H, *t*Bu).

3.1.7) 4-Methyl-4'-nitrobenzophenone (35)¹⁷³



To a solution of *p*-nitrobenzoyl chloride (1 g, 5.39 mmol) in toluene (40 mL) was added AlCl₃ (1 g, 7.54 mmol) and the resulting red solution stirred at room temperature for 2 h. H₂O (4 mL) was added dropwise and the resulting mixture was stirred for 15 min and then extracted with H₂O (50 mL) and 10 % NaHCO₃ (2 × 50 mL). The organic layer was dried (MgSO₄), filtered and evaporated to give a pale yellow solid. Recrystallisation from CHCl₃/hexane gave the product as pale yellow needles. Yield: 1.2 g (92 %). t.l.c system: dichloromethane-hexane 1:1, R_f= 0.27.

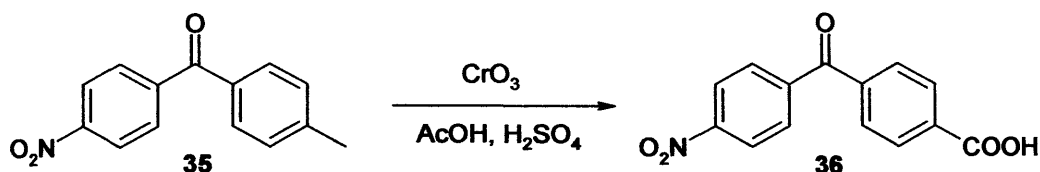
¹⁷² Sessler J.L., Wang B. and Harriman A.; Photoinduced energy transfer in associated, but noncovalent-linked photosynthetic model system. *J. Am. Chem. Soc.*, 1995, 117, 704-714.

¹⁷³ Findeis M.A. and Kaiser E.T.; Nitrobenzophenone oxime based resins for the solid phase synthesis of protected peptide segments. *J. Org. Chem.*, 1989, 54, 3478-3482.

$^1\text{H NMR}$: δ (CDCl_3): 8.36 (d, 2H, $J = 8.8$ Hz, Ar), 7.92 (d, 2H, $J = 8.0$ Hz, Ar), 7.70 (d, 2H, $J = 8.8$ Hz, Ar), 7.24 (d, 2H, $J = 8.0$ Hz, Ar), 2.49 (s, 3H, CH_3).

Melting point: 112-114 °C (lit m.p. 120-120.5 °C)¹⁷³.

3.1.8) 4-(4-Nitrobenzoyl)benzoic acid (36)¹⁷⁴

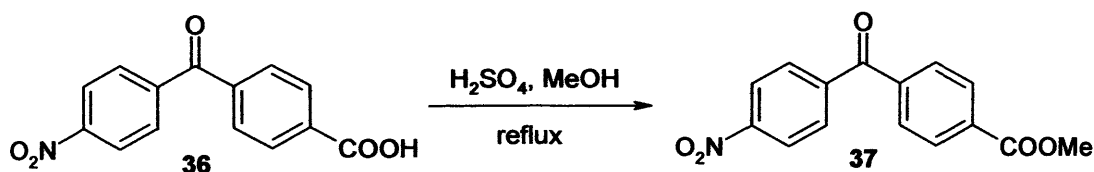


(4-Nitrophenyl)(*p*-tolyl)methanone (35) (2.35 g, 9.74 mmol) was dissolved in warm acetic acid (14 mL). A solution of chromic acid (3.41 g, 34.10 mmol) in H_2O /acetic acid/ H_2SO_4 (8/14/2.6 mL) was added slowly through the condenser while the reaction was kept just below boiling point. When all the oxidizing mixture had been added the preparation was refluxed gently for 1 h and the liquid portion then decanted into cold H_2O . The precipitated solid was collected and washed thoroughly with cold H_2O , then dried at 70 °C *in vacuo* to give the product as a white crystalline solid. Yield: 2.45 g (93 %). t.l.c analysis was impossible owing to limited solubility.

$^1\text{H NMR}$: δ ($\text{DMSO}-d_6$): 13.35 (bs, 1H, COOH), 8.40 (d, 2H, $J = 8.4$ Hz, Ar), 8.12 (d, 2H, $J = 8.0$ Hz, Ar), 7.98 (d, 2H, $J = 8.4$ Hz, Ar), 7.77 (d, 2H, $J = 8.0$ Hz, Ar).

Melting point: 243-244 °C (lit m.p. 255 °C)¹⁷⁴.

3.1.9) 4-(4-Nitrobenzoyl)benzoic acid methyl ester (37)¹⁷⁵



4-(4-Nitrobenzoyl)benzoic acid (36) (1 g, 3.68 mmol) was dissolved in H_2SO_4 (6 mL) with cooling (ice-bath), and the solution poured into dry MeOH (25

¹⁷⁴ Werther E.; Benzylbenzaldoxime. *J. Am. Chem. Soc.*, 1933, 55, 2540.

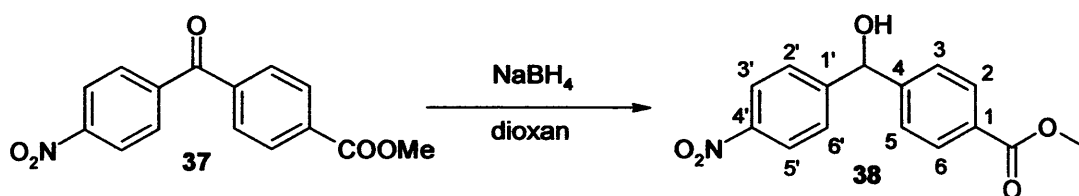
¹⁷⁵ Danishefsky S., Hiramama H., Gombatz K., Harayama T., Berman E. and Schuda P.; The use of trans-methyl β -nitroacrylate in Diels-Alder reaction. *J. Am. Chem. Soc.*, 1978, 100, 6536.

mL). The mixture was refluxed for 30 min and then allowed to cool to room temperature. The precipitated solid was filtered and washed with MeOH (2 × 20 mL) to give the product as a white solid. Yield: 0.94 g (89 %). t.l.c system: petroleum ether-ethyl acetate 1:1, R_f = 0.79.

$^1\text{H NMR}$: δ (DMSO- d_6): 8.41 (d, 2H, J = 8.7 Hz, Ar), 8.16 (d, 2H, J = 8.4 Hz, Ar), 8.03 (d, 2H, J = 8.7 Hz, Ar), 7.90 (d, 2H, J = 8.4 Hz, Ar), 3.96 (s, 3H, CH_3).

Melting point: 141-142 °C (lit m. p. 174-175 °C)¹⁷⁶.

3.1.10 Methyl 4-(hydroxy(4-nitrophenyl)methyl)benzoate (38)



To a cooled (0 °C) solution of 37 (5.84 g, 20 mmol) in anhydrous dioxane (100 mL) was added sodium borohydride (0.77 g, 20 mmol), then the mixture was allowed to stir at room temperature under nitrogen for 5 h. The solvent was concentrated under reduced pressure and aqueous HCl (1 M, 10 mL) added to the residue. The oil formed was extracted with Et_2O (2 × 50 mL) and washed with H_2O (2 × 50 mL), the organic layers were combined and dried with MgSO_4 and the solvent concentrated under reduced pressure to give a white solid. Yield: 5.74 g (99 %). t.l.c system: petroleum ether-ethyl acetate 1:1, R_f = 0.62.

$^1\text{H NMR}$: δ (CDCl_3): 8.12 (d, 2H, J = 8.7 Hz, Ar), 7.94 (d, 2H, J = 8.3 Hz, Ar), 7.52 (d, 2H, J = 8.7 Hz, Ar), 7.39 (d, 2H, J = 8.3 Hz, Ar), 5.88 (s, 1H, H-7), 3.87 (s, 3H, CH_3).

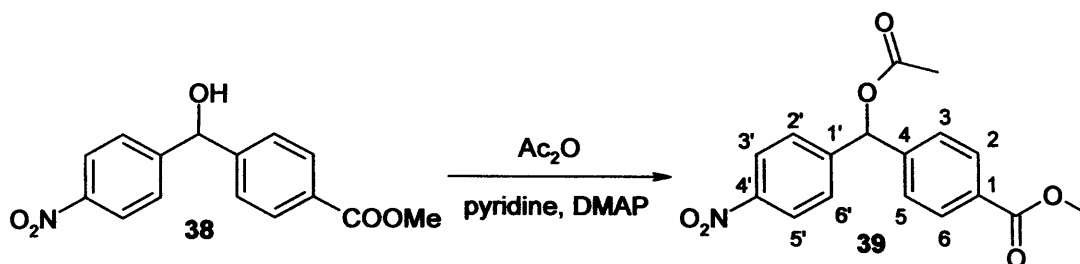
$^{13}\text{C NMR}$: δ (CDCl_3): 167.87 (C, C=O), 150.52 (C, C-1'), 148.13 (C, C-4), 147.25 (C, C-4'), 130.41 (CH, C-2, C-6), 129.51 (C, C-1), 127.46 (CH, C-2', C-6'), 126.48 (CH, C-3, C-5), 123.72 (CH, C-3', C-5'), 74.80 (CH, C-OH), 52.18 (CH_3).

Melting point: 122-124 °C.

HRMS (EI): Found: 287.0786 (M)⁺, Calculated: 287.0788.

¹⁷⁶ Salem O.A.I., Frotscher M., Scherer C., Neugebauer A., Biemel K., Streiber M., Maas R. and Hartmann R.W.; Novel 5 α -reductase inhibitors: synthesis, structure-activity studies, and pharmacokinetic profile of phenoxybenzoylphenyl acetic acid. *J. Med. Chem.*, 2006, 49, 748-759.

3.1.11) 4-[Acetoxy-(4-nitrophenyl)methyl]benzoic acid methyl ester (39)



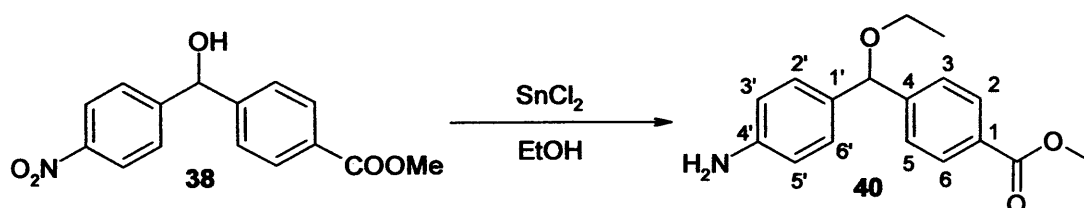
To a solution of **38** (1 g, 3.48 mmol) and DMAP (46 mg, 0.38 mmol) in dry pyridine (25 mL) was added acetic anhydride (0.71 g, 6.96 mmol) and the reaction was stirred under nitrogen at room temperature overnight. EtOH (10 mL) was added to quench the reaction, which was then diluted with CH₂Cl₂ (40 mL). The solution was washed with saturated aqueous NaHCO₃ (2 × 25 mL) and 10 % NaCl solution (2 × 25 mL). The organic layer was dried with MgSO₄ to give a yellow syrup. Yield: 1.07 g (93 %). t.l.c system: petroleum ether-ethyl acetate 1:1, R_f = 0.68.

¹H NMR: δ (CDCl₃): 8.11 (m, 2H, Ar), 7.97 (m, 2H, Ar), 7.50 (m, 2H, Ar), 7.39 (m, 2H, Ar), 6.90 (s, 1H, H-7), 3.83 (s, 3H, H-15), 2.16 (s, 3H, H-17).

¹³C NMR: δ (CDCl₃): 169.50 (C, OAc), 166.29 (C, Ar-C=O), 148.39 (C, C-1'), 147.53 (C, C-4), 146.61 (C, C-4'), 130.53 (CH, C-2, C-6), 130.38 (C, C-1), 128.17 (CH, C-2', C-6'), 127.77 (CH, C-3, C-5), 123.83 (CH, C-3', C-5'), 75.71 (C-OAc), 52.43 (CH₃, OCH₃), 21.32 (CH₃, CO-CH₃).

HRMS (EI): Found: 329.0895(M)⁺, Calculated: 329.0894.

3.1.12) 4-[(Aminophenyl)ethoxymethyl]benzoic acid methyl ester (40)



A mixture of **38** (0.20 g, 0.69 mmol) and SnCl₂ · 2 H₂O (0.47 g, 2.09 mmol) in 20 mL of absolute EtOH was heated at 70 °C under nitrogen. After 3 h, the starting material has disappeared and the solution was allowed to cool down and then poured into ice. The pH was made slightly basic (pH 8-9) by addition of 5 % aqueous

sodium bicarbonate. The product was then extracted with EtOH (20 mL) and the organic phase was thoroughly washed with brine (3 × 50 mL), treated with charcoal and dried over MgSO₄. After filtration, the solvent was removed under reduced pressure to give an orange solid which was washed with hot H₂O (2 × 30 mL) and MeOH (2 × 30 mL) to give the product as a yellow solid. Yield: 0.15 g (76 %).

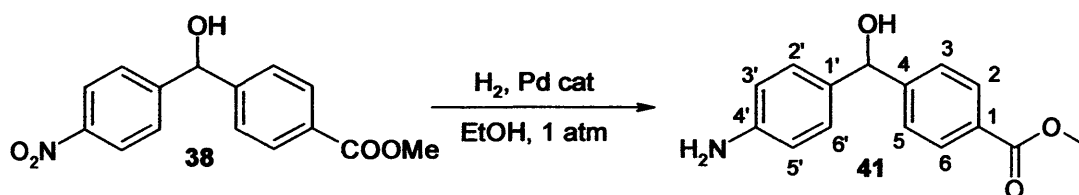
¹H NMR: δ (CDCl₃): 7.78 (d, 2H, J= 8.3 Hz, Ar), 7.31 (d, 2H, J= 8.3 Hz, Ar), 6.96 (d, 2H, J= 8.5 Hz, Ar), 6.52 (d, 2H, J= 8.5 Hz, Ar), 5.19 (s, 1H, H-7), 3.79 (s, 3H, H-15), 3.55 (bs, 2H, NH₂), 3.40 (q, 2H, J= 7.0 Hz, H-16), 1.13 (t, 3H, J= 7.0 Hz, H-17).

¹³C NMR: δ (CDCl₃): 166.06 (C, C=O), 147.39 (C, C-4), 144.99 (C, C-4'), 130.66 (C, C-1'), 129.01 (CH, C-2, C-6), 127.34 (C, C-1), 127.07 (CH, C-2', C-6'), 125.47 (CH, C-3, C-5), 114.36 (CH, C-3', C-5'), 82.03 (CH, CH-O), 63.35 (CH₂), 51.15 (CH₃, OCH₃), 14.27 (CH₃).

Melting point: 114-115 °C.

HRMS (EI): Found: 285.1361 (M)⁺, Calculated: 285.1365.

3.1.13 Methyl 4-((4-aminophenyl)(hydroxy)methyl)benzoate (41)¹⁷⁷



To a solution of 38 (5 g, 17.40 mmol) in EtOH (70 mL) was added Pd/C catalyst (1 g) and the reaction stirred under a H₂ atmosphere (H₂ balloon) for 30 min. The reaction was filtered through celite and the filtrate concentrated under reduced pressure. The resulting oil was extracted with CH₂Cl₂ (50 mL), washed with H₂O (2 × 50 mL), dried (MgSO₄) and concentrated in *vacuo* to give a yellow solid. Purification by column chromatography (petroleum ether/EtOAc 50:50) gave the product as a white solid. Yield: 3.38 g (76 %). t.l.c system: petroleum ether-ethyl acetate 1:1, R_f = 0.23.

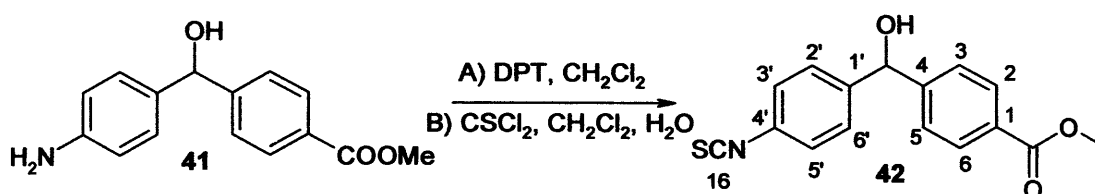
¹⁷⁷ Bridger G.J., Zhou Y. and Skerlj R.; Preparation of piperidines as chemokine receptor, particularly CCR5, modulators for treatment of inflammatory and autoimmune diseases. *PCT Int. Appl.*, 2005, 384 pp.

¹H NMR: δ (CDCl₃): 7.91 (d, 2H, J= 7.3 Hz, Ar), 7.39 (d, 2H, J= 7.2 Hz, Ar), 7.04 (d, 2H, J= 7.3 Hz, Ar), 6.56 (d, 2H, J= 7.2 Hz, Ar), 5.70 (s, 1H, H-7), 3.83 (s, 3H, CH₃), 3.61 (bs, 2H, NH₂), 2.09 (bs, 1H, OH).

¹³C NMR: δ (CDCl₃): 167.06 (C, C=O), 149.33 (C, C-4), 146.16 (C, C-4'), 133.63 (C, C-1'), 129.76 (CH, C-2, C-6), 128.91 (C, C-1), 128.08 (CH, C-2', C-6'), 126.21 (CH, C-3, C-5), 115.48 (CH, C-2, C-6), 75.59 (CH, CH-OH), 52.05 (CH₃).

Melting point: 117-118 °C.

3.1.14) *Methyl 4-(hydroxy(4-isothiocyanatophenyl)methyl)benzoate (42)*



Method A: Di-pyrimidyl-thiocarbonate (0.18 g, 0.76 mmol) was added to a solution of 41 and CH₂Cl₂ (25 mL) as a solvent. The mixture was stirred overnight at room temperature and then extracted with H₂O (2 × 25 mL). The recombined organic layers were dried on MgSO₄ and after filtration the solvent was reduced under reduced pressure to give an oil which was purified by column chromatography (petroleum ether/EtOAc 4:1) to obtain the product as a yellow syrup. Yield: 0.16 g (78 %).

Method B: To a solution of (41) (8.83 g, 34.50 mmol) in CH₂Cl₂ (100 mL) was added a mixture of ice (100 g) and H₂O (50 mL). Thiophosgene (3.16 mL, 41.40 mmol) was then added dropwise with vigorous stirring and the mixture stirred for 2 h at 0 °C and kept overnight in a refrigerator. The organic layer was separated and extracted successively with H₂O (2 × 50 mL), 10 % aqueous NaHCO₃ (50 mL) and H₂O again (50 mL), dried (MgSO₄) and concentrated under reduced pressure to obtain the pure product as a yellow solid. Yield: 9.17 g (89 %). t.l.c system: petroleum ether-ethyl acetate 1:1, R_f= 0.59.

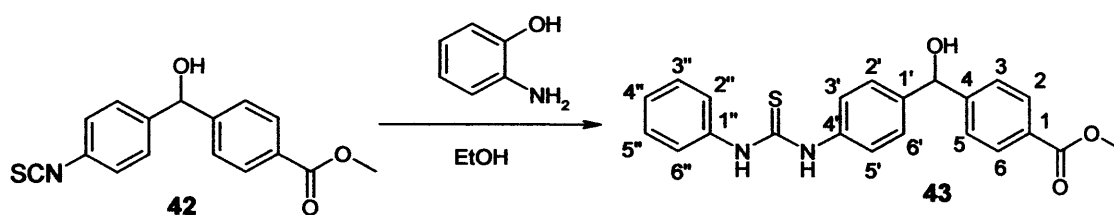
¹H NMR: δ (CDCl₃): 7.90 (d, 2H, J= 7.9 Hz, Ar), 7.31 (d, 2H, J= 7.9 Hz, Ar), 7.25 (d, 2H, J= 8.1 Hz, Ar), 7.09 (d, 2H, J= 8.1 Hz, Ar), 5.75 (s, 1H, H-7), 3.80 (s, 3H, CH₃), 2.51 (bs, 1H, OH).

^{13}C NMR: δ (CDCl_3): 166.83 (C, C=O), 148.17 (C, C-4), 142.48 (C, C-1'), 135.72 (C, NCS), 130.71 (C, C-1), 129.96 (CH, C-2, C-6), 129.90 (C, C-4'), 128.62 (CH, C-2', C-6'), 126.57 (CH, C-3, C-5), 125.92 (CH, C-3', C-5'), 75.18 (CH, CH-OH), 52.19 (CH_3).

Melting point: 114-115 °C.

HRMS (EI): Found: 299.0610(M)⁺, Calculated: 299.0610.

3.1.15) Methyl-4-(hydroxy(4-(3-(2-hydroxyphenyl)thioureido)phenyl)methyl)benzoate (43)



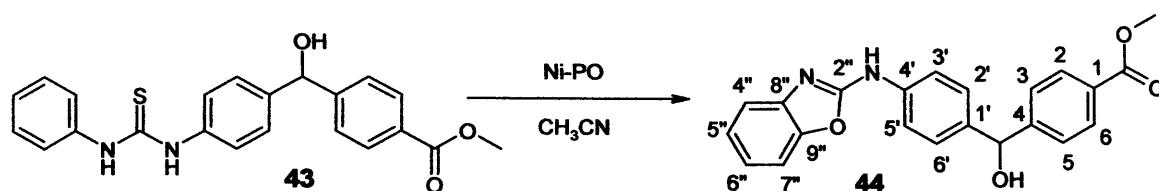
2-Aminophenol (38 mg, 0.24 mmol) was added to a solution of **42** (103 mg, 0.34 mmol) in absolute EtOH (10 mL). The mixture was then stirred overnight at room temperature. EtOH was removed under reduced pressure and the yellow oil was extracted with CH_2Cl_2 (20 mL) and washed with H_2O (2 \times 20 mL). The recombined organic layers were dried (MgSO_4) and the solvent evaporated in *vacuo* to give an oil which was purified by column chromatography (hexane/ EtOAc 100:0 to 50:50) to give a yellow syrup. Yield: 106 mg (76 %). t.l.c system: petroleum ether-ethyl acetate 1:1, R_f = 0.15.

^1H NMR: δ (CDCl_3): 8.09 (bs, 1H, NH), 7.84 (d, 2H, J = 8.1 Hz, Ar), 7.79 (bs, 1H, NH), 7.30 (d, 2H, J = 7.9 Hz, Ar), 7.23 (d, 2H, J = 7.7 Hz, Ar), 7.16 (d, 2H, J = 7.0 Hz, Ar), 7.07 (d, 2H, J = 8.3 Hz, Ar), 6.90 (d, 1H, J = 8.0 Hz, Ar), 6.71 (m, 1H, Ar), 5.71 (s, 1H, H-7), 3.82 (s, 3H, CH_3), 3.23 (bs, 1H, OH).

^{13}C NMR: δ (CDCl_3): 178.96 (C, C=S), 166.95 (C, C=O), 150.59 (C, C-1''), 142.48 (C, C-4'), 148.15 (C, C-4), 142.52 (C, C-1'), 134.44 (C, C-1), 129.92 (CH, C-2, C-6), 129.44 (CH, C-6''), 129.02 (CH, C-2''), 128.08 (CH, C-2', C-6'), 126.34 (CH, C-3, C-5), 126.15 (CH, C-4''), 125.48 (CH, C-3', C-5'), 121.40 (CH, C-3''), 119.26 (CH, C-5''), 75.22 (CH, CH-OH), 52.21 (CH_3).

HRMS (EI): Found: 409.1224 (M)⁺, Calculated: 409.1222.

3.1.16 Methyl-4-((4-(benzoxazol-2-ylamino)phenyl)(hydroxy)methyl)benzoate (44)



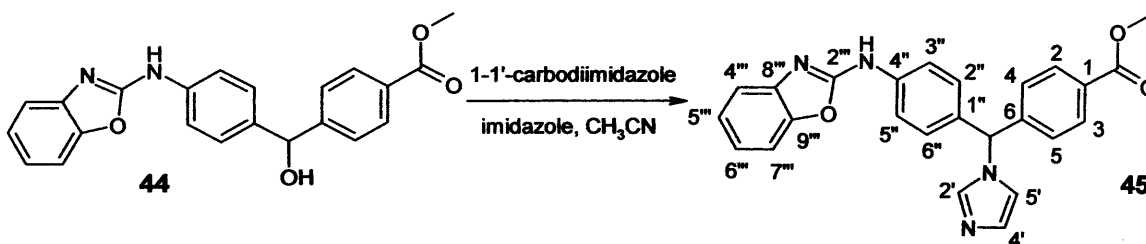
To a solution of (**43**) (0.35 g, 0.86 mmol) in CH_3CN (25 mL) was added nickel peroxide (0.29 g). The heterogeneous solution was stirred at room temperature overnight then the reaction mixture was filtered and washed repeatedly with CH_3CN . After evaporation of the solvent, the oil was extracted with CH_2Cl_2 (25 mL) and washed with H_2O ($2 \times 25\text{mL}$). The organic layer was dried (MgSO_4), concentrated under reduced pressure and the resulting oil purified by column chromatography (petroleum ether/EtOAc 80:20 v/v) to give the product as a yellow syrup. Yield: 0.19 g (61 %). t.l.c system: petroleum ether-ethyl acetate 1:1, $R_f = 0.45$.

$^1\text{H NMR}$: δ (CDCl_3): 7.92 (bs, 1H, NH), 7.91 (d, 2H, $J = 8.1$ Hz, Ar), 7.48 (d, 2H, $J = 8.1$ Hz, Ar), 7.38 (m, 3H, Ar), 7.25 (m, 3H, Ar), 7.12 (m, 1H, Ar), 7.03 (m, 1H, Ar), 5.77 (s, 1H, H-7), 3.81 (s, 3H, CH_3), 2.60 (bs, 1H, OH).

$^{13}\text{C NMR}$: δ (CDCl_3): 166.94 (C, C=O), 158.13 (C, C-2''), 148.70 (C, C-8''), 142.10 (C, C-4), 138.32 (C, C-4'), 137.53 (C, C-9''), 129.81 (CH, C-2, C-6), 129.27 (C, C-1'), 127.81 (CH, C-2', C-6'), 126.31 (CH, C-3, C-5), 124.35 (CH, C-6''), 122.01 (CH, C-5''), 118.65 (CH, C-3', C-5'), 117.18 (CH, C-7''), 109.14 (CH, C-4''), 75.45 (CH, CH-OH), 52.10 (CH_3).

HRMS (EI) : Found: 375.1337(M)⁺, Calculated: 375.1339.

3.1.17 4-[[4-(Benzoxazol-2-ylamino)phenyl]imidazol-1-ylmethyl]benzoic acid methyl ester (45)



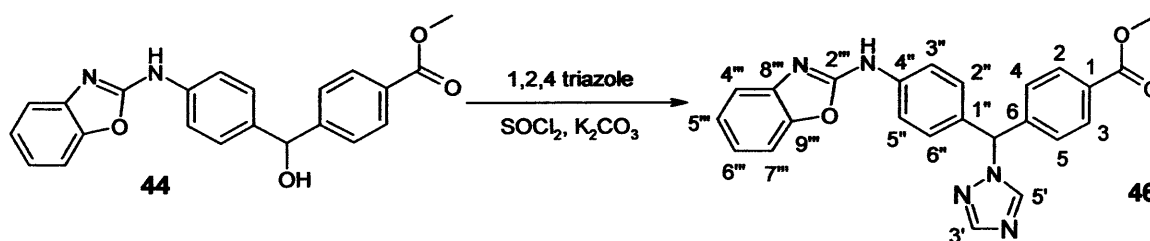
To a solution of **44** (2.28 g, 6.08 mmol) in CH₃CN (40 mL) was added imidazole (1.24 g, 18.25 mmol) and 1,1'-carbodiimidazole (1.18 g, 9.13 mmol). The mixture was heated under reflux for 2 h, then the reaction mixture was allowed to cool and the solvent removed under reduced pressure. The oil formed was then extracted with CH₂Cl₂ (50 mL) and washed with H₂O (2 × 50 mL). The organic layer was dried (MgSO₄), filtered and reduced in *vacuo*. Purification by column chromatography (EtOAc) gave the product as a yellow syrup. Yield: 2.33 g (90 %). t.l.c system: ethyl acetate, R_f = 0.21.

¹H NMR: δ (CDCl₃): 8.52 (bs, 1H, NH), 7.96 (d, 2H, J = 8.2 Hz, Ar), 7.59 (d, 2H, J = 8.5 Hz, Ar), 7.38 (d, 2H, J = 7.5 Hz, Ar), 7.22 (d, 1H, J = 7.9 Hz, Ar), 7.18 (m, 1H, Ar), 7.08 (m, 6H, Ar), 6.79 (m, 1H, Ar), 6.45 (s, 1H, H-7), 3.86 (s, 3H, CH₃).

¹³C NMR: δ (CDCl₃): 166.47 (C, C=O), 157.82 (C, C-2'''), 147.78 (C, C-8'''), 144.19 (C, C-4), 142.21 (C, C-4''), 139.82 (CH, C-2'), 138.67 (C, C-9'''), 132.46 (C, C-1''), 130.28 (C, C-1), 130.18 (CH, C-2, C-3), 129.57 (CH, C-2'', C-6''), 127.78 (CH, C-3, C-5), 125.94 (CH, C-5'), 124.32 (CH, C-6'''), 122.63 (CH, C-4'), 122.13 (CH, C-5'''), 119.33 (CH, C-3'', C-5''), 117.36 (CH, C-7'''), 109.12 (CH, C-4'''), 64.37 (CH, CH-N), 52.29 (CH₃).

HRMS (EI): Found: 425.1610 (M)⁺, Calculated: 425.1608.

3.1.18) Methyl 4-((4-(benzoxazol-2-ylamino)phenyl)(1H-1,2,4-triazol-1-yl)methyl)benzoate (46)



To a cooled (0 °C) solution of 1,2,4-triazole (0.22 g, 3.20 mmol) in anhydrous CH₃CN (10 mL) was added thionyl chloride (0.12 mL, 1.60 mmol) in anhydrous CH₃CN (6 mL) and the reaction stirred at 10 °C for 1 h. Potassium carbonate (0.22 g, 1.60 mmol) was then added followed by a solution of **44** (0.30 g, 0.80 mmol) in anhydrous CH₃CN (10 mL) and the reaction allowed to stir at room

temperature for 3 days. The suspension was filtered and the solution concentrated under reduced pressure to produce a mixture which was extracted with EtOAc (2 × 25 mL) and washed with H₂O (2 × 25 mL). The organic layers were dried with MgSO₄ and the solvent evaporated to give a yellow solid. Purification by flash-chromatography (EtOAc) gave the product as a yellow solid. Yield: 0.15 g (43 %). t.l.c system: ethyl acetate R_f = 0.10.

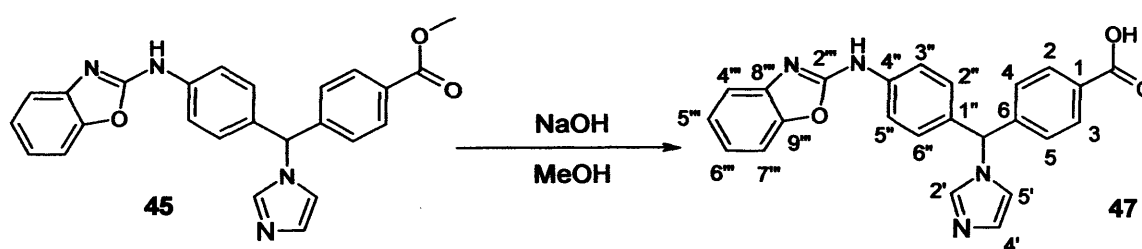
¹H NMR: δ (CDCl₃): 8.69 (bs, 1H, NH), 8.02 (m, 1H, Ar), 8.00 (d, 2H, J = 7.4 Hz, Ar), 7.97 (m, 1H, Ar), 7.68 (d, 2H, J = 8.2 Hz, Ar), 7.33 (d, 1H, J = 6.3 Hz, Ar), 7.27 (m, 6H, Ar), 6.79 (m, 1H, H-7), 3.91 (s, 3H, CH₃).

¹³C NMR: δ (CDCl₃): 165.63 (C, C=O), 157.03 (C, C-2'''), 151.64 (CH, C-5'), 146.95 (C, C-8'''), 142.75 (CH, C-3'), 142.27 (C, C-4), 141.18 (C, C-4''), 138.03 (C, C-9'''), 130.54 (C, C-1''), 129.51 (C, C-1), 129.35 (CH, C-2, C-6), 128.78 (CH, C-2'', C-6''), 126.93 (CH, C-3, C-5), 123.58 (CH, C-6'''), 121.35 (CH, C-5'''), 117.78 (CH, C-3'', C-5''), 116.45 (CH, C-7'''), 108.34 (CH, C-4'''), 66.26 (CH, CH-N), 51.46 (CH₃).

Melting point: 192-194 °C.

HRMS (EI): Found: 426.1559 (M)⁺, Calculated: 426.1561.

3.1.19) 4-[[4-(Benzoxazol-2-ylamino)phenyl]imidazol-1-ylmethyl]benzoic acid (47)



To a suspension of 45 (0.30 g, 0.7 mmol) in MeOH (6 mL) was added a 2 M solution of aqueous NaOH (3 mL) and the mixture was refluxed for 30 min. The mixture was then allowed to cool and was diluted with H₂O (5 mL), HCl was added until pH 1. After removing the solvent under reduced pressure, MeOH (5 mL) was added to the mix to precipitate the NaCl formed during the reaction. The solid was

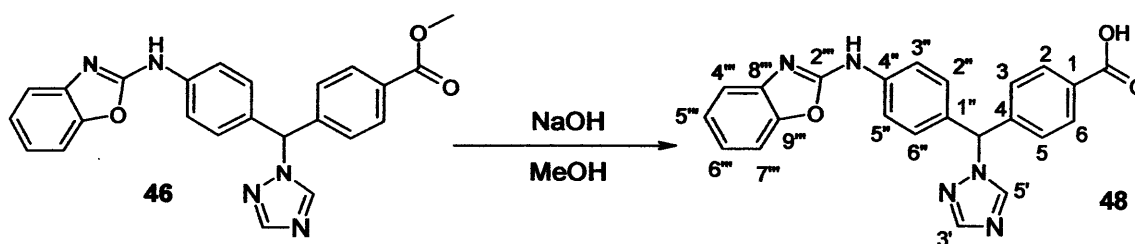
removed by filtration and the filtrate reduced *in vacuo* to give a yellow syrup. Yield: 0.18 g (62 %). t.l.c system: dichloromethane-methanol 98:2, $R_f = 0.16$.

$^1\text{H NMR}$: δ (DMSO- d_6): 13.11 (bs, 1H, COOH), 11.02 (bs, 1H, NH), 9.21 (s, 1H, Ar), 8.01 (m, 2H, Ar), 7.87 (m, 2H, Ar), 7.79 (m, 2H, Ar), 7.50 (m, 1H, Ar), 7.43 (m, 1H, Ar), 7.32 (m, 5H, Ar), 7.22 (m, 1H, Ar), 6.95 (s, 1H, H-7).

$^{13}\text{C NMR}$: δ (DMSO- d_6): 169.14 (C, C=O), 159.69 (C, C-2'''), 148.96 (C, C-8'''), 143.75 (C, C-4), 143.45 (C, C-4''), 141.13 (C, C-9'''), 132.74 (C, C-1''), 131.72 (C, C-1), 131.60 (CH, C-2'), 130.65 (CH, C-2, C-6), 129.03 (CH, C-2'', C-6''), 125.33 (CH, C-3, C-5), 123.34 (CH, C-4'), 123.22 (CH, C-6'''), 122.89 (CH, C-5'''), 120.23 (CH, C-5'), 120.23 (CH, C-3'', C-5''), 117.89 (CH, C-7'''), 110.11 (CH, C-4'''), 67.19 (CH, CH-N).

HRMS (EI) : Found: 411.1452 (M^+), Calculated: 411.1449.

3.1.20 4-{[4-(Benzoxazol-2-ylamino)phenyl]-1H-1,2,4-triazol-1-ylmethyl}benzoic acid (48)



To a suspension of **46** (50 mg, 0.12 mmol) in MeOH (2 mL) was added a 2M solution of aqueous NaOH (1 mL) and the mixture was refluxed for 30 min. The mixture was then allowed to cool and was diluted with H₂O (2 mL), HCl was added until pH 1. After removing the solvent under reduced pressure, MeOH (3 mL) was added to the mix to precipitate the NaCl formed during the reaction. The solid was removed by filtration and the filtrate reduced *in vacuo* to give a yellow syrup. Yield: 28 mg (56 %). t.l.c system: dichloromethane-methanol 98:2, $R_f = 0.20$.

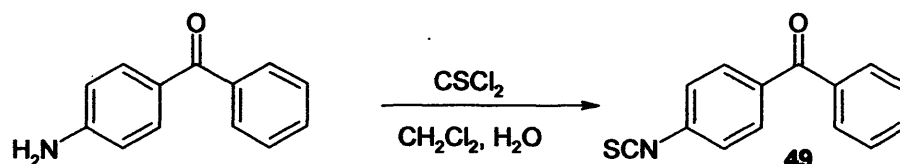
$^1\text{H NMR}$: δ (MeOD): 8.99 (s, 1H, Ar), 8.31 (s, 1H, Ar), 7.88 (m, 2H, Ar), 7.56 (m, 2H, Ar), 7.25 (m, 5H, Ar), 7.13 (m, 1H, Ar), 7.09 (m, 2H, Ar), 6.82 (s, 1H, H-7).

^{13}C NMR: δ (MeOD): 169.08 (C, C=O), 159.37 (C, C-2'''), 148.26 (C, C-8'''), 143.96 (C, C-4), 138.96 (C, C-4''), 138.72 (C, C-9'''), 134.45 (C, C-1'''), 132.26 (C, C-1), 131.30 (CH, C-5'), 131.09 (CH, C-2, C-3), 130.98 (CH, C-2'', C-6''), 129.47 (CH, C-3, C-5), 126.85 (CH, C-3'), 124.46 (CH, C-6'''), 122.86 (CH, C-5'''), 121.61 (CH, C-3'', C-5''), 116.40 (CH, C-7'''), 110.89 (CH, C-4'''), 68.66 (CH, CH-N).

HRMS (EI): Found: 412.1415 (M)⁺, Calculated: 412.1410.

3.2) Experimental results for the preparation of the unsubstituted derivatives 52, 53, 53' and 54

3.2.1) 4-Isothiocyanatobenzophenone (49)¹⁷⁸

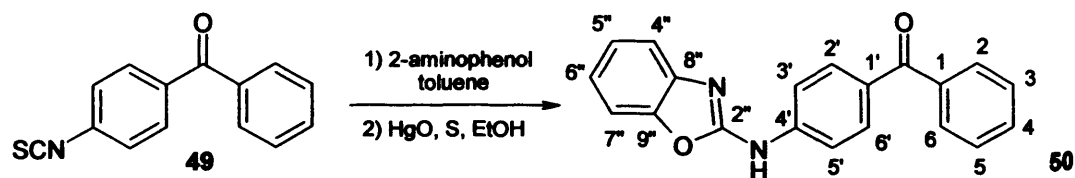


To a solution of 4-amino-benzophenone (10 g, 50.70 mmol) in CH₂Cl₂ (10 mL) was added a mixture of ice (30 g) and H₂O (70 mL) and subsequently dropwise with vigorous stirring thiophosgene (4.64 mL, 60.84 mmol). The mixture was stirred for 2 h at 0 °C and kept overnight in a refrigerator. The organic layer was separated and extracted successively with H₂O (2 × 50 mL), 10 % NaHCO₃ aq. (50 mL) and H₂O again (50 mL), dried (MgSO₄) and evaporated to dryness to obtain the pure product as a yellow syrup. Yield: 12 g (99 %). t.l.c system: petroleum ether-ethyl acetate 2:1, R_f = 0.88.

^1H NMR: δ (CDCl₃): 7.83 (d, 2H, J = 8.3 Hz, Ar), 7.79 (d, 2H, J = 7.2 Hz, Ar), 7.64 (m, 1H, Ar), 7.51 (m, 2H, Ar), 7.33 (m, 2H, Ar).

¹⁷⁸ Horakova K., Drobica L. and Nemeč P.; Cytotoxic and cancerostatic activity of isothiocyanates and related compounds. VI. Isothiocyanates of the R-C₆H₄-X-C₆H₄-NCS type. *Neoplasma*, 1970, 17, 9-14.

3.2.2) [4-(Benzoxazol-2-ylamino)phenyl]phenylmethanone (50)



2-Aminophenol (5.48 g, 50.21 mmol) was added to a solution of 49 (12 g, 50.21 mmol) in toluene (150 mL). The mixture was then refluxed for 1 h and left to stir overnight at room temperature. The solvent was removed under reduced pressure and the crude product was used for the cyclisation. The crude thiourea was then dissolved in EtOH (150 mL), mixed with HgO (16.94 g, 78.21 mmol) and sulphur (0.25 g, 7.82 mmol) and refluxed for 4 h. The cooled reaction mixture was filtered through a celite pad and then the dark residue was dissolved in THF and filtered again through celite to give the pure product as a yellow solid. Yield: 6.89 g (54 %). t.l.c system: petroleum ether-ethyl acetate 2:1, $R_f = 0.56$.

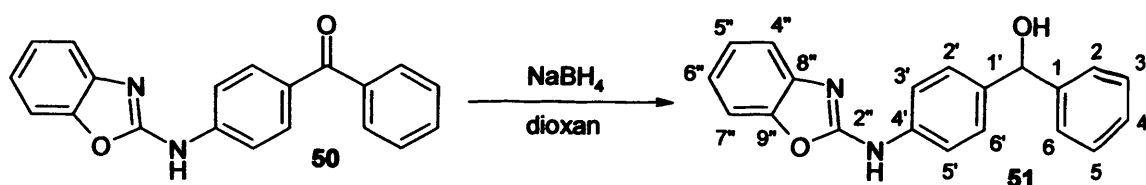
$^1\text{H NMR}$: δ (DMSO- d_6): 11.12 (bs, 1H, NH), 7.94 (d, 2H, $J = 8.2$ Hz, Ar), 7.83 (d, 2H, $J = 8.2$ Hz, Ar), 7.72 (d, 2H, $J = 7.7$ Hz, Ar), 7.67 (m, 1H, Ar), 7.55 (m, 4H, Ar), 7.26 (m, 1H, Ar), 7.18 (m, 1H, Ar).

$^{13}\text{C NMR}$: δ (DMSO- d_6): 194.35 (C, C=O), 157.28 (C, C-2''), 147.00 (C, C-4'), 142.89 (C, C-8''), 141.98 (C, C-9''), 137.68 (C, C-1), 132.12 (CH, C-4), 131.48 (CH, C-2', C-6'), 130.25 (C, C-1'), 129.35 (CH, C-2, C-6), 129.03 (CH, C-2', C-6'), 128.43 (CH, C-3, C-5), 122.25 (CH, C-5''), 117.02 (CH, C-7''), 116.81 (CH, C-3', C-5'), 109.20 (CH, C-4'').

Melting point: 193-194 °C.

HRMS (EI): Found: 315.1135 (M) $^+$, Calculated: 315.1134.

3.2.3) [4-(Benzoxazol-2-ylamino)phenyl]phenylmethanol (51)



To a cooled (0 °C) solution of **50** (6.78 g, 20.86 mmol) in anhydrous dioxan (100 mL) was added sodium borohydride (0.79 g, 20.86 mmol), then the mixture was allowed to stir at room temperature under nitrogen overnight. The solvent was concentrated under reduced pressure and aqueous HCl (1 M, 10 mL) added to the residue. The oil formed was extracted with Et₂O (2 × 50 mL) and washed with H₂O (2 × 50 mL), the organic layers were combined and dried with MgSO₄ and the solvent concentrated under reduced pressure to give a white solid. Yield: 5.84 g (86 %). t.l.c system: petroleum ether-ethyl acetate 2:1, R_f = 0.28.

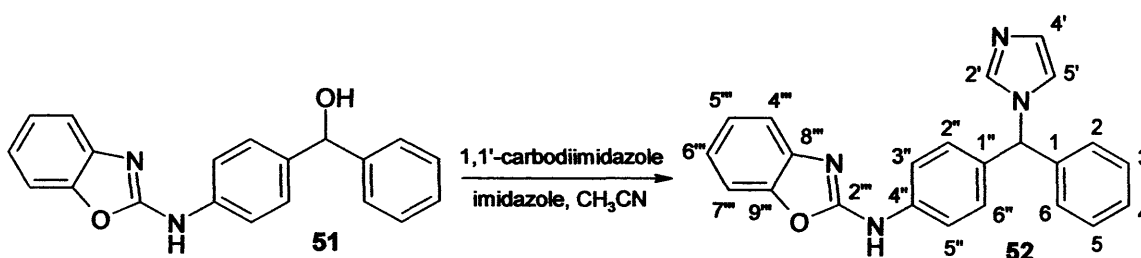
¹H NMR: δ (DMSO-*d*₆): 10.52 (bs, 1H, NH), 7.51 (d, 2H, J = 8.1 Hz, Ar), 7.45 (m, 4H, Ar), 7.40 (m, 2H, Ar), 7.22 (m, 2H, Ar), 7.14 (m, 1H, Ar), 5.83 (bs, 1H, OH), 5.20 (s, 1H, H-7).

¹³C NMR: δ (DMSO-*d*₆): 158.04 (C, C-2''), 147.00 (C, C-8''), 145.84 (C, C-4'), 142.44 (C, C-1), 139.59 (C, C-9''), 137.31 (C, C-1'), 128.45 (CH, C-2', C-6'), 127.99 (CH, C-3, C-5), 126.86 (CH, C-2, C-6), 126.17 (CH, C-4), 123.94 (CH, C-6''), 121.54 (CH, C-5''), 117.39 (CH, C-3', C-5'), 116.51 (CH, C-7''), 108.87 (CH, C-4''), 73.92 (CH, CH-OH).

Melting point: 160-162 °C.

HRMS (EI): Found: 317.1287 (M)⁺, Calculated: 317.1285.

3.2.4 *Benzoxazol-2-yl-[4-imidazol-1-ylphenylmethyl]phenyl]amine (52)*



To a solution of **51** (5.84 g, 17.85 mmol) in CH₃CN (100 mL) was added imidazole (3.67 g, 53.58 mmol) and 1,1'-carbodiimidazole (4.34 g, 26.78 mmol). The mixture was heated under reflux overnight, then the reaction mixture was allowed to cool and the solvent removed under reduced pressure. The oil formed was then extracted with CH₂Cl₂ (100 mL) and washed with H₂O (2 × 100 mL). The organic layer was dried (MgSO₄), filtered and reduced in *vacuo*. Purification by column

chromatography (EtOAc) gave the product as a pale yellow solid. Yield: 4.98 g (74 %). t.l.c system: ethyl acetate, $R_f = 0.11$.

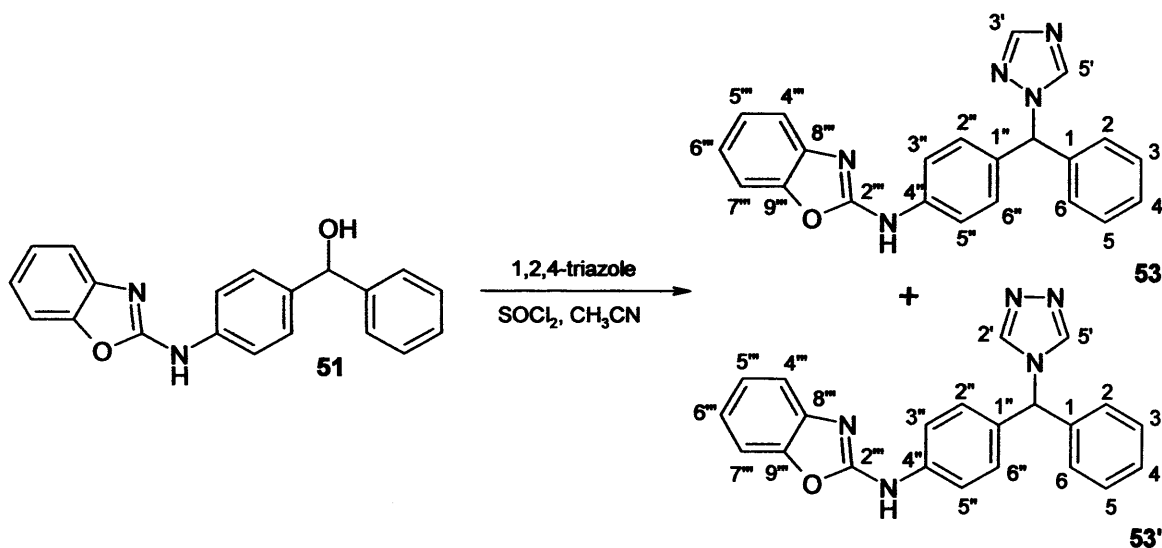
$^1\text{H NMR}$: δ (CDCl_3): 10.70 (bs, 1H, NH), 7.76 (m, 2H, Ar), 7.64 (s, 1H, Ar), 7.49 (m, 1H, Ar), 7.40 (m, 4H, Ar), 7.19 (m, 3H, Ar), 7.12 (m, 4H, Ar), 6.97 (s, 1H, Ar), 6.84 (s, 1H, H-7).

$^{13}\text{C NMR}$: δ (CDCl_3): 157.85 (C, C-2'''), 147.00 (C, C-8'''), 142.28 (C, C-4''), 140.27 (C, C-1), 138.42 (C, C-9'''), 137.13 (CH, C-2'), 133.39 (C, C-1''), 128.74 (CH, C-2'', C-6''), 128.26 (CH, C-3, C-5), 127.81 (CH, C-4), 127.54 (CH, C-2, C-6), 124.01 (CH, C-5'), 122.06 (CH, C-4'), 121.74 (CH, C-6'''), 119.14 (CH, C-5'''), 117.74 (CH, C-3'', C-5''), 116.64 (CH, C-7'''), 108.98 (CH, C-4'''), 62.98 (CH, CH-N).

Melting point: 214-216 °C.

HRMS (EI): Found: 367.1555 (M^+), Calculated: 367.1553.

3.2.5) Benzoxazol-2-yl-[4-(phenyl-[1,2,4]triazol-1-ylmethyl)phenyl]amine (53) and Benzoxazol-2-yl-[4-(phenyl-[1,3,4]triazol-1-ylmethyl)phenyl]amine (53')



To a cooled (0 °C) solution of 1,2,4-triazole (1.76 g, 6.39 mmol) in anhydrous CH_3CN (50 mL) was added thionyl chloride (0.94 mL, 12.78 mmol) in anhydrous CH_3CN (6 mL) and the reaction stirred at 10 °C for 1 h. Potassium carbonate (1.77 g, 12.78 mmol) was then added followed by a solution of **51** (2.09 g,

6.39 mmol) in anhydrous CH₃CN (10 mL) and the reaction allowed to stir at room temperature for 3 days. The suspension was filtered and the solution concentrated under reduced pressure to produce a mixture which was extracted with EtOAc (2 × 50 mL) and washed with H₂O (2 × 50 mL). The organic layers were dried with MgSO₄ and the solvent evaporated to give a yellow solid. Purification by flash-chromatography (EtOAc) gave the first product as a white solid. Yield: 0.85 g (35 %). t.l.c system: petroleum ether/ethyl acetate 2:1, R_f = 0.32. Purification with flash-chromatography (CH₂Cl₂-MeOH 9:1 v/v) gave the second as a brown-orange solid. Yield: 0.28 g (12 %). t.l.c system: ethyl acetate, R_f = 0.08.

- Benzoxazol-2-yl-[4-(phenyl-[1,2,4]triazol-1-ylmethyl)phenyl]amine (53)

¹H NMR: δ (CDCl₃): 8.18 (bs, 1H, NH), 8.10 (s, 1H, Ar), 7.99 (s, 1H, Ar), 7.67 (m, 2H, Ar), 7.48 (m, 1H, Ar), 7.39 (m, 4H, Ar), 7.28 (m, 1H, Ar), 7.17 (m, 5H, Ar), 6.80 (s, 1H, H-7).

¹³C NMR: δ (CDCl₃): 157.80 (C, C-2'''), 152.31 (CH, C-5'), 147.81 (C, C-8'''), 143.59 (CH, C-3'), 142.10 (C, C-4'''), 138.30 (C, C-1), 138.03 (C, C-9'''), 132.46 (C, C-1''), 129.35 (CH, C-2'', C-6''), 128.99 (CH, C-3, C-5), 128.62 (CH, C-4), 127.98 (CH, C-2, C-6), 124.39 (CH, C-6'''), 122.16 (CH, C-5'''), 118.50 (CH, C-3'', C-5''), 117.34 (CH, C-7'''), 109.17 (CH, C-4'''), 67.45 (CH, CH-N).

Melting point: 150-151 °C.

HRMS (EI): Found: 368.1510 (M)⁺, Calculated: 368.1511.

- Benzoxazol-2-yl-[4-(phenyl-[1,3,4]triazol-1-ylmethyl)phenyl]amine (53')

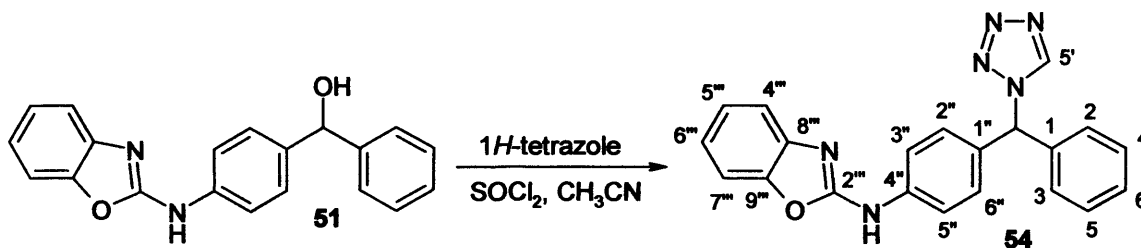
¹H NMR: δ (CDCl₃): 9.73 (bs, 1H, NH), 8.04 (s, 2H, Ar), 7.68 (m, 2H, Ar), 7.47 (m, 1H, Ar), 7.26 (m, 3H, Ar), 7.18 (m, 1H, Ar), 7.10 (m, 1H, Ar), 7.00 (m, 5H, Ar), 6.48 (s, 1H, H-7).

¹³C NMR: δ (CDCl₃): 158.23 (C, C-2'''), 147.72 (C, C-8'''), 142.22 (C, C-4''), 139.42 (C, C-1), 137.76 (C, C-9'''), 131.26 (C, C-1''), 129.27 (CH, C-2', C-5'), 128.97 (CH, C-2'', C-6''), 128.86 (CH, C-3, C-5), 128.67 (CH, C-4), 128.44 (CH, C-2, C-6), 124.34 (CH, C-6'''), 121.96 (CH, C-5'''), 118.78 (CH, C-3'', C-5''), 117.12 (CH, C-7'''), 109.10 (CH, C-4'''), 63.57 (CH, CH-N).

Melting point: 118-119 °C.

HRMS (EI): Found: 735.2940 (2M + H⁺)⁺, Calculated: 735.2944.

3.2.6) Benzoxazol-2-yl-[4-(phenyltetrazol-1-ylmethyl)phenyl]amine (54)



Thionyl chloride (0.4 mL, 4.89 mmol) in anhydrous CH₃CN (5 mL) was added dropwise to a stirred solution of 1*H*-tetrazole (0.45 M in CH₃CN, 22 mL) at a temperature of 10 °C. The white suspension formed was allowed to stand for 1 h at 10 °C. A solution of **51** (0.80 g, 2.44 mmol) in anhydrous CH₃CN (5 mL) was added to the mixture followed by activated potassium carbonate (0.68 g, 4.89 mmol). The suspension was stirred under nitrogen at room temperature for 3 days. The resulting suspension was filtered and the filtrate was evaporated *in vacuo* to yield a brownish oil. The oil was extracted with CH₂Cl₂ (50 mL) and H₂O (3 × 50 mL). The organic layer was dried with MgSO₄, filtered and reduced *in vacuo* to give an orange oil. The crude product was purified by flash column chromatography (petroleum ether/EtOAc 70:30 v/v) to give the product as a brown solid. Yield: 0.29 g (32 %). t.l.c system: petroleum ether-ethyl acetate 1:1, R_f = 0.68.

¹H NMR: δ (CDCl₃): 8.49 (s, 1H, tetrazole), 7.52 (m, 2H, Ar), 7.34 (m, 1H, Ar), 7.20 (m, 4H, Ar), 7.14 (m, 3H, Ar), 7.07 (m, 3H, Ar), 7.01 (s, 1H, H-7), 6.85 (bs, 1H, NH).

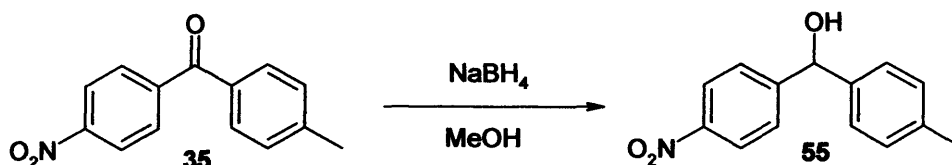
¹³C NMR: δ (CDCl₃): 157.28 (C, C-2''), 152.01 (CH, C-5'), 147.02 (C, C-8''), 140.46 (C, C-4''), 137.52 (C, C-1), 135.94 (C, C-9''), 130.35 (C, C-1''), 128.44 (CH, C-2'', C-6''), 127.81 (CH, C-3, C-5), 127.74 (CH, C-4), 126.94 (CH, C-2, C-6), 123.46 (CH, C-6''), 121.02 (CH, C-5''), 117.51 (CH, C-3'', C-5''), 115.83 (CH, C-7''), 108.27 (CH, C-4''), 69.66 (CH, CH-N).

Melting point: 116-118 °C.

HRMS (EI): Found: 369.1468 (M)⁺, Calculated: 369.1464.

3.3) Experimental results for the preparation of the methyl derivative 59

3.3.1) (4-Methylphenyl)-(4-nitrophenyl)methanol (55)¹⁷⁹

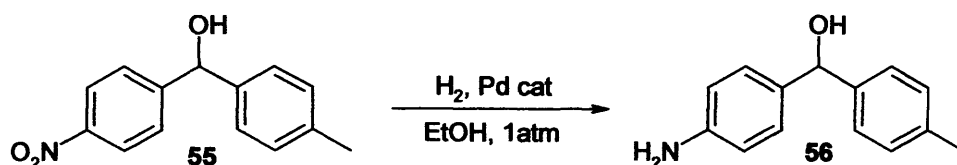


To a cooled (0 °C) solution of **35** (7 g, 29.02 mmol) in anhydrous MeOH (100 mL) was added sodium borohydride (1.10 g, 29.02 mmol), then the mixture was allowed to stir at room temperature under nitrogen for 1 h. The solvent was concentrated under reduced pressure and aqueous HCl (1 M, 10 mL) added to the residue. The oil formed was extracted with EtOAc (2 × 50 mL) and washed with H₂O (2 × 50 mL), the organic layers were combined and dried with MgSO₄ and the solvent concentrated under reduced pressure to give a white solid. Yield: 6.02 g (86 %). t.l.c system: petroleum ether-ethyl acetate 2:1, R_f = 0.70.

¹H NMR: δ (CDCl₃): 8.12 (d, 2H, J = 9.0 Hz, Ar), 7.48 (d, 2H, J = 9.0 Hz, Ar), 7.15 (d, 2H, J = 8.5 Hz, Ar), 7.08 (d, 2H, J = 8.5 Hz, Ar), 5.79 (s, 1H, CH), 2.29 (s, 3H, CH₃).

Melting point: 95-96 °C.

3.3.2) (4-Methylphenyl)-(4-aminophenyl)methanol (56)



¹⁷⁹ Massa S., Stefancich G., Corelli F., Silvestri R., Mai A., Artico M., Panico S. and Simonetti N.; Researches on antibacterial and antifungal agents, X. synthesis and antifungal activities of 1-[p-methyl-α-[4-(1H-pyrrol-1-yl)phenyl]-benzyl]azoles and some related products. *Archiv. Pharm.*, 1989, 322, 369-73.

To a solution of **55** (6.02 g, 24.77 mmol) in EtOH (150 mL) was added Pd/C catalyst (1 g) and the reaction stirred under a H₂ atmosphere (H₂ balloon) for 1 h. The reaction was filtered through celite and the filtrate concentrated under reduced pressure. The resulting oil was extracted with CH₂Cl₂ (100 mL), washed with H₂O (2 × 100 mL), dried (MgSO₄) and concentrated in *vacuo* to give a yellow solid. Purification by column chromatography (petroleum ether/EtOAc 70:30 v/v) gave the product as a white crystalline solid. Yield: 2.55 g (48 %). t.l.c system: petroleum ether-ethyl acetate 3:2, R_f = 0.21.

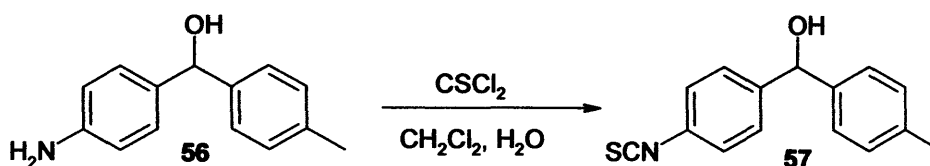
¹H NMR: δ (CDCl₃): 7.13 (d, 2H, J = 8.8 Hz, Ar), 7.03 (m, 4H, Ar), 6.50 (d, 2H, J = 8.8 Hz, Ar), 5.59 (s, 1H, CH), 3.11 (bs, 3H, NH₂ + OH), 2.21 (s, 3H, CH₃).

¹³C NMR: δ (CDCl₃): 144.22 (C, C-1), 140.74 (C, C-8), 132.43 (C, C-13), 131.82 (C, C-6), 124.57 (CH, C-11, C-12), 122.49 (CH, C-4, C-5), 117.17 (CH, C-9, C-10), 113.57 (CH, C-2, C-3).

Melting point: 97-98 °C.

HRMS (EI): Found: 196.1125 (M-H₂O)⁺, Calculated: 196.1126.

3.3.3) (4-Methylphenyl)-(4-isothiocyanatophenyl)methanol (57)



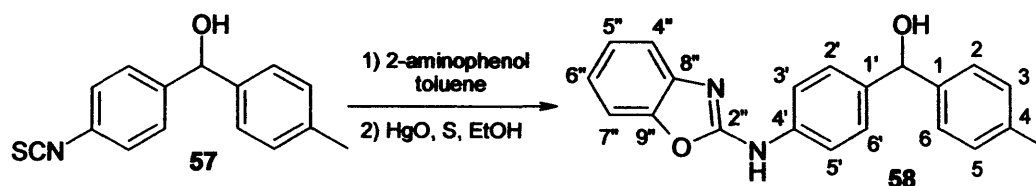
To a solution of **56** (1.9 g, 8.92 mmol) in CH₂Cl₂ (50 mL) was added a mixture of ice (5 g) and H₂O (30 mL) and subsequently dropwise with vigorous stirring thiophosgene (0.82 mL, 10.70 mmol). The mixture was stirred 2 h at 0 °C and kept overnight in a refrigerator. The organic layer was separated and extracted successively with H₂O (2 × 50 mL), 10 % NaHCO₃ aq. (50 mL) and H₂O again (50 mL), dried (MgSO₄) and evaporated to dryness to obtain the pure product as a brown syrup. Yield: 2.01 g (88 %). t.l.c system: petroleum ether-ethyl acetate 2:1, R_f = 0.81.

¹H NMR: δ (CDCl₃): 7.33 (m, 2H, Ar), 7.22 (m, 4H, Ar), 7.16 (m, 2H, Ar), 5.57 (s, 1H, CH), 3.56 (bs, 1H, OH), 2.44 (s, 3H, CH₃).

^{13}C NMR: δ (CDCl_3): 143.43 (C, C-6), 140.48 (C, C-8), 137.70 (C, C-13), 135.42 (C, C-15), 130.07 (C, C-1), 129.48 (CH, C-11, C-12), 127.68 (C, C-4, C-5), 126.71 (C, C-9, C-10), 125.77 (C, C-2, C-3), 75.36 (CH, C-7), 21.37 (CH_3 , C-14).

HRMS (EI): Found: 255.0718 (M^+), Calculated: 255.0718.

3.3.4 [4-(Benzoxazol-2-ylamino)phenyl]-p-tolylmethanol (58)



2-Aminophenol (0.68 g, 6.30 mmol) was added to a solution of **57** (1.61 g, 6.30 mmol) in EtOH (80 mL). After stirring overnight at room temperature, HgO (2.73 g, 12.60 mmol) and sulphur (40 mg, 1.26 mmol) were added to the crude thiourea and refluxed for 2 h. The cooled reaction mixture was filtered through a celite pad and the solvent evaporated. Purification by column chromatography (petroleum ether/EtOAc 60:40 v/v) gave the product as an orange solid. Yield: 0.75 g (35 %). t.l.c system: petroleum ether-ethyl acetate 1:1, R_f = 0.76.

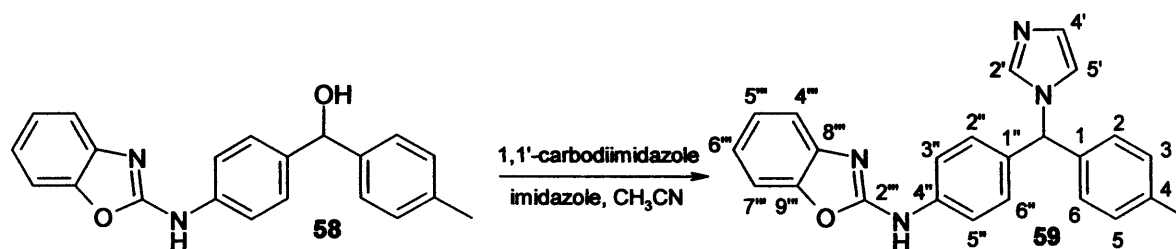
^1H NMR: δ (CDCl_3): 8.88 (bs, 1H, NH), 7.86 (m, 4H, Ar), 7.47 (m, 2H, Ar), 7.28 (m, 2H, Ar), 7.12 (m, 1H, Ar), 6.98 (m, 5H, Ar), 5.59 (s, 1H, H-7), 3.34 (bs, 1H, OH), 2.22 (s, 3H, CH_3).

^{13}C NMR: δ (CDCl_3): 147.89 (C, C-2''), 141.84 (C, C-4'), 141.00 (C, C-8''), 139.17 (C, C-9''), 137.25 (C, C-1), 137.16 (C, C-1'), 135.29 (CH, C-4), 129.21 (CH, C-3, C-5), 127.59 (CH, C-2', C-6'), 126.55 (CH, C-2, C-6), 124.39 (CH, C-5''), 121.78 (CH, C-6''), 118.77 (CH, C-3', C-5'), 116.81 (CH, C-7''), 109.23 (CH, C-4''), 75.63 (CH, CH-OH), 21.17 (CH_3).

Melting point: 157-158 °C.

HRMS (EI): Found: 331.1443 (M^+), Calculated: 331.1447.

3.3.5) Benzoxazol-2-yl-[4-imidazol-1-yl-p-tolylmethyl]phenyl]amine (59)



To a solution of **58** (0.25 g, 0.73 mmol) in CH₃CN (20 mL) was added imidazole (0.15 g, 2.19 mmol) and 1,1'-carbodiimidazole (0.18 g, 1.09 mmol). The mixture was then heated under reflux overnight, then the reaction mixture was allowed to cool and the solvent removed under reduced pressure. The oil formed was extracted with CH₂Cl₂ (50 mL) and washed with H₂O (2 × 50 mL). The organic layer was dried (MgSO₄), filtered and reduced in *vacuo*. Purification by column chromatography (EtOAc) gave the product as a yellow syrup. Yield: 0.19 g (66 %). t.l.c system: ethyl acetate, R_f = 0.08.

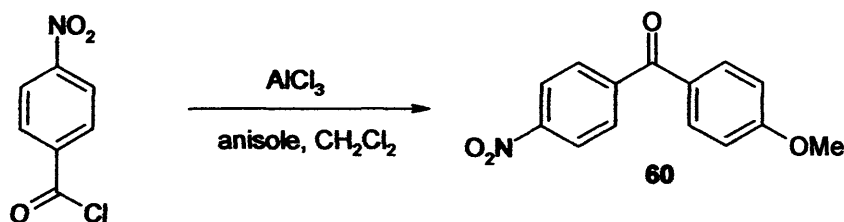
¹H NMR: δ (CDCl₃): 10.27 (bs, 1H, NH), 7.58 (m, 2H, Ar), 7.41 (s, 1H, Ar), 7.36 (m, 1H, Ar), 7.18 (m, 1H, Ar), 7.08 (m, 1H, Ar), 7.02 (m, 3H, Ar), 6.95 (m, 3H, Ar), 6.88 (m, 2H, Ar), 6.76 (s, 1H, Ar), 6.37 (s, 1H, H-7), 2.25 (s, 3H, CH₃).

¹³C NMR: δ (CDCl₃): 157.00 (C, C-2'''), 148.82 (C, C-8'''), 141.23 (C, C-4'''), 137.29 (C, C-9'''), 137.25 (C, C-1), 135.09 (C, C-4), 132.63 (C, C-1''), 129.87 (CH, C-2'), 128.55 (CH, C-3, C-5), 127.96 (CH, C-2'', C-6''), 127.79 (CH, C-5'), 126.91 (CH, C-2, C-6), 123.24 (CH, C-5'''), 122.06 (CH, C-4'), 120.98 (CH, C-6'''), 117.43 (CH, C-3'', C-5''), 116.24 (CH, C-7'''), 108.08 (CH, C-4'''), 63.49 (CH, CH-N), 21.96 (CH₃).

HRMS (EI): Found: 381.1712 (M)⁺, Calculated: 381.1715.

3.4) Experimental results for the preparation of the methoxy derivative 67 and the hydroxy derivative 68

3.4.1) 4-Methoxy-4'-nitrobenzophenone (60)¹⁸⁰

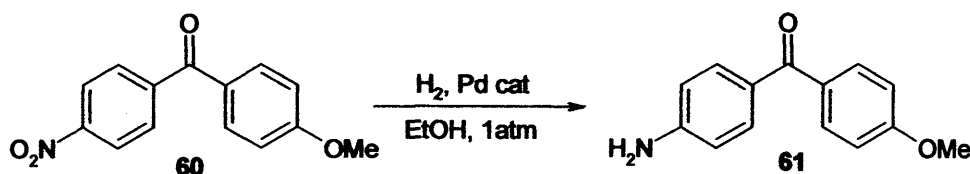


To a solution of *p*-nitrobenzoyl chloride (2.5 g, 13.37 mmol) in CH₂Cl₂ (50 mL) was added aluminum chloride (3.59 g, 26.94 mmol) and anisole (1.74 g, 16.16 mmol). The mixture was then stirred overnight at room temperature. HCl 1 M (10 mL) was then added to the mix before washing with H₂O (2 × 50 mL) and NaHCO₃ (50 mL). The organic layer was dried (MgSO₄), filtered and reduced in *vacuo*. Recrystallisation from EtOAc/petroleum ether gave the product as a pale yellow solid. Yield: 2.4 g (69 %). t.l.c system: petroleum ether-ethyl acetate 2:1, R_f = 0.61.

¹H NMR: δ (CDCl₃): 8.28 (d, 2H, J = 8.5 Hz, Ar), 7.81 (d, 2H, J = 9.0 Hz, Ar), 7.75 (d, 2H, J = 9.0 Hz, Ar), 6.92 (d, 2H, J = 8.5 Hz, Ar), 3.83 (s, 3H, CH₃).

Melting point: 108-109 °C (lit m.p. 123 °C)¹⁸¹.

3.4.2) 4-Methoxy-4'-aminobenzophenone (61)¹⁸²



¹⁸⁰ Gorvin J.H. and Whalley D.P.; Aromatic nitro-group displacement reactions. Part 1. A novel route to substituted 10-phenylacridones. *J. Chem. Soc. Per. Trans. 1: Org and Bio-org Chem.* 1979, 5, 1634-70.

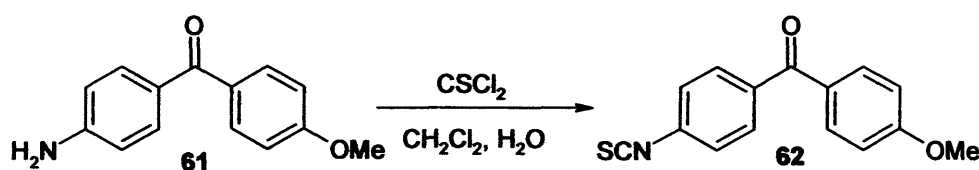
¹⁸¹ Shani J., Gazit A., Livshitz T. and Biran S.; Synthesis and receptor-binding affinity of fluorotamoxifen, a possible estrogen-receptor imaging agent. *J. Med. Chem.*, 1985, 28, 1504-1511.

¹⁸² Kaslow C.E. and Stayner R.D.; Substituted 4-aminodiphenylmethanes. *J. Am. Chem. Soc.*, 1946, 68, 2600-2.

To a solution of **60** (1 g, 3.88 mmol) in EtOH (50 mL) was added Pd/C catalyst (0.2 g) and the reaction stirred under a H₂ atmosphere (H₂ balloon) for 10 min. The reaction was filtered through celite and the filtrate concentrated under reduced pressure. The resulting oil was extracted with EtOAc (50 mL), washed with H₂O (2 × 50 mL), dried (MgSO₄) and concentrated in *vacuo* to give the pure product as a yellow syrup. Yield: 0.84 g (95 %). t.l.c system: petroleum ether-ethyl acetate 2:1, R_f = 0.32.

¹H NMR: δ (CDCl₃): 7.68 (d, 2H, J = 8.8 Hz, Ar), 7.58 (d, 2H, J = 8.6 Hz, Ar), 6.84 (d, 2H, J = 8.8 Hz, Ar), 6.59 (d, 2H, J = 8.6 Hz, Ar), 4.07 (bs, 2H, NH), 3.79 (s, 3H, CH₃).

3.4.3) 4-Methoxy-4'-isothiocyanatobenzophenone (**62**)¹⁸³



To a solution of **61** (0.84 g, 3.70 mmol) in CH₂Cl₂ (50 mL) was added a mixture of ice (2 g) and H₂O (20 mL) and subsequently dropwise with vigorous stirring thiophosgene (0.34 mL, 4.44 mmol). The mixture was stirred for 2 h at 0 °C and kept overnight in a refrigerator. The organic layer was separated and extracted successively with H₂O (2 × 50 mL), 10 % NaHCO₃ aq. (50 mL) and H₂O again (50 mL), dried (MgSO₄) and evaporated to dryness to obtain the pure product as an orange solid. Yield: 0.97 g (97 %). t.l.c system: petroleum ether-ethyl acetate 2:1, R_f = 0.72.

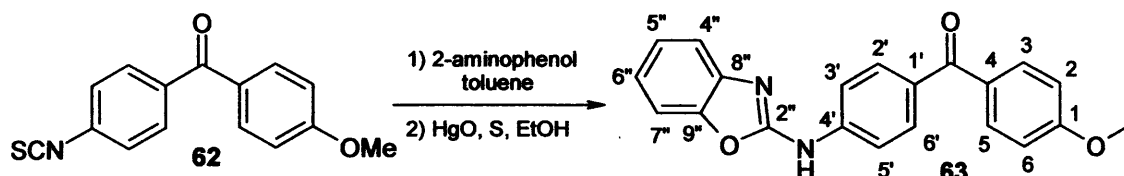
¹H NMR: δ (CDCl₃): 7.68 (d, 2H, J = 9.0 Hz, Ar), 7.66 (d, 2H, J = 8.5 Hz, Ar), 7.19 (d, 2H, J = 8.5 Hz, Ar), 6.81 (d, 2H, J = 9.0 Hz, Ar), 3.73 (s, 3H, CH₃).

¹³C NMR: δ (CDCl₃): 193.68 (C, C-7), 163.45 (C, C-13), 137.52 (C, C-15), 136.70 (C, C-6), 134.59 (C, C-1), 132.43 (CH, C-4, C-5), 131.21 (CH, C-9, C-10), 129.60 (C, C-8), 125.54 (CH, C-2, C-3), 113.76 (CH, C-11, C-12), 55.58 (CH₃, C-14).

¹⁸³ Antos K., Sura J., Knoppova V. and Prochozka J.; Synthesis and properties of 4'-substituted 4-isothiocyanatobenzophenone. *Coll. Czech. Chem. Com.*, 1973, 38, 1609-13.

Melting point: 112-114 °C.

3.4.4) [4-(Benzoxazol-2-ylamino)phenyl](4-methoxyphenyl)methanone (63)



2-Aminophenol (0.39 g, 3.59 mmol) was added to a solution of **62** (0.97 g, 3.59 mmol) in toluene (50 mL). After stirring overnight at room temperature, HgO (2.73 g, 12.60 mmol) and sulphur (40 mg, 1.26 mmol) were added to the crude thiourea and refluxed for 1.5 h. The cooled reaction mixture was filtered through a celite pad and the solvent evaporated. Purification by column chromatography (petroleum ether/EtOAc 60:40 v/v) gave the product as an orange solid. Yield: 0.57 g (46 %). t.l.c system: petroleum ether-ethyl acetate 2:1, $R_f = 0.41$.

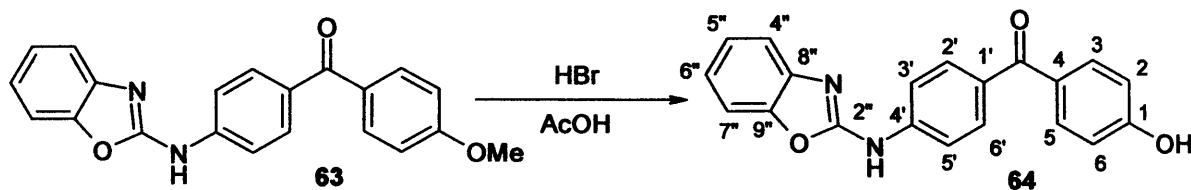
$^1\text{H NMR}$: δ (CDCl_3): 8.62 (bs, 1H, NH), 7.80 (m, 4H, Ar), 7.67 (d, 2H, $J = 8.5$ Hz, Ar), 7.46 (d, 1H, $J = 7.5$ Hz, Ar), 7.32 (d, 1H, $J = 8.0$ Hz, Ar), 7.20 (d, 1H, $J = 8.5$ Hz, Ar), 7.11 (m, 1H, Ar), 6.92 (m, 2H, Ar), 6.88 (d, 2H, $J = 9.0$ Hz, Ar), 3.83 (s, 3H, CH_3).

$^{13}\text{C NMR}$: δ (CDCl_3): 188.04 (C, $\text{C}=\text{O}$), 163.09 (C, C-1), 152.63 (C, C-2''), 149.35 (C, C-9''), 141.36 (C, C-4'), 139.65 (C, C-8''), 132.43 (CH, C-3, C-5), 131.83 (CH, C-2', C-6'), 130.46 (C, C-4), 129.52 (C, C-1'), 125.44 (CH, C-5''), 124.79 (CH, C-6''), 120.96 (CH, C-4''), 117.17 (CH, C-3', C-5'), 113.57 (CH, C-2, C-6), 110.07 (CH, C-7''), 55.53 (CH_3).

Melting point: 143-144 °C.

HRMS (EI): Found: 345.1236 (M^+), Calculated: 345.1239.

3.4.5) (4-(Benzoxazol-2-ylamino)phenyl)(4-hydroxyphenyl)methanone (64)



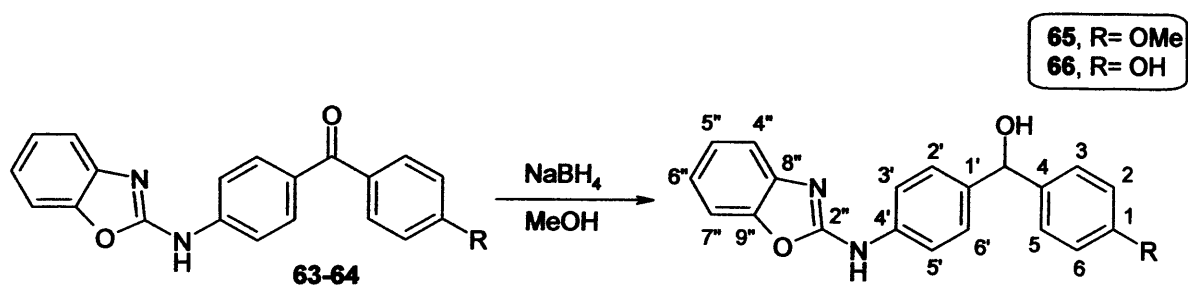
A mixture of **63** (0.46 g, 1.33 mmol) in 20 mL of a 48 % solution of HBr in acetic acid and 10 mL of acetic acid was heated at reflux for 6 h and then left to stir overnight at room temperature. The mixture was then evaporated to one-half the original volume on the rotary evaporator. The residue was diluted with H₂O (30 mL) and extracted with EtOAc (50 mL). The organic extract was washed with aq. NaHCO₃ (2 × 30 mL) and evaporated to give a yellow oil. Purification by column chromatography (petroleum ether/EtOAc 60:40 v/v) gave the product as a yellow syrup. Yield: 0.34 g (77 %). t.l.c system: petroleum ether-ethyl acetate 1:1, R_f = 0.37.

¹H NMR: δ (CD₃OD): 7.76 (d, 2H, J = 9.0 Hz, Ar), 7.71 (d, 2H, J = 9.0 Hz, Ar), 7.62 (d, 2H, J = 8.6 Hz, Ar), 7.39 (d, 1H, J = 7.8 Hz, Ar), 7.33 (d, 1H, J = 8.2 Hz, Ar), 7.18 (m, 1H, Ar), 7.10 (m, 1H, Ar), 6.81 (d, 2H, J = 8.6 Hz, Ar).

¹³C NMR: δ (CD₃OD): 196.81 (C, C=O), 163.43 (C, C-1), 152.79 (C, C-2''), 144.04 (C, C-9''), 143.91 (C, C-4'), 139.06 (C, C-8''), 133.94 (CH, C-3, C-5), 133.26 (C, C-4) 132.57 (CH, C-2', C-6'), 130.36 (C, C-1'), 125.37 (CH, C-5''), 125.12 (CH, C-6''), 123.53 (CH, C-4''), 118.18 (CH, C-3', C-5'), 116.14 (CH, C-2, C-6), 110.11 (CH, C-7'').

HRMS (EI): Found: 330.1004 (M)⁺, Calculated: 330.1004.

3.4.6) General procedure for the preparation of [4-(Benzoxazol-2-ylamino)phenyl](4-substitutedphenyl)methanol 65 and 66



To a cooled (0 °C) solution of **63-64** (1.20 mmol) in anhydrous MeOH (30 mL) was added sodium borohydride (53 mg, 1.20 mmol), then the mixture was allowed to stir at room temperature under nitrogen for 4 h (R= OMe) or 12 h (R= OH). The solvent was concentrated under reduced pressure and aqueous HCl (1 M, 5 mL) added to the residue. The oil formed was extracted with EtOAc (2 × 30 mL) and washed with H₂O (2 × 50 mL), the organic layers were combined and dried with MgSO₄ and the solvent concentrated under reduced pressure.

3.4.6.1) [4-(Benzoxazol-2-ylamino)phenyl](4-methoxyphenyl)methanol (**65**)

Orange solid (91 %), mp: 123-124 °C. t.l.c system: petroleum ether-ethyl acetate 2:1, R_f= 0.38.

¹H NMR: δ (CDCl₃): 8.74 (bs, 1H, NH), 7.38 (d, 2H, J= 8.0 Hz, Ar), 7.33 (d, 1H, J= 8.0 Hz, Ar), 7.20 (m, 3H, Ar), 7.15 (m, 2H, Ar), 7.10 (m, 1H, Ar), 7.01 (m, 1H, Ar), 6.76 (d, 2H, J= 8.5 Hz, Ar), 5.68 (s, 1H, H-7), 3.69 (s, 3H, CH₃).

¹³C NMR: δ (CDCl₃): 157.67 (C, C-1), 156.74 (C, C-2''), 146.76 (C, C-9''), 142.56 (C, C-4'), 140.73 (C, C-8''), 138.18 (C, C-4), 135.11 (C, C-1'), 129.00 (CH, C-5''), 127.21 (CH, C-3, C-5), 126.87 (CH, C-2', C-6'), 123.31 (CH, C-6''), 120.84 (CH, C-4''), 117.87 (CH, C-3', C-5'), 112.99 (CH, C-2, C-6), 108.10 (CH, C-7''), 76.96 (CH, CH-OH), 54.20 (CH₃).

HRMS (EI): Found: 347.1395 (M)⁺, Calculated: 347.1396.

3.4.6.2) [4-(Benzoxazol-2-ylamino)phenyl](4-hydroxyphenyl)methanol (**66**)

Purification by column chromatography (petroleum ether/EtOAc 60:40 v/v) gave the product as a yellow syrup (42 %). t.l.c system: petroleum ether-ethyl acetate 1:1, R_f= 0.51.

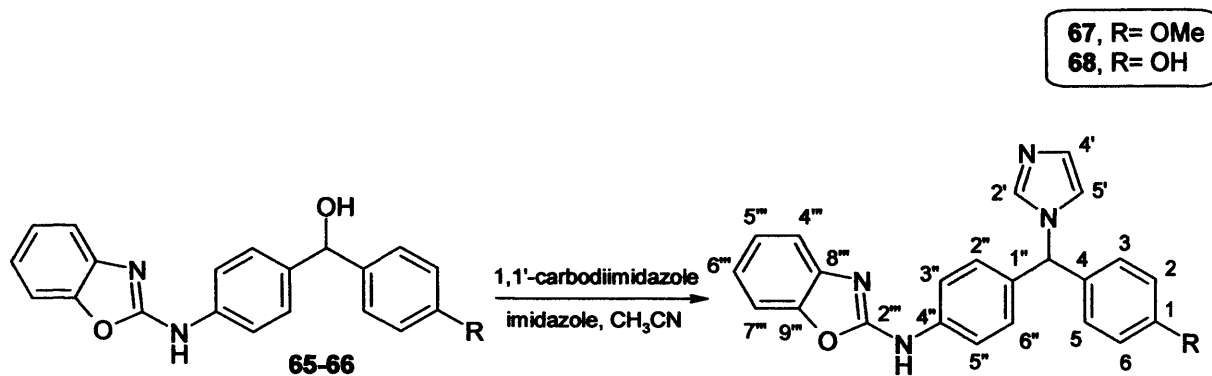
¹H NMR: δ (CD₃OD): 9.96 (bs, 1H, OH), 9.07 (bs, 1H, NH), 7.48 (d, 2H, J= 8.6 Hz, Ar), 7.22 (m, 4H, Ar), 7.11 (m, 3H, Ar), 6.95 (m, 1H, Ar), 6.65 (d, 2H, J= 8.6 Hz, Ar), 5.60 (s, 1H, H-7), 4.58 (bs, 1H, OH).

¹³C NMR: δ (CD₃OD): 160.34 (C, C-1), 157.68 (C, C-2''), 148.98 (C, C-9''), 143.50 (C, C-4'), 140.98 (C, C-8''), 138.72 (C, C-4), 136.96 (C, C-1'), 129.18 (CH, C-3, C-5), 128.46 (CH, C-2', C-6'), 125.25 (CH, C-5''), 123.02 (CH, C-6''), 119.48

(CH, C-4''), 117.54 (CH, C-3', C-5'), 116.07 (CH, C-2, C-6), 109.94 (CH, C-7''), 76.34 (CH, CH-OH).

HRMS (EI): Found: 333.1238 (M)⁺, Calculated: 333.1239

3.4.7) General procedure for the preparation of Benzoxazol-2-yl-{4-[imidazole-1-yl-(4-substitutedphenyl)methyl]phenyl}amine 67 and 68



To a solution of **65-66** (0.94 mmol) in CH₃CN (50 mL) was added imidazole (2.82 mmol) and 1,1'-carbodiimidazole (1.41 mmol). The mixture was heated under reflux overnight, then the reaction mixture was allowed to cool and the solvent removed under reduced pressure. The oil formed was then extracted with CH₂Cl₂ (50 mL) and washed with H₂O (2 × 50 mL). The organic layer was dried (MgSO₄), filtered and reduced in *vacuo*.

3.4.7.1)

Benzoxazol-2-yl-{4-[imidazol-1-yl-(4-methoxyphenyl)methyl]phenyl}amine 67

Purification by column chromatography (EtOAc) gave the product as a yellow syrup (38 %). t.l.c system: ethyl acetate, R_f = 0.09.

¹H NMR: δ (CDCl₃): 9.62 (bs, 1H, NH), 7.60 (d, 2H, J = 8.5 Hz Ar), 7.45 (s, 1H, Ar), 7.39 (d, 1H, J = 7.5 Hz, Ar), 7.23 (d, 1H, J = 8.0 Hz, Ar), 7.16 (m, 1H, Ar), 7.08 (m, 1H, Ar), 7.01 (m, 6H, Ar), 6.78 (d, 2H, J = 9.0 Hz, Ar), 6.39 (s, 1H, H-7), 3.75 (s, 3H, CH₃).

¹³C NMR: δ (CDCl₃): 158.59 (C, C-1), 157.28 (C, C-2''), 146.77 (C, C-9''), 141.29 (C, C-4''), 139.84 (CH, C-2'), 137.56 (C, C-8''), 132.51 (C, C-4), 130.00 (C,

C-1'), 128.34 (CH, C-3, C-5), 127.72 (CH, C-2'', C-6''), 125.92 (CH, C-5'), 123.18 (CH, C-5'''), 122.61 (CH, C-4'), 120.86 (CH, C-6'''), 117.47 (CH, C-3'', C-5''), 116.11 (CH, C-4'''), 113.24 (CH, C-2, C-6), 108.05 (CH, C-7'''), 63.31 (CH, CH-N), 54.33 (CH₃).

HRMS (EI): Found: 397.1667 (M)⁺, Calculated: 397.1665.

3.4.7.2)

Benzoxazol-2-yl-{4-[imidazol-1-yl-(4-hydroxyphenyl)methyl]phenyl}amine 68

Purification by column chromatography (EtOAc) gave the product as a colourless oil (74 %). t.l.c system: ethyl acetate, R_f = 0.10.

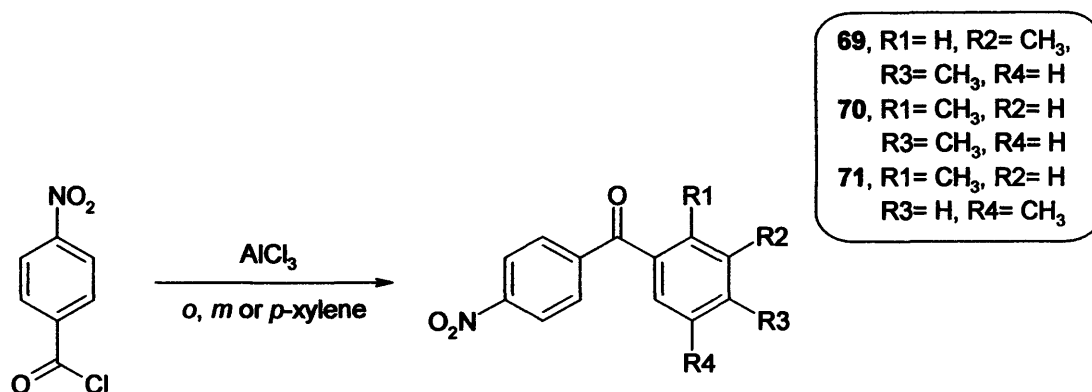
¹H NMR: δ (CD₃OD): 7.56 (d, 2H, J = 8.6 Hz, Ar), 7.45 (s, 1H, Ar), 7.26 (d, 1H, J = 7.4 Hz, Ar), 7.20 (d, 1H, J = 7.4 Hz, Ar), 7.07 (m, 1H, Ar), 6.98 (m, 5H, Ar), 6.80 (d, 2H, J = 8.2 Hz, Ar), 6.63 (d, 2H, J = 8.6 Hz, Ar), 6.46 (s, 1H, H-7).

¹³C NMR: δ (CD₃OD): 159.89 (C, C-1), 158.76 (C, C-2'''), 148.98 (C, C-9'''), 143.50 (C, C-4'), 139.90 (CH, C-8'''), 135.41 (C, C-4), 131.37 (C, C-1'), 130.58 (CH, C-3, C-5), 130.25 (CH, C-2'), 130.13 (CH, C-5'), 129.74 (CH, C-2', C-6'), 125.28 (CH, C-5'''), 123.28 (CH, C-6'''), 122.68 (CH, C-4'), 119.68 (CH, C-3', C-5'), 117.82 (CH, C-4'''), 116.68 (CH, C-2, C-6), 110.01 (CH, C-7'''), 65.48 (CH, CH-OH).

HRMS (EI): Found: 315.1130 (M-imidazole)⁺, Calculated: 315.1134.

3.5) Experimental results for the preparation of the dimethyl derivatives 84, 85 and 86

3.5.1) General procedure for the preparation of the dimethyl-4'-nitrobenzophenone 69, 70 and 71



To a solution of *p*-nitrobenzoyl chloride (10.77 mmol) in *o*, *m* or *p*-xylene (25 mL) was added AlCl₃ (15.15 mmol) and the resulting black solution stirred at room temperature for 3 h. H₂O (4 mL) was added dropwise and the resulting mixture was stirred for 15 min and then extracted with H₂O (50 mL) and 10 % NaHCO₃ (2 × 50 mL). The organic layer was dried (MgSO₄), filtered and evaporated.

3.5.1.1) 3,4-Dimethyl-4'-nitrobenzophenone 69¹⁸⁴

Purification by column chromatography (petroleum ether/EtOAc 80:20 v/v) gave the product as a white solid (41 %), mp: 114-115 °C (lit m.p. 82-83 °C)¹⁸⁵. t.l.c system: petroleum ether-ethyl acetate 2:1, R_f = 0.66.

¹H NMR: δ (CDCl₃): 8.13 (d, 2H, J = 9.0 Hz, Ar), 7.78 (d, 2H, J = 9.0 Hz, Ar), 7.46 (s, 1H, Ar), 7.34 (d, 1H, J = 7.8 Hz, Ar), 7.10 (d, 1H, J = 7.8 Hz, Ar), 2.22 (s, 6H, 2 × CH₃).

3.5.1.2) 2,4-Dimethyl-4'-nitrobenzophenone 70¹⁸⁴

¹⁸⁴ Kuhn H. and De Diesbach H.; Quinolyl ketones and their reduction products. *Hel. Chim. Acta*, 1958, 41, 894-903.

¹⁸⁵ Jin T.S., Yang M.N., Feng G.L. and Li T.S.; Synthesis of diaryl ketones catalysed by Al₂O₃-ZrO₂/S₂O₂-8 solid superacid. *Synth. Com.*, 2004, 34, 479-485.

White solid (85 %), mp: 80-81 °C (lit m.p. 87-88 °C)¹⁸⁵. t.l.c system: petroleum ether-ethyl acetate 2:1, R_f= 0.72.

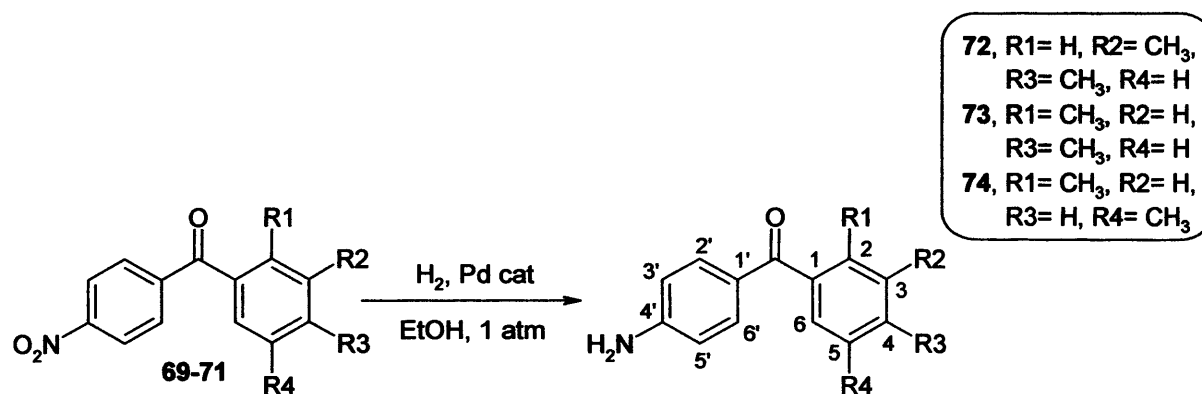
¹H NMR: δ (CDCl₃): 8.01 (d, 2H, J= 8.6 Hz, Ar), 7.70 (d, 2H, J= 8.6 Hz, Ar), 7.04 (d, 1H, J= 7.8 Hz, Ar), 6.92 (s, 1H, Ar), 6.86 (d, 1H, J= 7.8 Hz, Ar), 2.19 (s, 6H, 2 × CH₃).

3.5.1.3) 2,5-Dimethyl -4'-nitrobenzophenone 71¹⁸⁴

Yellow solid (90 %), mp: 72-74 °C (lit m.p. 84-86 °C)¹⁸⁵. t.l.c system: petroleum ether-ethyl acetate 2:1, R_f= 0.81.

¹H NMR: δ (CDCl₃): 8.09 (d, 2H, J= 8.6 Hz, Ar), 7.78 (d, 2H, J= 8.7 Hz, Ar), 7.09 (d, 1H, J= 7.7 Hz, Ar), 7.02 (d, 1H, J= 7.7 Hz, Ar), 6.95 (s, 1H, Ar), 2.13 (s, 6H, 2 × CH₃).

3.5.2) General procedure for the preparation of the dimethyl-4'-aminobenzophenone 72, 73 and 74



To a solution of **69-71** (9.75 mmol) in EtOH (70 mL) was added Pd/C catalyst (0.4 g) and the reaction stirred under a H₂ atmosphere (H₂ balloon) for 25 min. The reaction was filtered through celite and the filtrate concentrated under reduced pressure. The resulting oil was extracted with EtOAc (50 mL), washed with H₂O (2 × 50 mL), dried (MgSO₄) and concentrated in *vacuo*.

3.5.2.1) 3,4-Dimethyl-4'-aminobenzophenone 72¹⁸⁶

Yellow solid (94 %), mp: 96-97 °C. t.l.c system: petroleum ether-ethyl acetate 2:1, R_f= 0.47.

¹H NMR: δ (CDCl₃): 7.59 (d, 2H, J= 8.6 Hz, Ar), 7.38 (s, 1H, Ar), 7.33 (d, 1H, J= 7.7 Hz, Ar), 7.07 (d, 1H, J= 7.7 Hz, Ar), 6.49 (d, 2H, J= 8.6 Hz, Ar), 4.02 (bs, 2H, NH₂), 2.17 (s, 6H, 2 × CH₃).

¹³C NMR: δ (CDCl₃): 197.89 (C, C=O), 151.27 (C, C-4'), 140.77 (C, C-4), 136.99 (C, C-3), 136.52 (C, C-1), 132.87 (CH, C-2', C-6'), 130.70 (CH, C-2), 129.29 (CH, C-5), 127.76 (CH, C-6), 127.39 (C, C-1'), 113.94 (CH, C-3', C-5'), 19.77 (CH₃ × 2).

3.5.2.2) 2,4-Dimethyl-4'-aminobenzophenone 73¹⁸⁶

Yellow solid (96 %), mp: 119-120 °C. t.l.c system: petroleum ether-ethyl acetate 2:1, R_f= 0.59.

¹H NMR: δ (CDCl₃): 7.56 (d, 2H, J= 8.7 Hz, Ar), 7.08 (d, 1H, J= 7.7 Hz, Ar), 6.98 (s, 1H, Ar), 6.93 (d, 1H, J= 7.8 Hz, Ar), 6.52 (d, 2H, J= 8.6 Hz, Ar), 4.14 (bs, 2H, NH₂), 2.29 (s, 3H, CH₃), 2.19 (s, 3H, CH₃).

¹³C NMR: δ (CDCl₃): 197.15 (C, C=O), 151.36 (C, C-4'), 139.51 (C, C-4), 136.86 (C, C-2), 136.17 (C, C-1), 132.76 (CH, C-2', C-6'), 131.68 (CH, C-6), 128.17 (CH, C-3), 128.02 (C, C-1'), 123.58 (CH, C-5), 113.65 (CH, C-3', C-5'), 21.31 (CH₃), 19.74 (CH₃).

3.5.2.3) 2,5-Dimethyl-4'-aminobenzophenone 74¹⁸⁶

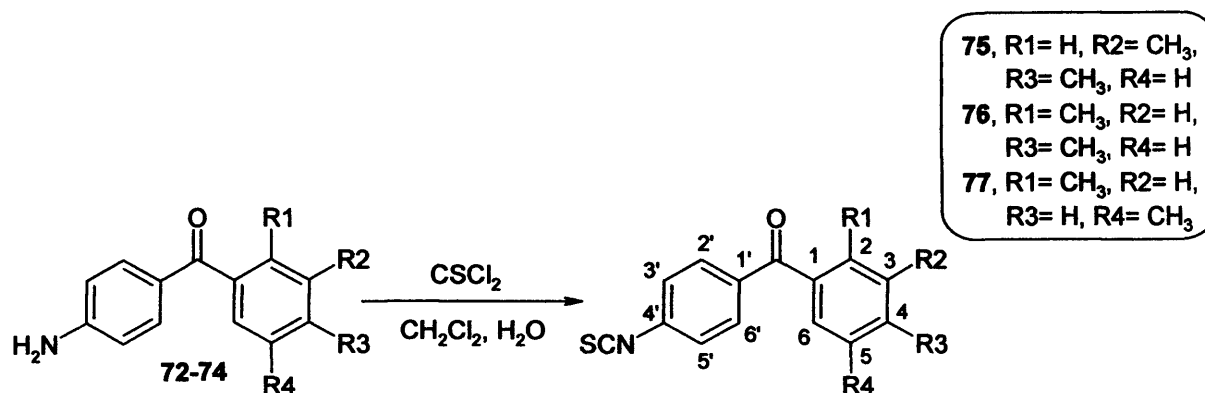
Yellow solid (94 %), mp: 130-131 °C. t.l.c system: petroleum ether-ethyl acetate 2:1, R_f= 0.48.

¹H NMR: δ (CDCl₃): 7.57 (d, 2H, J= 8.7 Hz, Ar), 7.05 (m, 2H, Ar), 6.97 (s, 1H, Ar), 6.53 (d, 2H, J= 8.8 Hz, Ar), 4.13 (bs, 2H, NH₂), 2.22 (s, 3H, CH₃), 2.14 (s, 3H, CH₃).

¹³C NMR: δ (CDCl₃): 197.38 (C, C=O), 151.56 (C, C-4'), 139.80 (C, C-1), 134.69 (C, C-2), 133.00 (CH, C-2', C-6'), 132.57 (C, C-5), 130.77 (CH, C-4), 129.93 (CH, C-6), 128.12 (CH, C-3), 127.36 (C, C-1'), 112.08 (CH, C-3', C-5'), 20.89 (CH₃), 19.20 (CH₃).

¹⁸⁶ Ernst M.; Isoindole pigments made from tetraphenylketazine and their use. *Ger. Offen.*, 1979, 42 pp.

3.5.3) General procedure for the preparation of the dimethyl-4'-isothiocyanatobenzophenone 75, 76 and 77



To a solution of 72-74 (2 g, 8.87 mmol) in CH₂Cl₂ (70 mL) was added a mixture of ice (2.5 g) and H₂O (30 mL) and subsequently dropwise with vigorous stirring thiophosgene (0.80 mL, 10.65 mmol). The mixture was stirred for 2 h at 0 °C and kept overnight in a refrigerator. The organic layer was separated and extracted successively with H₂O (2 × 50 mL), 10 % NaHCO₃ aq. (50 mL) and H₂O again (50 mL), dried (MgSO₄) and evaporated to dryness.

3.5.3.1) 3,4-Dimethyl-4'-isothiocyanatobenzophenone 75

Purification by column chromatography (petroleum ether/EtOAc 80:20 v/v) gave the product as an orange solid (75 %), mp: 81-82 °C. t.l.c system: petroleum ether-ethyl acetate 2:1, R_f= 0.85.

¹H NMR: δ (CDCl₃): 7.63 (d, 2H, J= 8.2 Hz, Ar), 7.42 (s, 1H, Ar), 7.32 (d, 1H, J= 7.8 Hz, Ar), 7.14 (d, 2H, J= 8.6 Hz, Ar), 7.08 (d, 1H, J= 7.4 Hz, Ar), 2.18 (s, 3H, CH₃), 2.14 (s, 3H, CH₃).

¹³C NMR: δ (CDCl₃): 195.10 (C, C=O), 142.42 (C, C-4), 137.00 (C, C-3), 136.49 (C, C-1'), 134.92 (C, C-4'), 134.84 (C, C-1), 133.60 (C, NCS), 131.44 (CH, C-2', C-6'), 131.07 (CH, C-2), 129.61 (CH, C-5), 127.89 (CH, C-6), 125.54 (CH, C-3', C-5'), 20.09 (CH₃), 19.82 (CH₃).

HRMS (EI): Found: 268.0791 (M)⁺, Calculated: 268.0796.

3.5.3.2) 2,4-Dimethyl-4'-isothiocyanatobenzophenone 76

Orange solid (96 %), mp: 39-40 °C. t.l.c system: petroleum ether-ethyl acetate 2:1, $R_f = 0.85$.

$^1\text{H NMR}$: δ (CDCl_3): 7.59 (d, 2H, $J = 8.6$ Hz, Ar), 7.08 (d, 2H, $J = 8.6$ Hz, Ar), 7.02 (d, 1H, $J = 7.4$ Hz, Ar), 6.95 (s, 1H, Ar), 6.88 (d, 1H, $J = 7.8$ Hz, Ar), 2.21 (s, 3H, CH_3), 2.16 (s, 3H, CH_3).

$^{13}\text{C NMR}$: δ (CDCl_3): 196.86 (C, C=O), 141.13 (C, C-4), 137.89 (C, NCS), 137.43 (C, C-2), 136.61 (C, C-1'), 135.50 (C, C-1), 134.94 (C, C-4'), 132.12 (CH, C-6), 131.56 (CH, C-2', C-6'), 129.22 (CH, C-3), 125.95 (CH, C-5), 125.69 (CH, C-3', C-5'), 21.44 (CH_3), 20.14 (CH_3).

HRMS (EI) : Found: 268.0792 (M^+), Calculated: 268.0796.

3.5.3.3) 2,5-Dimethyl-4'-isothiocyanatobenzophenone 77

Purification by column chromatography (petroleum ether/EtOAc 80:20 v/v) gave the product as an orange solid (61 %), mp: 49-50 °C. t.l.c system: petroleum ether-ethyl acetate 2:1, $R_f = 0.88$.

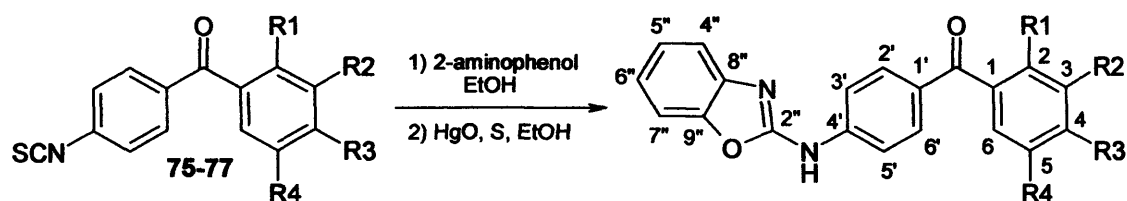
$^1\text{H NMR}$: δ (CDCl_3): 7.71 (d, 2H, $J = 8.6$ Hz, Ar), 7.18 (d, 2H, $J = 8.6$ Hz, Ar), 7.10 (m, 2H, Ar), 6.97 (s, 1H, Ar), 2.24 (s, 3H, CH_3), 2.17 (s, 3H, CH_3).

$^{13}\text{C NMR}$: δ (CDCl_3): 197.17 (C, C=O), 137.95 (C, C-1), 137.24 (C, NCS), 136.20 (C, C-2), 135.71 (C, C-4'), 134.99 (C, C-5), 133.60 (C, C-1'), 131.56 (CH, C-2', C-6'), 131.35 (CH, C-4), 131.09 (CH, C-6), 128.89 (CH, C-3), 125.78 (CH, C-3', C-5'), 20.93 (CH_3), 19.55 (CH_3).

HRMS (EI) : Found: 268.0791 (M^+), Calculated: 268.0796.

3.5.4) General procedure for the preparation of the [4-(Benzoxazol-2-ylamino)-phenyl](dimethylphenyl)methanone 78, 79 and 80

78, R1= H, R2= CH₃,
R3= CH₃, R4= H
79, R1= CH₃, R2= H,
R3= CH₃, R4= H
80, R1= CH₃, R2= H,
R3= H, R4= CH₃



2-Aminophenol (5.12 mmol) was added to a solution of **75-77** (5.12 mmol) in EtOH (100 mL). After stirring overnight at room temperature, HgO (10.24 mmol) and sulphur (1.02 mmol) were added to the crude thiourea and refluxed for 4-6 h. The cooled reaction mixture was filtered through a celite pad and the solvent evaporated.

3.5.4.1) [4-(Benzoxazol-2-ylamino)phenyl]-(3,4-dimethylphenyl)methanone 78

Purification by column chromatography (petroleum ether/EtOAc 70:30 v/v) gave the product as an orange solid (87 %), mp: 154-155 °C. t.l.c system: petroleum ether-ethyl acetate 2:1, R_f= 0.73.

¹H NMR: δ (CDCl₃): 8.94 (bs, 1H, NH), 7.81 (d, 2H, J= 9.0 Hz, Ar), 7.69 (d, 2H, J= 9.0 Hz, Ar), 7.53 (s, 1H, Ar), 7.45 (d, 2H, J= 7.8 Hz, Ar), 7.30 (d, 1H, J= 8.2 Hz, Ar), 7.14 (m, 3H, Ar), 2.29 (s, 3H, CH₃), 2.26 (s, 3H, CH₃).

¹³C NMR: δ (CDCl₃): 194.63 (C, C=O), 156.82 (C, C-2''), 146.12 (C, C-4'), 140.70 (C, C-9''), 138.04 (C, C-8''), 135.71 (C, C-4), 134.58 (C, C-3), 132.06 (C, C-1), 131.27 (C, C-1'), 130.99 (CH, C-2', C-6'), 130.04 (CH, C-2), 128.39 (CH, C-5), 126.81 (CH, C-6), 123.54 (CH, C-5''), 121.41 (CH, C-6''), 116.30 (CH, C-4''), 116.10 (CH, C-3', C-5'), 108.36 (CH, C-7''), 18.99 (CH₃), 18.77 (CH₃).

HRMS (ED): Found: 343.1446 (M)⁺, Calculated: 343.1447.

3.5.4.2) [4-(Benzoxazol-2-ylamino)phenyl]-(2,4-dimethylphenyl)methanone 78

Purification by column chromatography (petroleum ether/EtOAc 70:30 v/v) gave the product as a pale yellow solid (66 %), mp: 164-165 °C. t.l.c system: petroleum ether-ethyl acetate 2:1, R_f = 0.69.

$^1\text{H NMR}$: δ (CDCl_3): 7.79 (d, 2H, J = 8.6 Hz, Ar), 7.63 (d, 2H, J = 8.6 Hz, Ar), 7.45 (d, 1H, J = 7.8 Hz, Ar), 7.32 (d, 1H, J = 7.8 Hz, Ar), 7.16 (m, 3H, Ar), 7.03 (s, 1H, Ar), 6.98 (d, 2H, J = 7.8 Hz, Ar), 3.80 (bs, 1H, NH), 2.32 (s, 3H, CH_3), 2.28 (s, 3H, CH_3).

$^{13}\text{C NMR}$: δ (CDCl_3): 196.54 (C, C=O), 156.64 (C, C-2''), 146.73 (C, C-4'), 141.38 (C, C-9''), 140.26 (C, C-4), 139.35 (C, C-8''), 135.79 (C, C-2), 134.82 (C, C-1), 131.47 (C, C-1'), 131.02 (CH, C-2', C-6'), 130.76 (CH, C-6), 127.78 (CH, C-3), 124.78 (CH, C-5), 123.61 (CH, C-5''), 121.46 (CH, C-6''), 116.27 (CH, C-3', C-5'), 116.14 (CH, C-4''), 108.42 (CH, C-7''), 20.33 (CH_3), 18.95 (CH_3).

HRMS (EI) : Found: 343.1443 (M^+), Calculated: 343.1447.

3.5.4.3) [4-(Benzoxazol-2-ylamino)phenyl]-(2,5-dimethylphenyl)methanone 79

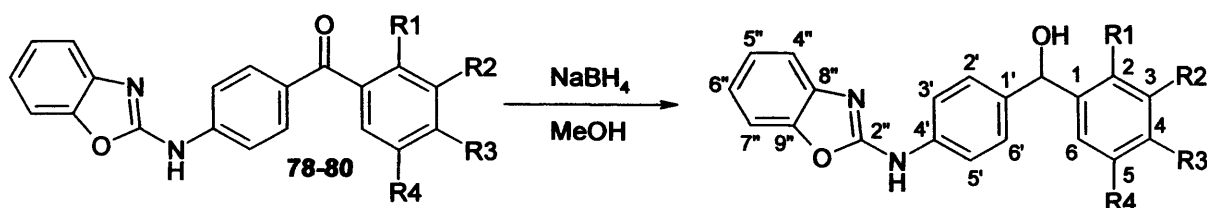
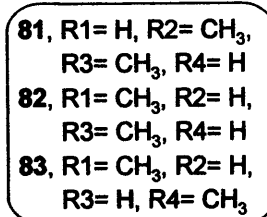
Purification by column chromatography (petroleum ether/EtOAc 70:30 v/v) gave the product as a light brown solid (64 %), mp: 173-174 °C. t.l.c system: petroleum ether-ethyl acetate 2:1, R_f = 0.67.

$^1\text{H NMR}$: δ (CDCl_3): 7.80 (d, 2H, J = 8.6 Hz, Ar), 7.64 (d, 2H, J = 9.0 Hz, Ar), 7.43 (m, 1H, Ar), 7.31 (d, 1H, J = 7.8 Hz, Ar), 7.19 (d, 1H, J = 7.8 Hz, Ar), 7.09 (m, 3H, Ar), 7.04 (s, 1H, Ar), 3.85 (bs, 1H, NH), 2.27 (s, 3H, CH_3), 2.19 (s, 3H, CH_3).

$^{13}\text{C NMR}$: δ (CDCl_3): 195.67 (C, C=O), 156.22 (C, C-2''), 145.97 (C, C-4'), 141.18 (C, C-9''), 137.95 (C, C-8''), 133.80 (C, C-1), 132.13 (C, C-2), 131.85 (C, C-5), 131.46 (C, C-1'), 131.04 (CH, C-2', C-6'), 129.78 (CH, C-4), 128.86 (CH, C-3), 127.57 (CH, C-6), 123.71 (CH, C-5''), 121.66 (CH, C-6''), 116.34 (CH, C-3', C-5'), 116.24 (CH, C-4''), 108.47 (CH, C-7''), 19.87 (CH_3), 18.39 (CH_3).

HRMS (EI) : Found: 343.1444 (M^+), Calculated: 343.1447.

3.5.5) General procedure for the preparation of the [4-(Benzoxazol-2-ylamino)phenyl](dimethylphenyl)methanol **81**, **82** and **83**



To a cooled (0 °C) solution of **78-80** (2.07 mmol) in anhydrous MeOH (50 mL) was added sodium borohydride (2.07 mmol), then the mixture was allowed to stir at room temperature under nitrogen for 4 h. The solvent was concentrated under reduced pressure and aqueous HCl (1 M, 5 mL) added to the residue. The oil formed was extracted with EtOAc (2 × 50 mL) and washed with H₂O (2 × 50 mL), the organic layers were combined and dried with MgSO₄ and the solvent concentrated under reduced pressure.

3.5.5.1) [4-(Benzoxazol-2-ylamino)phenyl]-(3,4-dimethylphenyl)methanol **81**

Orange solid (73 %), mp: 125-126 °C. t.l.c system: petroleum ether-ethyl acetate 2:1, R_f= 0.50.

¹H NMR: δ (CDCl₃): 7.70 (bs, 1H, NH), 7.33 (d, 2H, J= 8.6 Hz, Ar), 7.27 (m, 4H, Ar), 7.14 (m, 1H, Ar), 7.02 (m, 4H, Ar), 6.11 (s, 1H, H-7), 2.12 (s, 6H, 2 × CH₃).

¹³C NMR: δ (CDCl₃): 158.03 (C, C-2''), 146.84 (C, C-9''), 143.24 (C, C-4'), 140.30 (C, C-1), 138.23 (C, C-8''), 135.79 (C, C-3), 134.97 (C, C-4), 129.96 (C, C-1'), 126.75 (CH, C-4), 126.50 (CH, C-2', C-6'), 123.45 (CH, C-2), 122.92 (CH, C-6), 122.61 (CH, C-5''), 120.85 (CH, C-6''), 117.63 (CH, C-3', C-5'), 115.65 (CH, C-4''), 108.24 (CH, C-7''), 74.67 (CH, CH-OH), 18.83 (CH₃), 18.43 (CH₃).

HRMS (EI): Found: 345.1604 (M)⁺, Calculated: 345.1603.

3.5.5.2) [4-(Benzoxazol-2-ylamino)phenyl]-(2,4-dimethylphenyl)methanol 82

White solid (97 %), mp: 153-154 °C. t.l.c system: petroleum ether-ethyl acetate 2:1, R_f = 0.45.

$^1\text{H NMR}$: δ (CDCl_3): 7.56 (d, 2H, J = 8.6 Hz, Ar), 7.34 (m, 2H, Ar), 7.29 (m, 3H, Ar), 7.13 (m, 1H, Ar), 7.08 (m, 1H, Ar), 6.99 (d, 1H, J = 7.8 Hz, Ar), 6.90 (s, 1H, Ar), 5.89 (s, 1H, H-7), 2.27 (s, 3H, CH_3), 2.16 (s, 3H, CH_3).

$^{13}\text{C NMR}$: δ (CDCl_3): 160.27 (C, C-2''), 148.99 (C, C-9''), 143.54 (C, C-4'), 140.34 (C, C-1), 139.59 (C, C-8''), 138.89 (C, C-2), 137.84 (C, C-4), 136.31 (C, C-1'), 132.19 (CH, C-3), 129.27 (CH, C-2', C-6'), 127.56 (CH, C-6), 127.52 (CH, C-5), 125.23 (CH, C-5''), 123.00 (CH, C-6''), 119.40 (CH, C-3', C-5'), 117.61 (CH, C-4''), 109.96 (CH, C-7''), 73.54 (CH, CH-OH), 21.33 (CH_3), 19.72 (CH_3).

HRMS (EI) : Found: 345.1603 (M)⁺, Calculated: 345.1603.

3.5.5.3) [4-(Benzoxazol-2-ylamino)phenyl]-(2,5-dimethylphenyl)methanol 83

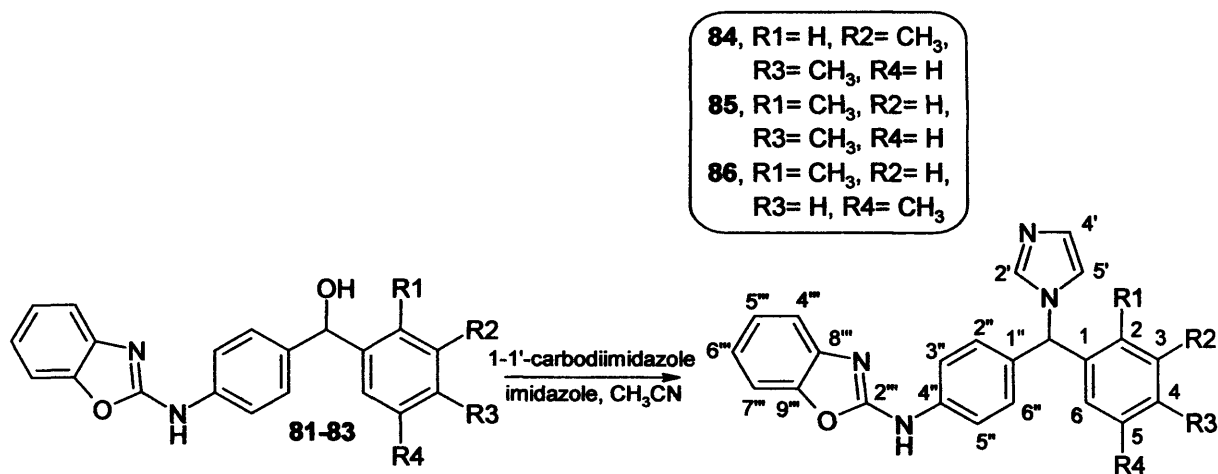
White solid (99 %), mp: 157-158 °C. t.l.c system: petroleum ether-ethyl acetate 2:1, R_f = 0.54.

$^1\text{H NMR}$: δ ($\text{DMSO-}d_6$): 10.54 (bs, 1H, NH), 7.71 (d, 2H, J = 8.4 Hz, Ar), 7.49 (d, 1H, J = 7.7 Hz, Ar), 7.45 (d, 1H, J = 7.7 Hz, Ar), 7.36 (s, 1H, Ar), 7.30 (d, 2H, J = 8.4 Hz, Ar), 7.22 (m, 1H, Ar), 7.17 (m, 1H, Ar), 7.02 (m, 2H, Ar), 5.84 (s, 1H, H-7), 5.70 (bs, 1H, OH), 2.32 (s, 3H, CH_3), 2.20 (s, 3H, CH_3).

$^{13}\text{C NMR}$: δ ($\text{DMSO-}d_6$): 158.04 (C, C-2''), 147.00 (C, C-9''), 142.97 (C, C-4'), 142.42 (C, C-1), 138.32 (C, C-8''), 137.25 (C, C-5), 134.32 (C, C-2), 131.38 (C, C-1'), 129.94 (CH, C-3), 127.51 (CH, C-2', C-6'), 127.14 (CH, C-6), 126.93 (CH, C-4), 123.92 (CH, C-5''), 121.53 (CH, C-6''), 117.31 (CH, C-3', C-5'), 116.48 (CH, C-4''), 108.85 (CH, C-7''), 71.06 (CH, CH-OH), 20.81 (CH_3), 18.57 (CH_3).

HRMS (EI) : Found: 345.1599 (M)⁺, Calculated: 345.1603.

3.5.6) General procedure for the preparation of the Benzoxazol-2-yl-*f*-4[*dimethylphenyl*]imidazol-1-ylmethyl}phenyl}amine **84**, **85** and **86**



To a solution of **81-83** (1.89 mmol) in CH₃CN (70 mL) was added imidazole (5.66 mmol) and 1,1'-carbodiimidazole (2.83 mmol). The mixture was heated under reflux overnight, then the reaction mixture was allowed to cool and the solvent removed under reduced pressure. The oil formed was extracted with CH₂Cl₂ (50 mL) and washed with H₂O (2 × 50 mL). The organic layer was dried (MgSO₄), filtered and reduced in *vacuo*.

3.5.6.1) Benzoxazol-2-yl-*f*-4[3,4-dimethylphenyl]imidazol-1-ylmethyl}phenyl}amine (84**)**

Purification by column chromatography (EtOAc) gave the product as a white solid (78 %), mp: 238-239 °C. t.l.c system: ethyl acetate, R_f= 0.18.

¹H NMR: δ (CDCl₃): 10.11 (bs, 1H, NH), 7.58 (d, 2H, J= 8.6 Hz, Ar), 7.42 (s, 1H, Ar), 7.33 (d, 1H, J= 7.8 Hz, Ar), 7.19 (d, 1H, J= 7.8 Hz, Ar), 7.06 (m, 2H, Ar), 6.98 (m, 4H, Ar), 6.76 (m, 2H, Ar), 6.70 (d, 1H, J= 7.8 Hz, Ar), 6.30 (s, 1H, H-7), 2.13 (s, 3H, CH₃), 2.09 (s, 3H, CH₃).

¹³C NMR: δ (CDCl₃): 157.60 (C, C-2'''), 146.68 (C, C-9'''), 141.11 (C, C-4'''), 137.74 (C, C-8'''), 136.18 (C, C-1), 135.88 (CH, C-2''), 135.41 (C, C-3), 132.18 (C, C-4), 129.02 (C, C-1'), 128.15 (CH, C-5), 127.83 (CH, C-2'', C-6''), 127.51 (CH, C-2), 124.34 (CH, C-5'), 124.21 (CH, C-4'), 123.12 (CH, C-6), 122.65 (CH, C-5'''),

120.70 (CH, C-6'''), 117.44 (CH, C-3'', C-5''), 115.85 (CH, C-7'''), 108.01 (CH, C-4'''), 63.59 (CH, CH-N), 18.80 (CH₃), 18.41 (CH₃, C).

HRMS (EI): Found: 395.1874 (M)⁺, Calculated: 395.1872.

3.5.6.2) **Benzoxazol-2-yl-{-4[2,4-dimethylphenyl]imidazol-1-ylmethyl}phenyl}amine (85)**

Purification by column chromatography (EtOAc) gave the product as a colourless oil (84 %). t.l.c system: ethyl acetate, R_f = 0.11.

¹H NMR: δ (CDCl₃): 10.32 (bs, 1H, NH), 7.62 (m, 2H, Ar), 7.33 (m, 2H, Ar), 7.19 (m, 1H, Ar), 7.09 (m, 2H, Ar), 6.96 (m, 4H, Ar), 7.85 (m, 1H, Ar), 6.77 (s, 1H, Ar), 6.55 (m, 1H, Ar), 6.48 (s, 1H, H-7), 2.20 (s, 3H, CH₃), 2.08 (s, 3H, CH₃).

¹³C NMR: δ (CDCl₃): 157.50 (C, C-2'''), 146.70 (C, C-9'''), 141.32 (C, C-4'), 137.90 (C, C-8'''), 137.13 (CH, C-2'), 136.41 (C, C-1), 134.91 (C, C-2), 133.52 (C, C-4), 131.38 (C, C-1''), 130.68 (CH, C-3), 127.90 (CH, C-2'', C-6''), 127.67 (CH, C-6), 126.44 (CH, C-5), 126.00 (CH, C-5'), 123.07 (CH, C-4'), 120.69 (CH, C-5'''), 118.83 (CH, C-6'''), 117.44 (CH, C-3'', C-5''), 115.95 (CH, C-4'''), 107.98 (CH, C-7'''), 60.69 (CH, CH-N), 20.02 (CH₃, C), 18.02 (CH₃, C).

HRMS (EI): Found: 395.1871 (M)⁺, Calculated: 395.1872.

3.5.6.3) **Benzoxazol-2-yl-{-4[2,5-dimethylphenyl]imidazol-1-ylmethyl}phenyl}amine (86)**

Purification by column chromatography (EtOAc) gave the product as a colourless oil (72 %). t.l.c system: ethyl acetate, R_f = 0.09.

¹H NMR: δ (CDCl₃): 9.82 (bs, 1H, NH), 7.63 (d, 2H, J = 8.6 Hz, Ar), 7.36 (d, 2H, J = 8.2 Hz, Ar), 7.22 (d, 1H, J = 7.8 Hz, Ar), 7.11 (m, 2H, Ar), 6.99 (m, 5H, Ar), 6.80 (s, 1H, Ar), 6.54 (s, 1H, Ar), 6.47 (s, 1H, H-7), 2.15 (s, 3H, CH₃), 2.07 (s, 3H, CH₃).

¹³C NMR: δ (CDCl₃): 157.36 (C, C-2'''), 146.71 (C, C-9'''), 141.24 (C, C-4''), 137.74 (C, C-8'''), 136.42 (C, C-1), 136.16 (CH, C-2'), 135.02 (C, C-5), 131.90 (C, C-2), 131.25 (C, C-1''), 129.81 (CH, C-3), 129.18 (CH, C-6), 128.08 (CH, C-2'', C-6''), 127.67 (CH, C-4), 126.88 (CH, C-5'), 123.14 (CH, C-4'), 120.79 (CH, C-5'''),

118.89 (CH, C-6'''), 117.40 (CH, C-3'', C-5'''), 116.01 (CH, C-4'''), 108.03 (CH, C-7'''), 60.89 (CH, CH-N), 20.15 (CH₃), 17.69 (CH₃).

HRMS (EI): Found: 395.1868 (M)⁺, Calculated: 395.1872.

CHAPTER 4

Haem and haem model binding studies

1) INTRODUCTION

The geometrical relationship between the iron atom of the haem and the nitrogen donor atom of the axial ligand acts as a major factor for the P450 inhibitors activity¹⁸⁷. Nitrogen donor ligands can form covalent complexes with the iron atom of porphyrins¹⁸⁸; it has consequently been proposed that some CYP26 drugs containing an aza-ring might coordinate to a porphyrin haem iron *via* a Fe-N covalent bond. It is well established that this coordination can be studied using NMR¹⁸⁹, mass spectrometry^{190,191}, UV-VIS spectroscopy¹⁹² and X-ray crystallography¹⁹³. This field has been especially investigated to study the mechanism of antimalarial drug-haem complex^{194,195}.

The haem of the P450 enzymes active site is a ferriprotoporphyrin IX (Fe(III)PPIX) containing a single iron coordinated to four planar pyrrole nitrogen atoms (Figure 4.1). This complex is commercially available with either chlorine (hemin) or hydroxyl group (hematin) coordinated in the axial position to the iron atom. The complex with the chlorine substituent has been chosen because it appeared

¹⁸⁷ Ekins S., De Groot M.J. and Jones J.P.; Pharmacophore and three-dimensional quantitative structure activity relationship methods for modeling cytochrome P450 active sites. *Drug Met. Dispo.*, **2001**, *29*, 936-944.

¹⁸⁸ Munro O.Q., Madlala P.S., Warby R.A.F., Seda T.B. and Madsen S.K.; Structural, Conformational, and Spectroscopic Studies of Primary Amine Complexes of Iron(II) Porphyrins. *Inorg. Chem.*, **1999**, *38*, 4724-4736.

¹⁸⁹ Alam S.L. Volkman B.F., Markley J.L. and Satterlee J.D.; Detailed NMR analysis of the heme-protein interactions in component IV *Glycemia dibranchiate* monomeric hemoglobin-CO. *J. Biomol. NMR*, **1998**, *11*, 119-133.

¹⁹⁰ Vinokur N. and Ryzhov V.; Using collision-induced dissociation with corrections for the ion number of degrees of freedom for quick comparisons of relative bonding strength. *J. Mass Spec.*, **2004**, *39*, 1268-1274.

¹⁹¹ Breuker K.; New mass spectrometric methods for the quantification of protein-ligand binding in solution. *Angew. Chem. Int. Ed.*, **2004**, *43*, 22-25.

¹⁹² Kelly J.X., Winter R., Riscoe M. and Peyton D.H.; A spectroscopic investigation of the binding interactions between 4,5-dihydroxyxanthone and heme. *J. Inorg. Biochem.*, **2001**, *86*, 617-625.

¹⁹³ Little R.G., Dymock K.R. and Ibers J.A.; The crystal and molecular structure of the ferrihemochrome bis(1-methylimidazole)-(protoporphyrin IX)iron-methanol-water. *J. Am. Chem. Soc.*, **1975**, *97*, 4532-4539.

¹⁹⁴ Leed A., Du Bay K., Ursos L.M.B., Sears D., De Dios A.C. and Roepe P.D.; Solution structures of antimalarial drug-heme complexes. *Biochem.*, **2002**, *41*, 10245-10255.

¹⁹⁵ Egan T.J.; Interactions of quinoline antimalarials with hematin in solution. *J. Inorg. Biochem.*, **2006**, *5*, 916-926.

to be more soluble (and thus easier to study) than the hydroxyl analogue. It has shown good solubility in DMF and DMSO.

A study of the binding of the benzoxazol-2-yl-[phenylimidazol-1-ylmethyl]phenyl]amine inhibitors to this complex could provide a rich source of information on the nature of the metal-ligand bonding involved in inhibition. It could show the influence of the type of aza-ring (imidazole, 1,2,4 triazole, 1,3,4 triazole and tetrazole) and the type of substituents (hydrogen, methyl, methyl ester and carboxylic acid) on the interaction between the drug and the haem. The data could then be correlated with the inhibitory activity of these compounds in order to determine the relative importance of ligand-iron interaction compared with the non-covalent ligand-protein interactions (e.g. π -stacking, hydrogen bonding and hydrophobic interactions).

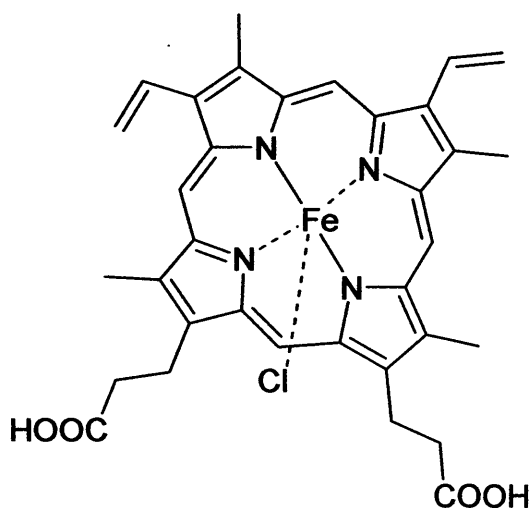


Figure 4.1: Structure of the haem used for this study (hemin).

A useful data on the haem-ligand binding interaction will be the determination of the ligand binding constant (or equilibrium constant) K which expresses the balance between the binding and dissociation processes after infinite reaction time (Figure 4.2) and has long been employed as an effective measure of the affinity of a ligand for a metal ion in solution¹⁹⁶. In order to determine the binding constant of the ligand, it is necessary to first determine the stoichiometry of the

¹⁹⁶ Martell A.E. and Motekaitis R.J.; Determination and use of stability constants. *VCH Publishers, Inc, New York, 1988*, p.1.

reaction and the number of species present in solution. In the case of haem, the central iron atom has two available binding sites; so it is possible to form the mono-substituted complex HL, the di-substituted complex HL₂ (Figure 4.3) or even to have a mixture of both.



Figure 4.2: Expression of the binding constant *K*.

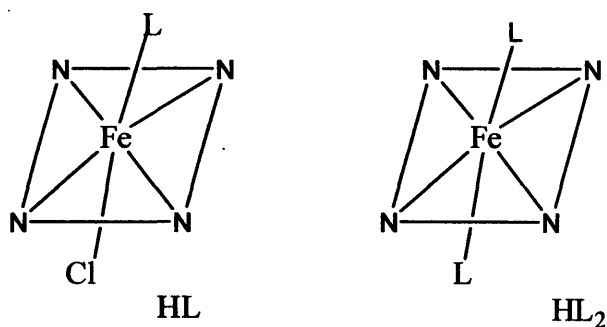


Figure 4.3: Structure of the haem-ligand complex HL and HL₂.

To determine the binding constant of the different ligands, a few different spectroscopy techniques were investigated: mass spectrometry, X-ray crystallography, ¹H NMR and UV/VIS spectroscopy. Because the analysis is performed in the gas phase, the mass spectra do not provide an accurate description of the haem-ligand binding in solution; however it provided useful data on the different species formed during the reaction. X-ray analysis of a haem-ligand crystal will be the most useful and accurate source of information especially on the properties (length, angle) of the Fe-N covalent bond and the stoichiometry of the reaction. Formation of the complex should also be easily identified by ¹H NMR and UV/VIS spectroscopy. The addition of a haem solution into a ligand solution or the inverse should lead to the progressive appearance of new peaks or new bands corresponding to the haem-ligand complex¹⁸⁹. The ratio observed between the bound

and unbound ligand or haem in ^1H NMR and UV/VIS spectrometry at different concentrations could then be used to determine the value of the binding constant K .

2) MASS SPECTROMETRY STUDIES

The formation of the haem-ligand complexes for **52**, **53**, **53'** and **54** was first studied using mass spectrometry. The mass spectrometry study presents some limitations. The presence of a complex in solution is not always correlated with the observation of the corresponding species in the gas-phase spectrum¹⁹⁷. Also, as dissociation processes could emerge during the ionisation process, the intensity of the peaks is not always correlated with the real concentration of the species. However, it will allow us to clearly identify (although it will be difficult to quantify) the products formed during the reaction (HL, HL₂) as well as the interaction of the haem with the different solvents. Thus it will be a good technique to study the stoichiometry of the reaction.

2.1) Material and method

Because of its poor solubility (only soluble in DMSO and DMF), hemin could not be used in these experiments in our laboratory, it was replaced by a similar and more soluble iron porphyrin: 5,10,15,20-tetraphenyl-21H,23H-porphine-iron(III)-chloride or TPP (Figure 4.4) which showed good solubility in chlorinated solvents. Spectra were recorded on a Micromass LCT premier XE using an electro-ionisation technique (ESI-MS).

A titration of TPP using four different ligands (**52**, **53**, **53'** and **54**) was performed. Eleven samples each containing a 50 µL mixture of a 2 mM solution of TPP in CH₂Cl₂ and a 2 mM solution of ligand in CH₂Cl₂ diluted in 1 mL of a 50:50 mixture of acetonitrile and water with 1 % of formic acid were used for this study.

¹⁹⁷ Clark M.S. and Konermann L.; Diffusion measurements by electrospray mass spectrometry for studying solution-phase noncovalent interactions. *J. Am. Soc. Mass Spectrom.*, **2003**, *14*, 430-441.

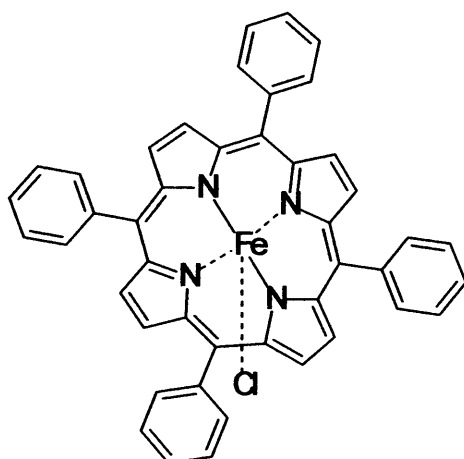


Figure 4.4: Structure of 5,10,15,20-tetraphenyl-21H,23H-porphine-iron(III)-chloride or TPP.

2.2) Experimental results and discussion

Although the mass spectra are difficult to interpret because of the molecular dissociation observed during the ionisation process, the experiments clearly showed the presence of haem-ligand species (HL and HL₂) for all the ligands (52, 53, 53' and 54) and could provide a rich source of information on the stoichiometry of the reaction and on the affinity between the haem and the different solvents (CH₂Cl₂, CH₃CN, H₂O, HCOOH) used for the experiment.

The TPP spectrum, shown on Figure 4.5, displayed 5 characteristic peaks. The presence of the TPP peak at 668 Da instead of 704 Da showed that the chloride ion is lost during the ionisation process. A loss of the chloride ion was also observed for all the other peaks; however the addition of a solution of silver nitrate to the solution showed no precipitation. The low intensity of the peak also proved that the haem always tend to have a sixth substitution by ligand or the different solvents. The peak at 709 Da represents one molecule of haem bonded to acetonitrile, the two peaks at 1353 Da and 1381 Da represent respectively a molecule of water and a molecule of formic acid bond to two molecules of haem (Figure 4.6). This demonstrates that the stoichiometry of binding for acetonitrile and water and formic acid is different. The acetonitrile is binding to only one molecule of haem while

water and formic acid seem to be responsible of aggregation of haem molecule (Figure 4.6). On the other hand, the presence of a dichloromethane-haem complex was not observed. This could be explained by the number of lone pair available for iron binding in these solvents (one on the acetonitrile nitrogen atom and two on the water oxygen atom, Figure 4.6).

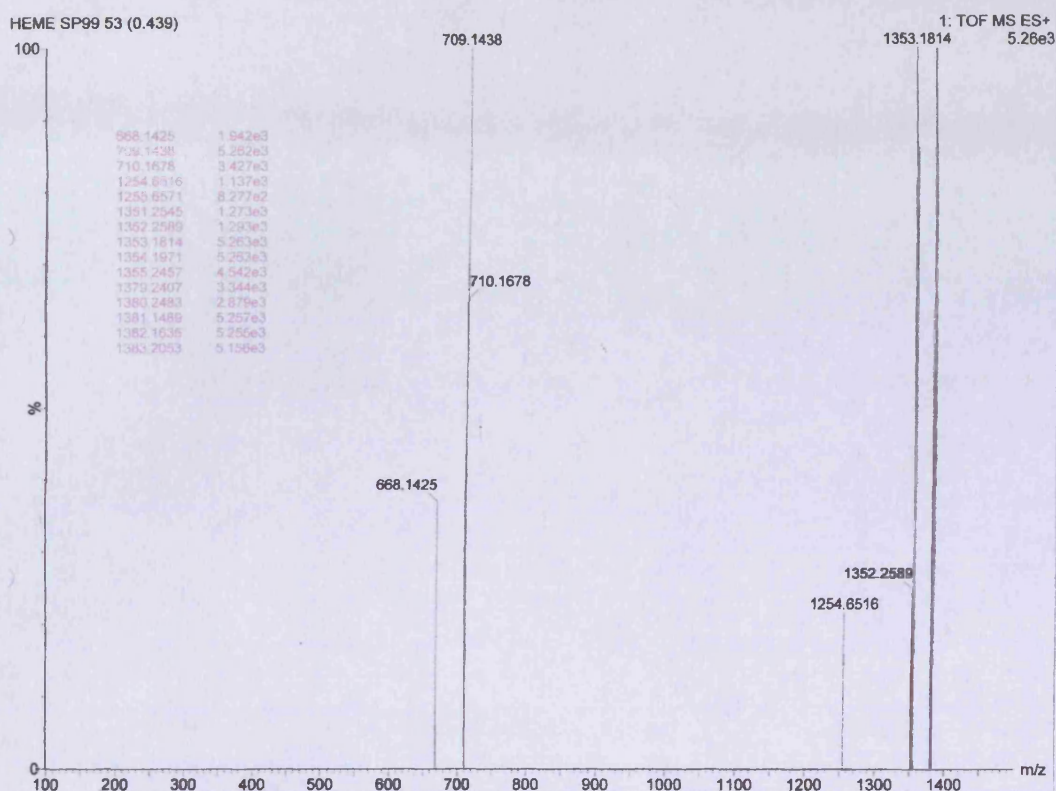


Figure 4.5: Mass spectrum of TPP.

Then, titration of TPP was performed with 4 different ligands **52**, **53**, **53'** and **54**. These experiments were designed to provide information on the binding properties of these ligands with iron porphyrin. An example is shown on Figure 4.7 with ligand **52**.

On the first addition of ligand (**B**), the spectrum displayed two new peaks at 299 Da and 1034 Da. The 299 Da peak is the main ligand peak corresponding to **52** minus its imidazole ring, previous experiments have shown that loss of the imidazole ring (or other type of aza-ring) is often observed during the ionisation process. The 1034 Da peak showed the formation of the haem-ligand complex.

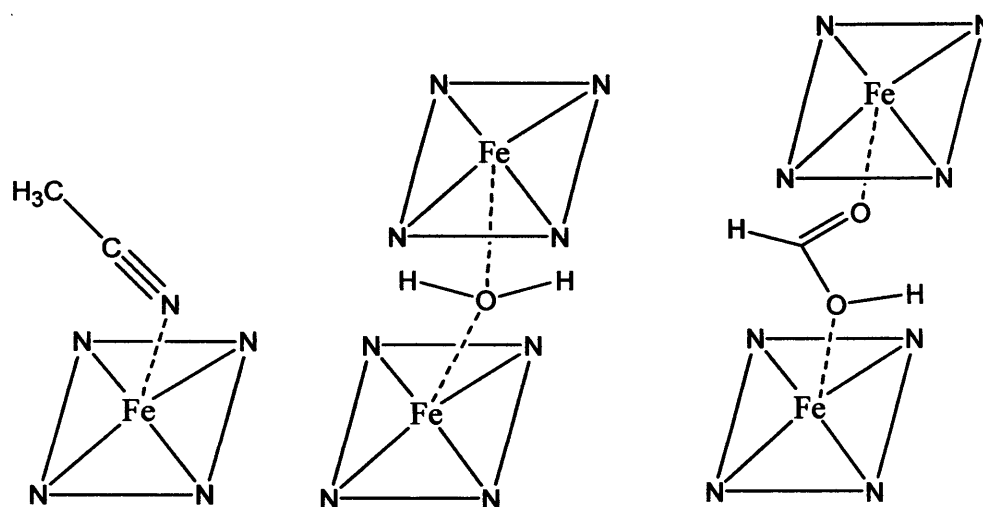
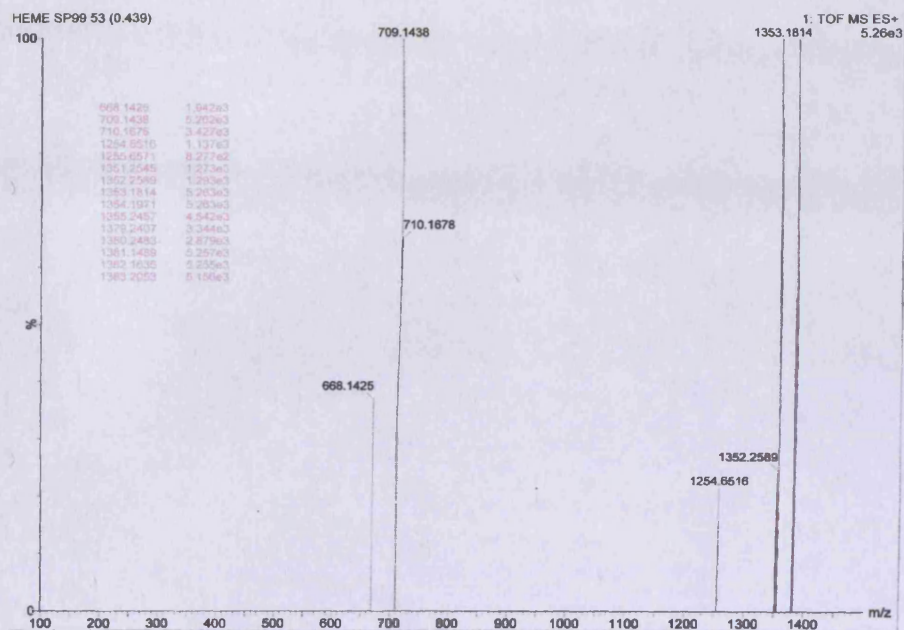


Figure 4.6: Structure of TPP-solvent (CH_3CN , H_2O and HCOOH) complexes observed in the mass spectrum.

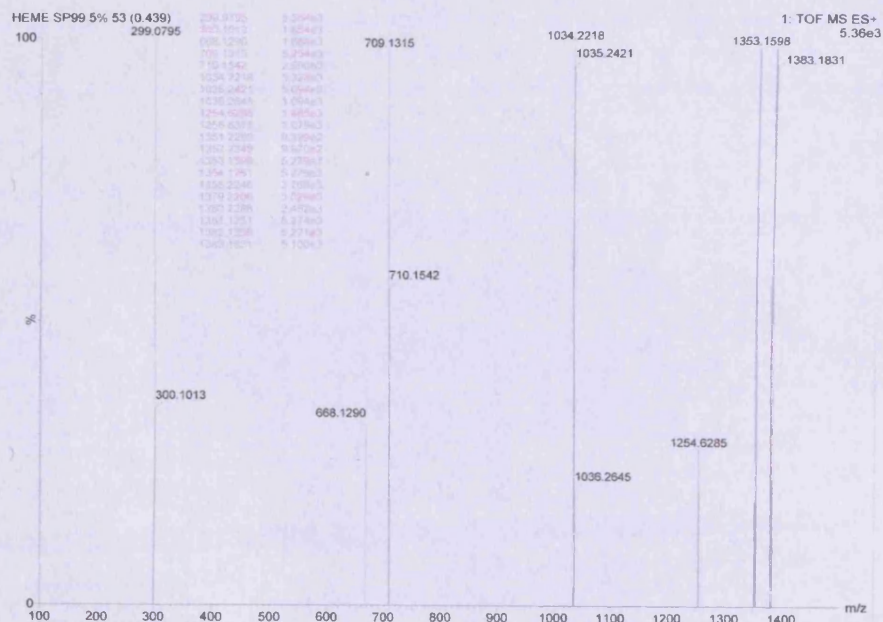
On the next addition (spectrum C), the “full” ligand peak appeared at 367 Da and a new complex involving a di-substitution of the haem by **52** also emerged at 1400 Da. Spectrum D was obtained using an equal concentration of haem and ligand ($47.61 \mu\text{M}$). It shows a big increase of the di-substituted species as well as new peak at 733 Da corresponding to the haem bound to free imidazole which is a consequence of the fragmentation of the ligand.

In the next spectra (spectrum E and F), equilibrium between the mono-substituted and the di-substituted species seem to be reached. The two species seem to exist at more or less equivalent intensity. This could be explained by some decomposition of the di-substituted complex. The last two spectra (E and F) also showed a slow disappearance of the haem + solvent peaks (haem + H_2O , haem + CH_3CN and haem + HCOOH), although the concentration of solvent is obviously much higher than the concentration of ligand (E: $[\mathbf{52}] = 66.66 \mu\text{M}$ and F: $[\mathbf{52}] = 104.76 \mu\text{M}$ while $[\text{H}_2\text{O}] = 27.5 \text{ M}$, $[\text{CH}_3\text{CN}] = 9.5 \text{ M}$ and $[\text{HCOOH}] = 0.26 \text{ M}$). When the haem/ligand ratio gets to 1:10 (F, $[\mathbf{52}] = 104.76 \mu\text{M}$), hardly any more haem + solvent species are observed, the peak at 1353 Da (water + 2 haem) has completely disappeared and the peaks at 709 Da (haem + acetonitrile) and 1381 Da (formic acid + 2 haem) are very minor compare to the two haem-ligand peaks. This

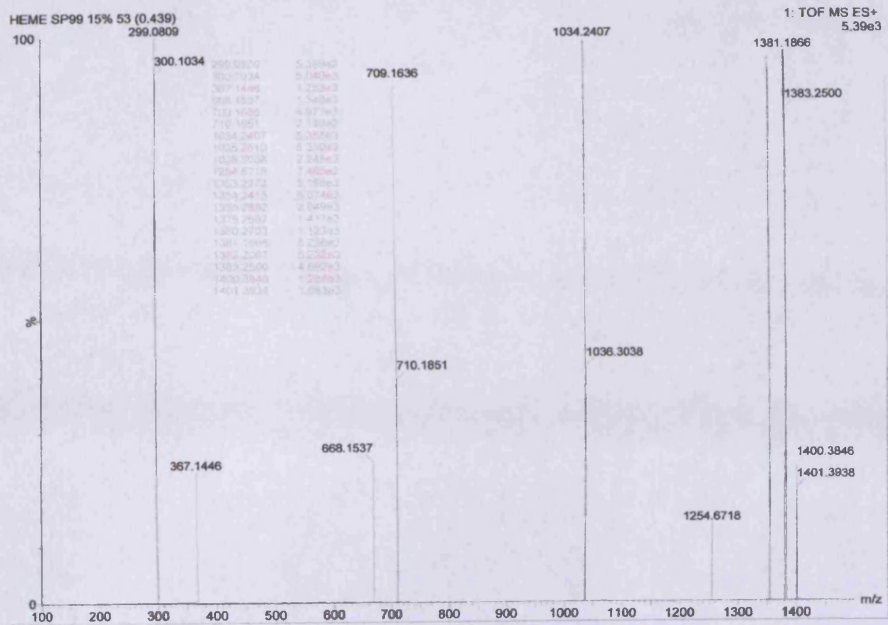
shows that **52** is a much better ligand than acetonitrile, water and formic acid, as, even when its concentration is much lower than all the solvent (about 100000 fold), it still competes successfully for binding.



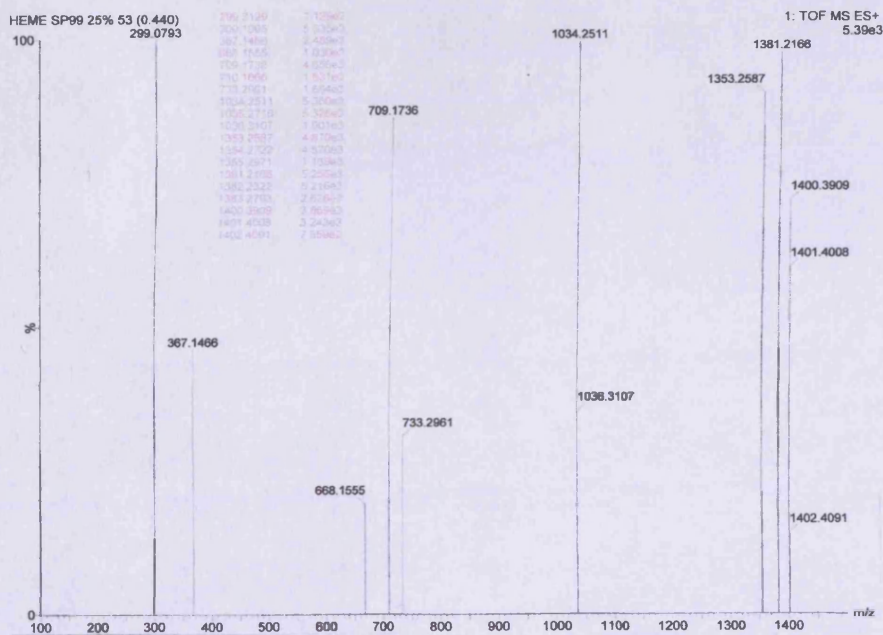
A:
[H]= 95.23 μ M



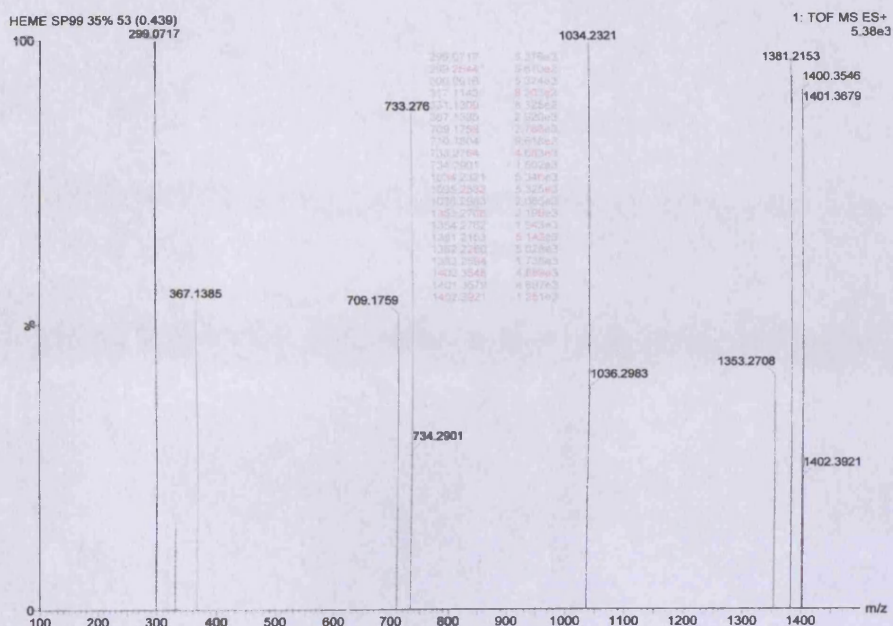
B:
[H]= 85.72 μ M
[L]= 9.52 μ M



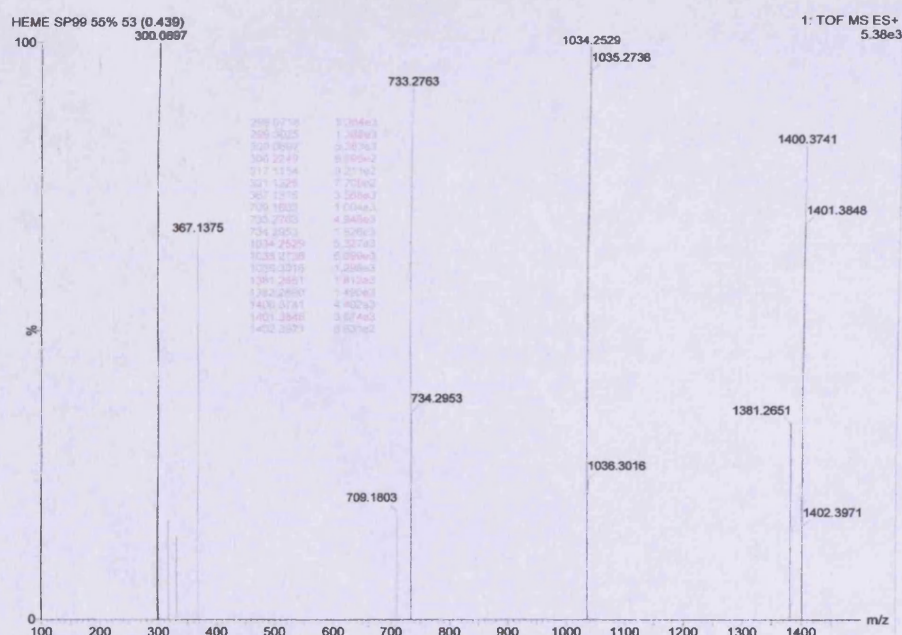
C:
[H]= 66.66 μ M
[L]= 28.57 μ M



D:
[H]= 47.61 μ M
[L]= 47.61 μ M



E:
[H]= 28.57 μ M
[L]= 66.66 μ M



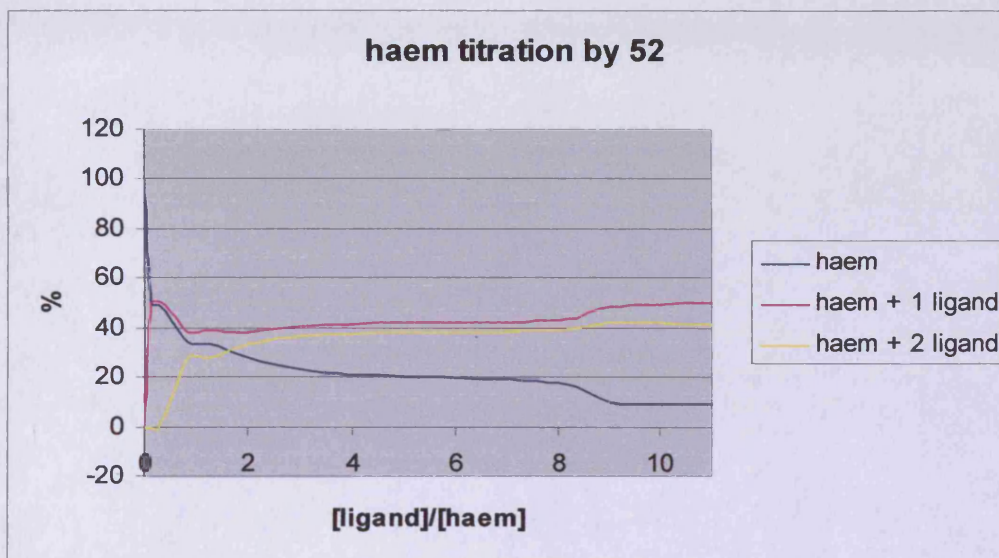
F:
[H]= 9.47 μ M
[L]= 104.76 μ M

Figure 4.7: Mass spectra of TPP titration with the imidazole ligand **52**, concentration of haem and ligand are indicated on the right of the spectrum.

Mass spectrometry is therefore a good technique to observe the evolution of the formation of different species. It allowed us to draw some conclusions on the

behaviour of the ligands and on the formation of mono or di-substituted haem complexes.

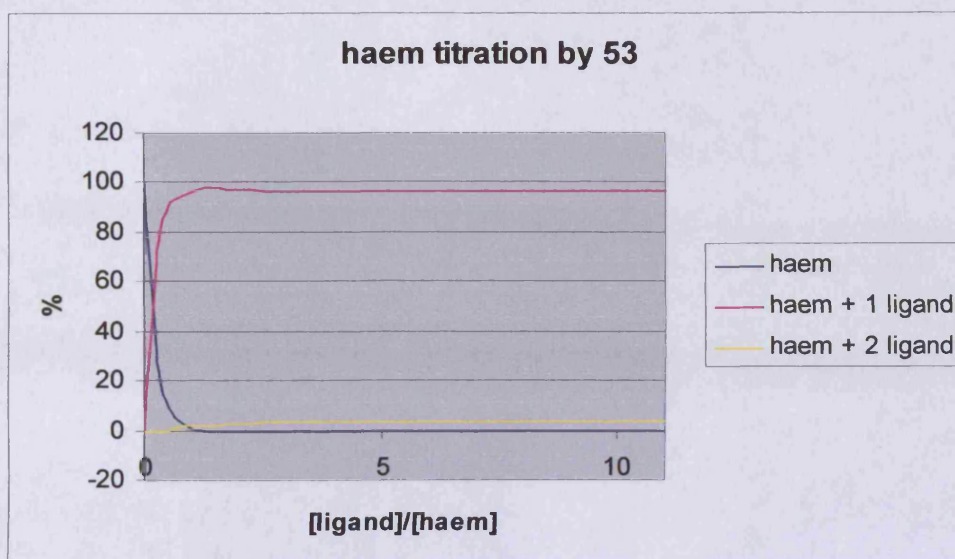
The evolution of the formation of the three species (free haem, mono-substituted haem-ligand complex and di-substituted haem-ligand complex), depending on the ligand/haem concentration ratio, is shown on Graph 1. This graph displays the percentage of each of the three species without considering any other peaks.



Graph 1: Percentage of haem, mono-substituted haem-ligand complex and di-substituted haem-ligand complex function of the ligand/haem concentration ratio for **52**. Concentrations of haem and **52** for each experiment are shown in Figure 4.4.

This graph clearly shows a disappearance of free haem and formation of first the haem + 1 ligand complex followed by the formation of the di-substituted species. The percentage of the three different species seems to stay constant at high concentration of ligand. Also the di-substituted compound never becomes the major species and the free haem never completely disappears. The presence of free haem at high concentration of ligand might be explained by the decomposition in the mass spectrometer of a certain proportion of complexes.

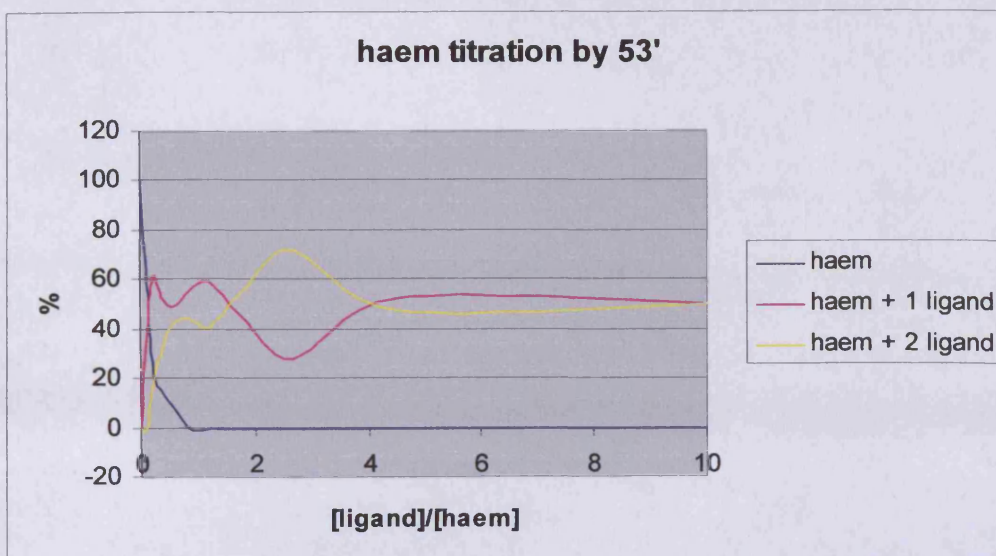
The following graphs show the evolution of the same three species with the other ligands **53** (Graph 2), **53'** (Graph 3) and **54** (Graph 4).



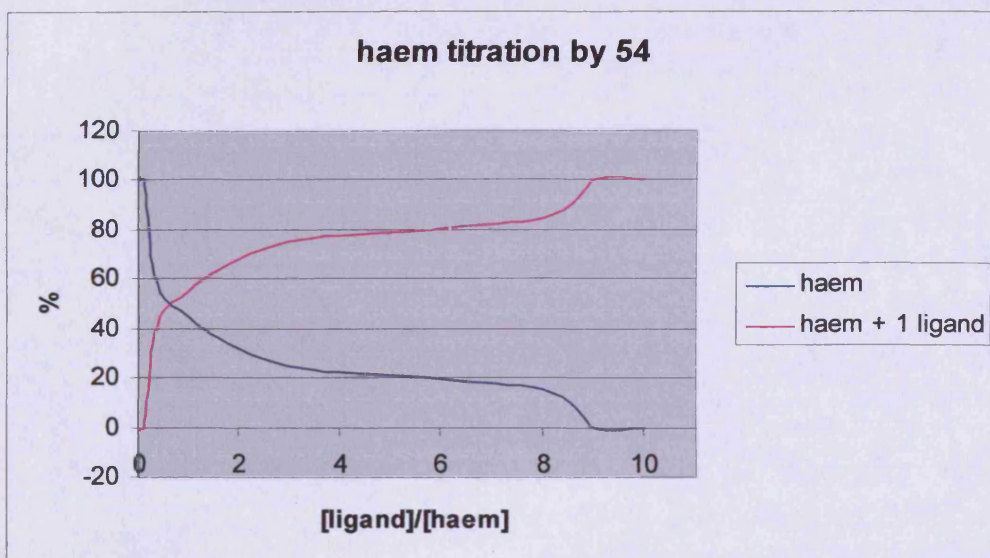
Graph 2: Percentage of haem, mono-substituted haem-ligand complex and di-substituted haem-ligand complex function of the ligand/haem concentration ratio for **53**. Concentrations used for this experiment are similar to concentrations of haem and ligand with **52** shown in Figure 4.4.

Concerning ligand **53** (Graph 2), almost no haem + 2 ligand species was observed, it never goes above 5 %. On the other hand the formation of the mono-substituted complex was observed at very low concentration of ligand ($[53] = 9.47 \mu\text{M}$). At a ligand/ haem concentration ratio of 0.5, half of the haem is already bound to one ligand. Then, the free ligand peak disappears completely when the concentration of ligand is double the concentration of haem.

The 1,3,4-triazole ligand **53'** display similar result to the imidazole **52** with the difference that no more free haem was observed when the concentration of ligand become higher than the concentration of haem (Graph 3). The presence of both haem-ligand species seems to stay constant after the concentration of ligand is more than double the concentration of haem. The chaotic curve of the percentage of haem + 1 ligand and haem + 2 ligands is probably due to the ionisation dissociation process of the di-substituted complex and shows the limitation of the technique.



Graph 3: Percentage of haem, mono-substituted haem-ligand complex and di-substituted haem-ligand complex function of the ligand/haem concentration ratio for **53'**. Concentrations used for this experiment are similar to concentrations of haem and ligand with **52** shown in Figure 4.4.



Graph 4: Percentage of haem, mono-substituted haem-ligand complex and di-substituted haem-ligand complex function of the ligand/haem concentration ratio for **54**. Concentrations used for this experiment are similar to concentrations of haem and ligand with **52** shown in Figure 4.4.

The tetrazole compound **54** displayed similarities with compound **53**, but the formation of the haem + 2 ligand complex was not observed at all for **54** (Graph 4). As well as **53**, an equal amount of free haem and haem + 1 ligand species was observed for a concentration ratio ligand/haem of 1:1. The haem is bound at 100 % to **54** for a haem/ligand ratio of 9:1.

In conclusion, although the techniques showed some limitations (the shape of the curve is occasionally chaotic), these mass spectrometry experiments provided a rich source of information on the binding properties of the ligands. Two different behaviours seem to occur. Experiments with ligand **52** and **53'** showed the formation of both the mono and the di-substituted complexes. Above a ligand/haem ratio of 2:1, the two species were present in more or less equal quantities in the gas phase. In the case of compound **53** and **54**, the percentage of the di-substituted complex was very low or even null for **54**. For **53**, the ligand bound species become major for a ligand/haem ratio of 0.25 and about 0.75 for **54**. The disappearance of the haem peak also happened at lower concentration of ligand with compound **53**. This might suggest that the 1,2,4-triazole compound **53** is a better ligand than the tetrazole **54**. All compounds also appeared to be much better ligands than all the solvents present in solution (water, acetonitrile and formic acid).

However, as the mass spectrometry data are recorded in the gas phase and display the presence of positively charged molecules in an excited state, the experiments do not accurately reflect what is actually happening in solution with ground state neutral molecules. It has been shown that false negative and false positive results could be obtained when the solution phase complexes dissociate prior to detection^{195, 198}. It was thus not possible to draw any quantitative conclusions on the binding properties of our ligands, such as a binding constant calculation, using these mass spectrometry data. But we could safely conclude that both the mono-substituted (HL) and the di-substituted complexes (HL₂) are formed and thus need to be considered in other experiments where the mono-substituted complex HL and the di-substituted complex HL₂ might have similar spectra.

¹⁹⁸ Cunniff J.B. and Vouros P.; False positives and the detection of cyclodextrin inclusion complexes by electrospray mass spectrometry. *J. Am. Soc. Mass Spectrom.*, 1995, 6, 437-447.

3) FORMATION OF COMPLEXES AND X-RAY CRYSTALLOGRAPHY STUDIES

A crystal structure of hemin or TPP bound to one of our ligands would be the most useful source of information on the binding geometry of the ligand. It would provide accurate data on the distance of the axial Fe-N bond for all the different ligands and the stoichiometry of the reaction.

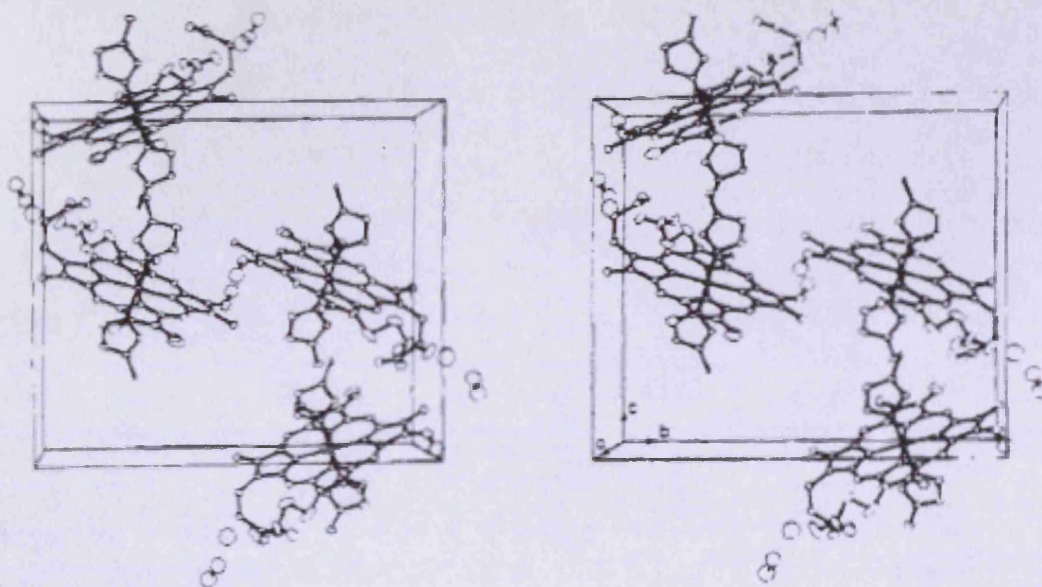


Figure 4.8: Stereoscopic view of the contents of one unit cell of the hemin-methylimidazole crystal structure¹⁹³.

Although only few X-ray structures of substituted haem system were found in the literature, a crystal structure of imidazole bound to TPP¹⁹⁹ and a crystal structure of methyl imidazole bound to hemin¹⁹³ have been achieved. They should display similar binding properties to our imidazole ligand **52**. The crystal structure of the hemin-methylimidazole complex is shown on Figure 4.8. The two axial Fe-N bond

¹⁹⁹ Collins D.M., Countryman R. and Howard J.L.; Stereochemistry of low-spin iron porphyrins. I. Bis(imidazole)- $\alpha,\beta,\gamma,\delta$ -tetraphenylporphyrinatoiron(III) chloride. *J. Am. Chem. Soc.*, 1972, 94, 2066-2072.

lengths are 1.966 Å and 1.988 Å and the average porphyrin Fe-N bond length is 1.990 Å. In this structure, the two propionate groups of the porphyrin core are connected together by a bridging water molecule.

The crystal structure of the imidazole-TPP complex (Figure 4.9) displayed two Fe-N bond lengths of 1.957 Å and 1.991 Å and an average porphyrin Fe-N bond length of 1.990 Å, all very similar to the hemin-methylimidazole structure. The complex also displays a very effective symmetry as it contains several plan of symmetry and the iron atom is the centre of symmetry of the complex.

In both crystals, the lengths of the two axial Fe-N bonds are non-equivalent. This could be explained by a small out of plane displacement of the iron atom of 0.009 (\pm 0.003) Å and also by the different steric interactions of the imidazole hydrogen atom with the porphyrin core.

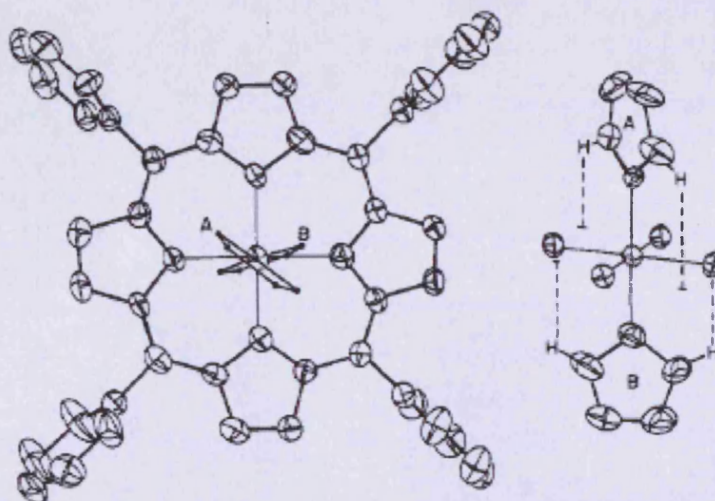


Figure 4.9: Computer-drawn models of at left the imidazole-TPP (Im_2FeTPP) complex and at right the coordination group¹⁹⁹.

Then, Little *et al.*¹⁹³ method's for the formation of hemin-methylimidazole crystal was applied to the formation of a hemin-52 crystal. Hemin was dissolved in a 5 % aqueous solution of KOH and then precipitated by addition of AcOH in order to remove the chloride ion. After being washed thoroughly with dilute AcOH, the solid was dissolved in a 1:1 mixture of $\text{CHCl}_3/\text{MeOH}$ containing the ligand 52. Then the sample was left to slowly evaporate for a few days until crystallisation occurred.

After 3 days black crystals formed on the bottom of the flask, unfortunately none of them were suitable for X-ray analysis. Consequently, the solid was collected and washed with a mixture of CHCl_3 and MeOH. Elemental analysis of the solid confirmed the formation of the complex as well as a 1:2 haem/ligand stoichiometry. Unfortunately, the poor solubility of the complex did not allow us to perform NMR and UV/VIS analysis and no conclusion could be drawn from the IR analysis because of the poor resolution of the peaks.

Many different techniques such as layering and slow evaporation and different solvents (MeOH, CHCl_3 , CH_2Cl_2 , hexane, petroleum ether, diethyl ether, H_2O) were investigated with unfortunately no success in gaining X-ray quality crystals both with hemin and TPP.

- Experimental procedure:

Hemin (0.4 g, 0.61 mmol) was dissolved in 40 mL of 5 % aqueous KOH and then precipitated by the addition of conc. AcOH. The precipitated solid was filtered off and washed with dilute AcOH. The dissolution and precipitation procedure was repeated until the filtrate was free from chloride ion, as indicated by the absence of a precipitate upon the addition of silver nitrate to the filtrate.

The washed, but still moist, solid was dissolved in 60 mL of a 1:1 mixture of CHCl_3 and MeOH containing **52** (0.6 g, 1.59 mmol). The solution was filtered to remove any undissolved material, the volume reduced to one third and more methanol added. The flask was then left to slow evaporation for 3 days. Then the precipitated black solid was collected and washed with a mixture of CHCl_3 and methanol. Anal. calcd. For $\text{C}_{80}\text{H}_{68}\text{FeN}_{12}\text{O}_6$: C, 71.21; H, 5.08; N, 12.46. Found: C, 71.16; H, 4.81; N, 14.20. The NMR analysis of the solid was impossible because of its limited solubility.

4) ¹H NMR STUDIES

NMR spectroscopy has become one of the most important methods for determining the binding constant of two molecules in solution²⁰⁰. ¹H NMR has been the most widely used NMR technique and will be used in our study; however it is also possible to use ¹³C NMR²⁰¹, ¹⁵N NMR²⁰², ³¹P NMR²⁰³ and NOESY²⁰⁴. This method uses the difference between the chemical shifts of the free ligand spectrum and the haem-ligand complex spectrum. Also, as paramagnetic iron atom exerts space effects on the relaxation rate of nearby proton spins depending on the iron-proton distance¹⁹⁴, it is possible to calculate the distance between the haem iron and the different proton ligand using the Solomon-Bloembergen equation^{205,206} (Figure 4.10).

T_1 : complex longitudinal relaxation time

S : total electron spin

r : distance between the proton and the paramagnetic Fe

τ_c : effective correlation time

$$\frac{1}{T_1} = \left(\frac{\mu_0}{4\pi} \right)^2 \frac{(\gamma_N^2 g_e^2 \mu_B^2)(S+1)}{r^6} \tau_c$$

²⁰⁰ Funasaki N., Nomura M., Ishikawa S. and Neya S.; NMR chemical shift references for binding constant determination in aqueous solutions. *J. Phys. Chem. B*, **2001**, *105*, 7361-7365.

²⁰¹ Rivera M. and Caignan G.A.; Recent developments in the ¹³C NMR spectroscopic analysis of paramagnetic hemes and heme protein. *Anal. Bioanal. Chem.*, **2004**, *378*, 1464-1483.

²⁰² Modi S., Behere D.V. and Mitra S.; ¹H and ¹⁵N-NMR study of the binding of thiocyanate to chemically modified horseradish peroxidase and involvement of saly bridge. *Biochim. Biophys. Acta*, **1994**, *1204*, 14-18.

²⁰³ Kabil O., Toaka S., Lo Brutto R., Shoemaker R. and Banerjee R.; Pyridoxal phosphate binding sites are similar in human heme-dependant and yeast heme-independant cystathionine β -synthase. *J. Biol. Chem.*, **2001**, *276*, 19350-19355.

²⁰⁴ Banci L., Bertini I., Marconi S., Pierattelli R. and Sligar S.G.; Cytochrome P450 and aromatic bases: a ¹H NMR study. *J. Am. Chem. Soc.*, **1994**, *116*, 4866-4873.

²⁰⁵ Martinez A., Olafsdottir S. and Flatmark T.; The cooperative binding of phenylalanine to phenylalanine 4-monooxygenase studied by ¹H NMR paramagnetic relaxation. *Eur. J. Biochem.*, **1993**, *211*, 259-266.

²⁰⁶ Novak R.F. and Vatsis K.P.; ¹H Fourier transform nuclear magnetic resonance relaxation rate studies on the interaction of acetanilide with purified isozymes of rabbit liver microsomal cytochrome P-450 and with cytochrome b₅. *Mol. Pharmacol.*, **1982**, *21*, 701-709.

γ_N : nuclear gyromagnetic ratio
 g_e : Lande factor for the metal ion
 μ_0 and μ_B : Bohr magneton

Figure 4.10: Solomon-Bloembergen equation

4.1) Materials and method²⁰⁷

All the spectra were recorded on a Bruker DPX400 and TMS was used as the internal standard. The chemical shifts are given in parts per million (ppm). NMR samples were prepared using 500 μL of a 1 mM solution of ligand in $\text{DMSO-}d_6$. To these samples 50 or 100 μL aliquots of a 2 mM solution of hemin in $\text{DMSO-}d_6$ were added. In order to keep the concentration of ligand constant during the experiment, the hemin solution also contained 1 mM of ligand.

4.2) Experimental results and discussion

^1H NMR spectroscopy has been shown to be a useful technique to study the interaction between a drug and a haem species. The broadening and the shift observed in the ligand peaks could be used to calculate the binding affinity of this ligand with the haem²⁰⁸. These changes in the NMR spectra are due to the influence of the paramagnetic iron on the ligand protons and are proof of the covalent binding between the haem and the ligand. It has been shown that the closer a particular proton on the ligand is to the Fe^{3+} atom, the greater the induced chemical shift^{194, 208}. Increasing the [ligand]/[hemin] molar ratio should also display a progressive modification of the chemical shift of some protons which could be used to calculate

²⁰⁷ Yao Y., Qian C., Wu Y., Hu J. and Tang W.; ^1H NMR study of 2-methylimidazole binding to cytochrome c: a comprehensive investigation of the role of the methyl substituent on the ligand binding affinity and haem electronic structure in imidazole-cytochrome c complexes. *J. Chem. Soc., Dalton Trans.*, 2001, 1841-1845.

²⁰⁸ Palma P.N., Moura I., Le Gall J., Van Beeumen J., Wampler J.E. and Moura J.J.G.; Evidence for a ternary complex formed between flavodoxin and cytochrome c3: ^1H NMR and molecular modelling studies. *Biochem.*, 1994, 33, 6397-6407.

the ligand binding constant. Changes in the ^1H NMR spectrum of the ligand upon the addition of a hemin solution were consequently investigated.

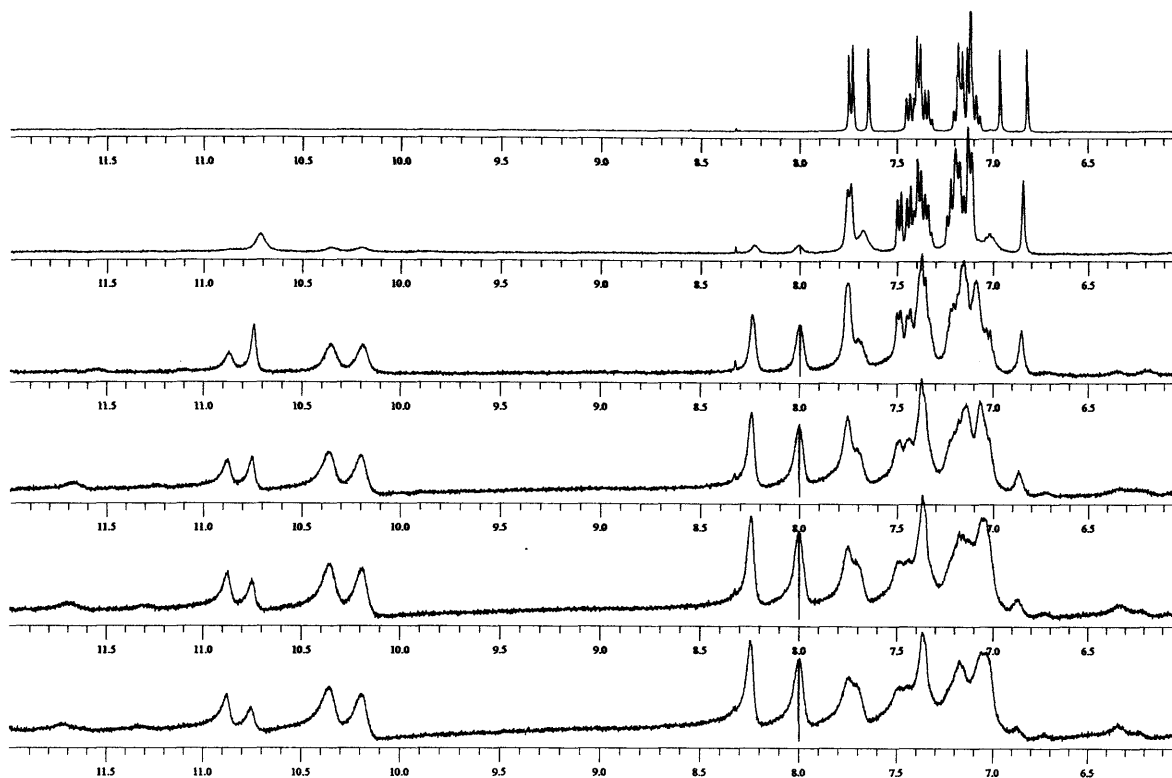
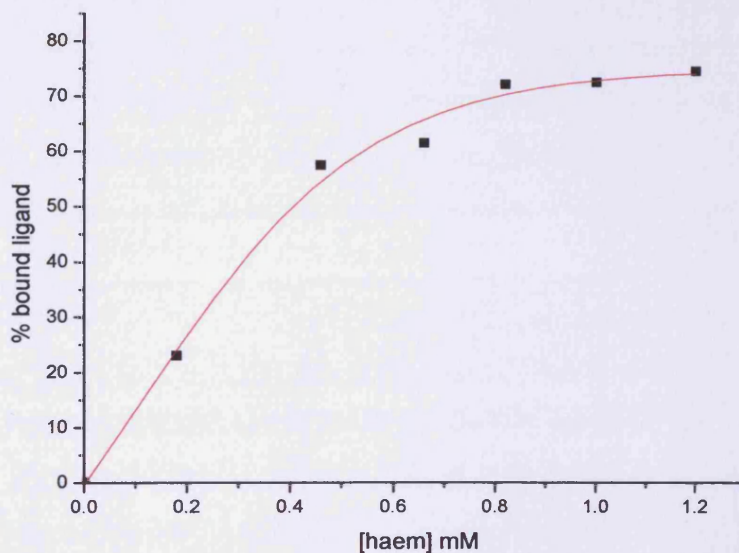


Figure 4.11: Changes in the ^1H NMR spectrum of a 1 mM solution of **52** upon the addition of hemin, concentration of hemin is respectively from the top to the bottom: 0 mM, 0.18 mM, 0.46 mM, 0.66 mM, 0.82 mM, 1 mM.

A spectrum of the ligand itself in $\text{DMSO-}d_6$ was first recorded and then a 2 mM hemin solution in $\text{DMSO-}d_6$ also containing 1 mM of ligand was slowly added to the tube. The results undoubtedly confirmed the binding of ligand **52** to the haem iron. Even with a low concentration of hemin, a broadening of some peaks as well as a large downfield shift of their value was observed for the imidazole ligand **52**. The shift in the peaks concerned the NH proton at 10.75 ppm (which does not appear in the original ligand spectrum), the three imidazole protons and the CH singlet H-7 which resulted in the formation of 5 new broad singlets at 10.82 ppm, 10.35 ppm, 10.18 ppm, 8.20 ppm and 7.96 ppm (Figure 4.11). This shows that these protons are the closest from the haem iron and thus confirms the coordination of the imidazole

ring of **52** with the iron atom of the haem *via* a Fe-N bond. The large broadening of all the other peaks also confirms that all the ligand protons are relatively close from the haem iron. Due to the large number of aromatic proton in the ligand, it was unfortunately impossible for us to assign the new peaks and thus to determine the distance between the different protons and the haem.

The plot of the percentage of bound ligand on the concentration of hemin (Graph 5) shows that no evolution in the formation of the complex was observed when the concentration of hemin was higher than the concentration of ligand. No more than 75 % of the ligand binds to the haem, this can be explained by the formation of DMSO bridged haem or haem aggregation at high concentration of haem. This graph also confirms the 1:2 stoichiometry as 50 % of the ligand is bound to some haem at a haem/ligand concentration ratio of 1:4.



Graph 5: Percentage of bound ligand **52** depending on the concentration of haem, the concentration of ligand is constant at 1mM.

The experiment was then repeated with ligand containing different azole rings such as the 1,2,4-triazole derivative **53**, the 1,3,4-triazole derivative **53'** and the tetrazole **54**, however no shifts or broadening of their peaks were observed. So the binding of these ligands with the haem iron observed in the gas phase in the mass

spectrometry studies (Graph 2, 3 and 4) could not be confirmed in solution with ^1H NMR spectrometry.

Changes in the ^1H NMR **52** spectra upon the addition of a haem solution undoubtedly confirmed the binding of ligand **52** to the haem iron as well as the 1:2 stoichiometry for the complex. However, the large number of aromatic peaks in the ligand did not allow us to assign all the peaks and consequently to use the Solomon-Bloembergen equation (Figure 4.10) to measure the distance between the different ligand protons and the haem iron. Another technique should therefore be used in order to calculate the ligand binding constant.

5) UV/VIS ANALYSIS AND DETERMINATION OF THE BINDING CONSTANT

5.1) UV/VIS analysis

Another useful technique to determine the binding constant of ligands with haem is to measure the changes in the UV/VIS spectra of the haem upon the addition of ligand¹⁹². Addition of ligand to a solution of haem should lead to the formation of new bands characteristic of the haem-ligand complex which can then be used to determine the binding constant. The UV/VIS experiments present major advantages compared to ¹H NMR. The measurement of a UV/VIS spectrum is very fast and allowed us to perform a large number of experiments in a relatively short time. The use of very dilute solutions (about 1000 fold more diluted than ¹H NMR solution) was also an advantage as experiments only consumed a very small amount of compounds.

The UV/VIS spectrum of the haem molecule is characteristic. It shows a very strong absorption band in the high energy region (390-450 nm) of the spectrum called the Soret band or B-band and a range of smaller bands in the visible region (450-700 nm) called the visible bands or Q-bands. These bands are susceptible to changes with the oxidation state and/or ligation of the haem iron atom.

Studies by Egan *et al.*²⁰⁹ on the effect of solvent on the interaction of quinoline antimalarials with hemin showed that a 40 % aqueous DMSO media is an excellent model of pure aqueous media. This solvent system also has the advantage of maintaining hemin in a monomeric state instead of the μ -oxo dimer observed in pure aqueous media²¹⁰. In this medium, DMSO (rather than H₂O) will be coordinated

²⁰⁹ Egan T.J. and Ncokazi K.K.; Effects of solvent composition and ionic strength on the interaction of quinoline antimalarials with ferritoporphyrin IX. *J. Inorg. Biochem.*, 2004, 98, 144-152.

²¹⁰ Collier G.S., Pratt J.M., De Wet C.R. and Tshabalala C.F.; Studies on haemin in dimethyl sulphoxide/water mixtures. *Biochem. J.*, 1979, 179, 281-289.

to the haem as an axial ligand. The use of DMSO will also allow us to dissolve both ligand and hemin.

The changes in the hemin absorption spectra were measured on a JASCO V570 spectrometer by titration of a 100 μM solution of hemin with a 1 mM solution of imidazole ligand **52** both in 40 % aqueous DMSO. As both hemin and **52** are insoluble in 40 % aqueous DMSO, a 1 mM solution of hemin and a 10 mM solution of **52** in pure DMSO had to be prepared before being diluted with a 40 % DMSO/water solution. Because of their different intensity, the 300-500 nm region was measured in a 1 mm glass UV flask and the 450-700 nm region was measured in a 1 cm glass UV flask in order to use the same 100 μM hemin solution. Spectra were baseline corrected and displayed the extinction coefficient (from the Beer-Lambert law) instead of the absorbance (Figures 4.12 and 4.13).

Beer-Lambert law: $A = \epsilon \cdot c \cdot l$

ϵ : extinction coefficient

A: absorbance

c: concentration of absorbing species

l: path length of the cuvette

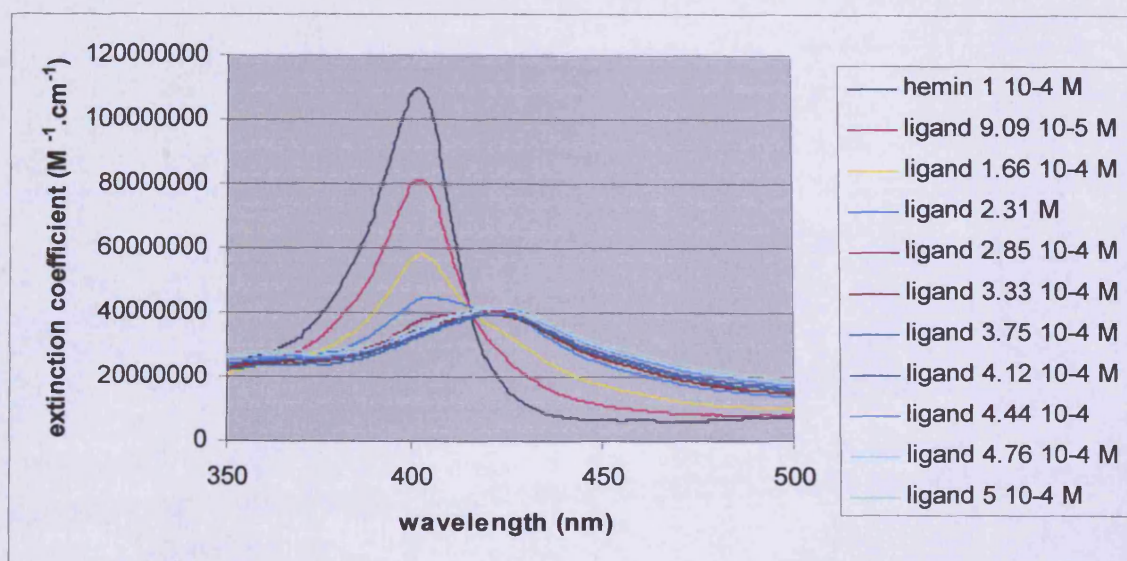


Figure 4.12: Changes in absorption of a 20 μM haem solution upon the addition of **52** in the 350-500 nm region with ligand concentrations as given in the legend.

The UV/VIS spectrum of hemin displays a Soret band at 400 nm and two visible bands at 502 nm and 626 nm. Ligand **52** displays an intense absorbance band at 292 nm but no absorption at higher wavelengths. Major changes in the hemin spectrum were observed when **52** was added to the solution and confirmed what was observed by ^1H NMR spectroscopy. A massive decrease in the intensity of the Soret band as well as the formation of a new band corresponding to the complex at 435 nm was observed. The most interesting information is the emergence of an isobestic point at 415 nm which suggest that the equilibrium involves only two different absorbing species present in significant concentrations throughout the titration (Figure 4.12).

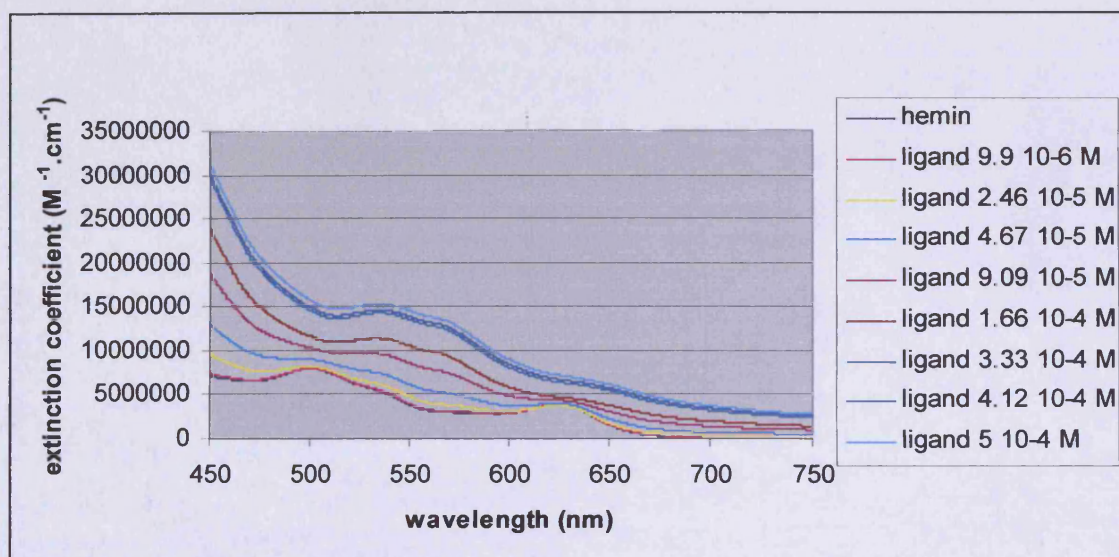


Figure 4.13: Changes in absorption of a 100 μM haem solution upon the addition of **52** in the 450-750 nm region with ligand concentrations as given in the legend.

A large increase in absorbance was also observed in the visible region with the appearance of two new bands at 534.5 nm and 561 nm (Figure 4.13). At a concentration of ligand of approximately 3.33×10^{-4} M, no further changes in the absorbance spectrum were observed across the whole hemin spectrum, indicating that all the haem present in solution is bound to **52**.

The experiment was also performed using TPP instead of hemin as a haem system. Only changes in the visible part (450-750 nm) of the spectrum were investigated (Figure 4.14). Though the same method and concentration of haem and ligand were used in this experiment, the 40 % aqueous DMSO media was replaced by pure dichloromethane for solubility reasons. The UV/VIS spectrum of TPP is different from that of hemin. It displays, in the visible region, one large band at 508 nm and three small bands at 578 nm, 652 nm and 692 nm.

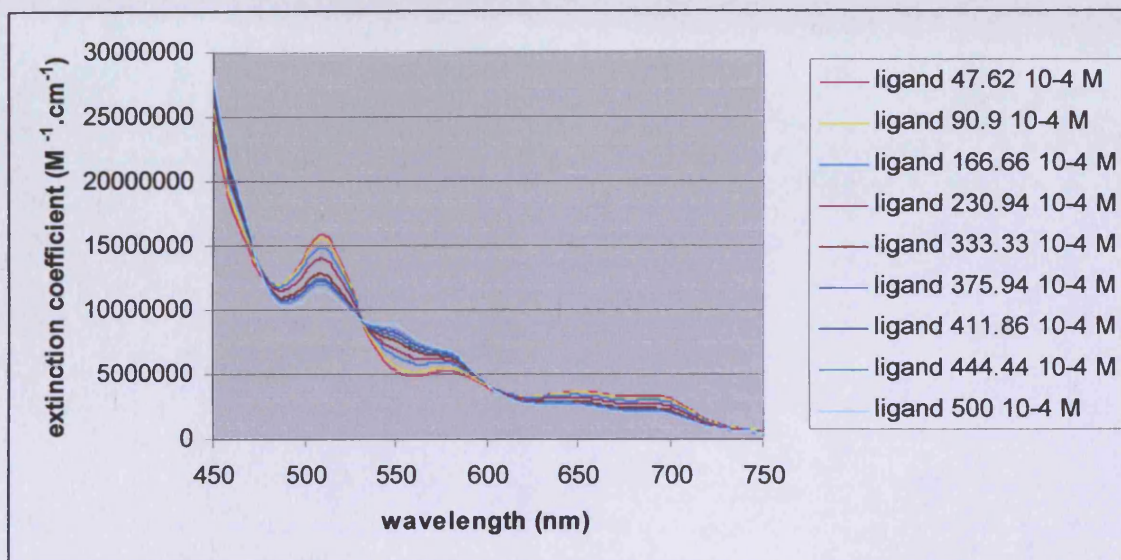


Figure 4.14: Changes in absorption of a 100 μM TPP solution upon the addition of **52** in the 450-750 nm region with ligand concentrations as given in the legend.

The addition of **52** to the solution led to dramatic changes in the TPP absorption spectrum (Figure 4.14). A decrease of the bands at 508, 652 and 692 nm was observed as well as an increase in intensity from 531 nm to 602 nm and formation of two new bands at 551 nm and 578 nm. The spectra also displayed three isobestic points at 477 nm, 530 nm and 603 nm instead of only one for the hemin spectra which also suggest that only two different absorbing species are present in solution throughout the titration. These changes in the TPP absorption spectrum are

also very similar to those observed with the imidazole titration which displayed isobestic points at 533 nm and 480 nm^{211, 212}.

The experiment was then repeated with different ligands. The titration of haem with ligands containing differentazole rings, such as 1,2,4-triazole (**53**), 1,3,4-triazole (**53'**) and tetrazole (**54**) did not display any changes in the haem absorption spectrum (hemin and TPP), there is thus no evidence of binding of these ligands with the haem in solution which confirmed what has been observed using ¹H NMR spectroscopy. On the other hand, all the other imidazole ligands such as the methyl derivative **59** and the methyl ester derivative **45** displayed very similar results to those observed for **52**, suggesting that para-substitution on the phenyl does not affect the binding properties of the ligand and that the difference observed in their activity is only due to their interactions (e.g. hydrogen bonding, hydrophobic interactions) with the protein residues.

UV/VIS spectroscopy is thus the technique of choice for the determination of binding constants for these systems. The major changes in absorbance observed both in the spectrum of hemin and TPP upon the addition of **52** will allow us to measure the concentration of complex formed at different concentrations of haem and ligand and as a result to determine the binding constant of the ligand. The presence of isobestic points also suggests an equilibrium involving only two species; only one complex is formed during the reaction.

5.2) Binding constant determination

The binding constant expresses the equilibrium between binding and dissociation process in a reaction and could be used to quantify the affinity of binding of a ligand to a metal in solution (Figure 4.2). The modification in the hemin and the TPP absorption spectrum upon the addition of ligand **52** should allow us to determine the binding constants of this ligand using the changes observed in the haem absorbance at different concentrations of ligand.

²¹¹ Duclos J.M.; Ligand binding to metalloporphyrin. 1. Thermodynamics constants for the association of imidazole with tetraphenylporphyrin iron (III) chloride in acetone. *Bioinorg. Chem.*, **1973**, *2*, 263-274.

²¹² Coyle C.L., Rafson P.A. and Abbott E.H.; Equilibria of imidazole with iron(III) tetraphenylporphine. *Inorg. Chem.*, **1973**, *12*, 2007-2010.

5.2.1) Stoichiometry of the reaction

Prior to determining the binding constant, the determination of the stoichiometry of the reaction is essential. Does binding involve one or two ligands? Does the reaction involve a simple equilibrium between two species or equilibrium between three or more species?

The mass spectrometry studies suggest a mixture of the mono-substituted, the di-substituted complex and free haem (Graph 1); however the presence of isobestic points in the UV/VIS spectra (Figure 4.12) clearly proves that only two absorbing species are present in detectable concentrations in solution. Literature precedent^{211, 213} for the binding of imidazole compounds to different haem systems also showed that two imidazole compounds are bound to the haem iron atom and that there is no evidence for the formation of the mono-substituted complex. This was confirmed by elemental analysis performed on our hemin-52 complex in solid form and by the two crystal structures of hemin-methylimidazole¹⁹³ and imidazole-TPP¹⁹⁹. It also suggests that our mass spectra results showed the mono-substituted complex HL as a result of a decomposition of the di-substituted complex HL₂. The equilibrium can consequently be described by Equation 4.1:



The stoichiometry of the reaction can be explained by the fact that the mono-substituted compound is high spin ($S = 5/2$) while the di-substituted is low spin ($S = 1/2$). The low spin Fe(III) has been shown to be smaller than the high spin Fe(III)²¹⁴, therefore it may drop into the porphyrin plane instead of being 0.5 Å out of plane for the high spin Fe(III)²¹⁵ and binds the ligands more tightly. The low spin ions should also bind ligands better because they have fewer e_g electrons which are antibonding²¹⁰. The five electrons in the iron 3d orbitals are accommodated in the nonbonding t_{2g} orbitals and the antibonding e_g orbitals. The low spin complex has a

²¹³ Cowgill R.W. and Clark W.M.; Metalloporphyrins. VII. Coordination of imidazoles with ferrimesoporphyrin. *J. Biol. Chem.*, **1952**, *198*, 33-61.

²¹⁴ Hu C., Noll B.C., Schulz C.E. and Scheidt W.R.; Proton-mediated electron configuration change in high-spin iron(II) porphyrinates. *J. Am. Chem. Soc.*, **2005**, *127*, 15018-15019.

²¹⁵ Nasri H., Ellison M.K., Shaevitz B., Gupta G.P. and Scheidt W.R.; Electronic, magnetic, and structural characterization of the five-coordinate, high-spin iron (II) nitrate complex [Fe(TpivPP)(NO₃)]. *Inorg. Chem.*, **2006**, *45*, 5284-5290.

$(t_{2g})^5(e_g)^0$ configuration while the high spin complex has a $(t_{2g})^3(e_g)^2$ configuration²¹⁶ (Figure 4.15). This suggests that the haem and the ligand system exhibit cooperative binding i.e. the binding of one ligand at one site increases the affinity of the ligand for the other site²¹⁷. The di-substituted complex haem(52)₂ will thus be far more stable.

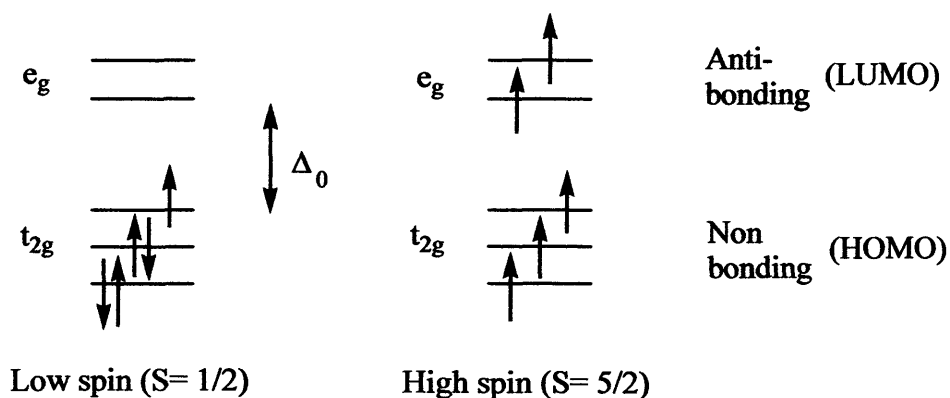


Figure 4.15: Electronic differences between the high spin ($S= 5/2$) and the low spin ($S= 1/2$) iron complexes.

5.2.2) Equations used

Two different equations (Equations 4.2 and 4.7), representing different types of binding, were used as global fitting models for the UV/VIS binding data. Equation 4.1 is based on the mass balance equation for an equilibrium involving consecutive independent binding events.



The mass balance equation describing such equilibrium results in a quadratic equation, which can be solved analytically²¹⁸ resulting in Equation 4.2.

(Equation 4.2):

$$signal_{obs} = background + signal_{free}[H]_t + \Delta_{binding} signal \frac{\left\{ 1 + K \frac{[L]_t}{N} + K[H]_t - \sqrt{\left(1 + K \frac{[L]_t}{N} + K[H]_t \right)^2 - 4K^2 \frac{[L]_t}{N} [H]_t} \right\}}{2K}$$

²¹⁶ Decker A. and Solomon E.; Dioxygen activation by copper, heme and non-heme iron enzymes: comparison of electronic structures and reactivities. *Curr. Opin. Chem. Biol.*, **2005**, *9*, 152-163.

²¹⁷ Cameron M.D., Wen B., Allen K.E., Roberts A.G., Schuman J.T., Campbell A.T., Kunze K.L. and Nelson S.D.; Cooperative binding of midazolam with testosterone and α -naphthoflavone within the CYP3A4 active site: a NMR T_1 paramagnetic relaxation study. *Biochem.*, **2005**, *44*, 14143-14151.

²¹⁸ <http://mathworld.wolfram.com/QuadraticFormula.html>.

Here, $signal_{obs}$ is the observed signal (here: absorbance), $signal_{free}$ is the molar free haem signal, $\Delta_{binding}signal$ is the change in the signal upon binding, $[H]_t$ is the total haem concentration, $[L]_t$ is the total ligand concentration, K is the binding constant which is assumed to be the same for the two consecutive binding processes and N is the binding stoichiometry so that concentration of binding sites added = $[L]_t/N$.

The mass balance equations for the cooperative binding of 2 ligands to 1 host molecule: $H+2L \rightleftharpoons HL_2$ result in a cubic equation (Equation 4.3).

$$(Equation 4.3): \quad [L]_f^3 + (2 \cdot [H]_t - [L]_t) \cdot [L]_f^2 + \frac{1}{K} \cdot [L]_f + \frac{-1 \cdot [L]_t}{K} = 0$$

This cubic equation can be solved to give the only real root (Equation 4.4)²¹⁹.

$$(Equation 4.4): \quad [L]_f = \left\{ \left[\left(\sqrt{(R^2 - Q^3)} + |R| \right)^{\frac{1}{3}} + \frac{Q}{\left[\left(\sqrt{(R^2 - Q^3)} + |R| \right)^{\frac{1}{3}} \right]} \right] - \frac{(2 \cdot [H]_t - [L]_t)}{3} \right\}$$

Here, Q and R are given by Equations 4.5 and 4.6, respectively:

$$(Equation 4.5): \quad R = \frac{\left(2 \cdot (2 \cdot [H]_t - [L]_t)^3 - 9 \cdot (2 \cdot [H]_t - [L]_t) \cdot \frac{1}{K} + 27 \cdot \frac{-1 \cdot [L]_t}{K} \right)}{54}$$

$$(Equation 4.6): \quad Q = \frac{\left[(2 \cdot [H]_t - [L]_t)^2 - 3 \cdot \frac{1}{K} \right]}{9}$$

This results in Equation 4.7 describing the change in an observed signal for titrations involving equilibrium $H+2L \rightleftharpoons HL_2$ which can then be used to fit our UV/VIS data.

$$(Equation 4.7): \quad signal_{obs} = background + signal_{free,m} [H]_t + \Delta_{binding} signal \cdot \left(\frac{[L]_t - [L]_f}{2} \right)$$

²¹⁹ Press W.H., Flannery B.P., Teukolsky S.A. and Vetterling W.T.; Numerical recipes in Pascal, the art of scientific computing. Cambridge University Press, 1989.

Here, $signal_{obs}$ is the observed signal (absorbance), $signal_{free,m}$ is the molar free haem signal, $\Delta_{binding}signal$ is the change in the signal upon binding, $[H]_t$ is the total haem concentration, $[L]_t$ is the total ligand concentration, K is the binding constant and $[L]_f$ is the free ligand concentration as calculated using Equation 4.3.

Both equations (4.2 and 4.7) were used to fit the data of the binding for our ligands to haem. Equation 4.7 is specific for cooperative binding of two ligands to one haem whereas Equation 4.2 can be used for equilibria involving an unknown number of independent binding sites as the stoichiometry of the reaction is one of the variables; however, we have here restricted N to a value of 2. Equation 4.2 assumes that the monosubstituted complex HL is formed in small quantity during the reaction before being transformed into the di-substituted complex HL_2 .

5.2.3) Fit of the data and binding constant determination

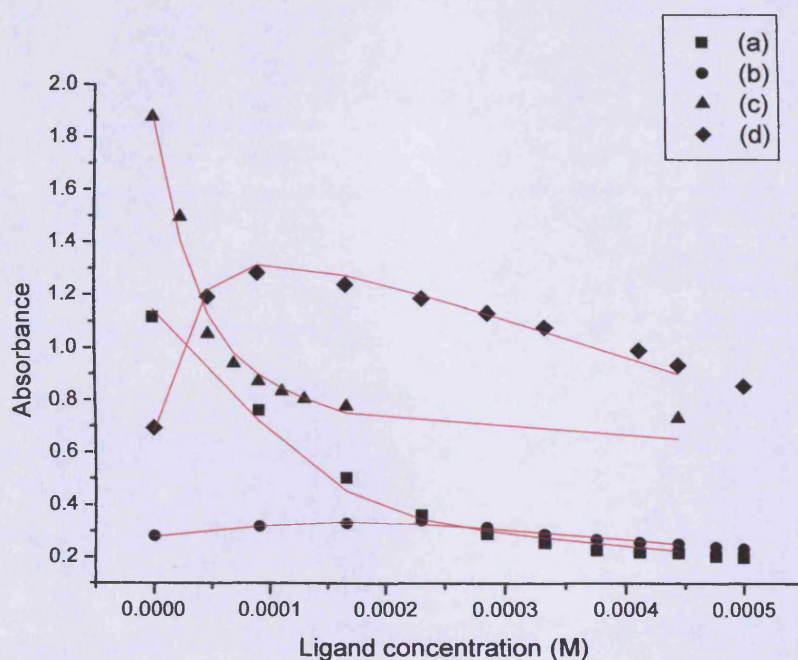


Figure 4.16: Absorbance for the hemin-52 complex at different concentrations of hemin and ligand. Lines are fitted curves using Equation 4.2. (a): [hemin]= 100 μ M at 402 nm; (b): [hemin]= 100 μ M at 420 nm; (c): [hemin]= 20 μ M

at 402 nm; (d): [hemin]= 20 μM at 420 nm. Optimised binding parameters are reported in Table 4.1.

Table 4.1: Optimised binding parameters (Equation 4.2) for the hemin-52 complex:

Variables	(a) [hemin]= 100 μM 402 nm	(b) [hemin]= 100 μM 420 nm	(c) [hemin]= 20 μM 402 nm	(d) [hemin]= 20 μM 420 nm
Binding constant K_{HI} (M^{-1})	$(1.69 \pm 0.31) \cdot 10^5$			
Stoichiometry	2			
$\Delta_{\text{binding}} \text{signal}$ ($\text{M}^{-1} \text{cm}^{-1}$)	-7933 ± 412.2	1565 ± 405.7	$(-5.40 \pm 0.22) \cdot 10^4$	$(4.54 \pm 0.21) \cdot 10^4$
$\text{Signal}_{\text{free}}$ ($\text{M}^{-1} \text{cm}^{-1}$)	$(1.11 \pm 0.03) \cdot 10^4$	2572 ± 312.0	$(9.35 \pm 0.16) \cdot 10^4$	$(3.05 \pm 0.17) \cdot 10^4$
Background	0.03	0.02	0.02	0.07
Chi^2/DoF	0.0012			
R^2	0.99498			

The two equations 4.2 and 4.7 were used to determine the binding constants of 52 with both hemin and TPP. For each combination of haem and ligand, the binding constant was determined from global non-linear least squares fitting of four different sets of data at different wavelengths and concentrations using the software Origin²²⁰. The results obtained with the two different equations were then compared and some conclusions were drawn about the best model and consequently about the type of binding.

For hemin, the decrease in absorption of the haem band at 402 nm and the increase in absorption of the complex at 420 nm were investigated. Two different concentrations of hemin were used: 100 μM and 20 μM while the ligand concentration was varied between 0 and 500 μM . The path length of the cuvette had

²²⁰ Origin v 7.0300 (B300), OriginLab Corporation, <http://www.OriginLab.com>

to be changed from 1 mm for the measurement of the 100 μM solution to 1 cm for the measurement of the 20 μM solution. With Equation 4.2, five variables had to be determined: the binding constant K_{H1} , the stoichiometry, the change in signal, the haem free signal and the background. The binding constant K_{H1} and the stoichiometry were shared between the four sets of data. As we previously demonstrated that there are two ligands binding to one haem, the stoichiometry was thus fixed as 2. The background was fixed to its measured value in each case. The binding constant K_{H1} and the variations in the $\Delta_{\text{binding}}\text{signal}$ and the $\text{signal}_{\text{free}}$ were optimised to their best fit values.

In the case of Equation 4.7, the stoichiometry is already fixed in the equation as 2. There are consequently only four variables: the binding constant K_{H2} , the change in signal, the haem free signal and the background. As for the Equation 4.2, the binding constant K_{H2} is shared between the four sets of data, the background is set to its measured value and the delta signal and the haem free signal are set as variables.

The goodness of fit is expressed for both equations by chi^2/DoF and R^2 . Chi^2/DoF compares the calculated values with the experimental values (Equation 4.8). A low value for this parameter suggests a good model.

$$\text{(Equation 4.8): } \text{chi}^2/\text{DoF} = \frac{\sum_n \left(\frac{(\text{calc.value} - \text{exp.value})}{\text{errormargin}} \right)^2}{\text{DoF}}$$

Here, n is the number of datapoints and DoF is the number of degrees of freedom which is expressed in Equation 4.9.

$$\text{(Equation 4.9): } \text{DoF} = n_{\text{datapoints}} - n_{\text{variables}}$$

The regression coefficient R^2 (Equation 4.10) corresponds to the slope of the straight line that most closely relates two correlated variables. It is a number between 0 and 1 and a value close to 1 suggests a good model.

(Equation 4.10):
$$R^2 = \frac{\left(\sum_{i=1}^n (x_i - \bar{x})(y_i - \bar{y}) \right)^2}{\left(\sum_{i=1}^n (x_i - \bar{x})^2 \right) \left(\sum_{i=1}^n (y_i - \bar{y})^2 \right)}$$

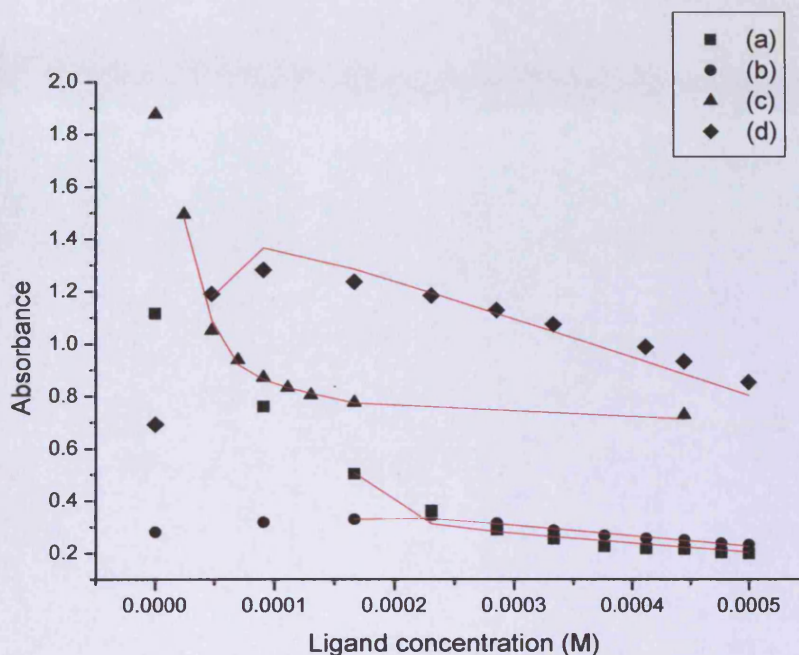


Figure 4.18: Absorbance for the hemin-52 complex at different concentrations of hemin and ligand. Lines are fitted curves using Equation 4.7. (a): [hemin]= 100 μ M at 402 nm; (b): [hemin]= 100 μ M at 420 nm; (c): [hemin]= 20 μ M at 402 nm; (d): [hemin]= 20 μ M at 420 nm. Optimised binding parameters are reported in Table 4.2.

Table 4.2: Optimised binding parameters (Equation 4.7) for the hemin-52 complex:

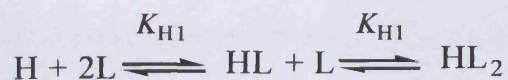
Variables	(a) [hemin]= 100 μ M 402 nm	(b) [hemin]= 100 μ M 420 nm	(c) [hemin]= 20 μ M 402 nm	(d) [hemin]= 20 μ M 420 nm
Binding constant K_{H2} (M^{-2})	$(1.34 \pm 0.004) \cdot 10^9$			

$\Delta_{\text{binding}}\text{signal}$ ($\text{M}^{-1}\text{cm}^{-1}$)	$(-0.91 \pm 1.04) \cdot 10^4$	884.1 ± 5769	$(-4.79 \pm 1.12) \cdot 10^4$	$(4.26 \pm 1.18) \cdot 10^4$
$\text{Signal}_{\text{free}}$ ($\text{M}^{-1}\text{cm}^{-1}$)	$(1.22 \pm 0.97) \cdot 10^4$	3113 ± 5190	$(8.77 \pm 0.81) \cdot 10^4$	$(3.28 \pm 0.96) \cdot 10^4$
Background	0.03	0.02	0.02	0.07
Chi ² /DoF	0.04402			
R ²	0.81543			

Although the error on the binding constant K_{H2} ($K_{\text{H2}} = (1.34 \pm 0.004) \cdot 10^9 \text{ M}^{-2}$) with Equation 4.7 is quite small, the equation could not fit all the data points properly (Figure 4.17). Errors on $\text{signal}_{\text{free}}$ and $\Delta_{\text{binding}}\text{signal}$ for all the graphs are also quite large, sometimes even bigger than the actual value. On the other hand, the fit with Equation 4.2 (Figure 4.16) gave better results. It displayed a binding constant $K_{\text{H1}} = (1.69 \pm 0.31) \cdot 10^5 \text{ M}^{-1}$ and an acceptable value for all the errors on the $\text{signal}_{\text{free}}$ and the $\Delta_{\text{binding}}\text{signal}$. Comparison of the values of both binding constants K_{H1} and K_{H2} showed that $K_{\text{H2}} \approx K_{\text{H1}}^2$. The difference between the values of K_{H1} and K_{H2} could be explained by the fact that Equation 4.2 considers the concentration of ligand and the concentration of binding sites ($[\text{ligand}] + [\text{binding sites}] \rightarrow [\text{ligand-binding sites}]$) while Equation 4.7 considers the binding of two ligand to one haem ($[\text{haem}] + 2[\text{ligand}] \rightarrow [\text{haem-ligand}_2]$). Consequently the units of the binding constant unit are different for the two equations: M^{-1} for K_{H1} and M^{-2} for K_{H2} . As a result of the difference in the length of the cuvette between experiments (a) and (b) (1 mm) and experiments (c) and (d) (1 cm) the values of the $\text{signal}_{\text{free}}$ and the $\Delta_{\text{binding}}\text{signal}$ vary. For (a) and (c), which measures the changes in absorption at 402 nm, the values of the $\text{signal}_{\text{free}}$ and the $\Delta_{\text{binding}}\text{signal}$ for (c) are about 10 fold those for (a). This is also observed with (b) and (d), which measures the changes in absorption at 420 nm, $\text{signal}_{\text{free}}$ and $\Delta_{\text{binding}}\text{signal}$ for (d) are about 10 fold those for (b).

The comparison of both goodness of fit variables chi^2/DoF and R^2 (Equation 4.2: $\text{chi}^2/\text{DoF} = 0.0012$ and $R^2 = 0.99498$; Equation 4.7: $\text{chi}^2/\text{DoF} = 0.04402$ and $R^2 = 0.81543$) shows that Equation 4.2 is a better model for the binding of ligand 52 to hemin. It suggests that, though never observed, the monosubstituted complex HL is

formed in minor quantities during the reaction prior to the formation of the disubstituted complex HL_2 and binding of 52 to hemin follows the following equilibrium:



Where H= hemin and L= 52

The determination of the binding constant K_T with TPP followed a similar method as that used for hemin and both equations 4.2 and 4.7 were used for data analysis. The decrease in the absorbance of the TPP band at 508 nm and the increase of the TPP-ligand complex at 548 nm were investigated, first with a 100 μ M solution of TPP and a ligand solution, which concentration was varied between 0 and 500 μ M, in a 1 cm cuvette and then with a 200 μ M solution of TPP and a ligand solution, which concentration was varied between 0 and 1 mM in a 0.5 cm cuvette. The fits of the data with both equations are shown in Figure 4.18 (Equation 4.2) and Figure 4.19 (Equation 4.7).

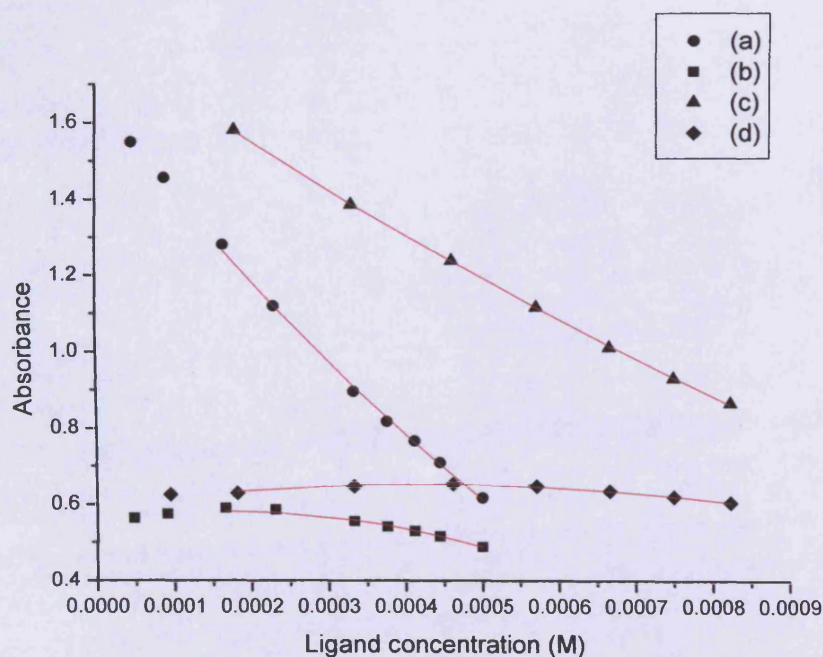


Figure 4.19: Absorbance for the TPP-52 complex at different concentrations of TPP and ligand. Lines are fitted curves using Equation 4.2. (a): [TPP]= 100 μM at 508 nm; (b): [TPP]= 100 μM at 548 nm; (c): [TPP]= 200 μM at 508 nm; (d): [TPP]= 200 μM at 548 nm. Optimised binding parameters are reported in Table 4.3.

Table 4.3: Optimised binding parameters (Equation 4.2) for the TPP-52 complex:

Variables	(a) [hemin]= 100 μM 402 nm	(b) [hemin]= 100 μM 420 nm	(c) [hemin]= 20 μM 402 nm	(d) [hemin]= 20 μM 420 nm
Binding constant K_{T1} (M^{-1})	557.3 \pm 304.6			
Stoichiometry	2			
$\Delta_{\text{binding}}\text{signal}$ ($\text{M}^{-1}\text{cm}^{-1}$)	(-4.23 \pm 1.99). 10^4	(3.18 \pm 1.50). 10^4	(-1.11 \pm 0.47). 10^4	(1.13 \pm 0.48). 10^4
$\text{Signal}_{\text{free}}$ ($\text{M}^{-1}\text{cm}^{-1}$)	(1.65 \pm 0.007). 10^4	5154 \pm 65.59	8958 \pm 59.23	2729 \pm 40.77
Background	0.04	0.04	0.04	0.04
Chi ² /DoF	0.00005			
R ²	0.99968			

Both equations (4.2 and 4.7) are able to reproduce the absorbance data for the formation of the TPP-52 complex. The values obtained for χ^2/DoF and R^2 with both equations (Equation 4.2: χ^2/DoF = 0.00005 and R^2 = 0.99968; Equation 4.7: χ^2/DoF = 0.00006 and R^2 = 0.99955) indicate that both binding models are suitable. Both binding models also displayed reasonable values for the errors of the binding constant K_T , the $\Delta_{\text{binding}}\text{signal}$ and the $\text{signal}_{\text{free}}$. Equation 4.2 (Figure 4.18) gave a binding constant K_{T1} = 557.3 \pm 304.6 M^{-1} and Equation 4.7 (Figure 4.19) gave a binding constant K_{T2} = (1.08 \pm 0.18). 10^7 M^{-2} . However, the errors with Equation 4.7 are much lower especially on the $\Delta_{\text{binding}}\text{signal}$ values. The difference in the path length of the cuvette (1 cm for (a) and (b) and 0.5 cm for (c) and (d)) acts on the

value of $signal_{free}$ and $\Delta_{binding}signal$. The value of $signal_{free}$ and $\Delta_{binding}signal$ for (a) is 2 fold that of (c) and the value of $signal_{free}$ and $\Delta_{binding}signal$ for (b) is 2 fold that of (d).

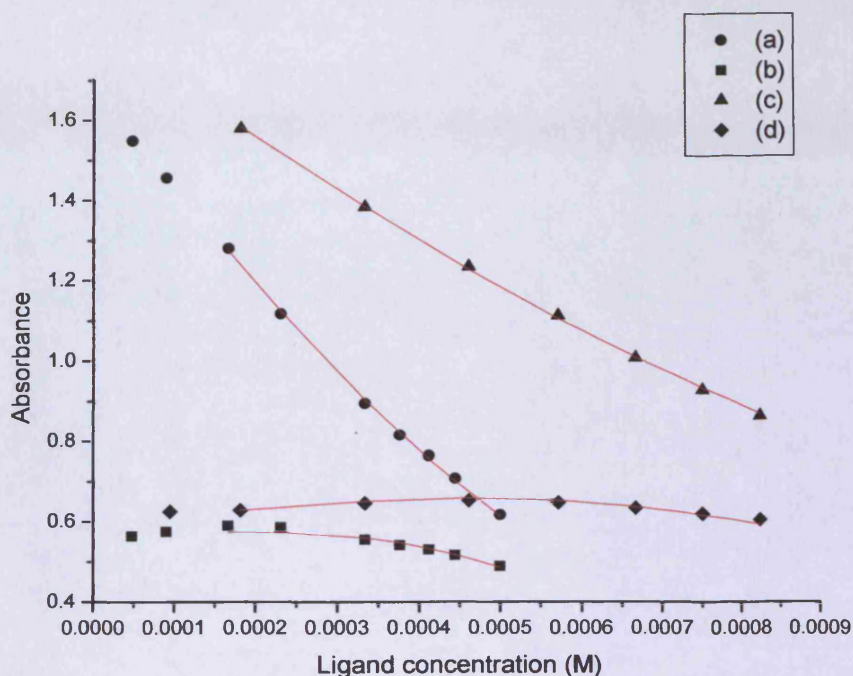


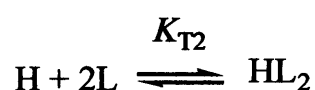
Figure 4.19: Fit of the absorbance for the TPP-52 complex at different concentration of TPP and ligand using Equation 4.7. (a): [TPP]= 100 μ M at 508 nm; (b): [TPP]= 100 μ M at 548 nm; (c): [TPP]= 200 μ M at 508 nm; (d): [TPP]= 200 μ M at 548 nm. Optimised binding parameters are reported in Table 4.4.

Table 4.4: Optimised binding parameters for Equation 4.7 in the fit of the TPP-52 complex:

Variables	(a)	(b)	(c)	(d)
Binding constant K_{T2} (M^{-2})	$(1.08 \pm 0.18) \cdot 10^7$			
$\Delta_{binding}signal$ ($M^{-1}cm^{-1}$)	-6729 ± 391.2	5024 ± 311.9	-2170 ± 98.10	2203 ± 90.87

<i>Signal</i> _{free} (M ⁻¹ cm ⁻¹)	(1.60 ± 0.07).10 ⁴	5550 ± 63.69	8818 ± 55.20	2912 ± 37.75
Background	0.04	0.04	0.04	0.04
Chi ² /DoF	0.00006			
R ²	0.99955			

Therefore, Equation 4.7 is a better model for the formation of the TPP-52 complex. In conclusion, the binding mode of ligand 52 to TPP appears to differ from that of 52 with hemin and follows the equilibrium.



Where H= TPP and L= 52

In conclusion, determination of the binding constants of ligand 52 has been successfully achieved using UV/VIS data both for binding with hemin and TPP. Unfortunately, binding constant determinations could not be done with ligands 53, 53' and 54. There is no evidence for the formation of the hemin and TPP complexes with these ligands in UV/VIS spectra, in agreement with what has been observed in ¹H NMR spectrometry. Consequently, the formation of complexes with ligands 53, 53' and 54 and TPP as observed in mass spectrometry studies in the gas phase has not been confirmed in solution.

Ligand 52 also seems to have a stronger affinity for hemin than for TPP as $K_{H1} \approx 10K_{T1}$ and $K_{H2} \approx 100K_{T2}$. This might be due to steric limitations caused by the orientation of the phenyl rings in TPP (Figure 4.9). Furthermore, the binding constant of imidazole ligand 52 ((1.69 ± 0.31).10⁵ M⁻¹) is comparable with the literature binding constant obtained for imidazole ((6.3 ± 0.9).10⁴ M⁻¹)²²¹ suggesting that there is no influence of the rest of the ligand on its binding properties and that the difference in activity is only due to the ligand interactions with the protein residues

²²¹ Wang J.T., Yeh H.J.C. and Johnson D.F.; Proton nuclear magnetic resonance study of equilibria and paramagnetisms of ferriprotoporphyrin IX-ligand complexations. *J. Am. Chem. Soc.*, 1978, 100, 2400-2405.

of the active site. The binding constant K_{T2} of **44** with TPP is also much lower than that of literature for imidazole ($\approx 4.8 \cdot 10^5 \text{ M}^{-1}$)¹⁹⁰. Consequently, TPP which appeared to be a good model for hemin in the titration with imidazole¹⁹⁰, is not a very accurate model for hemin interacting with **52**.

Formation of complex with hemin and TPP also displayed different behaviours. With hemin, the mono-substituted complex HL is formed prior to the disubstituted complex HL₂ and thus Equation 4.2 was found more satisfactory. With TPP, formation of the monosubstituted complex was never observed, the equilibrium followed a cooperative binding and Equation 4.7 was more suitable.

CHAPTER 6

Conclusion

6) CONCLUSION

In order to study the binding interaction between the cytochrome P450 haem and some of our ligands (**52**, **53**, **53'** and **54**), different spectroscopic techniques were used (mass spectrometry, X-ray crystallography, ^1H NMR and UV/VIS), each providing us with different data on the nature of the binding (stoichiometry, species formed in solution, binding constant). Although mass spectrometry provided some useful data on the different species formed during the reaction (HL, HL₂ and haem + solvents complexes), it did not provide quantitative information on the haem-ligand interactions in solution. ^1H NMR allowed us to conclude that the formation of the complex occurred but, because of the large number of aromatic protons and the broadening of the peaks, it did not lead to any accurate quantitative data either and was difficult to interpret. Here, UV/VIS spectroscopy emerged as the most useful source of data and allowed us to determine the binding constant of the ligand **52**.

Two different equations were used to fit the data from the UV/VIS study (Equations 4.2 and 4.7). Equation 4.2 was found to be more appropriate for **52** binding to hemin displaying a binding constant of $K_{\text{HI}} = (1.69 \pm 0.31) \cdot 10^5 \text{ M}^{-1}$ similar to that of imidazole binding to hemin $((6.3 \pm 0.9) \cdot 10^4 \text{ M}^{-1})^{221}$. This suggests that the imidazole ring, which coordinates the haem iron atom, is the only part of the ligand influencing the binding properties and the difference in activity observed between the different imidazole ligands might only be due to their interactions with the enzyme protein residues e.g. hydrogen bonding and hydrophobic interactions. The better fit observed with Equation 4.2 proves that a small amount of the mono-substituted complex HL is formed during the reaction before being transformed into the di-substituted complex HL₂.

Equation 4.7 was found more suitable for TPP interaction with **52** which shows that there is cooperative binding; none of the monosubstituted HL complex is formed during the reaction. **52** displayed a binding constant $K_{\text{T2}} = (1.08 \pm 0.18) \cdot 10^7 \text{ M}^{-2}$ with TPP which is about 100 fold lower than that of **52** interaction with hemin and also lower than TPP titration with imidazole $(\approx 4.8 \cdot 10^5 \text{ M}^{-1})^{190}$. Steric

interactions between the phenyl ring of TPP and **52** might be the cause of the low value of K_{T2} .

Unfortunately, the binding constant could not be calculated for ligands **53**, **53'** and **54**. There is no evidence for the formation of the complex in solution with these ligands and hemin and TPP. Complexes were only observed with TPP in mass spectrometry studies in the gas phase. It was thus not possible to correlate the binding constant of the ligands to their activity. However, the fact that these ligands do not form a covalent bond with the haem iron could explain their poor activity (**53**: $IC_{50} = 18 \mu\text{M}$; **53'** and **54**: $IC_{50} \geq 20 \mu\text{M}$) against CYP26 enzymes compare to **52** ($IC_{50} = 0.9 \mu\text{M}$). An imidazole ring seems to be necessary in the design of future CYP26 inhibitors.

Two new series of compounds the 1-[benzofuran-2-yl-(4-alkyl/arylphenyl)methyl]triazoles and the benzoxazol-2-yl-[phenylimidazol-1-ylmethyl]phenyl]amine were successfully synthesised and biologically tested as CYP26 inhibitors in MCF-7 cells. The binding constant of inhibitor **52** (benzoxazol-2-yl-[4-imidazol-1-ylphenylmethyl]phenyl]amine) was also calculated both with hemin and TPP.

The 1-[benzofuran-2-yl-(4-alkyl/arylphenyl)methyl]triazoles series displayed a moderate activity for CYP26 inhibition. The two most active compounds, the 4-ethyl derivative **26**, (IC_{50} = 4.5 μ M) and the 4-phenyl derivative **27**, (IC_{50} = 7 μ M) displayed an activity comparable with the well-known CYP26 inhibitor liarozole (IC_{50} = 6 μ M). The 4-cyclohexyl derivative (**22**, IC_{50} = 5-15 μ M) and the 4-*t*-Bu derivative (**21**, IC_{50} = 10-25 μ M) also displayed moderate activity. All the other derivatives (4-Me, 4-*i*-Pr, 4-*n*-Pr and *p*-Cl-C₆H₅) were poor inhibitors of the CYP26 enzyme.

The benzoxazol-2-yl-[phenylimidazol-1-ylmethyl]phenyl]amine were designed using our homology model of the CYP26A1 active site. In docking studies, they interacted closely with the haem iron and displayed multiple hydrophobic interactions and hydrogen bonds with the protein residues. However, they appeared to be only moderate inhibitors of the CYP26 enzyme. The most potent compound of the series was the unsubstituted compound **52** (IC_{50} = 0.9 μ M). The methyl derivative (**59**, IC_{50} = 8 μ M) and the hydroxy derivative (**68**, IC_{50} = 12 μ M) showed activity comparable with that of liarozole and the 1-[benzofuran-2-yl-(4-alkyl/arylphenyl)methyl]triazoles series. Para-substitution of the phenyl ring by larger substituents (**45**, **47** and **67**) or on another position (**84**, **85** and **86**) led to poor inhibitors (IC_{50} > 20 μ M), probably because of steric constraint within the active site. The disappointing results observed in the activity do not confirm what was observed on the docking studies and show the limitations of our CYP26A1 model.

In order to study the binding interaction between the cytochrome P450 haem and some of our ligands (**52**, **53**, **53'** and **54**), different spectroscopic techniques were investigated (mass spectrometry, X-ray crystallography, ¹H NMR and UV/VIS). All the techniques gave useful information on the binding properties of our ligand to haem and TPP; however UV/VIS spectroscopy emerged in our case as the most

appropriate tool and allowed us to calculate the binding constant of ligand **52** both with hemin ($K_{H1} = (1.69 \pm 0.31) \cdot 10^5 \text{ M}^{-1}$) and TPP ($K_{T2} = (1.08 \pm 0.18) \cdot 10^7 \text{ M}^{-2}$). The binding constant could not be determined for the triazole ligands **53** and **53'** and the tetrazole ligand **54**, which suggests that an imidazole ring is needed in the design of future CYP inhibitors.

Our future work will involve the replacement of the phenyl ring of the benzoxazol-2-yl-[phenylimidazol-1-ylmethyl]phenyl]amine series of inhibitors into a more flexible alkyl chain to enhance the activity. The disappointing results observed with the benzoxazole series also confirm that some improvements are needed in our model of the CYP26A1 enzyme.

In the binding studies, our effort should focus on the formation of a crystal structure of the haem-**52** complex which will allow us to study in detail the Fe-N covalent bond. A new method should also be found to determine the binding constant of ligand **53**, **53'** and **54** and then correlate the haem-ligand interaction of these ligands to their activity.

APPENDIX



Synthesis and CYP26A1 inhibitory activity of 1-[benzofuran-2-yl-(4-alkyl/aryl-phenyl)-methyl]-1*H*-triazoles

Stephane Pautus,^a Sook Wah Yee,^a Martyn Jayne,^a Michael P. Coogan^b and Claire Simons^{a,*}

^aWelsh School of Pharmacy, Cardiff University, King Edward VII Avenue, Cardiff CF10 3XF, UK

^bSchool of Chemistry, Cardiff University, Cardiff CF10 3TB, UK

Received 29 November 2005; revised 9 January 2006; accepted 10 January 2006

Available online 3 February 2006

Abstract—Methodology previously described by our group was applied to the preparation of a series of 4-alkyl/aryl-substituted 1-[benzofuran-2-yl-phenylmethyl]-1*H*-triazoles. The [1,2,4]-triazole derivatives were prepared for a range of alkyl and aryl substituents, and for the 4-methyl, 4-ethyl, 4-*i*-propyl, 4-*t*-butyl, 4-phenyl and 4-chlorophenyl derivatives, the minor [1,3,4]-triazole isomer also isolated. All the triazole derivatives were evaluated for CYP26A1 inhibitory activity using a MCF-7 cell-based assay. The 4-ethyl and 4-phenyl-1,2,4-triazole derivatives displayed inhibitory activity (IC₅₀ 4.5 and 7 μM, respectively) comparable with that of the CYP26 inhibitor liarozole (IC₅₀ 7 μM). Using a CYP26A1 homology model (based on CYP3A4) template, docking experiments were performed with MOE with multiple hydrophobic interactions observed in addition to coordination between the triazole nitrogen and the haem transition metal.

© 2006 Elsevier Ltd. All rights reserved.

1. Introduction

In humans, CYP26A1 is expressed in the liver, heart, pituitary gland, adrenal gland, testis, brain and placenta,¹ and has been mapped to chromosome 10q23-q24.² It is thought that the principal role of CYP26A1 is homeostatic, that is, the regulation of intracellular ATRA steady-state levels via a negative feedback loop similar to that of CYP24 in the metabolism of cholecalciferol.³ The enzyme therefore may have a protective function, as an important regulator of differentiation and a possible modulator of disease states indirectly by controlling ATRA and other retinoid concentrations.⁴

Retinoic acid has been used in a number of clinical situations, especially oncology and dermatology. In oncology, ATRA has shown spectacular success in the treatment of acute promyelocytic leukaemia,^{5,6} although remission seen is followed by relapse within 4–6 months; this appears to be due to increased RA metabolism as a result of RA induction so leading to decreased clinical

efficacy. Although other CYPs are also induced by ATRA and catalyse its metabolism, it is thought that CYP26A1 is likely to be the most important enzyme involved in its degradation⁷ (Fig. 1).

ATRA may improve the efficacy of other treatments such as radiation, cisplatin and interferon therapies.^{8,9} Retinoids have been used for some time in the treatment of psoriasis, cystic acne, cutaneous malignancies due to hyperkeratinisation as well as in the treatment of photo-damaged skin.^{10,11} As CYP26A1 appears to be so important in the management of intracellular levels of ATRA and the development of resistance to its effects in cancer, it presents a useful target in combating the development of resistance. Inhibition of CYP26A1 would elevate normal tissue levels of ATRA or maintain high therapeutic levels of ATRA preventing the resistance that develops to treatment. This might provide a leap forward in the prevention and treatment of a number of diseases including hormone refractory prostate cancer and psoriasis.

A number of inhibitors of ATRA metabolism have been developed over the last fifteen years.^{12–15} The discovery of the imidazoles as inhibitors led to further study into this class of compounds, resulting in the synthesis of

Keywords: 1-[Benzofuran-2-yl-(4-alkyl/aryl-phenyl)-methyl]-1*H*-triazoles; CYP26A1; Enzyme inhibition; MCF-7; Molecular modelling.

*Corresponding author. Tel.: +44 02920 876307; fax: +44 02920 874149; e-mail: SimonsC@Cardiff.ac.uk

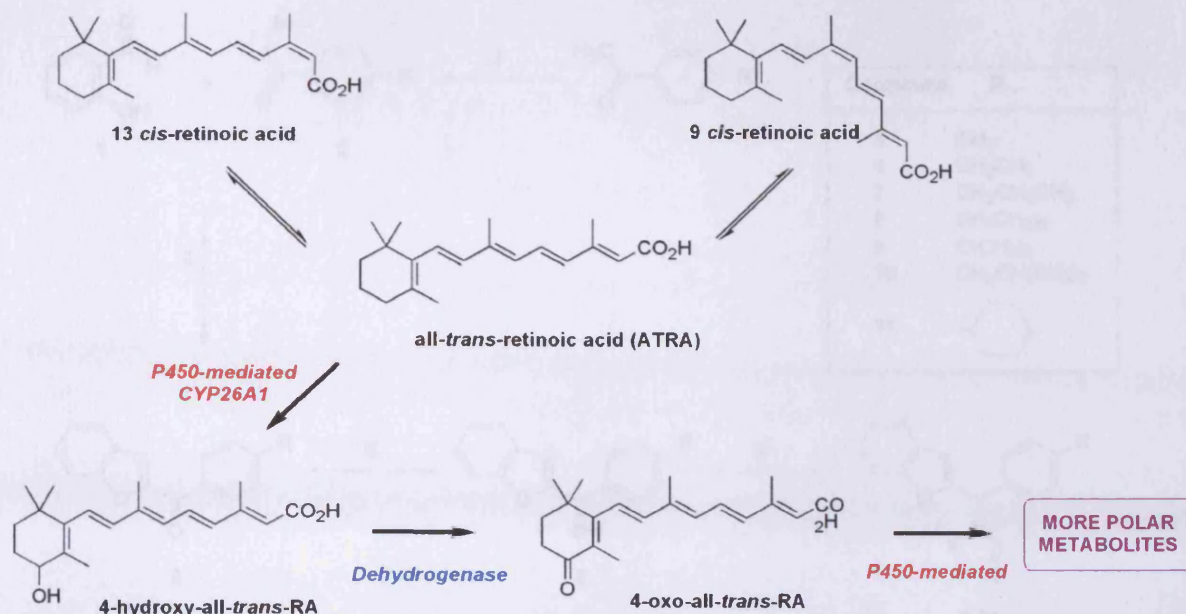


Figure 1. Metabolism of *all-trans* retinoic acid (RA = retinoic acid).

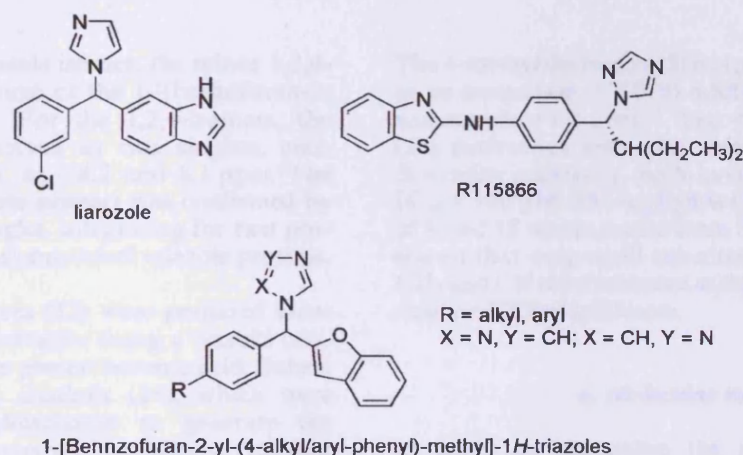


Figure 2. CYP26A1 metabolism inhibitors and target structures.

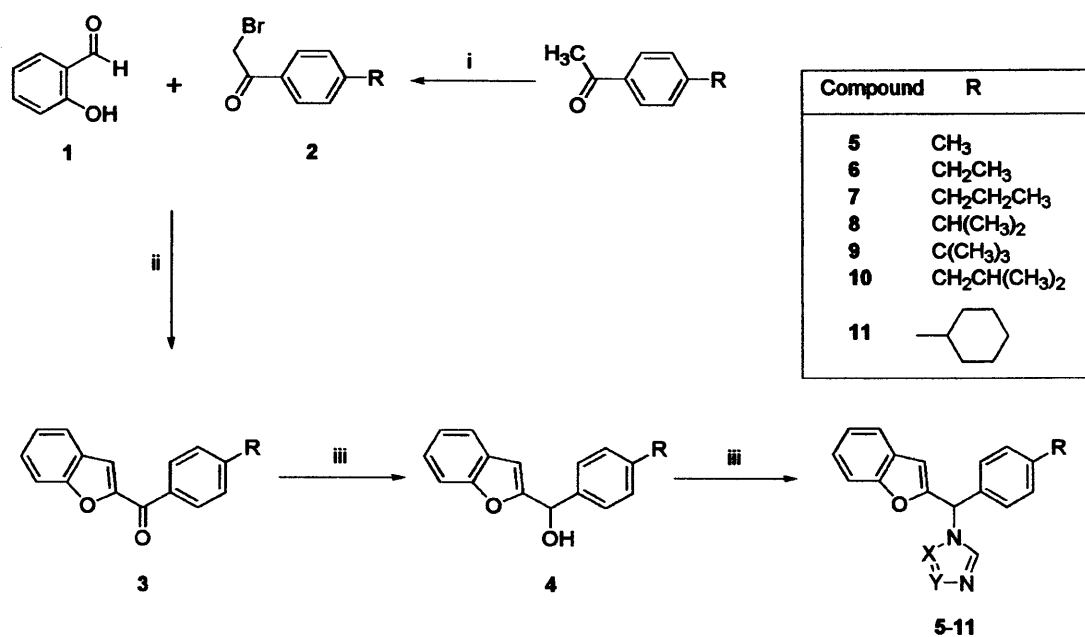
liarozole, which became the most studied inhibitor of ATRA metabolism.^{16–18} Though more specific and effective than the other imidazoles, liarozole is still a potent inhibitor of aromatase, preventing its use as an oral retinoic acid-mimetic for sex hormone-independent cancers, therefore clinical development of liarozole was discontinued.³ Further development has led to the discovery of the 1*H*-triazole derivative, R115866, a potent and selective inhibitor of ATRA metabolism (Fig. 2).¹⁹

As part of our ongoing research into the development of CYP26A1 inhibitors, we evaluated a number of compound classes for their inhibitory activity. The 4-alkyl-benzofuran derivatives were promising candidates owing to their structural similarity with liarozole as confirmed by molecular modelling. The synthesis, CYP26A1 inhibitory activity and bonding interactions at the CYP26A1 active site are described.

2. Chemistry

The required intermediates for the preparation of the 1-[(benzofuran-2-yl)phenylmethyl] triazoles were the corresponding ketones, benzo[*b*]furan-2-yl-phenylmethanones (**3**). The synthesis of the ketones was achieved by the Rap–Stoermer reaction,²⁰ and involved reaction of salicylaldehyde (**1**) with the α -bromoketones (**2**),²¹ generated by reaction of the appropriate acetophenone with bromine and aluminium trichloride according to literature methodology²² (Scheme 1).

The ketones were then reduced to the respective racemic carbinols (**4**) in quantitative yields by reaction with sodium borohydride. The target triazole derivatives (**5–11**) were then obtained by reaction with *N,N'*-thionyltriazole, which was prepared by the reaction of 1,2,4-1*H*-triazole with thionyl chloride at 10 °C for 1 h, for 4 days.



Scheme 1. Reagents and conditions: (i) Br₂, AlCl₃, Et₂O, 1 h; (ii) NaH, DMF, 80 °C, 2 h then NaOMe, 80 °C, 1 h; (iii) NaBH₄, dioxane, 2 h; (iv) *N,N'*-thionyliditriazole, K₂CO₃, CH₃CN, 4 days.

In addition to the 1,2,4-triazole isomer, the minor 1,3,4-isomer was obtained for some of the 1-[(benzofuran-2-yl)phenylmethyl] triazoles. For the 1,2,4-isomers, the triazole protons were observed as two singlets, each integrating for one proton, at ~8.2 and 8.1 ppm. The structure of the 1,3,4-triazole isomers was confirmed by ¹H NMR, which gave a singlet, integrating for two protons, at ~8.30 ppm for the symmetrical triazole protons.

The 4-aryl ketone derivatives (**13**) were prepared from the 4-bromoketone (**12**) derivative using a Suzuki coupling²³ with the appropriate phenyl boronic acid. Subsequent reduction gave the alcohols (**14**), which were reacted with *N,N'*-thionyliditriazole to generate the 1,2,4- and 1,3,4-triazole isomers of the phenyl (**15**) and 4-chlorophenyl (**16**) benzofurans (Scheme 2).

3. CYP26A1 inhibitory activity

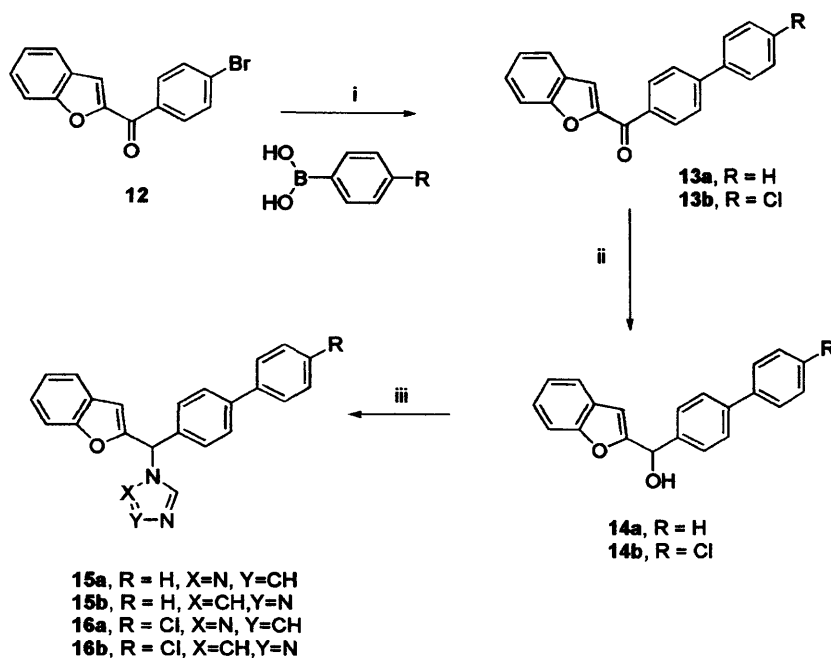
The 1-[(benzofuran-2-yl)-(4-alkyl/aryl-phenyl)-methyl]-1*H*-triazoles (**5–11**, **15** and **16**) were evaluated for their retinoic acid metabolism inhibitory activity using a MCF-7 cell assay,¹³ using radiolabelled [11,12-³H] all-*trans* retinoic acid as the substrate and liarozole and R115866 as standards for comparison. The 4-ethyl (**6a**, IC₅₀ = 4.5 μM; **6b**, IC₅₀ = 7 μM) and 4-phenyl (**15a**, IC₅₀ = 7 μM; **15b**, IC₅₀ = 9 μM) derivatives displayed inhibitory activity of CYP26A1 comparable with that of liarozole (IC₅₀ = 7 μM), and the cyclohexyl derivative (**11**, IC₅₀ = 5–15 μM) displayed moderate activity, the remaining alkyl/aryl derivatives all poor CYP26A1 inhibitors of retinoic acid metabolism (IC₅₀ > 20 μM) (Table 1). All the 1-[(benzofuran-2-yl)-(4-alkyl/aryl-phenyl)-methyl]-1*H*-triazoles were considerably less active than R115866 (IC₅₀ = 5 nM).

The 4-methyl derivative (**5**) has previously been evaluated as an aromatase (CYP19) inhibitor (IC₅₀ = 0.59 μM, cf. anastrozole = 0.6 μM).²¹ The 4-ethyl (**6**) and 4-phenyl (**15**) derivatives were also screened against CYP19 to determine selectivity, both having an inhibitory activity IC₅₀ > 100 μM. The negligible CYP19 inhibitory activity of **6** and **15** was expected from SAR studies²¹ which had shown that only small substituents, for example, F, Cl, CH₃ and CN were tolerated at the 4-position of the phenyl ring for CYP19 inhibitors.

4. Molecular modelling

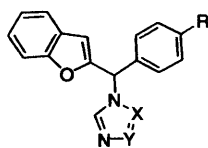
In order to rationalise the results obtained, MOE (Molecular Operating Environment)²⁴ docking studies of the inhibitors were performed using a human CYP26A1 model,²⁵ built using the recently crystallised human CYP3A4²⁶ as a template. Docking interactions at the enzyme active site were shown to be comparable with those of the CYP26 inhibitor liarozole with the benzofurans positioned above the haem with multiple hydrophobic interactions (Fig. 3). The inhibitor compounds are all racemic therefore both enantiomers of all the compounds were docked to determine any preference for (*R*)- or (*S*)-configuration; no preference was observed with both enantiomers exhibiting a similar 'fit' in the active site with the nitrogen of the heterocyclic ring coordinating with the Fe³⁺ of the haem, therefore for comparison Figure 3 shows the (*S*)-enantiomers of the 4-ethyl (**6a**) and the 4-phenyl (**15a**) 1,2,4-triazole benzofuran derivatives.

Docking of the 4-alkyl derivatives with a chain length of >2 indicated that steric hindrance was encountered preventing close (2.5–3.5 Å) interaction with the haem.



Scheme 2. Reagents and conditions: (i) Pd(PPh₃)₄, Na₂CO_{3(aq)} toluene, 100 °C, 5 h, then H₂O₂, rt, 1 h (60–70 %); (ii) NaBH₄, dioxane, 2–6 h; (iii) *N,N'*-thionyliditriazole, K₂CO₃, CH₃CN, 4 days.

Table 1. IC₅₀ data for the novel benzofuran derivatives using CYP26A1 MCF-7 assays



Compound	R	X	Y	IC ₅₀ (μM)
5a	CH ₃	N	CH	>40
5b	CH ₃	CH	N	>40
6a	CH ₂ CH ₃	N	CH	4.5
6b	CH ₂ CH ₃	CH	N	5
7	CH ₂ CH ₂ CH ₃	N	CH	50–100
8a	CH(CH ₃) ₂	N	CH	20–40
8b	CH(CH ₃) ₂	CH	N	50–100
9	C(CH ₃) ₃	N	CH	10–25
10	CH ₂ CH(CH ₃) ₂	N	CH	40–50
11	Cyclohexyl	N	CH	5–15
15a	C ₆ H ₅	N	CH	7
15b	C ₆ H ₅	CH	N	9
16a	<i>p</i> -Cl-C ₆ H ₅	N	CH	20–40
16b	<i>p</i> -Cl-C ₆ H ₅	CH	N	20–40
Ketoconazole	—	—	—	12
Liarozole	—	—	—	7
R115866	—	—	—	0.005

IC₅₀ values are the average (±5%) of two experiments.

The phenyl derivative (**15**, IC₅₀ = 7–9 μM) has a greater inhibitory activity despite its size owing to favourable conformation and enhanced hydrophobic bonding. This may strengthen the interaction of the phenyl derivative increasing its potency as an inhibitor of the enzyme; however, the unsubstituted phenyl was the limit with

the introduction of the chloro substituent (**16**, IC₅₀ = 20–40 μM) resulting in a reduction of inhibitory activity owing to steric/electronic factors.

The docking studies however fail to shed any light on the poor results obtained for the methyl compound (**5**,

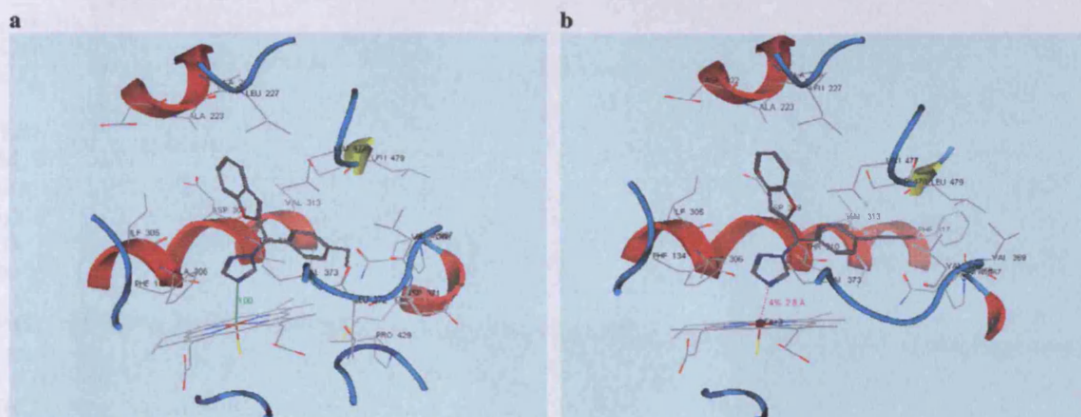


Figure 3. Active site region of CYP26A1 model showing (a) *S*-6a and (b) *S*-15a in ball and stick form. The distance from the haem is indicated with a green line, transition metal interaction with a purple line. Amino acid residues identified are involved in hydrophobic interactions.

$IC_{50} > 40 \mu M$), which was expected to possess potency similar to that of the ethyl derivative (**6**, $IC_{50} = 4.5\text{--}5 \mu M$).

A series of 4-alkyl/aryl benzofuran phenyl triazole derivatives has been prepared with the ethyl and phenyl derivatives shown to possess comparable inhibitory activity with that of the known CYP26 inhibitor liarozole.

5. Experimental

5.1. Materials and methods: chemistry

1H and ^{13}C NMR spectra were recorded with a Bruker Avance DPX500 spectrometer operating at 500 and 125 MHz, with Me_4Si as internal standard. Mass spectra were determined by the EPSRC Mass Spectrometry Centre (Swansea, UK). Microanalyses were determined by Medac Ltd (Surrey, UK). Flash column chromatography was performed with silica gel 60 (230–400mesh) (Merck) and TLC was carried out on precoated silica plates (kiesel gel 60 F₂₅₄, BDH). Melting points were determined on an electrothermal instrument and are uncorrected.

5.1.1. General method for the preparation of the ketones

3. To a solution of sodium hydride (60%, 11 mmol) in dry *N,N*-dimethylformamide (10 mL) was added a solution of salicylaldehyde (**1**, 10 mmol) in dry *N,N*-dimethylformamide (6 mL) dropwise. Hydrogen gas was liberated to give a yellow solution of the sodium salt. A solution of the α -bromoketone **2** (10 mmol) in dry *N,N*-dimethylformamide (10 mL) was then added dropwise and the reaction mixture was heated under nitrogen at 80 °C for 1.5 h. Sodium methoxide (2.5 mmol) was added to the mixture and heating was continued for another hour (TLC system: petroleum ether/ethyl acetate 4:1 v/v). After cooling, the reaction mixture was evaporated to about a third of its volume, diluted with dichloromethane (100 mL), washed with water (100 mL), dried ($MgSO_4$) and concentrated under reduced pressure.

5.1.1.1. Benzofuran-2-yl-(4-ethyl-phenyl)-methanone

(3a, R = CH_2CH_3). Brown solid (34%) after recrystallisation from methanol, mp 60–62 °C. 1H NMR ($CDCl_3$): δ 8.05 (d, $J = 8.1$ Hz, 2H, Ar), 7.78 (d, $J = 7.7$ Hz, 1H, Ar), 7.70 (d, $J = 7.9$, 1H, Ar), 7.55 (m, 2H, Ar), 7.37 (m, 3H, Ar), 2.81 (q, $J = 7.6$ Hz, 2H, CH_2), 1.36 (t, $J = 7.6$ Hz, 3H, CH_3). ^{13}C NMR ($CDCl_3$): δ 184.56 (C=O), 156.35 (C, C-7a), 152.83 (C, C-4'), 150.43 (C, C-1'), 135.22 (C, C-2), 130.19 (2 \times CH, CH-2' and CH-6'), 128.66 (CH, CH-6), 128.52 (2 \times CH, CH-3' and CH-5'), 127.48 (C, C-3a), 124.36 (CH, Ar), 123.70 (CH, Ar), 116.62 (CH, CH-3), 112.98 (CH, CH-7), 29.46 (CH_2), 15.71 (CH_3). Anal. Calcd for $C_{17}H_{14}O_2$ (250.296): C, 81.58; H, 5.64. Found: C, 81.44; H, 5.84.

5.1.1.2. Benzofuran-2-yl-(4-propyl-phenyl)-methanone

(3b, R = $CH_2CH_2CH_3$). Cream crystalline solid (42%) after recrystallisation from methanol, mp 64–66 °C. 1H NMR ($CDCl_3$): δ 7.92 (d, $J = 8.2$ Hz, 2H, Ar), 7.65 (d, $J = 7.9$ Hz, 1H, Ar), 7.57 (dd, $J = 0.40, 8.5$ Hz, 1H, Ar), 7.46 (d, $J = 0.6$ Hz, 1H, Ar), 7.42 (m, 1H, Ar), 7.26 (m, 3H, Ar), 2.62 (m, CH_2 , propyl), 1.64 (dt, $J = 7.4, 8.5$ Hz, CH_2 , propyl), 0.91 (t, $J = 7.3$ Hz, CH_3 , propyl). ^{13}C NMR ($CDCl_3$): δ 184.09 (C=O), 155.95 (C, C-7a), 152.51 (C, C-4'), 148.50 (C, C-1'), 134.84 (C, C-2), 129.67 (2 \times CH, CH-2' and CH-6') and 128.68 (2 \times CH, CH-3' and CH-5'), 128.19 (CH, Ar), 127.08 (C, C-3a), 123.92 (CH, Ar), 116.07 (CH, CH-3), 112.56 (CH, CH-7), 38.12 (CH_2), 24.25 (CH_2), 13.75 (CH_3). HRMS (EI^+) m/z Calcd for $C_{18}H_{16}O_2$ ($M+H$)⁺ 265.1223. Found 265.1224.

5.1.1.3. Benzofuran-2-yl-(4-isopropyl-phenyl)-methanone

(3c, R = $CH(CH_3)_2$). Pale orange solid (44%) after recrystallisation from methanol, mp 93–95 °C. 1H NMR ($CDCl_3$): δ 7.85 (m, 2H, Ar), 7.53 (m, 2H, Ar), 7.35 (m, 2H, Ar), 7.34 (s, 1H, H-7), 7.32 (m, 2H, Ar) 3.05 (septet, 1H, CH, isopropyl), 1.32 (s, 6H, isopropyl). ^{13}C NMR ($CDCl_3$): δ 186.36 (C=O), 155.81 (C, C-7a), 154.60 (C, C-2), 154.39 (C, C-4'), 152.39 (C, C-1'), 134.89 (C, C-3a), 131.15 (2 \times CH, CH-2' and CH-6'), 129.74 (2 \times CH, CH-3' and CH-5'), 126.62 (CH, Ar), 124.22 (CH, Ar), 123.27 (CH, Ar), 115.76 (CH, CH-3), 111.20 (CH,

CH-7), 34.24 (CH, isopropyl), 23.82 (CH₃, isopropyl). Anal. Calcd for C₁₈H₁₆O₂ (264.318): C, 81.79; H, 6.10. Found: C, 81.58; H, 6.07.

5.1.1.4. Benzofuran-2-yl-(4-*tert*-butyl-phenyl)-methanone (3d, R = C(CH₃)₃). Yellow solid (32%) after recrystallisation from methanol, mp 103–105 °C. ¹H NMR (CDCl₃): δ 7.87 (m, 2H, Ar), 7.67 (m, 2H, Ar), 7.53 (m, 2H, Ar), 7.34 (s, 1H, H-7), 7.32 (m, 2H, Ar), 1.35 (s, 9H, 'butyl). ¹³C NMR (CDCl₃): δ 184.08 (C=O), 167.76 (C, C-7a), 156.77 (C, C-2), 155.95 (C, C-4'), 155.95 (C, C-1'), 134.54 (C, C-3a), 130.89 (2× CH, CH-2' and CH-6'), 129.51 (2× CH, CH-3' and CH-5'), 127.09 (CH, Ar), 125.55 (CH, Ar), 123.92 (CH, Ar), 116.14 (CH, CH-3), 112.57 (CH, CH-7), 68.17 (C, 'butyl), 31.15 (CH₃, 'butyl). Anal. Calcd for C₁₉H₁₈O₂·0.6H₂O (289.159): C, 78.92; H, 6.69. Found: C, 79.17; H, 7.06.

5.1.1.5. Benzofuran-2-yl-(4-isobutyl-phenyl)-methanone (3e, R = CH₂CH(CH₃)₂). White solid (50%) after recrystallisation from methanol, mp 62–63 °C. ¹H NMR (CDCl₃): δ 7.90 (m, 2H, Ar), 7.59 (m, 2H, Ar), 7.52 (m, 2H, Ar), 7.34 (m, 2H, Ar), 7.32 (s, 1H, H-7), 2.56 (d, 2H, H-16), 1.96 (m, 1H, H-17), 1.01 (d, 6H, H-18, H-19). ¹³C NMR (CDCl₃): δ 184.08 (C=O), 155.95 (C, C-7a), 152.50 (C, C-2), 147.55 (C, C-4'), 134.86 (2× C, C-1' and C-3a), 129.63 (2× CH, CH-2' and CH-6'), 129.30 (2× CH, CH-3' and CH-5'), 128.19 (CH, Ar), 127.08 (CH, Ar), 123.92 (CH, Ar), 123.25 (CH, Ar), 116.09 (CH, CH-3), 112.55 (CH, CH-7), 45.48 (CH₂, isobutyl), 30.16 (CH, isobutyl), 22.39 (CH₃, isobutyl). Anal. Calcd for C₁₉H₁₈O₂ (278.345): C, 81.99; H, 6.52. Found: C, 81.55; H, 6.45.

5.1.1.6. Benzofuran-2-yl-(4-cyclohexyl-phenyl)-methanone (3f, R = C₆H₁₂).²⁷ Light yellow solid (29%) after recrystallisation from ethyl acetate. Mp 92–94 °C. ¹H NMR (CDCl₃): δ 7.93 (m, 2H, Ar), 7.24 (m, 2H, Ar), 7.19 (m, 4H, Ar), 6.62 (s, 1H, H-7), 2.51 (quintet, 1H, CH-cyclohexyl), and 1.56 (m, 10H, cyclohexyl).

5.1.2. General method for the preparation of the biphenyl ketones 13. Two molar aqueous Na₂CO₃ (11.65 mL) was added to a solution of benzo[*b*]furan-2-yl(4-bromophenyl)methanone²¹ (1.0 g, 3.32 mmol) in toluene (20 mL). The mixture was bubbled with nitrogen for one minute and then Pd(PPh₃)₄ (0.20 g, 0.166 mmol) was added to the mixture. Phenyl- or 4-phenyl-boronic acid (6.64 mmol) in ethanol (5 mL) was added to the above mixture and the reaction was refluxed at 100 °C for 4 h. After the reaction was complete, the residual borane was oxidised by the addition of H₂O₂ (30%, 2.5 mL) at room temperature for 1 h. The crude product was extracted with CH₂Cl₂ (100 mL) and water (3× 100 mL). The organic layer was dried with MgSO₄, filtered and reduced in vacuo to give a light yellow oily residue. Purification by flash column chromatography (petroleum ether/ethyl acetate 95:5 v/v increasing to 80:20 v/v) gave the product, which was recrystallised from petroleum ether.

5.1.2.1. Benzo[*b*]furan-2-yl-biphenyl-4-yl-methanone (13a). Light yellow fine crystals (58%), mp 150–152 °C (lit.²⁸ 153–155 °C). TLC system: petroleum ether/ethyl

acetate, 1:1 v/v, R_f: 0.63. ¹H NMR (CDCl₃): δ 8.21 (dd, *J* = 1.6, 8.2 Hz, 2H, Ar), 7.82 (m, 3H, Ar), 7.73 (m, 3H, Ar), 7.65 (s, 1H, H-3), 7.46 (m, 5H, Ar). ¹³C NMR (CDCl₃): δ 184.33 (C=O), 156.43 (C, C-7a), 152.80 (C, C-4'), 146.16 (C, C-1'), 140.29 (C, C-1'), 136.31 (C, C-2), 130.58 (2× CH, CH-2' and CH-6'), 129.46 (2× CH, CH-3' and CH-5'), 128.83 (2× CH, CH-3' and CH-5'), 128.76 (CH, Ar), 127.77 (2× CH, CH-2' and CH-6'), 127.66 (CH, Ar), 127.48 (C, C-3a), 124.46 (CH, Ar), 123.78 (CH, Ar), 116.83 (CH, CH-3), 113.03 (CH, CH-7).

5.1.2.2. Benzo[*b*]furan-2-yl(4'-chlorobiphenyl-4-yl)methanone (13b). Light yellow solid (73%), mp 76–78 °C. TLC system: petroleum ether/ethyl acetate, 4:1 v/v, R_f: 0.50. ¹H NMR (CDCl₃): δ 8.25 (dd, *J* = 1.7, 6.6 Hz, 2H, Ar), 7.81 (m, 4H, Ar), 7.69 (m, 2H, Ar), 7.52 (m, 5H, Ar). ¹³C NMR (CDCl₃): δ 184.18 (C=O), 156.44 (C, C-7a), 152.75 (C, C-4'), 144.82 (C, C-1'), 138.71 (C, C-2), 136.57 (C, C-1'), 134.96 (C, C-4'), 130.67 (2× CH, CH-2' and CH-6'), 129.64 (2× CH, CH-3' and CH-5'), 128.89 (2× CH, CH-3' and CH-5'), 128.65 (CH, CH-6), 127.49 (2× CH, CH-2' and CH-6'), 127.44 (C, C-3a), 124.49 (CH, Ar), 123.79 (CH, Ar), 116.87 (CH, CH-3), 113.02 (CH, CH-7). Anal. Calcd for C₂₁H₁₃ClO₂ (332.785): C, 75.79; H, 3.94. Found: C, 76.14; H, 4.00.

5.1.3. General method for the preparation of the alcohols 4 and 14. To a cooled (0 °C) solution of benzofuran-2-yl-(4-alkyl/aryl-phenyl)-methanone (5 mmol) in anhydrous dioxan (15 mL) was added sodium borohydride (5 mmol) and then the mixture was allowed to stir at room temperature under nitrogen for 2 h. The solvent was concentrated under reduced pressure and aqueous hydrochloric acid (1 M, 10 mL) was added to the residue. The oil formed was extracted with diethyl ether (2× 50 mL) and washed with water (2× 25 mL), the organic layers were combined and dried with MgSO₄ and the solvent concentrated under reduced pressure.

5.1.3.1. Benzofuran-2-yl-(4-ethyl-phenyl)-methanol (4a, R = CH₂CH₃). White solid (83%), mp 45–47 °C. TLC system: petroleum ether/ethyl acetate, 3:2 v/v, R_f: 0.64. ¹H NMR (CDCl₃): 7.60 (m, 1H, Ar), 7.50 (m, 3H, Ar), 7.32 (m, 4H, Ar), 6.61 (s, 1H, H-3), 5.96 (d, *J* = 4.6 Hz, 1H, CH-OH), 2.91 (d, *J* = 4.6 Hz, 1H, OH), 2.76 (q, *J* = 7.6 Hz, 2H, CH₂), 1.34 (t, *J* = 7.6 Hz, 3H, CH₃). ¹³C NMR (CDCl₃): δ 160.31 (C, C-2), 159.21 (C, C-7a), 155.54 (C, C-4'), 144.97 (C, C-1'), 138.12 (C, C-3a), 128.58 (2× CH, CH-3' and CH-5'), 127.34 (2× CH, CH-2' and CH-6'), 124.67 (CH, Ar), 123.25 (CH, Ar), 121.58 (CH, Ar), 111.81 (CH, CH-7), 104.35 (CH, CH-3), 71.02 (CH, CH-OH), 29.08 (CH₂), 16.05 (CH₃). LRMS (EI⁺) *m/z*: 252.1 (M⁺). Anal. Calcd for C₁₇H₁₆O₂ (252.311): C, 80.93; H, 6.39. Found: C, 80.73; H, 6.41.

5.1.3.2. Benzofuran-2-yl-(4-propyl-phenyl)-methanol (4b, R = CH₂CH₂CH₃). Yellow syrup (60%). TLC system: petroleum ether/ethyl acetate, 4:1 v/v, R_f: 0.64. ¹H NMR (CDCl₃): δ 7.50 (m, 4H, Ar), 7.26 (m, 4H, Ar), 5.70 (d, *J* = 9.5 Hz, 1H, CH-OH), 2.64 (m, CH₂, pro-

pyl), 2.50 (s, 1H, OH), 1.69 (m, CH₂, propyl), 0.10 (dt, $J = 3.5, 7.3$ Hz, CH₃, propyl). ¹³C NMR (CDCl₃): δ 157.20 (C, C-2), 155.25 (C-7a), 142.95 (C, C-4'), 135.72 (C, C-1'), 128.76 (2× CH, CH-3' and CH-5'), 128.15 (2× CH, CH-2' and CH-6'), 127.57 (C, C-3a), 126.78 (CH, Ar), 124.25 (CH, Ar), 122.82 (CH, Ar), 121.13 (CH, Ar), 111.48 (CH, CH-7), 105.09 (CH, CH-3), 75.22 (CH, CH-OH), 37.85 (CH₂), 24.51 (CH₂), 13.93 (CH₃). Anal. Calcd for C₁₈H₁₈O₂ (266.339): C, 81.17; H, 6.81. Found: C, 80.87; H, 6.92.

5.1.3.3. Benzofuran-2-yl-(4-isopropyl-phenyl)-methanol (4c, R = CH(CH₃)₂). White solid (96%), mp 69–70 °C. TLC system: petroleum ether/ethyl acetate, 4:1 v/v, R_f : 0.74. ¹H NMR (CDCl₃): δ 7.42 (m, 2H, Ar), 7.34 (m, 2H, Ar), 7.16 (m, 2H, Ar), 7.11 (s, 2H, Ar), 6.45 (s, 1H, H-7), 5.81 (s, 1H, CH-OH), 2.82 (m, 1H, isopropyl), 2.59 (s, 1H, OH), 1.18 (s, 6H, isopropyl). ¹³C NMR (CDCl₃): δ 157.64 (C, C-2), 154.03 (C, C-7a), 148.10 (C, C-4'), 136.71 (2× CH, CH-3' and CH-5'), 127.03 (2× CH, CH-2' and CH-6'), 125.81 (CH, Ar), 125.65 (CH, Ar), 123.16 (CH, Ar), 110.28 (CH, CH-7), 102.82 (CH, CH-3), 69.54 (CH, CH-OH), 32.84 (CH, isopropyl), 22.93 (CH₃, isopropyl). Anal. Calcd for C₁₈H₁₉O₂·0.5H₂O (276.3545): C, 78.23; H, 7.29. Found: C, 78.14; H, 7.05.

5.1.3.4. Benzofuran-2-yl-(4-tert-butyl-phenyl)-methanol (4d, R = C(CH₃)₃). White solid (99%), mp 87–88 °C. TLC system: petroleum ether/ethyl acetate, 4:1 v/v, R_f : 0.72. ¹H NMR (CDCl₃): δ 7.39 (m, 2H, Ar), 7.34 (m, 2H, Ar), 7.30 (m, 2H, Ar), 7.12 (m, 2H, Ar), 6.41 (s, 1H, H-7), 5.78 (s, 1H, CH-OH), 2.58 (s, 1H, OH), 1.21 (s, 9H, 'butyl'). ¹³C NMR (CDCl₃): δ 158.74 (C, C-2), 155.14 (C, C-7a), 151.24 (C, C-4'), 130.72 (2× CH, CH-3' and CH-5'), 129.36 (2× CH, CH-2' and CH-6'), 128.15 (CH, Ar), 126.64 (CH, Ar), 125.93 (CH, Ar), 111.39 (CH, CH-7), 103.92 (CH, CH-3), 70.57 (CH, CH-OH), 34.66 (C, 'butyl'), 31.39 (CH₃, 'butyl'). Anal. Calcd for C₁₉H₂₀O₂ (280.361): C, 81.40; H, 7.19. Found: C, 81.22; H, 7.01.

5.1.3.5. Benzofuran-2-yl-(4-isobutyl-phenyl)-methanol (4e, R = CH₂CH(CH₃)₂). Yellow syrup (99%), mp 87–88 °C. TLC system: petroleum ether/ethyl acetate, 4:1 v/v, R_f : 0.73. ¹H NMR (CDCl₃): δ 7.53 (m, 1H, Ar), 7.48 (m, 1H, Ar), 7.41 (m, 2H, Ar), 7.20 (m, 4H, Ar), 6.57 (s, 1H, H-7), 5.95 (s, 1H, CH-OH), 3.72 (s, 1H, OH), 2.52 (s, 2H, isobutyl), 1.91 (m, 1H, isobutyl), 0.96 (s, 6H, isobutyl). ¹³C NMR (CDCl₃): δ 158.74 (C, C-2), 155.12 (C, C-7a), 142.05 (C, C-4'), 137.66 (C, C-1'), 129.38 (2× CH, CH-3' and CH-5'), 128.10 (CH, Ar), 126.63 (2× CH, CH-2' and CH-6'), 124.23 (CH, Ar), 122.81 (CH, Ar), 121.12 (CH, Ar), 111.34 (CH, CH-7), 103.89 (CH, CH-3), 70.66 (CH, CH-OH), 45.16 (CH₂, isobutyl), 30.21 (CH, isobutyl), 22.38 (CH₃, isobutyl). Anal. Calcd for C₁₉H₂₀O₂ (280.361): C, 81.40; H, 7.19. Found: C, 81.07; H, 7.43.

5.1.3.6. Benzofuran-2-yl-(4-cyclohexyl-phenyl)-methanol (4f, R = C₆H₁₂). White solid (98%), mp 67–68 °C. TLC system: petroleum ether/ethyl acetate, 4:1 v/v, R_f :

0.63. ¹H NMR (CDCl₃): δ 7.59 (m, 1H, Ar), 7.48 (m, 3H, Ar), 7.25 (m, 4H, Ar), 6.58 (s, 1H, H-7), 5.89 (s, 1H, CH-OH), 3.72 (s, 1H, OH), 2.61 (m, 1H, cyclohexyl), 1.58 (m, 10H, cyclohexyl). ¹³C NMR (CDCl₃): δ 159.28 (C, C-2), 155.46 (C, C-7a), 144.09 (C, C-4'), 134.90 (C, C-1'), 128.72 (2× CH, CH-3' and CH-5'), 128.59 (2× CH, CH-2' and CH-6'), 124.00 (CH, Ar), 122.77 (CH, Ar), 120.91 (CH, Ar), 111.25 (CH, Ar), 103.24 (CH, Ar), 67.63 (CH, CH-OH), 45.00 (CH, CH-cyclohexyl), 35.40 (CH₂, cyclohexyl), 27.65 (CH₂, cyclohexyl), 26.95 (CH₂, cyclohexyl). HRMS (EI⁺) m/z Calcd for C₂₁H₂₂O₂ (M+H)⁺ 358.1914. Found 358.1910.

5.1.3.7. Benzo[b]furan-2-yl-biphenyl-4-yl-methanol (14a, R = phenyl). White solid (90%), mp 121–123 °C (lit.²⁸ 123–125 °C). TLC system: petroleum ether/ethyl acetate, 1:1 v/v, R_f : 0.63. ¹H NMR (CDCl₃): δ 7.63 (m, 6H, Ar), 7.46 (m, 4H, Ar), 7.30 (m, 3H, Ar), 6.64 (d, $J = 0.6$ Hz, 1H, H-3), 6.04 (d, $J = 3.1$ Hz, 1H, CH-OH), 2.73 (d, $J = 3.9$ Hz, 1H, OH). ¹³C NMR (CDCl₃): δ 158.84 (C, C-2), 155.57 (C, C-7a), 141.76 (C, C-1'), 141.10 (C, C-1''), 139.69 (C, C-4'), 129.28 (2× CH, CH-3' and CH-5''), 128.47 (C, C-3a), 127.92 (2× CH, CH-2' and CH-6''), 127.83 (2× CH, CH-3' and CH-5'), 127.72 (2× CH, CH-2'' and CH-6''), 127.60 (CH, Ar), 124.82 (CH, Ar), 123.34 (CH, Ar), 121.64 (CH, Ar), 111.83 (CH, CH-7), 104.57 (CH, CH-3), 70.91 (CH-OH).

5.1.3.8. Benzo[b]furan-2-yl-(4'-chlorobiphenyl-4-yl)methanol (14b, R = 4-chlorophenyl). White solid (75%), mp 76–78 °C. TLC system: petroleum ether/ethyl acetate, 1:1 v/v, R_f : 0.60. ¹H NMR (CDCl₃): δ 7.54 (m, 7H, Ar), 7.44 (m, 3H, Ar), 7.25 (m, 2H, Ar), 6.59 (s, 1H, H-3), 6.00 (d, $J = 4.5$ Hz, 1H, CH-OH), 2.65 (d, $J = 4.6$ Hz, 1H, OH). ¹³C NMR (CDCl₃): δ 158.69 (C, C-2), 155.55 (C, C-7a), 140.48 (C, C-1'), 140.31 (C, C-4'), 139.51 (C, C-1''), 134.02 (C, C-4''), 129.42 (2× CH, CH-3' and CH-5''), 128.81 (2× CH, CH-2'' and CH-6''), 128.41 (C, C-3a), 127.80 (2× CH, CH-2' and CH-6'), 127.64 (2× CH, CH-3' and CH-5'), 124.87 (CH, Ar), 123.36 (CH, Ar), 121.65 (CH, Ar), 111.82 (CH, CH-7), 104.59 (CH, CH-3), 70.82 (CH-OH). Anal. Calcd for C₂₁H₁₅ClO₂ (334.800): C, 75.20; H, 4.45. Found: C, 75.34; H, 4.52.

5.1.4. General method for the preparation of the triazole compounds 5–11, 15 and 16. Thionyl chloride (4 mmol) in anhydrous acetonitrile (10.0 mL) was added dropwise to a stirred solution of 1,2,4-triazole (16 mmol) in anhydrous acetonitrile (10.0 mL) at a temperature of 10 °C. The white suspension formed was stirred for 1 h at 10 °C. A solution of benzo[b]furan-2-yl-(4-alkyl/arylphenyl)methanol (4a–f, 14) (1.0 g, 4 mmol) in anhydrous acetonitrile (10.0 mL) was added to the mixture followed by activated potassium carbonate (1.10 g, 8 mmol). The suspension was stirred under nitrogen at room temperature for 4 days. The resulting suspension was filtered and the filtrate was evaporated in vacuo to yield a light brown oil. The oil was extracted with CH₂Cl₂ (150 mL) and water (3× 100 mL). The organic layer was dried with MgSO₄, filtered and reduced in vacuo.

5.1.4.1. 1-[Benzo[*b*]furan-2-yl-(4-methylphenyl)methyl]-1*H*-[1,2,4]triazole (5a) and 4-[benzo[*b*]furan-2-yl-(4-methylphenyl)methyl]-4*H*-[1,3,4]triazole (5b). Purified by column chromatography (petroleum ether/ethyl acetate, 1:1 v/v) to give the [1,2,4]triazole 5a, further elution (dichloromethane/methanol, 95:5 v/v) gave the [1,3,4]triazole 5b.

Data for 5a: orange crystals (28%), mp 106–108 °C. TLC system: petroleum ether/ethyl acetate, 4:1 v/v, R_f : 0.14. ^1H NMR (CDCl_3): δ 8.14 (s, 1H, H-3 $''''$), 8.05 (s, 1H, H-5 $''''$), 7.56 (d, $J = 7.7$ Hz, 1H, Ar), 7.48 (d, $J = 8.3$ Hz, 1H, Ar), 7.34 (m, 1H, Ar), 7.25 (m, 5H, Ar), 6.84 (s, 1H, H-1), 6.59 (s, 1H, H-3), 2.40 (s, 3H, CH_3). ^{13}C NMR (CDCl_3): δ 155.34 (C, C-2), 152.93 (C, C-7a), 152.21 (CH, CH-5 $''''$), 143.21 (CH, CH-3 $''''$), 139.24 (C, C-3a), 132.61 (C, C-1'), 129.80 and 127.67 (CH, Ar), 127.55 (C, C-4'), 125.17, 123.30 and 121.49 (CH, Ar), 111.54 (CH, CH-7), 107.58 (CH, CH-3), 62.10 (CH, CH-1), 21.19 (CH_3).

Data for 5b: white solid (12%), mp 64–66 °C. TLC system: dichloromethane/methanol, 9:1 v/v, R_f : 0.27. ^1H NMR (CDCl_3): δ 8.21 (s, 2H, H-2 $''''$ and H-5 $''''$), 7.57 (d, $J = 7.7$ Hz, 1H, Ar), 7.48 (d, $J = 8.3$ Hz, 1H, Ar), 7.36 (m, 1H, Ar), 7.28 (m, 3H, Ar), 7.17 (d, $J = 8.1$ Hz, 2H, Ar), 6.64 (s, 1H, H-1), 6.59 (s, 1H, H-3), 2.41 (s, 3H, CH_3). ^{13}C NMR (CDCl_3): δ 155.39 (C, C-2), 152.42 (C, C-7a), 142.43 (2 \times CH, CH-2 $''''$ and CH-5 $''''$), 139.72 (C, C-1'), 132.27 (C, C-4'), 130.08 and 127.38 (CH, Ar), 127.22 (C, C-3a), 125.56, 123.56 and 121.57 (CH, Ar), 111.62 (CH, CH-7), 107.60 (CH, CH-3), 58.00 (CH, CH-1), 21.18 (CH_3). HRMS (EI^+) m/z Calcd for $\text{C}_{18}\text{H}_{15}\text{N}_3\text{O}$ ($\text{M}+\text{H}$) $^+$ 290.1288. Found 290.1287.

5.1.4.2. 1-[Benzo[*b*]furan-2-yl-(4-ethylphenyl)methyl]-1*H*-[1,2,4]triazole (6a) and 4-[benzo[*b*]furan-2-yl-(4-ethylphenyl)methyl]-4*H*-[1,3,4]triazole (6b). Purified by column chromatography (petroleum ether/ethyl acetate, 7:3 v/v) to give the [1,2,4]triazole 6a, further elution (dichloromethane/methanol, 99:1 v/v) gave the [1,3,4]triazole 6b.

Data for 6a: yellow syrup (67%). TLC system: petroleum ether/ethyl acetate, 1:1 v/v, R_f : 0.42. ^1H NMR (CDCl_3): δ 8.19 (s, 1H, H-3 $''''$), 8.09 (s, 1H, H-5 $''''$), 7.58 (d, $J = 8.4$ Hz, 1H, Ar), 7.51 (d, $J = 9.3$ Hz, 1H, Ar), 7.39–7.27 (m, 6H, Ar), 6.89 (s, 1H, H-1), 6.63 (s, 1H, H-3), 2.73 (q, $J = 7.6$ Hz, 2H, CH_2), 1.30 (t, $J = 7.6$ Hz, 3H, CH_3). ^{13}C NMR (CDCl_3): δ 155.75 (C, C-2), 153.342 (C, C-7a), 152.65 (CH, CH-5 $''''$), 145.91 (C, C-4'), 143.67 (CH, CH-3 $''''$), 133.20 (C, C-1'), 129.06 (2 \times CH, CH-2' and CH-6'), 128.16 (2 \times CH, CH-3' and CH-5'), 127.96 (C, C-3a), 125.59 (CH, Ar), 123.73 (CH, Ar), 121.93 (CH, Ar), 111.97 (CH, CH-7), 108.06 (CH, CH-3), 62.51 (CH, CH-1), 28.99 (CH_2), 15.85 (CH_3). HRMS (EI^+) m/z Calcd for $\text{C}_{19}\text{H}_{17}\text{N}_3\text{O}$ ($\text{M}+\text{H}$) $^+$ 304.1444. Found 304.1442.

Data for 6b: White solid (13%), mp 126–128 °C. TLC system: dichloromethane/methanol, 9:1 v/v, R_f : 0.31. ^1H NMR (CDCl_3): δ 8.25 (s, 2H, H-2 $''''$ and H-5 $''''$),

7.57 (d, $J = 6.8$ Hz, 1H, Ar), 7.46 (d, $J = 8.4$ Hz, 1H, Ar), 7.37–7.19 (m, 6H, Ar), 6.75 (s, 1H, H-1), 6.62 (s, 1H, H-3), 2.70 (q, $J = 7.6$ Hz, 2H, CH_2), 1.26 (t, $J = 7.6$ Hz, 3H, CH_3). ^{13}C NMR (CDCl_3): δ 155.76 (C, C-2), 152.90 (C, C-7a), 146.26 (C, C-4'), 142.95 (2 \times CH, CH-2 $''''$ and CH-5 $''''$), 132.98 (C, C-1'), 129.27 (2 \times CH, CH-2' and CH-6'), 127.89 (2 \times CH, CH-3' and CH-5'), 127.67 (C, C-3a), 125.91 (CH, Ar), 123.94 (CH, Ar), 122.01 (CH, Ar), 112.01 (CH, CH-7), 108.04 (CH, CH-3), 58.28 (CH, CH-1), 28.95 (CH_2), 15.83 (CH_3). Anal. Calcd for $\text{C}_{19}\text{H}_{17}\text{N}_3\text{O}$ (303.362): C, 75.23; H, 5.65; N, 13.84. Found: C, 75.19; H, 5.74; N, 13.61.

5.1.4.3. 1-[Benzo[*b*]furan-2-yl-(4-propylphenyl)methyl]-1*H*-[1,2,4]triazole (7). Purified by column chromatography (petroleum ether/ethyl acetate, 1:1 v/v) to give the [1,2,4]triazole 7 as a yellow syrup (2%). TLC system: petroleum ether/ethyl acetate, 4:1 v/v, R_f : 0.25. ^1H NMR (CDCl_3): δ 8.03 (s, 1H, H-3 $''''$), 7.94 (s, 1H, H-5 $''''$), 7.46 (d, $J = 7.7$ Hz, 1H, Ar), 7.38 (d, $J = 8.3$ Hz, 1H, Ar), 7.23 (m, 1H, Ar), 7.16 (m, 5H, Ar), 6.74 (s, 1H, H-1), 6.49 (s, 1H, H-3), 2.53 (t, $J = 7.6$ Hz, CH_2 , propyl), 1.57 (dt, $J = 7.5$, 15 Hz, CH_2 , propyl), 0.87 (t, $J = 7.3$ Hz, CH_3 , propyl). ^{13}C NMR (CDCl_3): δ 154.32 (C, C-2), 151.92 (C, C-7a), 151.17 (CH, CH-5 $''''$), 142.96 (C, C-3a), 131.77 (C, C-1'), 128.17 (2 \times CH, CH-2' and CH-6'), 126.61 (2 \times CH, CH-3' and CH-5'), 126.53 (C, C-4'), 124.13, 122.27 and 120.46 (CH, Ar), 110.52 (CH, CH-7), 106.55 (CH, CH-3), 61.11 (CH, CH-1), 36.68 (CH_2), 23.34 (CH_2), 12.79 (CH_3). HRMS (EI^+) m/z Calcd for $\text{C}_{20}\text{H}_{19}\text{N}_3\text{O}$ ($\text{M}+\text{H}$) $^+$ 318.1601. Found 318.1601.

5.1.4.4. 1-[Benzo[*b*]furan-2-yl-(4-isopropylphenyl)methyl]-1*H*-[1,2,4]triazole (8a) and 4-[benzo[*b*]furan-2-yl-(4-isopropylphenyl)methyl]-4*H*-[1,3,4]triazole (8b). Purified by column chromatography (hexane/ethyl acetate, 9:1 v/v) to give the [1,2,4]triazole 8a, further elution (dichloromethane/methanol, 9:1 v/v) gave the [1,3,4]triazole 8b.

Data for 8a: yellow syrup (78%). TLC system: petroleum ether/ethyl acetate, 1:1 v/v, R_f : 0.72. ^1H NMR (CDCl_3): δ 8.42 (s, 1H, H-3 $''''$), 8.33 (s, 1H, H-5 $''''$), 7.31 (m, 1H, Ar), 7.24 (m, 2H, Ar), 7.06 (m, 5H, Ar), 6.62 (s, 1H, H-1), 6.37 (s, 1H, H-3), 2.73 (septet, 1H, isopropyl), 1.05 (d, 6H, isopropyl). ^{13}C NMR (CDCl_3): δ 155.25 (C, C-2), 153.15 (CH, C-7a), 152.11 (CH, CH-5 $''''$), 149.79 (C, C-3a), 143.35 (C, C-1'), 133.09 (C, C-4'), 127.76 (2 \times CH, CH-2' and CH-6'), 126.84 (2 \times CH, CH-3' and CH-5'), 125.04 (CH, Ar), 123.22 (CH, Ar), 112.44 (CH, Ar), 111.42 (CH, CH-7), 107.07 (CH, CH-3), 62.03 (CH, CH-1), 34.47 (C, isopropyl), 24.16 (CH_3 , isopropyl). HRMS (EI^+) m/z Calcd for $\text{C}_{20}\text{H}_{19}\text{N}_3\text{O}$ (M) $^+$ 318.1601. Found 318.1601.

Data for 8b: yellow syrup (7%). TLC system: petroleum ether/ethyl acetate, 1:1 v/v, R_f : 0.11. ^1H NMR (CDCl_3): δ 8.12 (s, 2H, H-2 $''''$ and H-5 $''''$), 7.47 (m, 1H, Ar), 7.39 (m, 1H, Ar), 7.27 (m, 1H, Ar), 7.20 (m, 4H, Ar), 7.13 (m, 3H, Ar), 6.56 (s, 1H, H-1), 6.49 (s, 1H, H-3), 2.75 (septet, 1H, isopropyl), 1.18 (d, 6H, isopropyl). ^{13}C

NMR (CDCl₃): δ 155.39 (C, C-2), 152.30 (C, C-7a), 150.63 (2 \times CH, CH-2''' and CH-5'''), 142.47 (C, C-4'), 132.46 (C, C-1'), 127.72 (C, C-3a), 127.52 (2 \times CH, CH-2' and CH-6'), 127.21 (2 \times CH, CH-3' and CH-5'), 125.58 (CH, Ar), 123.58 (CH, Ar), 121.59 (CH, Ar), 111.64 (CH, CH-7), 107.67 (CH, CH-3), 58.08 (CH, CH-1), 33.89 (C, isopropyl), 23.85 (CH₃, isopropyl). HRMS (EI⁺) *m/z* Calcd for C₂₀H₁₉N₃O (M+H)⁺ 318.1601. Found 318.1603.

5.1.4.5. 1-[Benzo[*b*]furan-2-yl-(4-*tert*-butyl-phenyl)-methyl]-1*H*-[1,2,4]triazole (9). Purified by column chromatography (hexane/ethyl acetate, 9:1 v/v) to give the [1,2,4]triazole **9**, as a yellow syrup (62%). TLC system: petroleum ether/ethyl acetate, 1:1 v/v, *R_f*: 0.61. ¹H NMR (CDCl₃): δ 8.15 (s, 1H, 1H, H-3'''), 8.01 (s, 1H, H-5'''), 7.49 (m, 1H, Ar), 7.40 (m, 3H, Ar), 7.25 (m, 3H, Ar), 7.19 (m, 3H, Ar), 6.76 (s, 1H, H-1), 6.57 (s, 1H, H-3), 1.32 (s, 9H, 'butyl). ¹³C NMR (CDCl₃): δ 156.98 (C, C-2), 154.16 (CH, CH-5'''), 150.30 (C, C-7a), 148.52 (CH, CH-3'''), 136.47 (C, C-4'), 132.56 (2 \times CH, CH-2' and CH-6'), 129.94 (C, C-1'), 129.08 (C, C-3a), 127.92 (2 \times CH, CH-3' and CH-5'), 123.37 (CH, Ar), 122.14 (CH, Ar), 120.55 (CH, Ar), 110.82 (CH, CH-7), 101.37 (CH, CH-3), 61.90 (CH, CH-1), 34.80 (C, 'butyl), 31.41 (CH₃, 'butyl). HRMS (EI⁺) *m/z* Calcd for C₂₁H₂₁N₃O (M)⁺ 332.1757. Found 332.1761.

5.1.4.6. 1-[Benzo[*b*]furan-2-yl-(4-isobutylphenyl)methyl]-1*H*-[1,2,4]triazole (10). Purified by column chromatography (hexane/ethyl acetate, 9:1 v/v) to give the [1,2,4]triazole **10** as a yellow syrup (56%). TLC system: petroleum ether/ethyl acetate, 1:1 v/v, *R_f*: 0.63. ¹H NMR (CDCl₃): δ 8.28 (s, 1H, 1H, H-3'''), 8.22 (s, 1H, 1H, H-5'''), 7.60 (m, 2H, Ar), 7.40 (m, 2H, Ar), 7.31 (m, 2H, Ar), 7.23 (m, 2H, Ar), 6.82 (s, 1H, H-1), 6.54 (s, 1H, H-3), 2.54 (d, 2H, CH₂, isobutyl), 1.95 (m, 1H, CH, isobutyl), 1.02 (s, 6H, isobutyl). ¹³C NMR (CDCl₃): δ 155.27 (C, C-2), 153.21 (CH, CH-5'''), 152.11 (CH, CH-3'''), 136.47 (C, C-7a), 132.51 (2 \times CH, CH-2' and CH-6'), 131.47 (2 \times CH, CH-3' and CH-5'), 131.36 (C, C-4'), 129.94 (C, C-1'), 128.88 (C, C-3a), 123.37 (CH, Ar), 122.14 (CH, Ar), 120.55 (CH, Ar), 110.89 (CH, CH-7), 101.37 (CH, CH-3), 56.50 (CH, CH-1), 45.54 (CH₂, isobutyl), 27.57 (CH, isobutyl), 22.23 (CH₃, isobutyl). Anal. Calcd for C₂₁H₂₁N₃O·0.3-H₂O (336.821): C, 74.89; H, 6.46; N, 12.48. Found: C, 74.87; H, 6.45; N, 12.15.

5.1.4.7. 1-[Benzo[*b*]furan-2-yl-(4-cyclohexylphenyl)-methyl]-1*H*-[1,2,4]triazole (11). Purified by column chromatography (hexane/ethyl acetate, 9:1 v/v) to give the [1,2,4]triazole **11** as a yellow syrup (14%). TLC system: petroleum ether/ethyl acetate, 1:1 v/v, *R_f*: 0.70. ¹H NMR (CDCl₃): δ 8.28 (s, 1H, 1H, H-3'''), 8.22 (s, 1H, 1H, H-5'''), 7.60 (m, 2H, Ar), 7.40 (m, 2H, Ar), 7.31 (m, 2H, Ar), 7.23 (m, 2H, Ar), 6.82 (s, 1H, H-1), 6.54 (s, 1H, H-3), 2.54 (m, 1H, CH, cyclohexyl), 1.48 (m, 10H, cyclohexyl). ¹³C NMR (CDCl₃): δ 156.98 (C, C-2), 154.16 (CH, C-7a), 148.52 (CH, CH-5'''), 143.74 (CH, CH-3'''), 136.47 (C, C-4'), 131.56 (2 \times CH, CH-2' and CH-6'), 129.81 (2 \times CH, CH-3' and CH-5'), 128.64 (C, C-3a), 123.37 (CH, Ar), 122.14 (CH, Ar), 120.55

(CH, Ar), 110.89 (CH, CH-7), 101.37 (CH, CH-3), 56.50 (CH, CH-1), 45.00 (CH, cyclohexyl), 35.40 (2 \times CH₂, cyclohexyl), 27.65 (2 \times CH₂, cyclohexyl), 26.95 (1 \times CH₂, cyclohexyl). HRMS (EI⁺) *m/z* Calcd for C₂₃H₂₃N₃O₂ (M+H)⁺ 358.1914. Found 358.1910.

5.1.4.8. 1-(Benzo[*b*]furan-2-yl-biphenyl-4-yl-methyl)-1*H*-[1,2,4]triazole (15a) and 4-(benzo[*b*]furan-2-yl-biphenyl-4-yl-methyl)-4*H*-[1,2,4]triazole (15b). Purified by column chromatography (petroleum/ethyl acetate, 9:1 v/v increasing to 65:35 v/v) to give the [1,2,4]triazole **15a**, further elution (dichloromethane/methanol, 99:1 v/v) gave the [1,3,4]triazole **15b**.

Data for 15a: White solid (53%), mp 130–132 °C. TLC system: petroleum ether/ethyl acetate, 1:1 v/v, *R_f*: 0.41. ¹H NMR (CDCl₃): δ 8.24 (s, 1H, H-3'''), 8.12 (s, 1H, H-5'''), 7.68 (d, *J* = 8.3 Hz, 2H, Ar), 7.63 (m, 3H, Ar), 7.53 (m, 3H, Ar), 7.45–7.31 (m, 5H, Ar), 6.96 (s, 1H, H-1), 6.69 (s, 1H, H-3). ¹³C NMR (CDCl₃): δ 155.80 (C, C-2), 152.99 (C, C-7a), 152.78 (CH, CH-5'''), 143.76 (CH, CH-3'''), 142.61 (C, C-1'), 140.55 (C, C-1'), 134.92 (C, C-4'), 129.36 (2 \times CH, CH-2' and CH-6'), 128.58 (2 \times CH, CH-3'' and CH-5''), 128.27 (2 \times CH, CH-2'' and CH-6''), 128.23 (2 \times CH, CH-3' and CH-5'), 127.92 (C, C-3a), 127.60 (CH, CH-4''), 125.75 (CH, Ar), 123.83 (CH, Ar), 122.02 (CH, Ar), 112.02 (CH, CH-7), 108.34 (CH, CH-3), 62.41 (CH, CH-1). Anal. Calcd for C₂₃H₁₇N₃O (351.406): C, 78.61; H, 4.88; N, 11.95. Found: C, 78.38; H, 4.74; N, 11.89.

Data for 15b: Light yellow solid (6%), mp 56–58 °C. TLC system: dichloromethane/methanol, 9:1 v/v, *R_f*: 0.31. ¹H NMR (CDCl₃): δ 8.41 (s, 2H, H-2'' and H-5'''), 7.79 (d, *J* = 8.4 Hz, 2H, Ar), 7.72 (m, 3H, Ar), 7.61 (m, 3H, Ar), 7.58–7.40 (m, 5H, Ar), 6.87 (s, 1H, H-1), 6.79 (s, 1H, H-3). ¹³C NMR (CDCl₃): δ 155.85 (C, C-2), 152.44 (C, C-7a), 143.02 (C, C-1''), 142.93 (2 \times CH-2'' and CH-5'''), 140.23 (C, C-1'), 134.50 (C, C-4'), 129.42 (2 \times CH, CH-2' and CH-6'), 128.51 (2 \times CH, CH-3'' and CH-5''), 128.41 (2 \times CH, CH-2'' and CH-6''), 128.31 (CH, CH-4''), 127.59 (2 \times CH, CH-3' and CH-5' and C, C-3a), 126.12 (CH, Ar), 124.07 (CH, Ar), 122.09 (CH, Ar), 112.10 (CH, CH-7), 108.34 (CH, CH-3), 58.33 (CH, CH-1). Anal. Calcd for C₂₃H₁₇N₃O (351.406): C, 78.61; H, 4.88; N, 11.95. Found: C, 78.77; H, 4.62; N, 11.79.

5.1.4.9. 1-[Benzo[*b*]furan-2-yl-(4'-chloro-biphenyl-4-yl)-methyl]-1*H*-[1,2,4]triazole (16a) and 4-[benzo[*b*]furan-2-yl-(4'-chloro-biphenyl-4-yl)-methyl]-4*H*-[1,2,4]triazole (16b). Purified by column chromatography (petroleum/ethyl acetate, 9:1 v/v increasing to 65:35 v/v) to give the [1,2,4]triazole **16a**, further elution (dichloromethane/methanol, 99:1 v/v) gave the [1,3,4]triazole **16b**.

Data for 16a: white solid (67%), mp 34–36 °C. TLC system: petroleum ether/ethyl acetate, 1:1 v/v, *R_f*: 0.26. ¹H NMR (CDCl₃): δ 8.24 (s, 1H, H-3'''), 8.11 (s, 1H, H-5'''), 7.64 (d, *J* = 8.3 Hz, 2H, Ar), 7.60–7.52 (m, 3H, Ar), 7.49–7.29 (m, 7H, Ar), 6.95 (s, 1H, H-1), 6.69 (s, 1H, H-3). ¹³C NMR (CDCl₃): δ 155.80 (C, C-2), 152.80 (CH, CH-5'' and C, C-7a), 143.74 (CH, CH-

3'''), 141.36 (C, C-1'), 138.97 (C, C-1''), 135.32 (C, C-4'), 134.38 (C, C-4''), 129.52 (2× CH, CH-2' and CH-6'), 128.83 (2× CH, CH-3'' and CH-5''), 128.67 (2× CH, CH-2'' and CH-6''), 128.10 (2× CH, CH-3' and CH-5'), 127.87 (C, C-3a), 125.80 (CH, Ar), 123.86 (CH, Ar), 122.02 (CH, Ar), 112.02 (CH, CH-7), 108.40 (CH, CH-3), 62.35 (CH, CH-1). Anal. Calcd for C₂₃H₁₆ClN₃O (385.852): C, 71.60; H, 4.18; N, 10.89. Found: C, 71.45; H, 4.10; N, 10.62.

Data for 16b: Light yellow solid (13%), mp 68–70 °C. TLC system: dichloromethane/methanol, 9:1 v/v, R_f: 0.50. ¹H NMR (CDCl₃): δ 8.31 (s, 2H, H-2''' and H-5'''), 7.65 (d, *J* = 8.3 Hz, 2H, Ar), 7.61–7.43 (m, 6H, Ar), 7.41–7.31 (m, 4H, Ar), 6.79 (s, 1H, H-1), 6.70 (s, 1H, H-3). ¹³C NMR (CDCl₃): δ 155.85 (C, C-2), 152.29 (C, C-7a), 142.89 (2× CH, CH-2''' and CH-5'''), 141.75 (C, C-1'), 138.66 (C, C-1''), 134.93 (C, C-4'), 134.58 (C, C-4''), 129.59 (2× CH, CH-2' and CH-6'), 128.82 (2× CH, CH-3'' and CH-5''), 128.42 (2× CH, CH-2'' and CH-6''), 128.35 (2× CH, CH-3' and CH-5'), 127.56 (C, C-3a), 126.16 (CH, Ar), 124.10 (CH, Ar), 122.10 (CH, Ar), 112.10 (CH, CH-7), 108.37 (CH, CH-3), 58.26 (CH, CH-1). Anal. Calcd for C₂₃H₁₆ClN₃O·0.1H₂O (387.653): C, 71.26; H, 4.21; N, 10.83. Found: C, 71.05; H, 4.09; N, 10.75.

5.2. MCF-7 (CYP26A1) assay for inhibition of metabolism of atRA

Human MCF-7 breast cancer cells were cultured in phenol red free RPMI 1640 medium supplemented with 5% (v/v) charcoal free foetal calf serum, antibiotics (penicillin and streptomycin) and fungizone at the same concentration of 10 iU/mL. Cells were grown in a humidified incubator (5% CO₂, 95% air) at 37 °C. MCF-7 cells were seeded in 12-well cell culture plates (Corning Inc., New York, USA) at 2.5 × 10⁵ cells per well in a total volume of 1.5 mL. Cells were allowed to adhere to the well for 24 h. After 24 h, the medium from each well was removed, washed once with phosphate-buffered saline (PBS) and replaced by fresh medium plus 10 μL inhibitor/solvent (acetonitrile) and 10 μL of atRA (to give a final concentration of 1 × 10⁻⁷ M atRA and 0.1 μCi [11,12-³H] *all-trans* retinoic acid). The plates were foil wrapped and incubated at 37 °C for 9 h. Each treatment was performed in duplicate. The incubation was stopped by addition of 1% acetic acid (100 μL/well), the medium removed into separate glass tubes. Two hundred microlitres of distilled water was added to each well and the cells were scrapped off and the contents added to the appropriate glass tube. This procedure was repeated with a further 400 μL water but without scraping. Ethyl acetate containing 0.05% (w/v) butylated hydroxyanisole (2 × 2 mL) was added to each tube. After vortexing for 15 s, the tubes were spun down at 3000 rpm for 15 min. The organic layer was then evaporated using a Christ centrifuge connected to a vacuum pump and a multitrap at -80 °C.

5.3. High performance liquid chromatography (HPLC)

The HPLC system was equipped with a high pressure pump (Milton-Roy pump), injector with a 50 μL loop

connected to a β-RAM radioactivity detector, connected to a Compaq™ computer running Laura® data acquisition and analysis software. This enabled on-line detection and quantification of radioactive peaks. The HPLC column (10 μM C₁₈ μBondapak™ 3.9 × 300 mm HPLC column from Waters, UK) operating at ambient temperature was used to separate the metabolites which were eluted with acetonitrile/1% ammonium acetate in water/acetic acid (75:25:0.1 v/v/v) at a flow rate of 1.9 mL/min. Ecoscint™ was used as the flow scintillation fluid.

5.4. Molecular docking

All molecular modelling studies were performed on a RM Innovator Pentium IV 2.4 GHz running either Linux Fedora Core 3 or Windows XP using Molecular Operating Environment (MOE) 2004.03²⁴ software. All the minimisations were performed with MOE until a RMSD gradient of 0.05 Kcal mol⁻¹ Å⁻¹ with the forcefield specified and the partial charges were automatically calculated.

Ligands were docked within the active site of the CYP26A1 homology model²⁵ using the MOE-Dock with simulated annealing used as the search protocol with a total of 5 runs, 10 cycles per run, 8000 steps per cycle and an initial temperature of 1000 K. Molecular dynamics was performed with MOE using the NVT environment for 100 ps and constant temperature of 300 K using the MMFF94X forcefield with all other default settings in MOE-dynamics chosen. The lowest energy conformation was selected and subjected to an energy minimisation using the MMFF94X forcefield. The scoring.svl script was used to identify interaction types between ligand and protein.

Acknowledgments

One of us (S.W.Y.) would like to acknowledge the ORS Awards Scheme for a United Kingdom Scholarship. We also acknowledge the technical staff of the Tenovus Cancer Centre for the preparation of cells and media, and the EPSRC Mass Spectrometry Centre, Swansea, UK, for mass spectroscopy data.

References and notes

1. Ray, W. J.; Bain, G.; Yao, M.; Gottlieb, D. I. *J. Biol. Chem.* **1997**, *272*, 18702–18708.
2. White, J. A.; Beckett, B.; Scherer, S. W.; Herbrick, J. A. *Genomics* **1998**, *48*, 270–272.
3. Njar, V. C. O. *Mini-Rev. Med. Chem.* **2002**, *2*, 261–269.
4. Marill, J.; Idres, N.; Capron, C. C.; Nguyen, E.; Chabot, G. G. *Curr. Drug Metab.* **2003**, *4*, 1–10.
5. Estey, E. H.; Giles, F.; Kantarjian, H.; O'Brien, S.; Cortes, J.; Freireich, E.; Lopez-Berestein, G.; Keating, M. *Blood* **1999**, *94*, 2230–2235.
6. Fenaux, P.; Chastang, C.; Chevret, S.; Sanz, M.; Dombret, H.; Archimbaud, E.; Fey, M.; Rayon, C.; Huguet, F.; Sotto, J. J.; Gardin, C.; Makhoul, P. C.; Travade, P.; Solary, E.; Fegueux, N.; Bordessoule, D.; San Miguel, J.;

- Link, H.; Desablens, B.; Stamatoullas, A.; Deconinck, E.; Maloysel, F.; Castaigne, S.; Preudhomme, C.; Degos, L. A. *Blood* **1999**, *94*, 1192–1200.
7. Marill, J.; Cresteil, T.; Lanotte, M.; Chabot, G. G. *Mol. Pharmacol.* **2000**, *58*, 1341–1348.
8. Weiss, G. R.; Liu, P. Y.; Alberts, D. S.; Peng, Y. M.; Fisher, E.; Xu, M. J.; Scudder, S. A.; Baker, L. H.; Moore, D. F.; Lippman, S. M. *Gynecol. Oncol.* **1998**, *71*, 386–390.
9. Pettersson, F.; Colston, K. W.; Dalgleish, A. G. *Pancreas* **2001**, *23*, 273–279.
10. Ahmad, N.; Mukhtar, H. *J. Invest. Dermatol.* **2004**, *123*, 417–425.
11. Brecher, A. R.; Orlow, S. J. *J. Am. Acad. Dermatol.* **2003**, *49*, 171–182.
12. Smith, H. J.; Nicholls, P. J.; Simons, C.; LeLain, R. *Exp. Opin. Ther. Patents* **2001**, *11*, 789–824.
13. Yee, S. W.; Jarno, L.; Gomaa, M. S.; Elford, C.; Ooi, L.-L.; Coogan, M. P.; McClelland, R.; Nicholson, R. I.; Evans, B. A. J.; Brancale, A.; Simons, C. *J. Med. Chem.* **2005**, *48*, 7123–7131.
14. Patel, J. B.; Huynh, C. K.; Handratta, V. D.; Gediya, L. K.; Brodie, A. M. H.; Goloubeva, O. G.; Clement, O. O.; Nanne, N. P.; Soprano, D. R.; Njar, V. C. O. *J. Med. Chem.* **2004**, *47*, 6716–6729.
15. Mulvihill, M. J.; Kan, J. L. C.; Beck, P.; Bittner, M.; Cesario, C.; Cooke, A.; Keane, D. M.; Nigro, A. I.; Nillson, C.; Smith, V.; Srebernak, M.; Sun, F. L.; Vrkjan, M.; Winski, S. L.; Castelhana, A. L.; Emerson, D.; Gibson, N. *Bioorg. Med. Chem. Lett.* **2005**, *15*, 1669–1673.
16. Kuijpers, A. L. A.; Van Pelt, J. P. A.; Bergers, M.; Boegheim, P. J.; Den Bakker, J. E. N.; Siegenthaler, G.; Van de Kerkhof, P. C. M.; Schalkwijk, J. *Br. J. Dermatol.* **1998**, *139*, 380–389.
17. Luckner, G. P. H.; Heremans, A. M. C.; Boegheim, P. J.; Van de Kerkhof, P. C. M.; Steijlen, P. M. *Br. J. Dermatol.* **1997**, *136*, 71–75.
18. Denis, L.; Debruyne, F.; De Porre, P. *Eur. J. Cancer* **1998**, *34*, 469–475.
19. Stoppie, P.; Borgers, M.; Borghgraef, P.; Dillen, L.; Goossens, J.; Sanz, G.; Szel, H.; Van Hove, C.; Van Nyen, G.; Nobels, G.; Vanden Bossche, H.; Venet, M.; Willemsens, G.; Van Wauwe, J. *J. Pharmacol. Exp. Ther.* **2000**, *293*, 304–312.
20. Stoermer, R. *Annalen der Chemie* **1900**, *312*, 237.
21. Vinh, T. K.; Yee, S. W.; Kirby, A. J.; Nicholls, P. J. *Anticancer Drug Des.* **2001**, *16*, 217–225.
22. Cowper, R. M.; Davidson, L. H. *Organic Syntheses Collective Volumes*. 1943, Vol. 1, p 480.
23. Miyaura, N.; Yanagi, T.; Suzuki, A. *Synth. Commun.* **1981**, *11*, 513–519.
24. Molecular Operating Environment (MOE). Chemical Computing Group, Inc. Montreal, Quebec, Canada. <http://www.chemcomp.com>. Code 'scoring svl' obtained from SVL Exchange website <http://svl.chemcomp.com>, Chemical Computing Group, Inc. Montreal, Canada.
25. Gomaa, M.; Yee, S. W.; Milbourne, C. E.; Chiara, M. B.; Simons, C.; Brancale, A. Submitted for publication.
26. Yano, J. K.; Wester, M. R.; Schoch, G. A.; Griffin, K. J.; Stout, D.; Johnson, E. F. *J. Biol. Chem.* **2004**, *279*, 38091–38094.
27. Richter, P. H.; Elsner, H.; Vogt, B. Preparation of benzo[b]furan-derived ketone amidinohydrazome class III antiarrhythmic agents. *Eur. Pat. Appl.*, 1997, 32 pp.
28. Pestellini, V.; Giolitti, A.; Pasqui, F.; Abelli, L.; Cutrufo, C.; De Salvia, G.; Evangelista, S.; Meli, A. *Eur. J. Med. Chem.* **1988**, *23*, 203–206.

